THE EFFECT OF TOOTH GEOMETRY

on

POWER HACKSAW BLADE PERFORMANCE

by

William Malcolm Manson Hales BSc

A Thesis submitted to the Council for National Academic Awards in partial fulfilment of the requirements for the degree of Doctor of Philosophy.

Sponsoring Establishment : Department of Mechanical and Production Engineering
Sheffield City Polytechnic

Collaborating Establishment : James Neill Limited
Handsworth, Sheffield

November 1986

DECLARATION

I declare that, while registered as a candidate for the Council's research degree, I have not been a registered candidate or enrolled student for another award of the CNAA or other academic or professional institution.

Signed:

ABSTRACT

The effect of tooth geometry on hacksaw blade performance.

Author: W M M Hales

Published work concerning the influence of tooth geometry on hacksaw blade performance has been reviewed.

By testing standard and modified hacksaw blades the author has shown that, contrary to previous belief, pitch is not a parameter which affects blade performance. Furthermore experimental evidence is presented to show that gullet size and shape significantly affect blade performance.

The author proposes that restriction of chip flow by the gullet causes very inefficient metal removal. This is supported by examination of hacksaw chips, and a theoretical model has been developed to show how rapidly cutting forces increase when the chip is restricted from flowing.

Two testing procedures have been developed to examine chip formation in the gullet. The first procedure employs video equipment to show chip formation and cutting forces simultaneously on one VDU, during cutting with single hacksaw teeth. This test is of limited use due to the slow cutting speeds employed. The second procedure, also using single teeth but cutting at realistic speeds, was capable of testing any tooth/gullet geometry cutting any material. The test results confirmed that restriction of chip flow by the gullet produces inefficient cutting. It has been shown that a particular tooth/gullet geometry can only cut efficiently over a limited range of feeds and workpiece lengths.

The author has developed a method for accurately predicting sawing rates from the single tooth data gathered.

The information gathered from the single tooth tests has enabled the author to isolate the most important aspects of tooth geometry affecting blade performance, and as a result, a new tooth design has been developed which performs better than the standard tooth.

ACKNOWLEDGEMENTS

The author is particularly grateful to his supervisors, Professor D S Dugdale and Dr M Sarwar for their guidance and encouragement.

Many thanks are also due to Dr B Worthington, Dr S Hashmi and Dr D Gillibrand for their constructive and pertinent criticism and advice.

The continual and willing assistance of all the laboratory technicians has been gratefully received. In particular the author wishes to thank Mr S J Leigh, Mr R C Wainwright, Mr T J O'Hara, Mr R C Wilkinson, Mr M Jackson and Mr J Taylor.

The author wishes to thank the members of the Product Development Department, Eclipse Tools Limited, for their advice and generous supply of blades and materials. Special thanks go to Mr K Pascoe, Mr A Fleming and Mr P Wilkinson.

CONTENTS

LIST OF FIGURES

FIGURE	CAPTION
4.7	The performance of a 4 TPI tooth cutting aluminium: (a) showing thrust force/unit width of tooth versus undeformed chip thickness, and (b) showing specific thrust pressure versus undeformed chip thickness.
4.8	The performance of a 4 TPI tooth cutting aluminium, and the performance of a 6 TPI tooth cutting aluminium. Length of cut 50 mm.
4.9	The performance of a 4 TPI tooth cutting aluminium at three different lengths of cut.
4.10	Some mild steel chips produced by single hacksaw teeth cutting at a realistic speed.
4.11	Cutting and thrust force traces for a standard 4 TPI tooth cutting 25 mm of mild steel. Undeformed chip thickness 0.071 mm.
4.12	Typical surface finish of the slot bed caused by a 4 TPI tooth cutting 50 mm mild steel at 30 m/min.
4.13	Performance of a standard 4 TPI tooth cutting aluminium. Length of cut 75 mm. Cutting speed 30 m/min.
4.14	Thrust force traces for points X, Y and Z in Figure 4.13.
4.15	Chips relating to points X, Y and Z in Figure 4.13.
4.16	Graph showing, for a standard 4 TPI tooth cutting aluminium: (a) the average performance over each cut; (b) the instantaneous maximum specific thrust pressure, and (c) the instantaneous specific thrust pressure before restriction to chip flow occurred.

FIGURE	CAPTION
4.17	Aluminium chips cut by: (a) a standard 4 TPI tooth, and (b) a standard 10 TPI tooth Undeformed thickness: (a) 0.04 mm (b) 0.039 mm Length of cut: (a) 75 mm (b) 12 mm
4.18	Graph showing the length of cut at which chip flow was first restricted in standard 4, 6 and 10 TPI teeth cutting aluminium at 30 m/min.
4.19	Graph showing the data in Figure 4.18 normalised by the height of the gullet.
4.20	The performance of a standard 4 TPI tooth cutting mild steel. Length of cut 75 mm. Cutting speed 30 m/min.
4.21	Chip and associated thrust force trace for point X on Figure 4.20.
4.22	Performance of a standard 4 TPI tooth cutting stainless steel. Length of cut 75 mm. Cutting speed 30 m/min.
4.23	The thrust force trace relating to point X on Figure 4.22.
4.24	The chip relating to point X on Figure 4.22.
4.25a-c	The performance 4, 6 and 10 TPI single teeth cutting various lengths of aluminium workpiece at 30 m/min cutting speed.
4.26a-c	The performance 4, 6 and 10 TPI single teeth cutting various lengths of mild steel workpiece at 30 m/min cutting speed.
4.27a-c	The performance 4, 6 and 10 TPI single teeth cutting various lengths of stainless steel workpiece at 30 m/min cutting speed.

FIGURE	CAPTION
4.28a-c	Performance of different pitch standard single teeth cutting aluminium: (a) 50 mm (b) 25 mm (c) 12 mm
4.29a-c	Performance of different pitch standard single teeth cutting mild steel: (a) 50 mm (b) 25 mm (c) 12 mm
4.30a-c	Performance of different pitch standard single teeth cutting stainless steel: (a) 50 mm (b) 25 mm (c) 12 mm
5.1	Diagram of the shear planes OX and OA along which the chip material shears when the chip is restricted from flowing along the rake face. The associated hodograph shows the relative velocity of chip material along OX and OA.
5.2	Diagram of alternate secondary shear planes OA, OB and OC and the associated hodograph.
5.3	Diagram of chip shape when the tool has travelled 3 t after the chip flow has been restricted.
5.4	Modelled chip shape at a distance; (a) 6 t, (b) 15 t, (c) 24 t, (d) 36 t and (e) 54 t, after chip restriction occurred. Rake angle, 0°.
5.5	Modelled chip shape at a distance; (a) 6 t, (b) 15 t, (c) 24 t, (d) 36 t and (e) 54 t, after chip restriction occurred. Rake angle, -4°.
5.6	Diagram showing the geometrical relationship between the cutting and thrust forces and the force acting along the shear plane.
5.7	Equivalent stress and logarithmic strain for mild steel and aluminium. Data taken from compression tests. Straight line extrapolation has been used.

FIGURE	CAPTION
5.8a	Theoretical and experimental values of cutting force subsequent to chip flow restriction occurring, for a standard 4 TPI tooth cutting aluminium. UCT is 0.067 mm.
5.8b	Theoretical and experimental values of cutting force subsequent to chip flow restriction occurring, for a standard 6 TPI tooth cutting aluminium. UCT is 0.074 mm.
5.8c	Theoretical and experimental values of cutting force subsequent to chip flow restriction occurring, for standard 4 and 6 TPI tooth cutting mild steel. UCT is 0.067 mm.
5.9	Chip and force trace showing the effect of the chip sticking and then slipping. The peaks are caused by the chip sticking and the subsequent drop in force occurs when the chip slips up the rake face.
6.1	Single tooth data used to predict sawing times, showing thrust force per unit width of tooth versus undeformed chip thickness.
6.2	Thrust force trace generated by a hydralic hacksaw machine.
7.1	4 TPI tooth having no restricting gullet with: (a) a zero degree rake angle; (b) a 11° rake angle.
7.2	Standard 4 TPI tooth/gullet geometry with: (a) a zero degree rake angle (b) a 10° rake angle
7.3	Performance of 4 TPI hacksaw tooth with no restricting gullet: (a) with zero degree rake angle (b) with 11° rake angle. Mild steel workpiece. Length of cut 50 mm.

FIGURE	CAPTION
7.4	Performance of standard 4 TPI tooth: (a) with zero degree rake angle (b) with 10° rake angle. Mild steel workpiece. Length of cut 50 mm.
7.5	Specific cutting energy versus undeformed chip thickness for single hacksaw teeth having no restricting gullet. Workpiece mild steel. 0° rake angle and 11° rake angle.
7.6	Single hacksaw teeth having a single radius root: (a) 1.25 mm radius (b) 1.75 mm radius
7.7	New tooth/gullet geometry for improved chip curl.
7.8	The performances of: (a) the single root radius teeth, Figure 7.6; and (b) the new tooth/gullet, Figure 7.7, compared to the performance of a standard 4 TPI tooth cutting a 50 mm workpiece.
7.9	The single tooth shown in Figure 7.6 with chips which have curled to the same radius as the roots. There is sufficient spring in these chips to prevent them from falling out of the gullet.
7.10	Chip created by a hacksaw tooth having no restricting gullet.
7.11	Chips produced by the new tooth/gullet, Figure 7.7.
7.12	The performances of a standard 4 TPI tooth/gullet and the new tooth/gullet, Figure 7.7, cutting a 75 mm mild steel workpiece.
7.13	The performances of a standard 4 TPI tooth/gullet and the new tooth/gullet, Figure 7.7, cutting 25 and 50 mm aluminium workpieces.

CHAPTER ONE

INTRODUCTION

Cutting-off is the first process in many manufacturing sequences, because material is rarely delivered in suitable lengths for subsequent forging or machining processes.

Sawing is one of the most common cut-off processes used in industry, because it provides good output rates and tolerances. The sawing processes in commonest use are:

(i) Power hacksawing;

(ii) Bandsawing;

(iii) Circular sawing.

The relative merits of each are briefly considered below.

Power hacksawing has the slowest output rate because it is not a continuous cutting process. The blade does not cut on the return stroke and therefore the return time is unproductive. Both bandsaws and circular saws cut continuously, having no unproductive cutting time. Circular sawing has the highest output rate of the three processes, because the blade is the most rigid, and can therefore apply the highest cutting forces.

Hacksaw machines are generally cheaper than either circular saw machines or bandsaw machines. Also the cost of circular saw blades is higher than for bandsaw and hacksaw blades. Circular saws are often specials,

designed for particular applications thus making production costs high. They are not throw-away tools, like band- and hacksaw blades, but have to be re-sharpened throughout their cutting lives. Some circular saws have replaceable segmental teeth which prolongs the life of the blade.

Bandsaw and hacksaw blades are throw-away tools, hacksaw blades being considerably cheaper. The price of the blade in a sawing process is particularly important if the material is difficult to cut, causing rapid or inconsistent blade wear.

Kerf loss is greatest in circular sawing. The thickness of a circular saw blade determines the rigidity of the blade and is therefore thicker than band- and hacksaw blades in which rigidity is obtained by longitudinal tensioning. Kerf loss is particularly important when expensive materials or short pieces are being cut.

Bandsaw blades, being the least rigid, have the worst run-out. This is particularly severe when cutting broad workpieces because the blade guides have to be positioned far apart.

Circular saws cut the mot accurately, this is partly due to the rigidity of the blade, but it is also due to the close tolerances to which these blades are manufactured.

The competition which hacksawing has received from bandsawing and circular sawing is considerable, but there still appears to be a share of the cut-off market best served by power hacksawing. The process is particularly suited to cutting large workpieces of difficult-to-machine materials.

1.1 Hacksaw Machines

The essential features of a power hacksaw machine are the swing-arm assembly, which carries the saw blade and its bow, a mechanical drive to reciprocate the blade, and a device for developing thrust load between the blade and the workpiece. The thrust load is required to feed the blade into the workpiece. It is applied during the cutting stroke and relieved to lift the blade on the return stroke. A number of different types of machines are available, and they can be classified according to the method used to develop the thrust load.

Gravity fed machines develop the thrust load from the gravity force acting on a massive blade bow and swing arm assembly. In some machines an adjustable mass is provided on the swing arm assembly so that the gravity force can be adjusted.

These machines are for light-duty work, because of the practical limitations on the mass of the swing arm assembly.

In hydraulic machines the thrust load is produced by the action of a hydraulic device. The control which the operator has over the thrust load generated by the hydraulic device is imprecise, and varies over the length of the stroke. However, this type of machine is common and is capable of applying large thrust loads which makes it applicable for heavy duty work.

Positive feed machines control the feed rate to the blade directly by a mechanical screw device. The feed rate per stroke is pre-set and remains constant throughout the cut. When using gravity fed or hydraulic machines, feed rate is controlled by the thrust load. Positive feed machines, however, control the thrust load by the feed rate. The developed thrust load increases as the blade wears, for a given feed rate, and this can lead to premature blade fracture. This lack of control over the thrust load and the resultant tendency to break blades are the main disadvantages of the positive displacement machines.

1.2 Power Hacksaw Blades

There are many brands of hacksaw blade on the market. The types of blade available can be categorised by the material from which they are made.

(i) **Low alloy steel blades**

These blades contain more than 1% tungsten. The whole blade is hardened and tempered uniformly, and only a small portion of the blade around the pinholes is softened. Blades which have been heat-treated in this manner are known as 'all-hard' blades. (BS 1919).

'All-hard' blades are rigid and will break into a number of pieces if bent beyond a critical radius.

(ii) **High speed steel blades. All-hard.**

The high speed steel usually contains molybdenum. Often M2 or M42 steels are used for these blades.

(iii) **Bi-metal high speed steel blades**

These blades are manufactured with the toothed edge formed from high speed steel joined to a spring steel backing strip. The toothed edge is fully hardened and tempered, whilst the backing strip is retained in a spring-like condition. Bi-metal blades are therefore flexible and shatter-proof. Shatter-proof means that if the blade fractures it will only fracture into two parts. Thus bi-metal blades are safer than all-hard blades.

1.2.1 Power hacksaw blade nomenclature

BS 1919 defines the nomenclature used for power hacksaw blades as below:

Nomenclature

Centre line The longitudinal line which passes through the centres of the pin holes.

Pin hole The hole at each end of the blade by means of which the blade is held and tensioned when in use.

Teeth The serrations formed across the thickness of the blade to provide cutting edges.

Toothed edge The longitudinal edge along which the teeth have been formed.

Cutting edge The transverse edge of each tooth, formed by the intersection of the flank and the face.

Face The surface of the tooth adjacent to the cutting edge on which the chip impinges as it is cut from the material being sawn.

Flank The surface behind the cutting edge of the tooth which extends to the root radius.

Root radius The radius connected to the face of one tooth and the flank of the preceding one.

Back edge The longitudinal edge parallel to the toothed edge.

Side The flat surface between the toothed edge and the back edge.

Set The projection of teeth from the sides of the blade to provide cutting clearance.

Linear dimensions and size designation

Blade length The dimension between the centres of the pin holes, measured along the centre line of the blade.

Overall length The dimension between the ends of the blade measured along its centre line.

Width The dimension between the toothed edge and the back edge.

Thickness The dimension between the two sides, excluding the set.

Pitch (P) The distance between adjacent cutting edges measured in millimetres.

Number of teeth (N) Number of complete teeth contained in any 25 mm length measured along the toothed edge.

Size designation The blade length, width, thickness and pitch and (number of teeth per 25 mm) are always expressed in this order as given in the following example:

250 x 13 x 0.65 x 1.4 (18)

1.2.2 BS 1919

The BS for hand and power blades places few constraints on blade design, and manufacturers are free to design any tooth geometry, set pattern and side clearance.

1.3 Blade Performance Assessment Methods

To know how well a blade 'performs' is necessary for manufacturers' of hacksaw blades;

(a) for quality control; and
(b) for comparison with other manufacturers' blades

Hacksaw blade performance does not have a clearly defined standard, and as a result there are several methods of testing performance.

Three of these methods are now discussed:

1.3.1 A blade manufacturer's testing procedure

In this test the performance of blades are tested over their complete cutting lives. A blade tested is set in a gravity fed machine to cut through a workpiece, of standard dimensions and material, several times until it is "worn out". A blade is adjudged to be worn out, when it takes more than a prescribed number of strokes to cut one section of the workpiece. The number of strokes taken to cut

each section is recorded, and from this a peformance criterion is evaluated, which is a measure of both the starting performance and wear rate of the blade. Figure 1.1 shows the performance of three blades; it is clear that blade A performs worse than the other two blades, because it takes more strokes to cut through the workpiece and wears out faster than the other two blades. However, the relative performance levels of blades B and C are more difficult to assess. Blade B's initial output rate is better than C's, but it wears out faster.

In this test the applied thrust force is not measured for each blade tested, but is arranged to be constant from test to test and is assumed to be constant from one machine to another. However, fundamental studies of hacksaw machines (2) carried out at Sheffield City Polytechnic, have shown that the thrust force characteristics of various machines differ considerably and therefore to compare the performance of two blades using this method, both must be tested on the same machine. A better performance test would eliminate the effect of the machine characteristics from the performance of the blade, so that the performance of the blade itself would be obtained.

Two testing methods have been proposed to solve the problem of variable machine characteristics.

1.3.2 The BS 1919 British Standard performance test

The British Standard performance test, based on work carried out at Sheffield City Polytechnic and the British Hacksaw Manufacturers' Association, attempts to eliminate as many unwanted test variables (eg machine characteristics, workpiece length and material, etc) as possible.

To this end, the proposal specifies the material to be cut, and the width of the workpiece which varies depending on the pitch of the blade. It also specifies the machine characteristics in detail. The specified machine parameters are:

(a) gravity feed;

(b) cutting in one direction only;

(c) cutting speed;

(d) stroke length;

(e) blade angle;

(f) stroke rate;

(g) level of lift off on return stroke;

(h) the average thrust force per cutting stroke; and

(i) the coolant used.

For each blade tested the number of sections cut is specified.

The procedure followed to test a blade is:

(i) set up the workpiece of specified width;

(ii) cut the number of sections specified;

(iii) record the number of strokes to cut each section;

(iv) calculate the 'wear rate' and 'total time' and compare them with the standards given. Wear rate is a measure of the increase in cutting time per section cut for the whole test.

Figure 1.2 shows one of the proposed standards for power hacksaw blades.

1.3.3 The performance test developed by Sarwar and Thompson

Tests carried out by Sarwar and Thompson (1) had shown that for a given workpiece width and material, the depth of cut per stroke is dependent on the thrust force applied to the blade. Any performance criterion, therefore, should be able to take account of the effect of varying thrust forces which occur during hacksawing.

The performance criterion, proposed by Sarwar and Thompson, gave consistent results when various hydraulic and gravity feed machines were used (2). This suggested that the machine characteristics of the sawing process had been eliminated from the measure of performance.

The procedure followed in testing a blade is:

(a) Set up a rectangular cross-section workpiece of known dimensions in a hacksaw machine equipped with a load measuring device.

(b) Cut through the workpiece, measuring the time to cut through the workpiece, and the thrust force for one stroke at approximately mid-way through the specimen.

(c) A few more cuts are taken at different thrust forces as in (b) above.

(d) The performance criterion is calculated using the time to cut through each section, and the force measurements.

The performance criterion (K) is calculated by dividing the average depth of cut per stroke per tooth (δa) by the average thrust force per unit width of tooth per tooth in contact with the workpiece (f_{tm}).

$$\delta a = \frac{D}{N} \cdot \frac{1}{s.p^{-1}} \cdot \frac{w}{t} \qquad (1.1)$$

$$f_{tm} = \frac{F_{tm}}{B.p^{-1}} \cdot \frac{1}{t} \qquad (1.2)$$

where:

D = Depth of workpiece

w = Width of the saw slot

B = Breadth of workpiece

t = Thickness of saw teeth

p = Tooth pitch

s = Stroke length

$s.p^{-1}$ = Number of teeth cutting per stroke

N = Number of strokes to cut through the workpiece

F_{tm} = The average thrust force applied to the blade per stroke

$B.p^{-1}$ = The number of teeth in contact with the workpiece.

$K = \frac{\delta a}{f_{tm}}$

Thus from (1.1) + (1.2) $K = \frac{D.w.B}{F_{tm}.N.S}$ (1.3)

Sarwar (2) showed that:

$$F_{tm} = C.F_{cm} \quad (1.4)$$

where:

F_{cm} = the average cutting force applied to the blade per stroke; and

C = a constant

Substituting (1.4) in (1.3):

$$K = \frac{D.w.B}{C.F_{cm}N.S}$$

D.w.B is the volume of material cut by the blade per section.

$C.F_{cm}.N.S$ is the total cutting energy required to cut the section.

Thus K, the blade performance criterion, is proportional to the inverse of specific cutting energy.

The Sarwar and Thompson blade performance test is generally used to give the performance of a blade in its new state. However the test can be used to give the performance of a blade at different stages of its cutting life, and can be used to measure blade wear rate. (3)

1.4 Tooth Geometry

The aim of this research project was to gain more understanding of the influences of the various elements of tooth geometry on the cutting performance of power hacksaw blades so that their performance can be improved.

Hacksaw tooth geometry varies from one brand of blade to another. The only feature common to all brands is the pitch, for which there is an internationally agreed standard. Table 1.1.

Pitch of teeth (mm)	0.8	1.0	1.4	1.8	2.5	4.0	6.3
Number of teeth/25 mm	32	24	18	14	10	6	4

These values are nominal and subject to a variation of $\pm$6%.

Table 1.1

Some manufacturers make blades with a larger tooth pitch than 6.3 mm, but there are no pitches produced between those shown in Table 1.1.

Two tooth geometries are shown in Figure 1.3 to illustrate the difference between brands of hacksaws.

In the following sections of this chapter, various aspects of tool geometry are discussed in relation to hacksaw teeth.

1.4.1 Rake angle and cutting edge radius

Figures 1.4 a-d show the effect of rake angle on continuous chip formation in orthogonal cutting. The positive rake angle tool , Figure 1.4a, produces a larger shear plane angle, ϕ, than the zero rake angle tool, Figure 1.4b. Its shear plane length AB is therefore shorter and the forces required to shear the chip across this plane are less. As the rake angle becomes more negative, Figure 1.4 c, the

shear plane angle decreases, and the shear plane length and shear force increase. When the rake angle becomes very negative, Figure 1.4d, the force required to shear along the chip/tool interface AC will approach that required to shear along the shear plane AB. This model of cutting cannot occur in practice because the area of metal AOC is unable to flow under these conditions. Thus AOC becomes a dead metal zone and shear planes are created along AO, OC and OB, Figure 1.4d (2).

In most metal cutting operations, eg turning, milling, shaping, the rake angle is never more negative than -15^{o}. However, for some processes, eg grinding and hacksawing, the effective rake angle can be more negative than -15^{o} ranging between 0^{o} and -90^{o}. This is due to the small undeformed chip thickness to cutting edge radius ratio. Early work carried out at Sheffield City Polytechnic (1, 4) showed that the cutting edge radii, Figure 1.5, of hacksaw teeth are large and can vary in size from 0.02 mm to 0.08 mm. The blunt cutting edge is a result of the heat treatment process which is carried out after the teeth have been milled to size. (There is no sharpening of the teeth after heat treatment). The average undeformed chip thickness per tooth was estimated (4) to vary between 0.002 mm and 0.030 mm which is small compared

to the cutting edge radius. Figure 1.6 shows the effective rake angle when the cutting edge radius, (R), to undeformed chip thickness, $(\frac{t}{tc})$, ratio is large.

Cutting tests (2, 5) have shown that tools with large cutting edge radii to undeformed chip thickness ratios, cut significantly less efficiently than sharper tools. During these tests (2,5,6), cutting copper, Sarwar and Thompson observed that a dead metal cap formed in front of the blunt tools at the start of each cut. Furthermore they reported that a transient phase of chip formation occurred during the beginning of the cut until a steady state of chip formation was produced. The chip was thinner in the transient phase and required less force to be produced than in the steady state phase, despite the undeformed chip thickness remaining constant throughout the cut. Thus chip formation was more efficient in the transient phase than the steady state phase.

Sarwar (2,5) produced a slip-line field model of the chip formation of a tool with a large cutting edge radius/undeformed chip thickness ratio. The model includes a dead metal cap in front of the tool cutting edge. Shear planes bound the dead metal cap next to the chip and the workpiece. The predicted cutting forces from this model correlate well with empirical data.

Sarwar and Hales also carried out tests on blunt cutting tools (7) which had nominal rake angles varying from 0^{o} to 15^{o}. The cutting edge radii tested were nominally sharp, 0.3 mm and 0.5 mm.

Nominal rake angle had no effect on performance when cutting EN1A, a leaded mild steel, but when cutting copper the 5^{o} rake angle tool performed better than the 0^{o} rake angle tool. The conclusion drawn from these tests was that when the cutting edge radius to undeformed chip thickness ratio is high then nominal rake angle does not affect cutting performance for mild steel but does for copper. The relevance of these tests to hacksawing is discussed in Chapter Seven.

When the cutting edge radius to undeformed chip thickness ratio is very large, the chip formed during the time that the tooth traverses the workpieces will not grow large enough to give chip contact on the tooth face beyond the end of the edge radius. Under these conditions, rake angle of the tooth face must be irrelevant to the cutting action.

1.4.2 Set

The teeth on a hacksaw blade are set to give clearance between the blade and the slot wall which, if not provided, would cause frictional forces

sufficient to break the blade and/or temperatures capable of softening the blade.

The author is unaware of any published work which covers theoretical or experimental examinations of set angle with regard to blade performance. However, Thompson & Taylor (8) have considered the effect of set on the lateral displacement of a blade. They conclude that "setting angle errors are the prime cause of the lateral displacements produced by new un-worn blades".

Soderberg (9) makes a passing reference to the effect of set on the undeformed chip thickness cut by each tooth on a blade. He reports that there is a variation in undeformed chip thickness along the tooth cutting edge. Soderberg showed, Figure 1.7, that some parts of a new tooth edge do not cut at all. Chips from hacksawing are frequently not as wide as the teeth on the blade, which corroborates Soderberg's suggestion.

There are three set patterns, wavy set, alternate set and raker set. Wavy set is rarely used for power blades. For alternate set the teeth are set alternately left and right. For the raker pattern the teeth are set left, right, centre.

1.4.3 Clearance angle

The clearance angle on a standard hacksaw tooth, 34^{o} - 38^{o}, Figure 1.5, is much larger than that found on conventional tools used for turning, shaping, milling, etc. A larger clearance angle will obviously lead to a smaller size of land wear. However a large clearance angle produces a small wedge angle which reduces the strength of the tool, and decreases the wear resistance of the tool further because heat conduction from the tool tip is restricted. Therefore a compromise must be made between the size of the clearance angle and the wedge angle.

The clearance angle also affects the size of the gullet. Some manufacturers have two clearance angles on each tooth, Figure 1.3. The primary clearance angle provides a large wedge angle, and the secondary angle provides space in the gullet for the chip to form.

1.4.4 Tooth pitch

Performance tests carried out by Sarwar and Thompson (1,2) have shown that blades with large pitches cut better than those with small pitches, Figure 1.8. Thompson (4) explains this effect by reference to the transient cutting force build-up produced by

blunt tools (6). The model Thompson (4) proposed, showed that pitch affected cutting performance. The pitch effect is discussed in Chapter Two.

1.4.5 Gullet

The effect of the gullet on the cutting performance of hacksaw blades has not been investigated in the past. Thompson (10) reports that "A number of gullet shapes are used, but it is believed that they do not have a major influence on cutting performance providing that 'clogging' of the teeth does not occur. The primary cause of clogging is the adhesion of the metal removed to the teeth so that it is carried by the blade to the beginning of the subsequent cut".

A major proportion of the author's work, for this research project, is concerned with gullet shape and size.

1.5 Blade Wear

Like all other cutting tools, the performance of a hacksaw blade depends on the rate at which it wears. Wright and Trent (11) proposed the following system of classification of wear processes and mechanisms for HSS:

(i) Superficial plastic deformation by shear at high temperatures.

(ii) Plastic deformation of the cutting edge.

(iii) Wear based on diffusion.

(iv) Attrition wear.

(v) Abrasive wear.

Thompson & Taylor (3) proposed that mechanisms (i) and (ii) were the main processes by which hacksaw blades wear. Figure 1.9 shows the wear model of a hacksaw tooth as proposed by Thompson and Taylor. They suggest that flank wear of this type maintains the blunt cutting edge profile.

Thompson and Taylor (3) also proposed a model which could determine the effects of various cutting conditions on the wear rate of hacksaw blades. Wear rate being a measure of the loss in cutting efficiency per cutting stroke. They report that cutting speed and thrust load had the greatest effect on wear rate: doubling cutting speed increased wear rate by six-fold, and doubling thrust force tripled wear rate. Also small workpiece breadths were shown to induce a higher wear rate than large workpiece breadths.

Thompson and Taylor (3) suggested three applications for their model:

(i) To validate improvements, applications and developments in blade design;
(ii) To test the effectiveness of coolants; and
(iii) To compare one blade with another.

A more detailed study of wear mechanisms in power hacksawing has been carried out by Soderberg et al (9). They report that wear mechanisms vary depending on workpiece material. When cutting a quenched and tempered carbon steel (0.36% C, 322 VHN) flank and crater wear were caused by abrasion. However, when cutting an austenitic stainless steel (18% Cr, 183 VHN) they report that flank wear was caused by plastic deformation due to high temperatures, and that wear on the rake face was caused by spalling. Figure 1.10 shows the characteristic profile of a tooth after cutting each of the materials mentioned above.

An interesting recent development in hacksaw technology is that some hacksaw manufacturers have produced blades which have the corners of each tooth ground away. Standard hacksaw teeth generally wear most severely on the corners due to poor heat conduction from the corners. By grinding off the corners of the teeth, a tooth shape with better heat conduction is created.

CHAPTER TWO

BLADE PERFORMANCE TESTS

Work carried out by Sarwar and Thompson (1,2) had shown that, for one make of hacksaw blade, there was a difference in performance between 4, 6 and 10 TPI blades; the 4 TPI blade cutting better than the 6 TPI blade which cut better than the 10 TPI blade, Figure 1.8. Furthermore it had been shown that cutting performance, for a particular blade, varied according to width of workpiece. As workpiece width increases, cutting performance falls, Figure 2.1. These tests have been repeated by the author using a Kasto hydraulic feed machine, and the results, Figures 2.2 and 2.3 corroborated those of Sarwar. The reason given by Thompson (4) for the difference in performance as workpiece width increases is that, a smaller proportion of the teeth in contact are cutting in the transient chip formation phase section for a wide workpiece than for a narrow workpiece. Cutting in the transient phase is more efficient than in the steady state phase, because the cutting forces are not as high. Furthermore, Thompson (4) produced a mathematical model showing that as the number of teeth in contact with the workpiece (Nc) increases the cutting performance falls.

Because Nc = B/p, where B = Breadth of workpiece (mm), and P = pitch of teeth (mm), it was suggested (4) that cutting performance would not only fall as breadth of workpiece increased, but also as pitch of teeth decreased.

The above supposition would explain why performance varies with breadth of workpiece, Figure 2.3, assuming that the transient phase was large in proportion to the breadth of workpiece. However, whether or not pitch affects performance needed further investigation.

2.1 Performance Tests on Modified Blades to Determine the Effect of Pitch

The following results are given in terms of the Sarwar and Thompson performance criterion, section 1.3.3, in which the depth of cut per tooth is plotted against thrust force per tooth; the steeper the curve the better the performance.

Test machine:	Kasto hydraulic feed
Cutting conditions:-	
Cutting rate:	50 strokes/min
Stroke length:	135 mm
Coolant:	None

Workpiece specification:

Mild Steel (0.17% C, 0.73% Mn, 0.24% Si, 0.06% S, 0.13% P, 0.20% Ni, 0.10% Cr, 0.06% Cu, 0.06% Mo, 0.012% Al).

50 mm wide x 25 mm deep.

An initial test compared the cutting performance of a 400 x 40 x 2 mm 4 TPI blade, raker set in its new condition, Figure 2.4a, and the cutting performance of the same blade modified by the removal of the cutting edge of every other tooth, Figure 2.4b. (The modification did not change the raker set pattern). The modified blade was effectively a 2 TPI blade, and would therefore cut better than the new 4 TPI blade if pitch affected cutting performance. As can be seen from Figure 2.5, there was no appreciable difference in cutting performance between the 4 TPI blade and the 2 TPI blade which suggests that pitch is not a parameter which affects performance.

The blade used for the above test was modified further by the removal of every other tooth, see Figure 2.4c, and its performance tested once again.

Figure 2.5 shows that the further modification improved the cutting performance of the blade.

2.1.1 Discussion of results

From the evidence provided by these results it was suggested that the size of the gullet affects cutting performance of hacksaw blades. The reasoning behind this suggestion is that the first modification did not alter the gullet size of the

blade and did not alter the cutting performance of the blade, but the second modification enlarged the gullet and improved the cutting performance of the blade.

It is indeed feasible that a small gullet would restrict the flow of a chip more than a large gullet would, and that this restriction could cause a fall in cutting efficiency. (Chapter Five).

2.2 Performance Tests on Modified Blades to Determine the Effect of Gullet Size

To check the above conclusion concerning gullet size and cutting performance, three more tests were carried out using the same experimental set-up as before, but in this test a 400 x 40 x 2 mm - 6 TPI blade was used.

Initially the blade was tested in its new condition, Figure 2.6a. Every other tooth was then removed down to the root of the gullet, Figure 2.6b, thus creating a 3 TPI blade with a larger gullet area than the 6 TPI blade.

The 3 TPI blade cut more efficiently than the 6 TPI blade, Figure 2.7, however, it did not perform as well as the new 4 TPI blade, despite having a larger gullet area than the new 4 TPI blade.

A further modification of the 3 TPI blade was made which enlarged every gullet so that the height of the gullet was the same as that of a new 4 TPI blade, Figure 2.6c. The performance of this blade was better than that of the 3 TPI blade with the smaller gullet, but it was no better than the 4 TPI blade which had a smaller gullet, Figure 2.7.

These results show that size is not the only aspect of the gullet geometry which affects cutting performance. Shape is also important when considering gullet geometry.

2.3 Hacksaw Chip Formation

The premise that gullet size and shape affects the performance of hacksaw blades has been made in section 2.2. Evidence to support this assumption has been found in the formation of hacksaw chips.

The sizes and shapes of hacksaw chips vary greatly, Figure 2.8 a-c. There are several factors in the hacksawing process which cause the variations in chip size.

(i) The variable thrust load applied during each stroke by hydraulic feed machines causes the depth of cut per tooth to vary during each stroke.

(ii) Hacksaw teeth vary in size, Appendix 1, thus a large tooth will remove more material than a small tooth.

(iii) The set of the teeth varies along the length of the blade. A tooth having a large set will remove more material than one with a smaller set.

(iv) Chip thickness varies from tooth to tooth due to variations in cutting edge radius.

(v) Due to the set of the teeth some teeth do not cut across the full width of the cutting edge, Figure 1.7 (9).

When studying hacksaw chips, it is therefore, impossible to know which tooth cut which chip, the undeformed chip thicknesses, or even whether the chips are broken or whole. Despite these limitations it is possible to glean some information by studying hacksaw chips.

2.3.1 Chip formation affected by the gullet

Some chips have been mounted in bakelite, sectioned and etched in 2% Nital solution, Figures 2.9 a-f. Consider Figure 2.9, a chip taken from a 10 TPI blade cutting a 50 mm broad mild steel workpiece on a hydraulic feed hacksaw machine. The bottom part of the chip is 3-4 times thicker than the top. This suggests that considerably more energy was required

to cut the bottom part of the chip than the top. The flow lines show that the shear plane angle has decreased towards the bottom of the chip. It is possible that this type of chip formation is caused by the gullet restricting the flow of the chip up the rake face. (Chapter Five).

Figures 2.9 b-d also show thickening at the base of the chip.

CHAPTER THREE

SINGLE TOOTH & GULLET TESTS AT SLOW CUTTING SPEEDS

The effect of gullet size and shape on blade performance appeared to be sufficiently important for a study of gullet size and shape to be initiated.

3.1 Test Objectives

A testing procedure was developed with three major objectives in mind:

(i) To determine the difference in cutting performance of 4, 6 and 10 TPI teeth-gullet combinations for various workpiece materials.

(ii) To determine the effect of length of cut on cutting performance for various workpiece materials.

(iii) To determine the effect of modifications to gullet shape and size cutting performance for various workpiece materials.

3.2 Testing & Instrumentation

In order to avoid the complexities of the hacksawing process, single teeth were tested on the same rig as was used by Sarwar (2) for testing the cutting performance of single point cutting tools.

A universal miller was used to provide the relative motion of the tool and workpiece. The workpiece was securely mounted on a flat reference plate which was bolted to a three force component dynamometer which in turn was secured to a ground steel plate, bolted on the milling machine. The dynamometer measured the cutting and thrust forces and its output signals were amplified and recorded on an X-Y plotter.

The tools used for this test were straight teeth taken from new all-hard HSS hacksaw blades. The geometry and dimensions of the teeth are shown in Figure 3.1, and for the purposes of this thesis will be referred to as the "standard" tooth/gullet geometries. Each tooth was viewed under a microscope and checked for uniformity of geometry, and the cutting edge radius was estimated using a shadow-graph projector. Teeth having cutting edge radii of 0.05 mm $\pm$ .01 mm were used. When under test, a tooth was secured in a holder, Figure 3.2, which was clamped to the headstock of the milling machine.

The height of the slot surface cut by the tool, was measured relative to the reference plate, using a DTI mounted on a bridge, Figure 3.3, before and after each cut. The difference in height gave the undeformed chip thickness. Readings were taken in

three places along the slot and an average value of undeformed chip thickness was calculated for each cut. The test went through three stages of development.

METHOD 1 Figure 3.4

The procedure for this method was:

(i) Set an undeformed chip thickness by raising the mill table.

(ii) Start the cut by traversing the table. The tool cut on the surface of the workpiece, not in a groove, so that the chip could be viewed as it formed.

(iii) An X-Y plotter recorded the cutting and thrust forces during the cut. The characteristics of the chip formation was recorded during the cut.

(iv) The depth of cut was measured before and after each cut in three places using a DTI, to determine an accurate value for the average undeformed chip thickness.

The limitation of this method was the imprecise nature of the recording of the chip formation. It was impossible to write down, in sufficient detail, the exact chip formation throughout the cut.

METHOD 2

The procedure for this method was the same as for Method 1, with the exception that instead of writing down how the chips formed, every cut was filmed using video equipment. An oblique view of the cutting tool was filmed so that both the front and one side of the chip could be seen at the same time.

Despite the vast improvement made by filming each cut, it was still difficult to relate a particular event on the film, such as the chip breaking, to the relevant part of the force trace. The need to relate chip formation to the cutting forces was particularly important owing to large variations occurring in the cutting forces for a single cut, at a constant undeformed chip thickness. Figure 3.5 shows a cutting force trace exhibiting considerable variation as the chip formed.

METHOD 3

This method was the same as Method 2, but with the addition of a storage oscilloscope and a second video camera. A diagram of the test set-up is shown in Figure 3.6 and photos of the instrumentation in Figure 3.7.

The storage oscilloscope recorded the same cutting and thrust forces as the X-Y plotter. The second

camera filmed the oscilloscope during each cut, and its picture was superimposed on that of the first camera giving a picture of the force traces and chip formation simultaneously on one screen.

This enabled a study of both chip formation and force variations to be made simultaneously.

3.3 Cutting Conditions & Tests

Machine Tool	Universal Milling Machine
Cutting speed	95 mm/min
Lubricant	None
Material	Mild Steel (0.17% C, 0.73% Mn, 0.24% Si, 0.06% S, 0.03% P, 0.20% Ni, 0.10% Cr, 0.06% Cu, 0.06% Mo, 0.01% Al).

Table 3.1 below, shows the length of workpieces cut by the various teeth tested.

TOOTH	LENGTH OF WORKPIECE (mm)
10 TPI	25
10 TPI* (Modified)	25
10 TPI	50
6 TPI	50
4 TPI	50

* The modified 10 TPI tooth, Figure 3.8, has an enlarged gullet.

3.4 Discussion of Results

The comprehensive set of tests covering a range of workpiece lengths and materials, and gullet shapes and sizes, was not carried out with this testing procedure, owing to problems relating to cutting speed and chip formation, see Section 3.4.3. Indeed all the results related to this testing procedure must be considered in the light of Section 3.4.3.

The maximum cutting forces developed by the 10 TPI teeth cutting 25 mm length of workpiece have been plotted against undeformed chip thickness, Figure 3.9. At undeformed chip thicknesses of less than

0.03 mm the two teeth perform the same. However at 0.037 mm there is a significant difference in cutting force. The force traces for the points A and B, Figure 3.10 show that, for the tooth in its new state there was a rapid rise in cutting force towards the end of the cut. This did not happen with the modified tooth, points C and D, Figure 3.11, nor did it happen when cutting at smaller undeformed chip thicknesses with the tooth in its new state. The rapid rise in cutting force, Figure 3.10 was caused by restriction of the chip flow by the gullet.

Figure 3.12 shows sketches of the chip formation at various stages during a cut in which restriction by the gullet occurred. These sketches have been made from the video film of the cut. (It was not possible to take still photographs from the video screen, because the video equipment used could not provide a still picture with good definition). The chip forms, initially, with a tight curl, Figure 3.12a and does not curl sharply again until the chip makes contact with the root, Figure 3.12b. At this stage in the chip formation the cutting forces started to rise rapidly. Because the chip cannot flow upwards it thickens at its base and continues to thicken until the end of the cut, Figure 3.12d. The rapid build-up in cutting forces occurs,

therefore, when the chip is restricted from flowing. The cuts made at small undeformed chip thickness values did not produce chips large enough for their flow to be restricted by the gullet and therefore the rapid increase in cutting forces did not occur. Cutting with the modified tooth, Figure 3.8, did not cause any rapid increase in cutting force because there was no gullet to restrict chip flow.

It is interesting to note that restriction of chip flow by the gullet occurs before the gullet is completely full of chip material. The area of the 10 TPI gullet profile was approximately 2 mm^2. To completely fill this gullet, an undeformed chip thickness of 0.08 mm would be needed, assuming a 25 mm length of cut. The force traces, Figure 3.10a and b, suggest that the chip flow is restricted when the gullet is approxmately 35% full of chip material. The specific cutting energy curve for the tool in its new state, Figure 3.13, shows the rise in average specific cutting energy as undeformed chip thickness increases past 0.03 mm.

Several other tests, cutting with 10 TPI teeth having restricting gullets, have shown the same characteristic force trace as in Figure 3.10. Two more sets of traces and sketches of the chip formation are shown in Figures 3.14 a and b and 3.15 a and b. The length of cut for these tests was 50 mm,

and as a result the undeformed chip thickness required to cause chip flow restriction (0.027 mm) was less than for the 25 mm length of cut.

3.4.1 Relevance of the results to hacksawing

The results of the above tests can be related directly to positive feed hacksawing operations. They show that if too high a feed is set on the machine, then very high cutting forces will be induced, possibly resulting in tooth and/or blade fracture.

The relevance of the above results to gravity and hydraulic feed hacksawing machines is not so direct. Feed is controlled by thrust force in these machines but in the simulation test the thrust force was controlled by the applied feed. The thrust force created by cutting in the simulation test had the same characteristic shape as the cutting force, when restriction of the chip flow occurred, Figure 3.10. On a hydraulic hacksaw, the rise in thrust force would partially or completely relieve the thrust force acting between the workpiece and the other teeth, thus reducing the blade's cutting performance.

Blade life may be reduced, due to tooth failure at the high cutting forces generated by the gullet restricting chip flow.

3.4.2 Comparison of 4, 6 and 10 TPI teeth

The performance of the 4, 6 and 10 TPI teeth cutting 50 mm length workpieces is shown in Figure 3.16. Lines of best fit have been drawn through the data points using linear regression. The 4 TPI tool performs better than the 6 TPI tool which in turn performs better than the 10 TPI tool. This trend is the same as for hacksaw blades, Figure 2.7.

3.4.3 Effects of slow cutting speed

At this stage it is necessary to report on a limitation in this simulation test which did not come to light, until after a great amount of time had been spent setting up and carrying out the test.

The cutting speed for this test was 95 mm/min. This is slow compared to that available on hacksaw machines, but was used to facilitate observation and filming of the chip formation. Hacksaws cut over a range of speeds, eg 0 to 30 m/min, during each stroke due to the crank action of the drive. However, most of the material is removed whilst the blade is moving at its fastest, because the thrust forces are highest during this time (9).

Cutting at such a slow speed in the simulation test produced a very rough surface finish, Figure 3.17, after the first 7-10 mm length of cut, which made

accurate measurement of undeformed chip thickness difficult. Also the backs of the chips had several transverse cracks, Figure 3.18, and the forces developed during the cuts were very uneven, Figure 3.5. The chips produced by the 4 to 6 TPI Teeth appeared to be very weak, frequently breaking when coming in contact with the gullet root. This was attributed to the cracks in the backs of the chips. A study of the microstructure of the chips was made to determine the size of the cracks. Some typical chips were taken from a 4 TPI tooth cutting on the simulation rig. They were mounted in bakelite, sectioned and etched using 2% Nital, Figure 3.19. The chips appear to be discontinuous in the photographs, however the sides of the chips, which cannot be seen in the central section shown, were continuous.

The chip formation bears a close similarity to that described by Chandiramani and Cook (12) in the section "Non-built-up-edge". They report that at low cutting speeds, below those at which built-up-edge occurs, a discontinuous chip is formed. The chip formation follows a cycle which is repeated throughout the cut. The first stage of the cycle is the chip sticking to the tool rake face due to high frictional forces. This causes the shear plane to lengthen, increases the chip thickness, and

increases the stresses around the tool tip.

In the second stage a crack, caused by the high stresses is formed in the chip at the tool tip. This crack propogates through the chip, breaking it. The broken part of the chip no longer applies a force to the workpiece, and therefore the forces, stresses, and shear plane length decrease.

In the third stage, the chip flows up the rake face until again the frictional forces increase to a level high enough for the chip to stick. The cycle then repeats itself. Figure 3.20 shows a diagram of the chip formation described above.

Furthermore the authors report (12) that at very low cutting speeds surface finish was very poor.

The simulation test did not produce a chip formation similar to that which it was designed to simulate. The number of cracks in the simulation test chips was far greater than those in hacksawing chips, Figures 2.8 and 2.9. The cracked chips being very weak, prevented any useful data being obtained when cutting with 4 and 6 TPI teeth, because when the gullet restricted chip flow the chips broke thus relieving the restriction. The data obtained from cutting with 10 TPI tools is however more reliable. The initial parts of the chips were free from cracks and therefore relatively strong, Figure 3.19. The

10 TPI gullet was small enough to restrict the flow of this inital part of the chip, which, being free from cracks did not break. The restriction was therefore maintained as the cut progressed, causing the chip to thicken and the cutting forces to increase.

A true picture of the effect of the gullet size on hacksawing performance could not be obtained on this simulation rig, because the chip formation was significantly dissimilar to that produced in hacksawing, Figure 3.19.

3.4.4 Examinations of video films

The use of the video films was found to be severely limited for the 4 and 6 TPI tools, because the cracks in the chips were only visible on the backs of the chips and therefore not in the view of the camera. Thus, rises and falls in the cutting forces could not be explained by reference to the video films.

However, for the 10 TPI tools the video film gave a good macro view of the chip restriction in the gullet.

CHAPTER FOUR

SINGLE TOOTH & GULLET TESTS AT HIGHER CUTTING SPEEDS

The test rig and procedure described below was developed to fulfil the objectives stated in Section 3.1 at realistic power hacksaw cutting speeds.

4.1 The Test Rig

A screw cutting lathe, Figure 4.1, was used to provide the relative motion between the workpiece and tooth. The workpiece holder, Figure 4.3, was held in the three jaw chuck and centred for rigidity. The tool was mounted in a holder, Figure 4.2, which was secured to a Kistler three force dynamometer platform, which in turn was bolted to the cross-slide of the lathe.

The toolholder, Figure 4.2, was designed to hold tools of the dimensions shown in Figure 3.1. The function of the two side pieces was to simulate the slot wall in hacksawing which prevents the chip from moving sideways out of the gullet whilst a tooth is cutting.

The workpiece and holder, Figures 4.3 and 4.4 were designed such that, by traversing at an appropriate screw feed, the tool would cut the workpiece once only per test cut. This was necessary because the gullet had to be cleared between each cut and each

chip collected and identified.

The holder has a large diameter for the following reasons:

(i) To keep the helix angle, at which the tool cuts to less than 1^{o}, ie to create orthogonal cutting conditions;

(ii) To simulate the flat slot bed produced in hacksawing; and

(iii) To maintain rigidity.

The workpiece is both simple and inexpensive to produce. The length of workpiece can be varied from 10-100 mm and any workpiece material can be tested. The locating pins provide accurate relocation of the workpiece if required.

The instrumentation used is shown in Figures 4.5a and b. The cutting and thrust force outputs from the Kistler charge amplifiers were fed into a digital storage oscilloscope. A hard copy of the force traces which had been stored by the oscilloscope, was taken by an X-Y plotter. (The oscilloscope was necessary as an intermediate data store, because the X-Y plotter's response time was too long to read data as each test cut was made). The analogue output from the oscilloscope was also amplified and fed through an A/D converter to an Apple microcomputer.

The microcomputer sampled the output from the oscilloscope 256 times per force trace, and from this data calculated and recorded the average and maximum cutting and thrust forces for each test cut. Using the Apple in this way is not only a time-saver, but also leads to greater accuracy in determining average and maximum cutting and thrust forces. (Section 4.4 comments on the data handling facilities of the Apple).

The cutting speed of a hacksaw blade varies throughout a stroke, owing to the reciprocating action of the mechanism. However, the speed of an individual tooth on a blade depends on its position on the blade and the breadth of the workpiece. For example, a tooth in contact with the workpiece at the beginning of a stroke will initially have a cutting speed of zero, it will then accelerate rapidly leaving the workpiece at a much higher cutting speed. However, a tooth cutting during the middle of a stroke will commence cutting at a high speed and will leave the workpiece at much the same speed. The difference between the entry and exit cutting speeds of a tooth also depends on the breadth of the workpiece. For the purposes of the single tooth tests a constant cutting speed (30 m/min) was used to simulate the cutting speed of the teeth in the mid-stroke region. (These teeth cut

more material than those at the beginning and end of the stroke (9) because the thrust loading is highest at mid-stroke and are therefore the most important teeth to investigate).

4.2 The Testing Procedure

1 The workpiece was clamped to the holder, and the tooth secured in the holder and adjusted to the centre height on the bar.

2 An appropriate screw cutting feed was set, so that the tooth would cut the workpiece once only per traverse.

3 A depth of cut was set by moving the cross-slide towards the workpiece.

4 The workpiece was set revolving at 30 m/min, and the saddle engaged with the screw feed, so that the tool traversed the workpiece taking a single cut.

5 During the cut the oscilloscope read, and stored the cutting and thrust forces.

6 The traverse and workpiece were stopped after each cut.

7 The chip was collected and identified.

8 The X-Y plotter took a hard copy of the cutting

and thrust forces for the cut, and the microcomputer calculated and recorded the average and maximum cutting and thrust forces.

9 Steps 3-8 were repeated for increasing undeformed chip thicknesses until restriction of the chip flow caused excessively large cutting and thrust forces.

10 Each chip was weighed to determine the amount of material removed per test cut.

11 The chip weights were typed into the microcomputer which calculated the volume of material in each chip and the undeformed chip thickness, and stored the data on disk for subsequent analysis.

4.3 Measurement of Undeformed Chip Thickness

Weighing the chips to determine the volume of material removed during each cut, was considered to be both sufficiently accurate and convenient for these tests. The undeformed chip thickness, UCT, is calculated by:

$$UCT = \frac{\text{Weight of chip}}{\text{Density of chip material}} \times \frac{1}{\text{Length of cut} \times \text{Width of tooth}}$$

Thus the average value of undeformed chip thickness is an average over the length and width of the cut.

The electronic balance used to weigh the chips, measured to 10 micro gms.

4.4 Data Handling

The tests produced several hundred chips all of which were examined often by comparison with one another. Each chip had to be identifiable with its force traces, cutting tool and workpiece.

Perspex display trays were made, Figure 4.6, having a matrix of flat-bottomed holes drilled in them. The chips were thus kept separate from one another, but could be compared easily.

The quantity of numerical data generated by the tests was also large (the weight of each chip, the undeformed chip thickness and related cutting forces, all had to be recorded for each test cut). The ease with which the Apple microcomputer can handle numerical data made storage, recall and manipulation of data very rapid. Storage was made on a floppy disk from which data can be retrieved within seconds. Repetitive calculations using the data were made rapidly using simple programs (Appendix 4). Graphs and tables of relevant data can be drawn and printed accurately by connecting the Apple to a suitable piece of hardware, eg a plotter or printer.

The author found that commercially produced software was often cumbersome to use, and inappropriate for the needs of this project. All the software was therefore written by the author (Appendix 4).

4.5 Tests Carried Out at Higher Cutting Speeds

4.5.1 Tools

The first tests were performed using standard tooth and gullet combinations from new 4, 6 and 10 TPI all-hard blades as described in Section 3.2 (Figure 3.1).

4.5.2 Workpiece materials

Three materials were tested.

(a) Aluminium (BS 1474 HE 30 TF)
(10% Cu, .5/12% Mg, .7/1.3% Si, 0.5% Fe
0.4/1.0% Mn, .2% Z, .25% Cr, 0.2% Ti)
66 HV

(b) Mild Steel
(0.17% C, 0.73% Mn, 0.24% Si, 0.06% S, 0.013% P,
0.20% Ni, 0.10% Cr, 0.06% Cu, 0.06% Mo, 0.012% Al)
218 HV

(c) Austenitic Stainless Steel EN58J
(0.064% C, 1.74% Mn, 0.53% Si, 0.009% S, 0.027% P,
10.01% Ni, 16.57% Cr, 2.23% Mo, 0.01% Ti)
200 HV

The length of workpiece that each tooth and gullet combination cut is shown in Table 4.1 below for each workpiece material.

Aluminium

Pitch of Tooth	4			6			10	
Length of workpiece (mm)	75	50	25	50	25	12	25	12

Mild Steel

Pitch of Tooth	4			6			10		
Length of workpiece (mm)	75	50	25	50	25	12	50	25	12

Stainless Steel

Pitch of Tooth	4			6			10	
Length of workpiece (mm)	75	50	25	50	25	12	25	12

4.6 The Improvements Caused by Testing at Higher Cutting Speeds

The chips produced by this testing procedure, Figure 4.10, were similar to those produced in power hacksawing, Figure 2.8, and more continuous than those produced at lower cutting speeds, Figure 3.19.

The cutting and thrust force traces were more consistent than those produced at lower cutting speeds. Compare Figures 4.11 and 3.5.

The surface finish of the slot bed, Figure 4.12, was similar to that produced in hacksawing and considerably better than the surface finish generated at lower cutting speeds, Figure 3.17.

4.7 Cutting Performance of Single Tooth Tools

The performance of metal-cutting tools is often stated in terms of specific cutting energy, which is the cutting energy required to remove a unit volume of material. However, in power hacksawing the metal removal rate is dependent more on thrust force than cutting force (1), Section 1.3.3. For this reason the performances of the single teeth have been measured by relating the thrust force to the amount of material removed. This has been done in two ways:

(i) by relating the average thrust force per unit width of tooth to the undeformed chip thickness; and

(ii) by relating the specific thrust force pressure to the undeformed chip thickness. (Specific thrust force pressure =

$$\frac{\text{Average Thrust Force}}{\text{Cross-sectional area of undeformed chip}}$$

The second performance criterion has the same units as the Thompson and Sarwar (1) performance criterion for power hacksaw blades.

The above performance criteria for single tools are best represented graphically (Figure 4.7). Comparisons of performance can be made between different tools, (Figure 4.8) and the variation in performance of a tool as length of cut increases can be compared (Figure 4.9). (The shape and nature of the curves is discussed in detail in Section 4.8.1)

4.8 Results & Discussion

4.8.1 Restriction of chip flow by the gullet

4.8.1.1 ALUMINIUM WORKPIECES

Figure 4.13 shows the performance of a 4 TPI tooth cutting a 75 mm wide Aluminium workpiece at various undeformed chip thicknesses. At low undeformed chip thicknesses, region 'A', Figure 4.13, the specific thrust pressure is high. In region 'B', the performance improves and in region 'C', the performance deteriorates. The tool performs poorly at low undeformed chip thicknesses because of "ploughing" forces (13, 14 and 15). Cutting performance improves as undeformed chip thickness increases, region 'B', because the ploughing forces become less significant as a factor of the total cutting and thrust forces. The performance continues to improve until the flow of the chip is restricted, as in region 'C', Figure 4.13.

The force traces relating to points X, Y and Z in Figure 4.13 are shown in Figure 4.14. The traces for points X and Y were even from the start of the cut to the end, however, the thrust forces for point Z, rose as the gullet restricted the chip flow.

The chips which relate to points X, Y and Z, Figure 4.13, are shown in Figure 4.15. The chips for points X and Y each had a consistent thickness. The chip for point Z, however, is considerably thicker at its base than at its tip, which suggests that the base of the chip was formed less efficiently than its tip. (See Figure 4.14c).

Figure 4.16 shows the same data as Figure 4.13 with the addition of the instantaneous performance of the tooth at the beginning and at the end of each cut in region C, Figure 4.13. This highlights the drop in performance caused by restriction of chip flow. The specific thrust pressure at the end of cut Z, Figure 4.16, is five times that at the beginning of the cut.

The chips collected showed that there were two ways in which the gullet restricted chip flow. Which form the chip took depended on the thickness of the chip, the height of the gullet and the curvature of the root. Figure 4.17 a, b, shows how a particular thickness of chip may be restricted in two diffeent

gullet sizes. The chip, Figure 4.17a was thin enough to curl around the root but the same thickness of chip was unable to curl around the smaller radius root, Figure 4.17b. In neither case was the gullet full of chip material when chip flow was restricted. How far a chip can flow without restriction will be important in further design considerations.

The relationship between undeformed chip thickness and the length of cut at which chip flow restriction occurred is shown in Figure 4.18, for 4, 6 and 10 TPI tooth geometries. The results show that the smaller gullets restrict chip flow at a shorter length of cut than the larger gullets.

An attempt to normalise the results of Figure 4.18 has been made by dividing the length of cut at which chip flow restriction took place by the height of the gullet, see Figure 4.19. Over the range of undeformed chip thicknesses tested, height is not the normalising factor, ie it is not solely the height of the gullet which determines when the chip will be restricted. The size of the gullet radius affects how far a chip can flow before it is restricted as well as the height of the gullet, Figure 4.17.

4.8.1.2 MILD STEEL WORKPIECES

The performance of a 4 TPI tooth cutting 75 mm of mild steel is shown in Figure 4.20. The curve shows that performance improves as undeformed chip thickness increases despite the gullet restricting chip flow at the higher undeformed chip thickness (see Figure 4.21 for the force trace and chip for point X on Figure 4.20). However, the difference between the specific thrust pressure at the beginning of the cut, and the average specific thrust pressure, indicates that the tooth's performance is severely hampered by the gullet restricting chip flow.

4.8.1.3 STAINLESS STEEL WORKPIECES

When cutting stainless steel gullet restriction of chip flow had the same characteristic effect on cutting performance as it did when cutting the aluminium and mild steel workpieces, Sections 4.6.1.1 and 4.6.1.2. (See Figures 4.22 and 4.24).

4.8.2 The effect of length of workpiece on cutting performance

The effect of length of workpiece (ie length of cut) on cutting performance showed the same trend for all the materials tested.

As length of workpiece increased the cutting performance fell, Figures 4.25 - 4.27, which is the same trend as shown in the hacksawing process, Figures 2.1 and 2.3, Chapter 2.

Performance is better for a shorter workpiece, because a larger undeformed chip thickness is required to cause chip flow restriction in the gullet. In other words, the efficient cutting region of the specific thrust force v undeformed chip thickness curve, extends further for a shorter workpiece than a longer workpiece, Figure 4.25a.

In some cases the workpiece length was too great for a tooth to cut efficiently at any undeformed chip thickness. For example, in Figure 4.29a, the 10 TPI tooth performs very poorly at all undeformed chip thicknesses tested. Also in Figure 4.29b, the 6 TPI tooth does not improve in performance. In both cases the tools are either cutting inefficiently at very low undeformed chip thicknesses, or inefficiently with the gullet restricting chip flow at higher undeformed chip thicknesses.

4.8.3 The effect of gullet size on performance

Figures 4.28 - 4.30 show the performance of 4, 6 and 10 TPI teeth cutting various workpiece lengths. For the three materials tested, the 4 TPI teeth

performed better than the 6 TPI teeth, and these in turn performed better than the 10 TPI teeth. This is because the smaller gullet restricts chip flow at lower undeformed chip thicknesses than larger gullets.

It is of interest to note that a low undeformed chip thicknesses, when there is no restriction to chip flow, all the teeth performed much the same as each other.

4.9 Summary of Results

These tests have confirmed that:

(a) the gullet can restrict chip flow, and when this occurs specific thrust pressure increases, and cutting efficiency falls.

(b) for a particular undeformed chip thickness, the length of cut required to cause restriction of chip flow will be shorter for a small gullet than a large gullet of the same geometry.

(c) for a particular length of cut, the range of undeformed chip thicknesses, and therefore thrust loads, at which a tooth can cut efficiently varies according to the gullet size: the smaller the gullet the smaller the efficient cutting range.

The above summary of results corroborates the results discussed in Chapter 2, which were gained by testing complete blades.

The tests reported on in this chapter have met objectives (i) and (ii) as stated in Section 3.1. The tests which were carried out to meet the third objective are reported on in Chapter Seven.

CHAPTER FIVE

THEORETICAL MODEL OF THE INEFFICIENT CHIP FORMATION CAUSED BY RESTRICTION IN THE TOOTH GULLET

Previously the author has claimed that the thickening in the chip and the rise in the cutting and thrust forces is due to the chip flow in the gullet being restricted. In this chapter a simple analytical model is presented, showing why the chip thickens and why the rate of increase in cutting force is so rapid when the chip flow is restricted. The model is not presented for the purpose of accurate prediction of cutting force and chip thickness, but rather for the purpose of highlighting the inefficient chip formation which occurs when the chip flow is restricted.

5.1 The Model

When the chip is no longer able to flow over the tooth face, due to it being obstructed by the tooth gullet, shearing is considered to occur along two planes OX and OA as shown in Figure 5.1.

Measurements of chip thickness show that a typical value of chip thickness ratio, $\frac{t}{tc}$, is 0.2, and this value has been used in the model examined here. This fixes the length of shear plane OX as a multiple of undeformed chip thickness, t. When the inclination of the secondary shear plane is selected, its length OA is also determined relative to t.

Let the velocity of the incoming work material, relative to the hacksaw tooth, ie the cutting velocity, be V_1. The shear plane OX is assumed to be straight, and the relative velocity of material either side of this plane is Vox. Similarly the relative velocity on either side of the secondary shear plane is Voa. Both Vox and Voa are determined as multiples of V_1 from the velocity diagram, Figure 5.1.

It is assumed that the shear flow stress, k, is the same on the two shear planes. Then the principle that rate of work input equals rate of energy absorption gives cutting force, F_v, from the equation:

$$F_v \cdot V_1 = w.k\ (OX.Vox + OA.Voa)$$

where w is the width of the tool

The objective is to apply an iterative upper bound technique (16). It is assumed that the secondary shear plane takes up the position in which the cutting force is a minimum.

Figure 5.2 shows alternative inclinations OA, OB and OC. It should be noted that when the inclination is changed, the relative velocity for the secondary shear plane is changed and also the relative velocity for the primary plane OX.

Assuming unit values of t and V_1 values measured from the diagram give:

$$\frac{Fv}{t.w.k} = (OX.Vox + OA.Voa) = 8.48$$

$$\text{or} \quad = (OX.Vox + OB.Vob) = 8.34$$

$$\text{or} \quad = (OX.Vox + OC.Voc) = 8.44$$

This suggests that the appropriate secondary shear plane is OB. This plane gives minimum work per unit volume of material removed.

The validity of this prediction depends on the general suitability of the simple model adopted.

After the tool has travelled a small distance, in this case 3t, with shear taking place along OX and OB, the wedge OXD is formed, Figure 5.3. For the sake of this analysis it is assumed that shearing along OB causes a thin wedge of material either side of OB to strain harden. The increase in shear stress of this wedge prevents shear from continuing along OB and thus the secondary shear plane alters position, for example to OA or OC, Figure 5.3. A value of 6^{o} has been taken for the wedge angle AOC β because this provides an acceptable value of increase in shear stress due to strain hardening as shown below.

The work used to slip a distance BD over the area per unit width of OB.1 is:

$$k.OB.1.BD \text{ (Nm)} \quad \ldots \quad 5.2$$

For homogeneous strain γ in the volume of the wedge, V, work done is:

$$k.\gamma.V \text{ (Nm)} \quad \ldots \quad 5.3$$

However:

$$V = \frac{\beta}{2} . OB^2 .1 \quad \ldots \quad 5.4$$

Therefore combining 5.2, 5.3 and 5.4:

$$k.OB.BD = k . \gamma . \frac{\beta}{2} . OB^2$$

Thus:

$$\gamma = \frac{2}{\beta} . \frac{BD}{OB}$$

From Figure 5.3, OB = 0.96 units;

BD = 0.06 units; and

$\beta = 6^o = 0.105$ radians

Therefore:

$$\gamma = 1.19 \text{ m.m}^{-1}$$

The slopes of the compression test results, Figure 5.7, show that a shear strain of 1.19 would increase the shear stress of the mild steel by about 50 N/mm^2 and the aluminium by about 40 N/mm^2.

Now considering the strain energy required to shear the chip along OA, OB and OC, Figure 5.3, for the mild steel and assuming that the material along OB has work hardened:

$$k\ (OX.Vox + OA.Voa) = 8.8k\ Nms^{-1}$$

$$k\ (OX.Vox) + (k + 50)(OB.Vob) = 8.55k + 112\ Nms^{-1}$$

$$k\ (OX.Vox + OC.Voc) = 8.6k\ Nms^{-1}$$

Thus the chip shears along OC for another 3 units of travel; again the chip material is assumed to work harden in a wedge around OC, and again the secondary shear plane deviates. Continuing the iterative analysis it is found that the secondary shear plane deviates from one side of the original secondary shear plane to the other, which results in a chip form similar to that created in practical tests when chip flow was restricted by the gullet (see Figures 5.4 and 5.5).

5.2 Estimation of Shear Stress (k)

The shear stress used in the model is assumed to have the same value on both the shear planes. Three methods were used to obtain a value of k.

5.2.1 Estimation of shear stress using cutting & thrust force data

Cutting data, ie cutting and thrust forces,

undeformed chip thicknesses and chip thicknesses, was taken from tests carried out using a hacksaw tooth having no restricting gullet, cutting on the test rig described in Chapter 4. The geometrical relationship of the elements of cutting data is shown in Figure 5.6 (17) for zero rake angle. Thus the shear force (Fs), along the primary shear plane is:

$$Fs = R.Eos\ (\phi + \beta)$$

Shear stress, k, is then found by:

$$k = \frac{Fs}{A}$$

where A is the area of the shear plane. Values of k obtained by this method were for:

mild steel 600 to 700 N/mm^2

AND

aluminium 300 to 450 N/mm^2

5.2.2 Estimation of shear stress from hardness tests

Vickers hardness tests were made on mild steel chips cut by hacksaw teeth, giving a range from 335 to 400 HV which, from tables (18) gives a range from 540 to 650 N/mm^2 for shear stress.

5.2.3 Estimation of shear stress from compression tests

Compression tests were carried out on the mild steel and aluminium workpieces. The specimens were approximately 6 mm diameter and 6 mm high. The height of the specimen was measured, after each strain increment, with the load relieved. Lubrication was applied to both the specimen and the plattens before each strain increment (17, pp 80). Figure 5.7 shows the results obtained, normalised to give equivalent shear stress.

The values of shear stress obtained from the cutting data and those obtained from the hardness tests appear to be verified by the compression test results. At high strains, 2-3, the mild steel has a shear stress of around 600 N/mm^2 and the aluminium has a shear stress of around 300 N/mm^2.

5.3 The Correlation between the Model and Empirical Data

5.3.1 Chip shape

The modelled chip shape thickens at its base the further the tooth travels. This simulates the chip formation which was observed during the single tooth tests, Section 3.4, and the shape of chips formed during hacksawing, Section 2.3.1, and by the simulation tests, Section 4.6.

5.3.2 Cutting force

The cutting forces predicted by the model show good correlation in both magnitude and rate of increase with practical results taken from the simulation tests, Chapter Four. Figure 5.8 shows both experimental and theoretical results.

The prediction has not been taken further than 3 mm, of tooth travel after the chip flow was restricted. The model assumes that when the chip flow is restricted the chip does not flow up the rake face any further. In practice, however, it appears that the chip does move up the rake face when the forces, increased by the inefficient chip formation, reach a high enough level.

Slipping up the rake face relieves the cutting force to a greater or lesser degree and the chip sticks again. The model is unable to predict when the chip will slip or by how much and can therefore only apply to a few millimetres of tooth travel.

The chip and force trace, Figure 5.9, show that chip flow has been restricted five times, the chip slipping up the rake face after each of the first four restrictions thus relieving the cutting force. The distance that the chip slips determines by how much the forces will be relieved.

CHAPTER SIX

PREDICTION OF SAWING TIME FROM SINGLE TOOTH & GULLET DATA

In Chapter Four, the performances of single teeth are measured in terms of specific thrust pressure. In this chapter an attempt is made, using data from the single point tooth tests, to predict the number of strokes a hacksaw blade will take to cut through a particular size of workpiece on a particular thrust force setting. The single point cutting data will be used in the form shown in Figure 6.1 from which can be read the expected undeformed chip thickness for a particular thrust load when cutting a 25 mm wide mild steel workpiece with a 4 TPI tooth. (The 4 TPI tooth having the dimensions shown in figure 3.1). A performance criterion based on the number of strokes to cut through a workpiece would be of considerable practical use.

6.1 Theory

As described in Section 1.1, the application of thrust force by a hydraulic hacksaw machine varies along the length of the stroke. Figure 6.2 shows a typical thrust force trace for the Kasto machine used to test the performance of blades as reported in Section 1.3.3. Using this trace the instantaneous thrust force applied to each tooth of a hacksaw blade in contact with the workpiece is given by:

$$Ft_i = \frac{FT_i}{N_c . t}$$

Therefore:

$$Ft_i = \frac{FT_i}{(B/P) . t} \quad \ldots \quad 6.1$$

Where:

Ft_i is the Instantaneous thrust force per tooth per unit thickness of tooth;

FT_i is the Instantaneous applied thrust force;

N_c is the Number of teeth in contact;

B is the Breadth of workpiece;

P is the Pitch of the teeth;

and t is the thickness of the tooth.

The instantaneous value of undeformed chip thickness (d_i) which is caused by Ft_i can be read off from the single tooth data, Figure 6.1.

The volume of material removed per stroke (V_s) can be calculated thus:

$$V_s = \sum_{i=o}^{i=S} (d_i \times Nc \times t \times d)$$

$$V_s = Nc.t.d \sum_{i=o}^{i=S} d_i$$

where S is the length of the stroke/distance between i and i + 1.

and d is the distance travelled by the blade between the interval i and i+1, Figure 6.2.

The number of strokes to cut through a rectangular workpiece N_s is found as follows:

$$N_s = \frac{V}{V_s}$$

Therefore:

$$N_s = \frac{D.B.w}{V_s}$$

where V is the Volume of material removed from a saw slot;
D is the depth of the workpiece; and
w is the width of the slot.

To carry out this analysis the single tooth data must be collected using:

(a) the same tooth/gullet geometry as on the hacksaw blade;
(b) the same workpiece material as used in the hacksawing; and
(c) the same length of cut as the breadth of the workpiece used in the hacksawing.

6.2 Predicted Hacksawing Rates

Table 6.1 shows that predicted and actual hacksawing rates were very close for the narrower workpieces.

However for wider workpieces, Table 6.1, the predicted rates were lower than the actual rates. This is due to the estimation of Ft_i, the thrust force per tooth per unit width of tooth (equation 6.1) being inaccurate when the workpiece width is wide.

When cutting wide workpieces the calculated value of Nc is large, giving a low value of Fti and di. This suggests that all the teeth are cutting at a low inefficient undeformed chip thickness. However in the hacksawing process some teeth are larger than others, and therefore cut at a greater undeformed chip thickness than others. High-speed film of a hacksaw cutting, Appendix *2*, has shown that some teeth cut considerably more material than others, indeed some teeth do not appear to remove any material.

In order to use this model for predicting cutting rates on wide workpieces therefore, a value of number of teeth in contact must be assumed. This area of work needs further investigation, but the author decided that work in other areas would prove more profitable.

However, the predicted results from this model, show that the simulation tests do provide data which is relevant to hacksawing.

Table 6.1.

TPI	Theoretical No. of strokes.	Experimental No.of strokes.	Machine Setting.	Workpiece Dimensions(mm) Width	Depth
ALUMINIUM, WORKPIECE.					
4	26	31	3.5	25	20
4	29	40	3	25	20
4	41	51	2	25	20
6	28	55	3.5	25	20
6	34	61	3	25	20
6	63	90	2	25	20
4	72	88	3	50	25
4	128	113	2	50	25
6	238	266	2	50	25
6	12	13	3.5	12	20
6	18	25	2	12	20
10	15	19	3.5	12	20
10	23	35	2.5	12	20
MILD STEEL, WORKPIECE.					
4	34	45	3.5	25	25
4	82	76	2.5	25	25
4	113	103	2	25	25
6	63	54	3.5	25	25
6	90	80	2.5	25	25
6	125	113	2	25	25
10	165	90	3	25	25
6	31	25	3	12	25
10	24	30	3	12	25
10	35	37	2.5	12	25

Theoretical and experimental no. of strokes to saw through rectangular cross-section workpieces at various thrust load settings.

6.3 Undeformed Chip Thickness in Hacksawing

An important point arose from the calculations involved in predicting cutting time as regards the range of undeformed chip thicknesses which occur in hacksawing. Thompson (4) has suggested that hacksaw blades cut inefficiently because the average undeformed chip thickness per tooth is very small (0.002 - 0.030 mm). However relating typical applied thrust loads (Figure 6.2) to the single tooth data (Figure 6.1) has shown that undeformed chip thicknesses of 0.04 - 0.08 mm occur. Furthermore most of the material removed by a hacksaw blade is removed at this range of undeformed chip thickness.

CHAPTER SEVEN

THE EFFECT OF TOOTH AND GULLET GEOMETRY ON THE PERFORMANCE OF HACKSAW BLADES

The experimental work of Chapter Four has conclusively shown that increased tooth pitch improves cutting performance of the standard hacksaw teeth, because the gullet size is increased. However, it was still to be determined whether performance could be improved by altering the gullet shape while the pitch remained the same.

The experimental work reported on in this chapter was carried out to determine whether tooth/gullet performance could be improved:

(a) by improving the chip formation mechanism, eg by increasing the nominal rake angle, (see Section 7.1); and

(b) by reducing the restriction to chip flow imposed by the gullet (see Section 7.2).

(The Sections 7.1 and 7.2 each contain an introduction, details of experimental work and a discussion of the results obtained).

7.1 Improving Tooth/Gullet Performance by Altering the Nominal Rake Angle

In section 1.4.1 it has been suggested that nominal rake angle has no effect on cutting performance if the cutting edge radius to undeformed chip thickness ratio is large, because the effective rake angle is negative. The results of the tests carried out by Sarwar & Hales (7) appeared to uphold this argument. However, the relevance of the above tests to power hacksawing is in doubt because:

(a) the cutting speed (95 mm/min) was much slower than in power hacksawing;

(b) the ratio of undeformed chip thickness to cutting edge radius was kept less than unity, which the author has shown is dissimilar to hacksawing (see section 6.3); and

(c) the simulation tools were considerably larger than hacksaw teeth, which resulted in dimensional inconsistencies.

The effect of nominal rake angle on the cutting performance of hacksaw teeth when cutting at realistic speeds and undeformed chip thicknesses, therefore, required further investigation. The author devised two tests, the first of which tested hacksaw tooth performance at nominal rake angles of 0^{o} and 11^{o} when there was no gullet to restrict chip

flow. The second experiment tested hacksaw tooth performance at nominal rake angles of 0^{o} and 10^{o} when chip flow was restricted by a standard 4 TPI gullet.

The hacksaw teeth used in the first test are shown in Figure 7.1 a and b. The tooth in Figure 7.1a is a standard 4 TPI tooth having a 0^{o} rake angle with an enlarged gullet which did not affect chip flow. This tooth, Figure 7.1a, was tested using the rig and procedure described in Chapter Four, cutting a 50 mm long mild steel workpiece cutting at a range of undeformed chip thicknesses (0.01 - 0.08 mm). The rake angle of the tooth was then altered by grinding down the back of the tooth shank, Figure 7.1b. When replaced in the test rig the tooth was thus presented to the workpiece with a nominal rake angle of 11^{o}. It should be noted that altering the rake angle by this method does not alter the cutting edge radius, or the rake face of the tooth. The zero rake angle hacksaw tooth/gullet used in the second test is shown in Figure 7.2a. It was a standard 4 TPI tooth and was tested cutting a 50 mm long mild steel workpiece at a range of undeformed chip thicknesses (0.01 - 0.094 mm). The rake angle of the tooth was then altered to 10^{o} (Figure 7.2b) by the method described above and retested.

The results of the two tests described above are shown in Figure 7.3 and 7.4. In the first test, when chip flow was not restricted by the gullet, the increase in rake angle caused an improvement in cutting performance. Thus it was concluded that nominal rake angle does affect the chip formation mechanism of hacksaw teeth. The results of the second test also showed that performance was improved by increasing the rake angle. Cutting performance was improved not only as a result of improved chip formation at the cutting edge, but also as a result of the restriction of chip flow being reduced. The standard 0^{o} rake angle tooth effectively restricted chip flow at 0.055 mm undeformed chip thickness, but the 10^{o} rake angle tooth did not restrict chip flow until the undeformed chip thickness reached 0.074 mm. The reason for this was that increasing the rake angle increased the chip thickness ratio; ie the chips were more slender than those produced using smaller rake angles, and thus were able to curl further round the gullet.

Despite the improvement in cutting performance caused by increasing the rake angle, the hacksaw tooth, Figure 7.1b, did not cut as efficiently as a sharp lathe tool would be expected to cut. Figure 7.5 shows the specific cutting energy versus

undeformed chip thickness curves for the hacksaw teeth, Figures 7.1a and 7.1b, cutting mild steel at 30 m/min. The lowest value of specific cutting energy for the 11^{o} rake angle tool is 3 kN/mm^2. When cutting mild steel with a sharp lathe tool at 30 m/min, the specific cutting energy would not be expected to exceed 2 kN/mm^2 at 0.08 mm undeformed chip thickness (17). The difference in performance is due to the bluntness of the tooth (7,20); it had a cutting edge of radius of 0.04 - 0.05 mm which compared to that of a sharp tool, 0.008 mm, is large.

7.2 Improving the Performance of a 4 TPI Tooth/Gullet by Reducing the Restriction to Chip Flow Imposed by the Gullet

It was evident from the work reported on in Chapters Three and Four that one method of reducing the restriciton to chip flow was to enlarge the gullet. However, there is obviously a practical limit to the size of the gullet, imposed by the strength of the tooth. Appendix 2 contains a theoretical analysis of tooth strength, developed by the author, from which it is possible to determine whether a particular tooth shape will withstand the applied cutting forces.

Three 4 TPI tooth/gullet geometries were designed by the author, see Figures 7.6a and 7.6b and 7.7. The

gullet sizes of these teeth are larger than those of the standard 4 TPI tooth. The increase in size was obtained:

1 by heightening the gullet root;
2 by increasing the rake angle; and
3 by reducing the clearance angle and shortening the flank of the tooth.

The teeth in Figures 7.6a and 7.6b had 10^{o} rake angles, and single root radii of 1.25 and 1.75 mm respectively. The tooth in Figure 7.7 also had a 10^{o} rake angle, but had three radii in the root. All the teeth were tested using the rig described in Chapter Four cutting 50 mm mild steel workpieces over a range of undeformed chip thicknesses (0.01 - 0.09 mm) at a cutting speed of 30 m/min.

7.2.1 Results and discussion

Each of the three teeth performed better than the standard 4 TPI tooth and better than the tooth, Figure 7.2b, which had the standard 4 TPI shape and a 10^{o} rake angle (see Figures 7.8a and 7.8b). thus it was clearly shown that tooth/gullet performance can be improved by altering gullet geometry in such a manner as to reduce the restriction to chip flow.

An important result of the tests on the single root radius teeth was that the chips possessed a small

amount of elastic recoil which prevented them from falling out of the gullet, see Figure 7.9. Chip ejection at the end of the stroke is essential for power hacksawing to be efficient. If a chip remains in a gullet of a hacksaw blade from one stroke to the next, then the effective size of the gullet is reduced which has a detrimental effect on the performance of the blade. Therefore, although the teeth in Figures 7.6a and 7.6b cut efficiently on the single-tooth test rig, a hacksaw blade having that tooth/gullet geometry would perform inefficiently.

A further interesting result of the above tests was that the chips curled to the same radius as that of the root, which suggested that the curl of the chip could be controlled by the shape of the gullet. Figure 7.10 shows a mild steel chip which was formed by a 4 TPI tooth having an 11^{o} rake angle with no restricting gullet to affect the curl of the chip. The natural chip curl was much larger than the root radius of any of the standard gullets. Therefore, it can be presumed that all the standard gullets affect the chip curl. If a gullet could be designed which curled the chip tightly, then more chip material would be accommodated by the gullet before restriction of chip flow occurred, which would result in more efficient metal removal by the tooth.

The tooth in Figure 7.7 had three radii in the root, the first of which was 1.2 mm, the second 1.7 mm and the third 2.9 mm. The purpose of the two small radii was to curl the chip tightly, thus producing a compact chip form. The third radius was made large to provide clearance for the chip to fall out of the gullet. The chips, Figures 7.11a and 7.11b, were produced by this tooth cutting a 50 mm long mild steel workpiece. The chip, Figure 7.11a, has curled tightly and its shape appears to have been controlled by the two smaller root radii. However, the thicker chip, Figure 7.10b, has not curled tightly and its final radius of curl is larger than the two smaller root radii. The amount of control over chip curl which can be obtained by altering the root radius/radii of a hacksaw gullet, was thus shown to be dependent on the thickness of the chip.

The tooth/gullet, Figure 7.7, also performed better than the standard 4 TPI tooth/gullet when cutting 75 mm long mild steel workpieces, and when cutting 25 and 50 mm long aluminium workpieces, see Figures 7.12 and 7.13. Although the new tooth/gullet, Figure 7.7, is an improvement over the standard, it does not follow that this is the best tooth/gullet geometry that could be produced. Further tests are, therefore, required to determine the effect of further tooth/gullet geometry modifications.

CHAPTER EIGHT

CONCLUSIONS AND FURTHER WORK

Introduction

At the initiation of the work reported on in this thesis, the state of knowledge as regards the effect of tooth geometry on hacksaw blade performance was as follows. Thompson and Sarwar had shown (1,2) that blades with large pitches cut faster than blades with small pitches. Also it had been shown (1,2) that a hacksaw blade cut faster through a narrow workpiece than a wider workpiece. In order to explain why the above phenomena occurred, Thompson (4) produced a mathematical model showing that tooth pitch directly affected the performance of a hacksaw blade. However, the validity of the model was unconvincing (see Chapter Two). Furthermore, Thompson (10) claimed that gullet shape had a negligible effect on blade cutting performance, although no experimental evidence was provided to substantiate this claim.

Thompson and Sarwar (5) had also concluded from an analysis of their experimental work, that hacksaw teeth were blunt cutting tools because their cutting edge radii were larger than the "average undeformed chip thickness". Sarwar (2) went on to show that blunt cutting tools had a chip formation mechanism which was significantly less efficient than that of a sharp cutting tool.

The following conclusions drawn from the work in this thesis are hoped to broaden the understanding of why the performances of different hacksaw blades vary, and how this understanding can be used to improve the performance of hacksaw blades.

8.1 Conclusions

(i) Pitch is not a parameter which directly affects the performance of a hacksaw blade. A change in pitch only influences hacksaw blade performance if it is accompanied by a change in gullet size and/or geometry (see Chapter Two).

(ii) Both the size and shape of the gullet significantly affect the performance of power hacksaw blades (see Chapter Two).

(iii) Experimental work using single hacksaw teeth has shown that, when cutting mild steel at low undeformed chip thicknesses (less than 0.2 mm), the performances of the standard 4, 6 and 10 TPI teeth were the same. However, as undeformed chip thickness increased, the 4 TPI cut more efficiently than the 6 TPI tooth which, in turn, cut more efficiently than the 10 TPI tooth. Thus, it can be concluded that the performances of individual teeth of

different gullet size vary for identical cutting conditions. (See Chapters 3 & 4).

(iv) The performance of a single hacksaw tooth decreases as length of cut increases, when cutting mild steel, aluminium and stainless steel. (See Chapter 4).

(v) The effects stated in conclusions (iii) and (iv) occur because the gullets of hacksaw teeth restrict the flow of the chips and, when this restriction occurs, the chip formation mechanism alters, becoming continually less efficient in terms of specific cutting energy and specific thrust pressure.

(vi) Using the upper-bound technique, a theoretical model has been developed of the chip formation process after the chip has been restricted from flowing. The model shows that the chip formation mechanism alters when restriction occurs causing a continual increase in the shear plane length and the cutting and thrust forces as the cut progresses. The model highlights the extremely inefficient metal removal mechanism caused by restricting chip flow. (See Chapter 5).

(vii) Restriction of chip flow has been shown to occur before the gullet is completely full of chip material. Typically, chip material filled less than one third of the gullet when the chip flow was restricted. Therefore, the volume of the gullet must be at least three to four times larger than the volume of chip material which it has to accommodate. (See Chapters 3 & 4).

(viii) A mathematical analysis of the empirical data collected from the single tooth tests, and power hacksaw blade tests, has enabled hacksawing rates to be predicted from the performance of a single tooth. Thus, in order to test a new tooth/gullet design, it is not necessary to produce a complete blade; it is only necessary to test a small number of single teeth.

The analysis only predicts the sawing rates of blades in an unworn state.

(ix) Experimental work has shown that the performance of a hacksaw tooth and gullet combination can be improved by altering the tooth and gullet geometry but without altering pitch. Increasing the nominal rake angle improved tooth/gullet performance

despite the cutting edge radius being large compared to the undeformed chip thickness. Also enlarging the root radius improved tooth/gullet performance owing to the restriction of chip flow being reduced. (See Chapter 7).

8.2 Suggestions for Further Work

8.2.1 Power hacksaw blades

The performance of other tooth/gullet geometries should be investigated on the single-tooth-test-rig. The data collected could be used to determine the optimum tooth/gullet a blade should have to cut a particular workpiece size and material (see also 8.2.2). The scale of these investigations would be immense, but the information could also be related to bandsaw and broach tooth/gullet geometry.

8.2.2 Wear tests

The single-tooth-test-rig should be used to investigate the performance of various hacksaw tooth/gullet geometries at various stages of wear. The overall performance of a hacksaw blade, as with other cutting tools, is largely dependent on its wear rate.

8.2.3 Chipbreaking

Methods of chipbreaking in hacksaw gullets should be investigated as a means for reducing restriction of chip flow in the gullet. Breaking hacksaw chips into smaller pieces would enable more chip material to be accommodated in the gullet before restriction of chip flow occurred and hence performance would be improved.

8.2.4 Removal of chips from the gullet and saw slot

Chips which remain in the gullet of a hacksaw tooth effectively reduce the size of the gullet and thus reduce the performance of the blade. Some chips also fall onto the bed of the saw slot, during the return stroke, and thus produce a barrier between the teeth and the workpiece on the subsequent stroke. Mechanisms could be designed to remove chips both from the gullet and slot bed.

REFERENCES

1 "Power Hacksawing", P J Thompson & M Sarwar. Proceedings of the 15th International Machine Tool Design and Research Conference, Macmillan Press Ltd, 1975, p 217.

2 "The mechanics of power hacksawing and the cutting action of blunt tools", M Sarwar, PhD Thesis, 1982.

3 "An investigation into factors influencing the wear rate of power hacksaw blades using dimensional analysis - Blade wear testing", P J Thompson & R W Taylor, 16th MTDR Conference, 1976.

4 "A theoretical study of the cutting action of power hacksaw blades", P J Thompson, Int. J. Mach Tool Des. Res., Vol 14, pp 199-209, Pergammon Press, 1974.

5 "Cutting action of blunt tools", M Sarwar & P J Thompson, MTDR Conference, Manchester, Pergammon Press, 1981, pp 292-304.

6 "Simulation of the cutting action of a single hacksaw blade tooth", The Production Engineer, June 1974, pp 175.

7 "The effect of tooth geometry on blade performance in power hacksawing", M Sarwar & W Hales, Proceedings of first conference Irish Manufacturing Committee, 1984, Dublin, pp 85.

8 "An analysis of the lateral displacement of a power hacksaw blade, and its influence on the quality of the cut", P J Thompson & R W Taylor, Int. J. Mach. Tool Des. Res., Vol 16, pp 51-70, Pergammon Press, 1976.

9 "Wear and wear mechanisms during power hacksawing", S Soderberg et al, Fagersta, Sweden, Technical Bulletin.

10 "Factors influencing the sawing rate of hard ductile metals during power hacksaw and bandsaw operations", P J Thompson, Metals Technology, October, 1974, pp 437.

11 "Metallurgical appraisal of wear mechanisms and processes on high speed steel cutting tools", P K Wright & E M Trent, Metals Technology, January 1974.

12 "Investigations on the nature of surface finish and its variations with cutting speed", K L Chandiramani & N H Cook, Transactions of the ASME, May 1964, Journal of Engineering for Industry, May 1964, pp 134 - 140.

13 "New developments in the thery of the metal cutting process", Part 1, "The ploughing process in metal cutting", P Albrecht, Trans. ASME J. Eng. for Industry, November 1960, pp 348-358.

14 "Fundamental researches on metal cutting. A new analysis of cutting force", M Masuku, Trans. Soc. of Mech. Engrs., (Japan), V19, 1953, pp 32-39.

15 "Force measurement during cutting tes s with single point tools simulating the action of a single abrasive grit", C Rubenstein, F K Grozman, F Koenigsberger, Science and Technology of Industrial Diamonds, Ed John Burles, International Industrial Diamond Conference, September 1966.

16 "Plasticity for mechanical engineers", W Johnson & P Mellor, Van Nostrand Press, pp 289-293.

17 "Fundamentals of metal machining", G Boothroyd, Arnold, 1965, pp 22.

18 "Materials and Processes in Manufacturing", 4th Ed E Paul de Garmo, Collier Macmillan, pp 42-43, 1969.

19 "Present knowledge of chip control", W Kluft, W König et al, Annals of the CIRP, Vol 28/2/79, pp 441-445.

20 "Metal cutting mechanics", N N Zorev, Pergammon Press.

BIBLIOGRAPHY

1 Emerson C, "How to cut-off metal", American Machinist Special Report, pp 428, 1956.

2 Anderson R A, "Band machining and friction sawing", I. Mech. E. Proc. Conf. Tech. of Eng. Manufacture, 1958.

3 Remmerswaal J L, Mathysen M J C, "Economics of the cutting-off of metals", Microtecnic, 1961, 15(4), August, pp 140-150.

4 Nelson R E, "Bandsawing or hacksawing?", Am. Mach., Vol 109, No 24, November 22, 1965, pp 90-93.

5 "Sawing to blueprint tolerances", Machine and Tool Blue Book, Vol 60, No 2, February 1965, pp 98-102.

6 "Pushbutton bandsaw handles huge loads", The Iron Age, August 11, 1966, pp 230.

7 Bilston S & L, "High speed hot sawing", Iron & Steel, December 1967, pp 524.

8 Mortimer J, "Blade breakthrough to get the edge in hacksaw exports", The Engineer, 16 November 1972, pp 42.

9 Greenslade A, "Metal sawing today", Sheet Metal Industries, August 1976, pp 125.

10 "Sawing developments lift cut-offs status", Metalworking Production, December 1975, pp 43.

11 Jabionowski J, "Fundamentals of sawing", American Machinest, April 15, 1975, pp 54-68.

12 "Trends in sawing", Tooling and Production, January 1978, pp 70.

13 Rakowski R Leo, "Know your saw blades", Machine and Tool Blue Book, July 1978, pp 84.

14 "Cutting survey tests hacksaw's bite", Metalworking Production, June 1979, pp 133.

15 Thompson P J & Taylor R W, "A computer simulation of the power hacksaw operation and its use in estimating blade life, cutting rate and cost", The Production Engineer, January 1976, pp 25, Vol 55, No 1.

16 Albrecht P, "The ploughing process in metal cutting", Trans. Am. Soc. Mech. Engrs., Vol 82 (Series B), 1959, pp 263.

17 Connolly R & Rubenstein C, "The mechanics of continuous chip formation in orthogonal cutting", Int. J. Mach. Tool. Des. Res., Vol 8, 1968, pp 159-187.

18 Van Vlack L H, "Materials Science for Engineers", Adison-Wesley Publishing Company, (1975), p 198.

19 Palmer W B & Oxley P L B, "Mechanics of orthogonal machining", Proc Inst Mech Engrs, vol 173, No 24, 1959.

20 Johnson W & Mellor P B, "Engineering plasticity", Van Nostrand, pp 483-484, 1973.

21 Pugh H U D, "Mechanics of the cutting process", The Institution of Mech Engrs, London, Conf on Tech of Engrg Manuf, 1958.

22 Childs T H C, "A new visio-plasticity technique and a study of curly chip formation", Int. J. Mech. Sci., Pergammon Press, 1971, Vol 13, pp 373-387.

23 Childs T H C, "Rake face action of cutting lubricants ...carbon tetrachloride", Proc. Inst. Mech. Engrs, 1972, Vol 186, 63/72.

24 Childs T H C, "Elastic effects in metal cutting chip formation", 1980, Int. J. Mech. Sci., Vol 22, pp 457-466.

25 Aghan R L and Wilms G R, "Scale formation on workpiece surface from built-up edge", Metals Technology, December 1981, pp 488-490.

26 Watson D W & Murphy M C, "The effect of machining on surface integrity", The Metallurgist and Materials Technologist, April 1979, pp 199-204.

27 Williams J E, Smart E F and Milner D R, "The metallurgy of machining. Part 1: Basic Considerations and the Cutting of Pure Metals", Metallurgia, January 1970, pp 3-10.

28 Williams J E, Smart E F and Milner D R, "The metallurgy of machining. Part 2: The Cutting of Single Phase, Two-Phase and some Free Machining Alloys", Metallurgia, February 1970, pp 51-59.

29 Williams J E, Smart E F and Milner D R, "The metallurgy of machining. Part 3: The Effect of a Lubricant and an Assessment of the Current Understanding of Materials Behaviour in Machinery", Metallurgia, March 1970, pp 89-93.

30 McNulty G J, "The effect of blade wear on noise levels of power hacksaws", Proc 15th IMTDR, pp 305-308.

A Blade Manufacturer's Performance Criterion

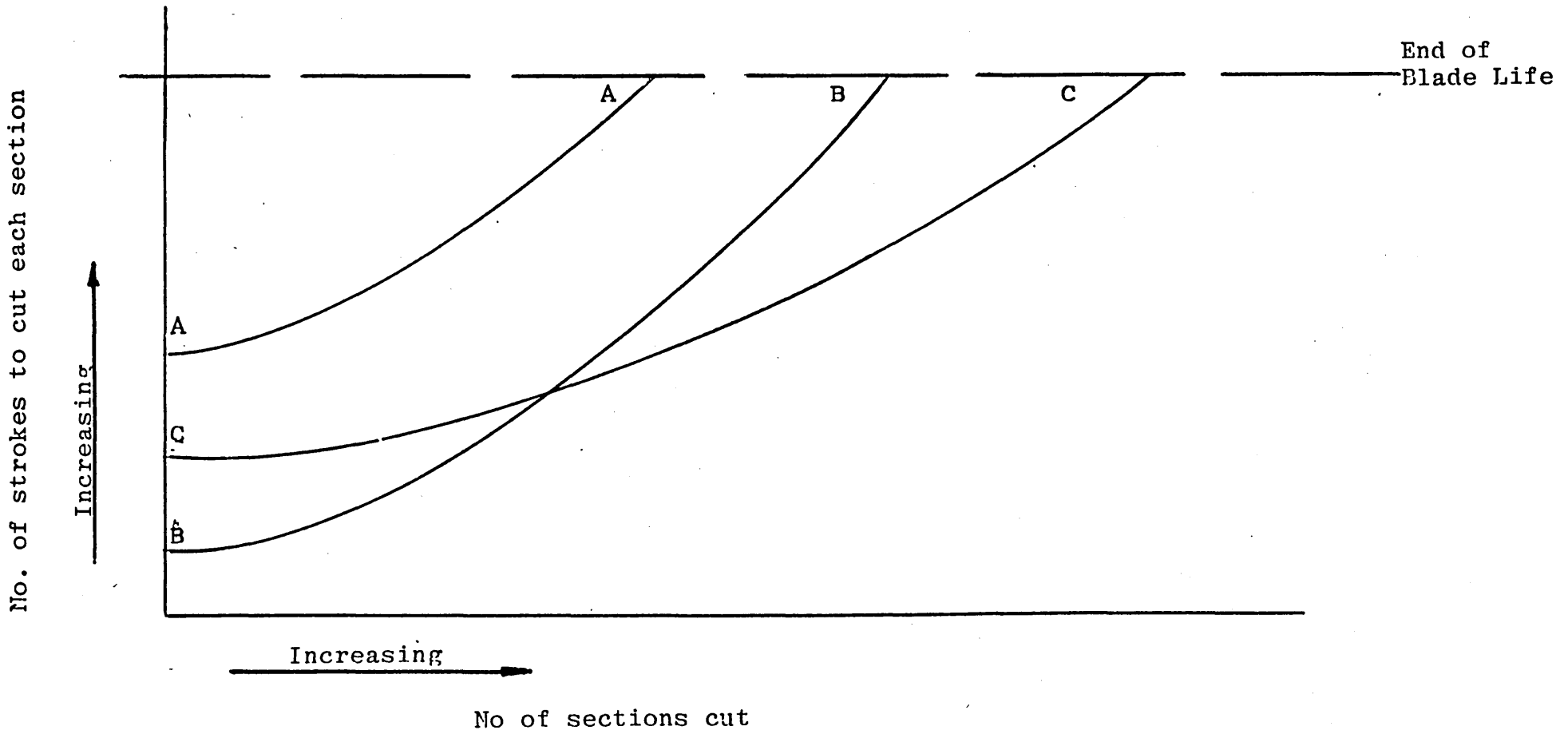

Fig. 1.1. A Blade Manufacturer's Performance Criterion

Table 5. Test conditions and acceptance limits for power blade cutting tests (high speed steel, all hard and bi-metal)

Blade dimensions				Speed	No. of cuts	Test bar		Wear rate	Total time
Length	Width	Thickness	Pitch			No. of strips	Thickness of strip		
mm	mm	mm	mm	strokes/ min			mm		min
300 and 350	25	1.25	1.8	124	10	15	2.6 ± 0.05	66	66
300 and 350	25	1.25	2.5	124	10	20	2.6 ± 0.05	56	61
350 400 450	32	1.60	2.5	124	10	20	2.6 ± 0.05	65	87
350 400 450	32	1.60	4.0	124	10	25	2.6 ± 0.05	47	60
400 450	40	2.00	4.0	124	10	25	2.6 ± 0.05	81	80
400 450	40	2.00	6.3	124	10	25	2.6 ± 0.05	69	76

Fig 1.2 BS 1919. Test Conditions and Acceptance Limits for Power Hacksaw Blades

SINGLE CLEARANCE ANGLE TOOTH GEOMETRY

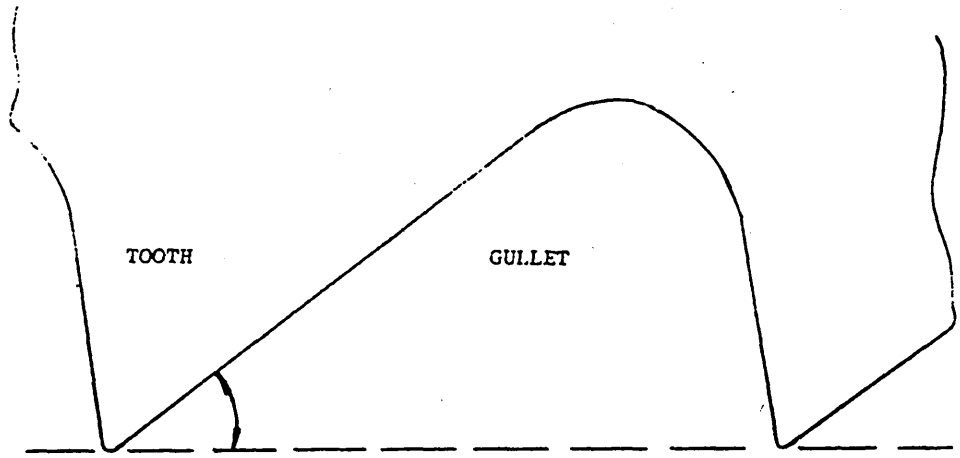

(a)

PRIMARY AND SECONDARY CLEARANCE ANGLE

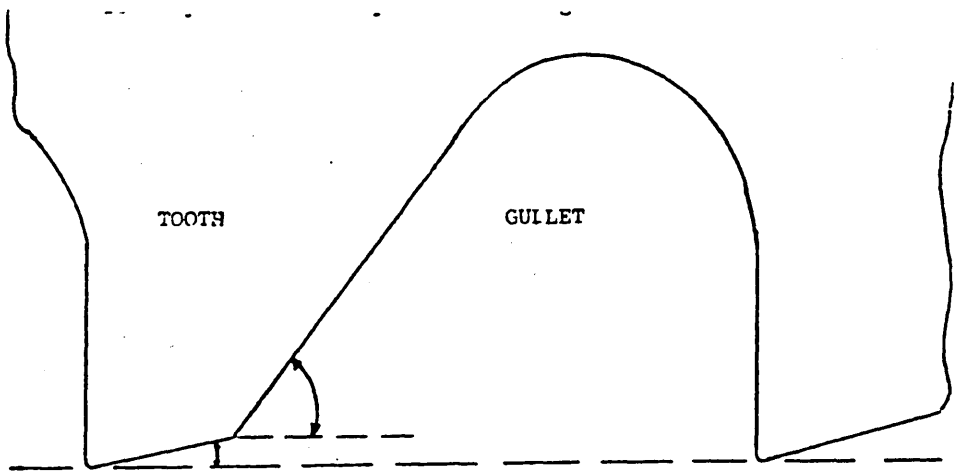

(b)

Fig. 1.3. Two different tooth and gullet geometries

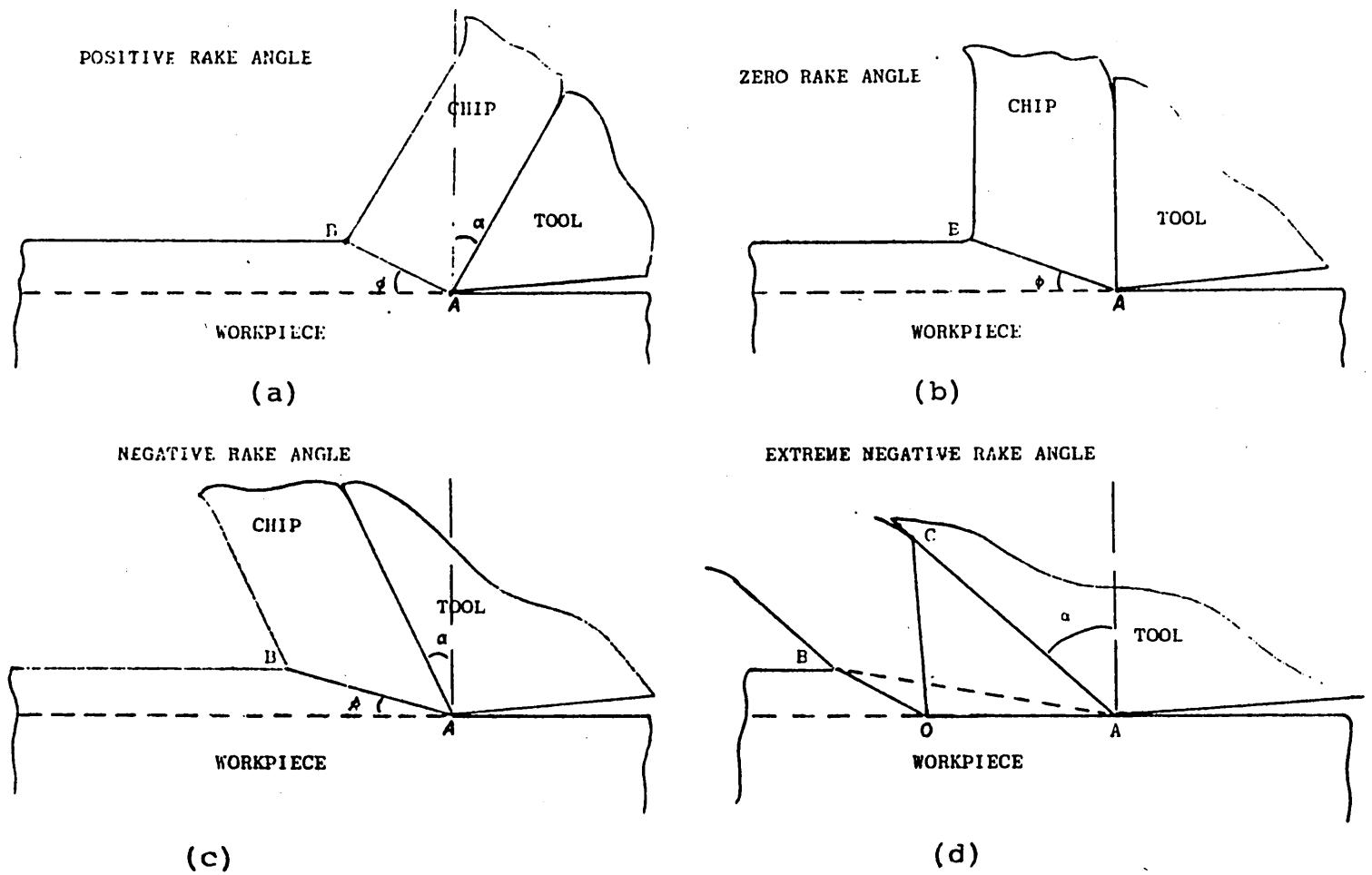

Fig. 1.4. Models of Chip Formation at Various Rake Angles.

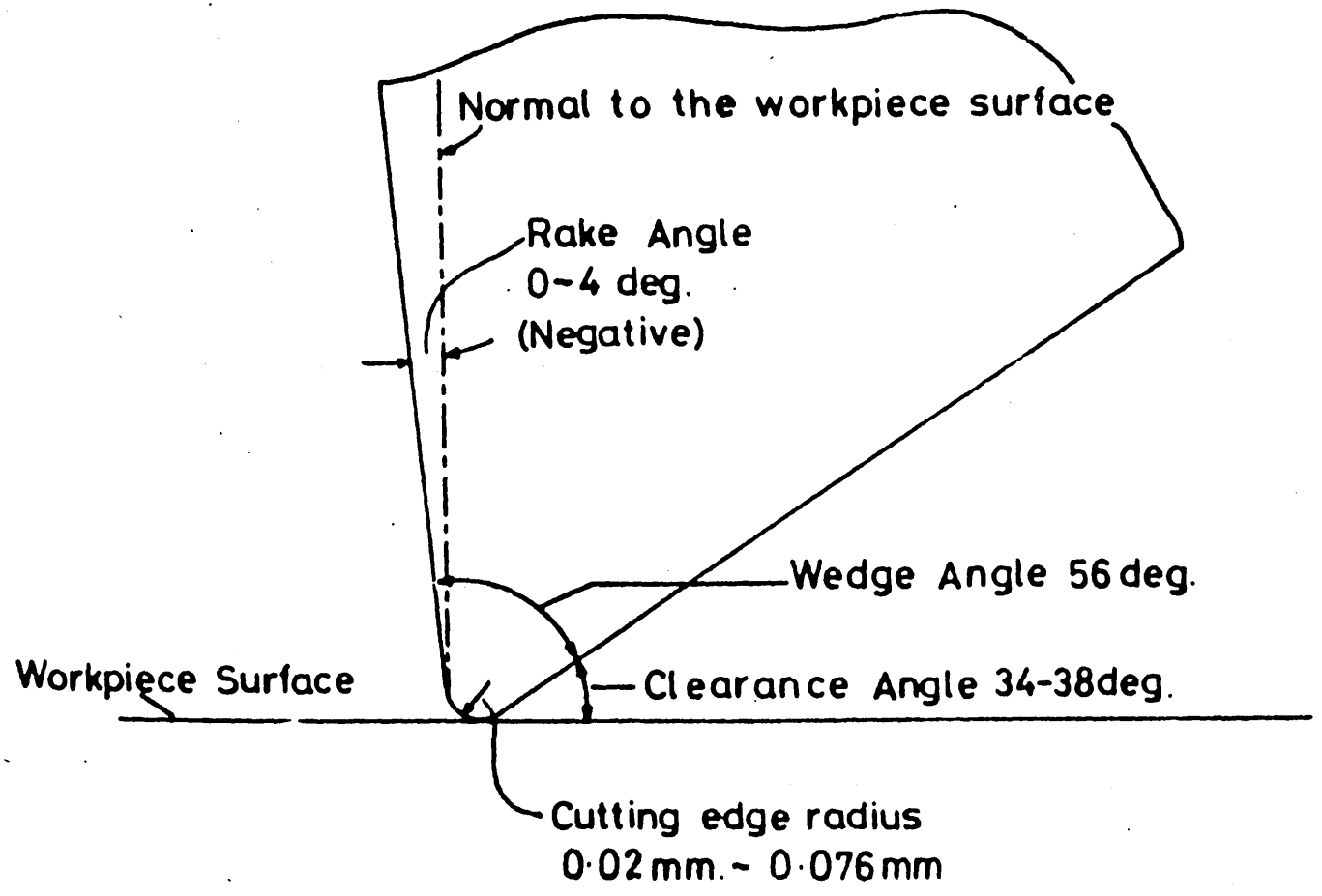

FIG.1.5 CUTTING EDGE GEOMETRY OF A HACKSAW BLADE TOOTH.

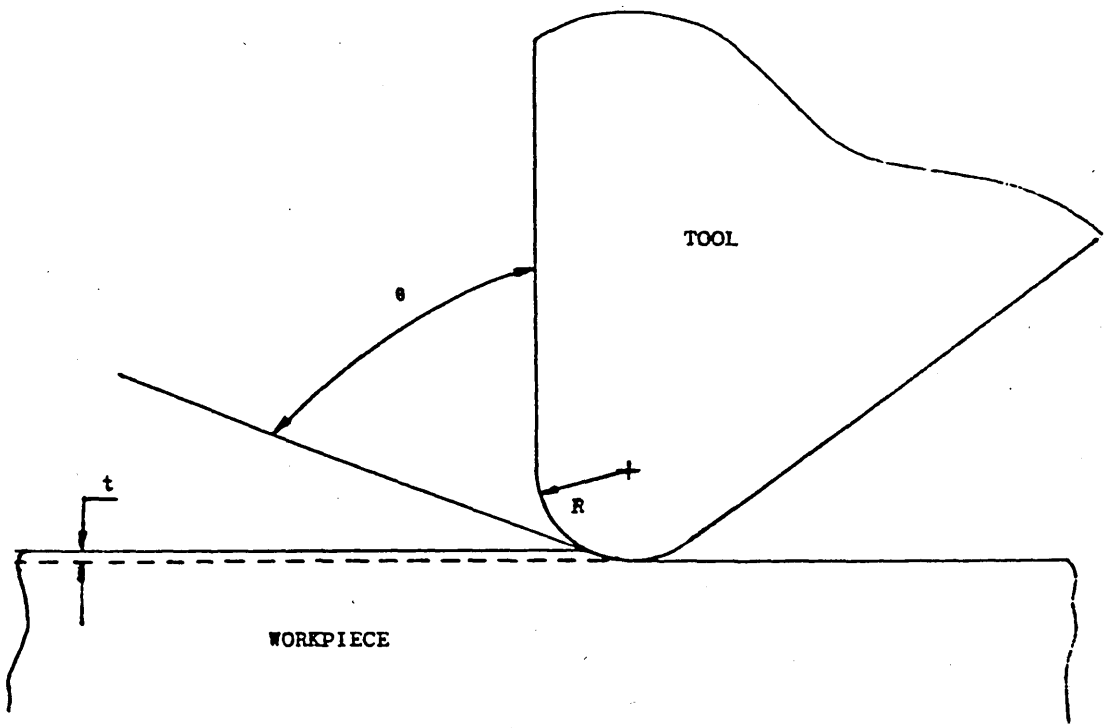

Fig. 1.6. Diagram of effective rake angle θ, when cutting edge radius R is large compared to undeformed chip thickness t. Nominal rake angle is zero degrees.

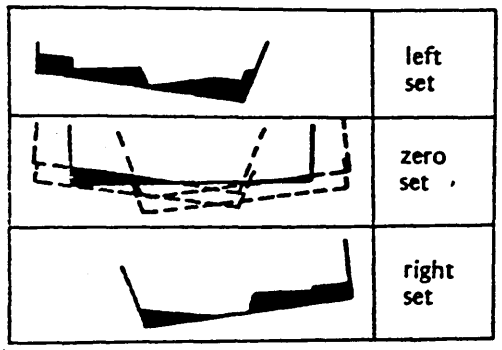

Fig. 1.7. Söderberg's model showing the variation in undeformed chip thickness (shaded area) along the edge for an averaged feed per tooth of 50 μm (9).

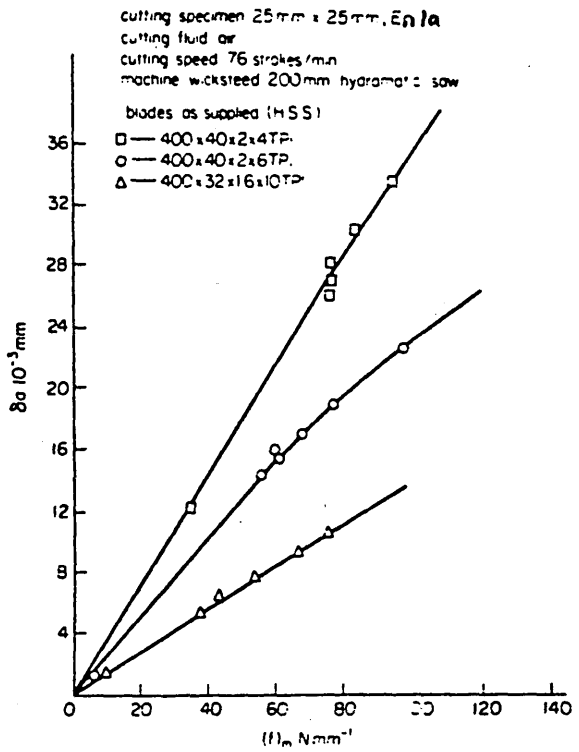

The average depth of cut per tooth against the thrust load per tooth per unit thickness for blades having different teeth pitch.

Fig. 1.8. Experimental data presented by Sarwar and Thompson (1,2).

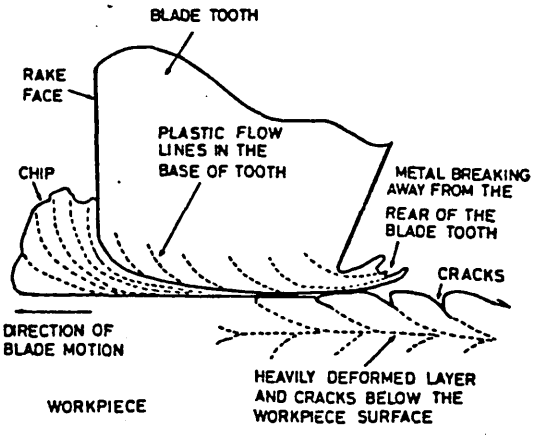

. Deformation occurring in both the blade tooth and workpiece, compiled from microscopic observations during wear tests on En 44E in phase II wear.

Fig. 1.9. Thompson and Taylor's wear model for hacksaw teeth.

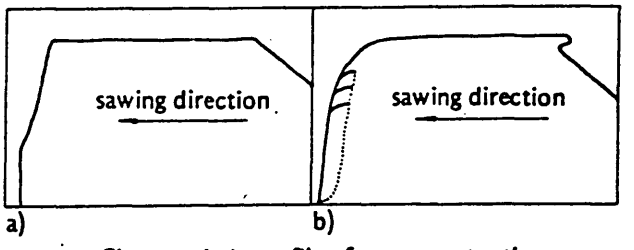

Characteristic profile of worn saw tooth. a) Work material AISI 4337 and b) AISI 316 (dotted line examplifies extension of future tooth spalling).

Fig. 1.10. Soderberg's wear model for hacksaw teeth cutting
(a) a quenched and tempered carbon steel, and
(b) an austenitic stainless steel

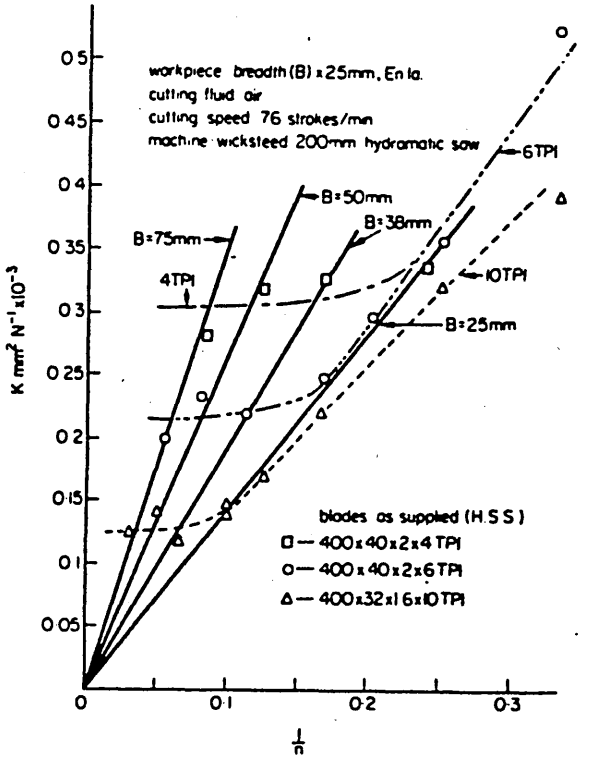

The cutting constant against the reciprocal of the number of teeth in contact with the workpiece.

Fig. 2.1. Experimental data presented by Sarwar and Thompson showing the effect of workpiece width on cutting performance. (1,2).

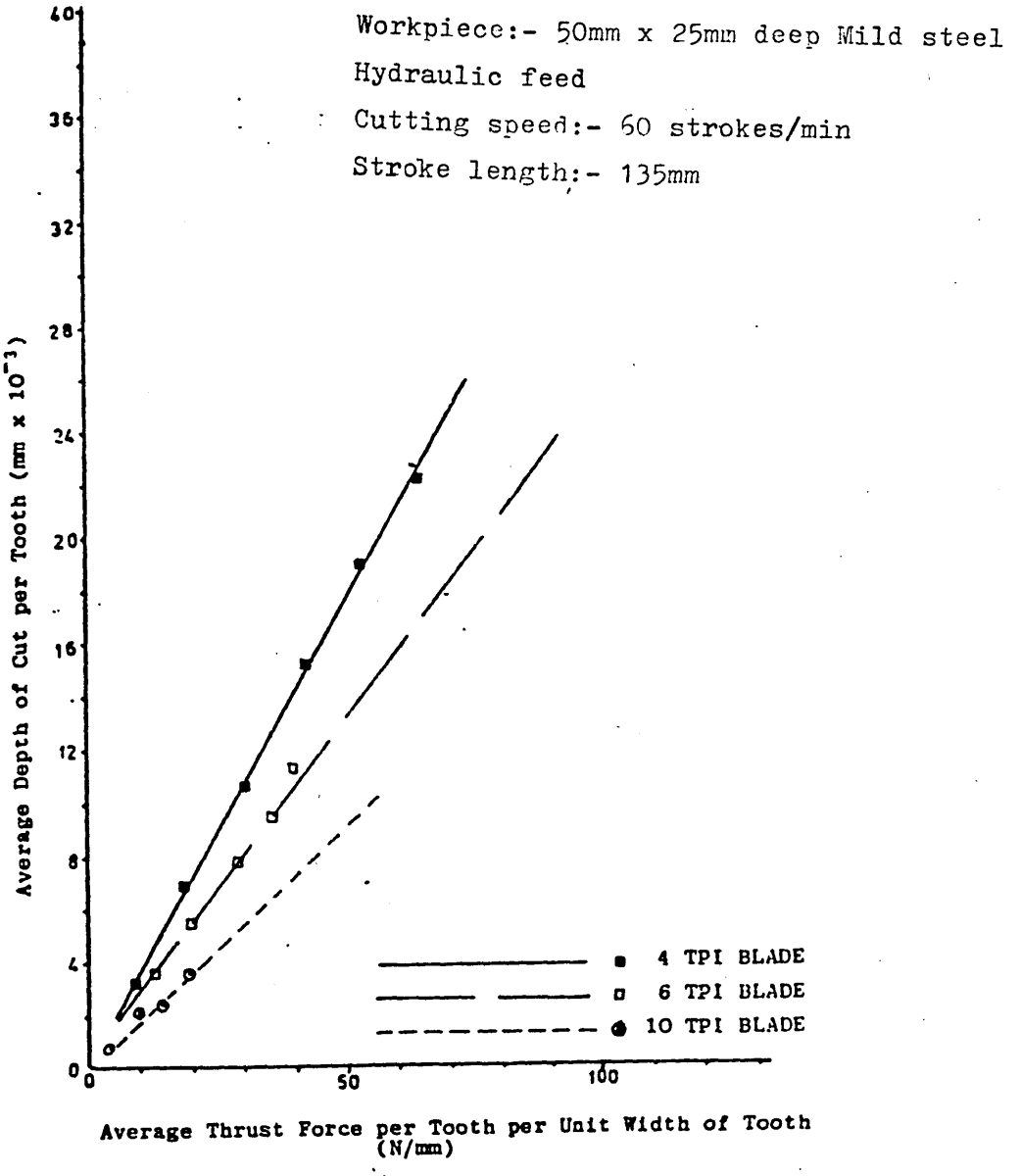

Fig. 2.2. Performance curves of blades. (as new condition). 50 mm wide by 25 mm deep Mild Steel Workpiece.

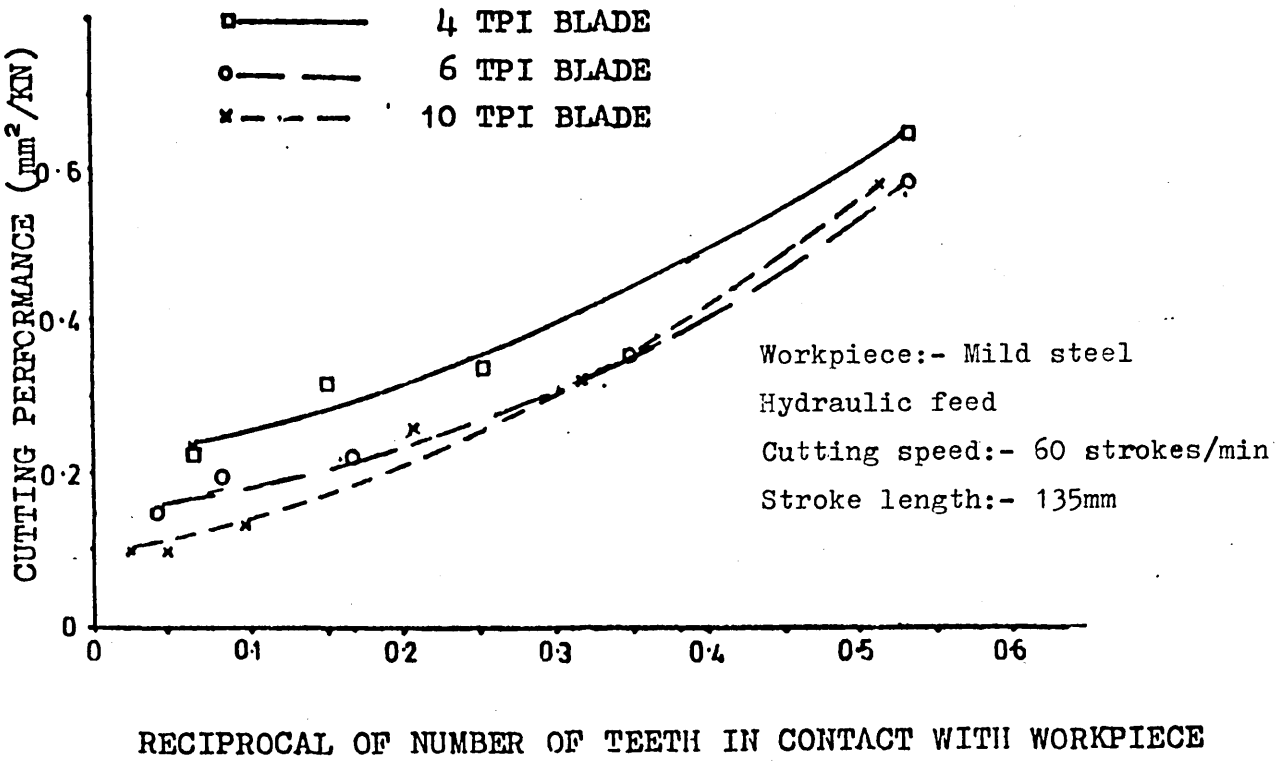

Fig. 2.3. Performance of Blades as Workpiece width increases.

(a) 4 TPI Blade profile as new

(b) 4 TPI Blade profile with every other cutting edge removed ie. 2 TPI blade.

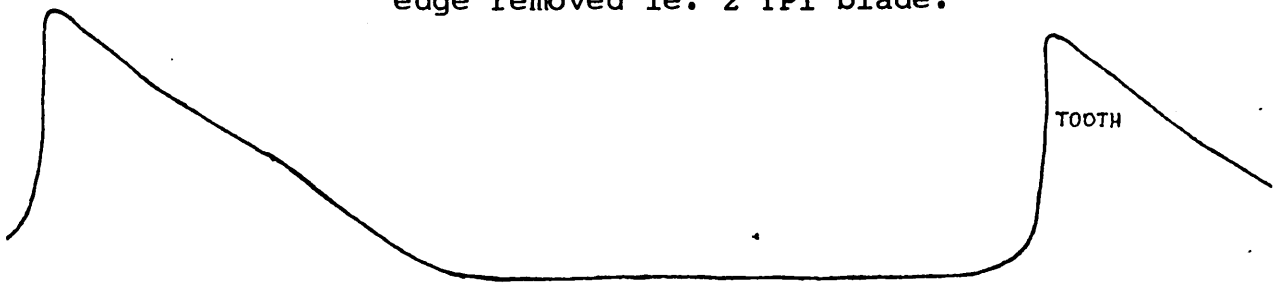

(c) 4 TPI Blade with every tooth ground out to root height.

Fig. 2.4. Profile of 4 TPI blade as new and modified. Traces were taken on a shadowgraph.

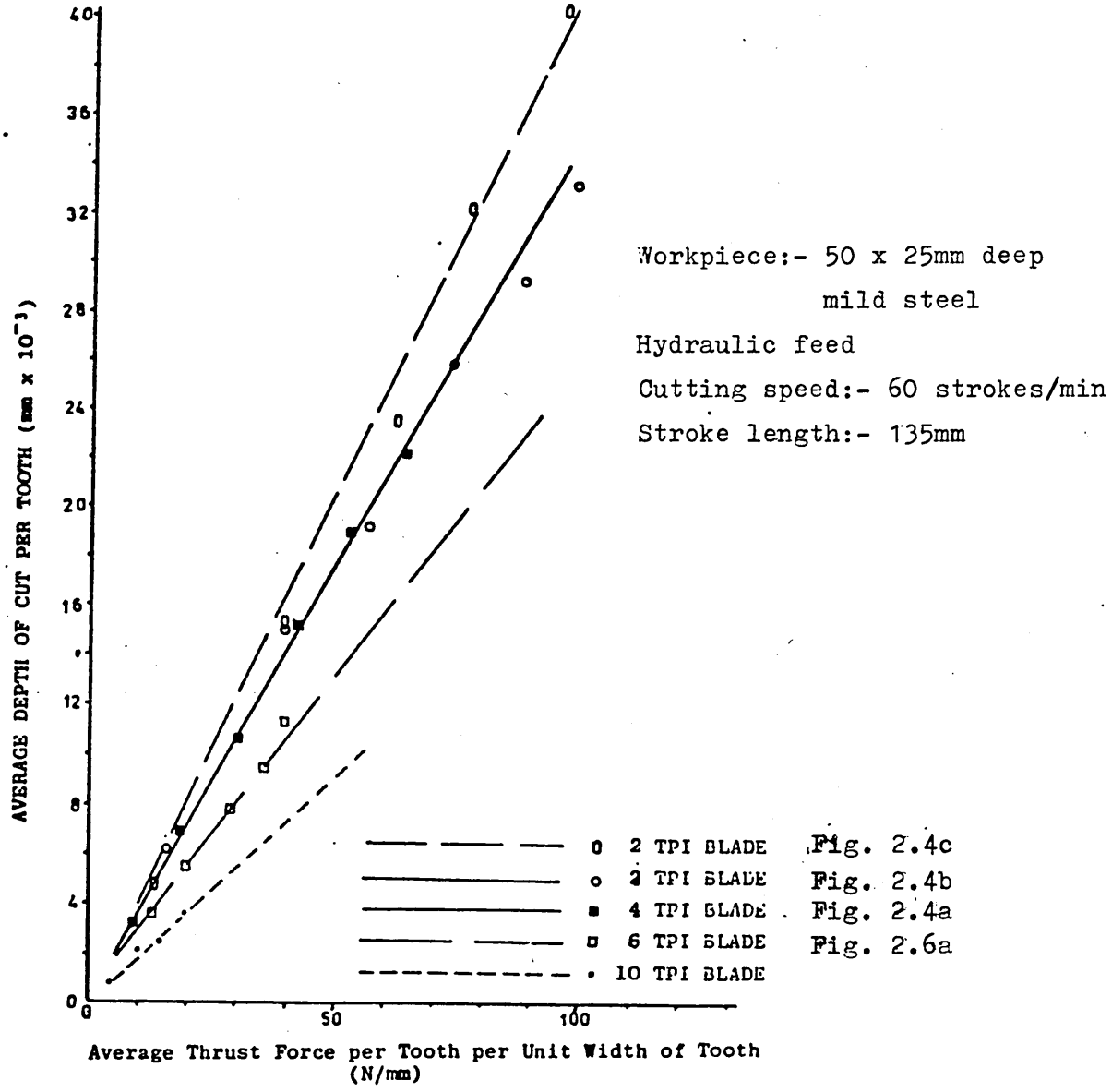

Fig. 2.5. Performance of blades with modified gullets. 50 mm wide x 25 mm deep Mild Steel Workpiece.

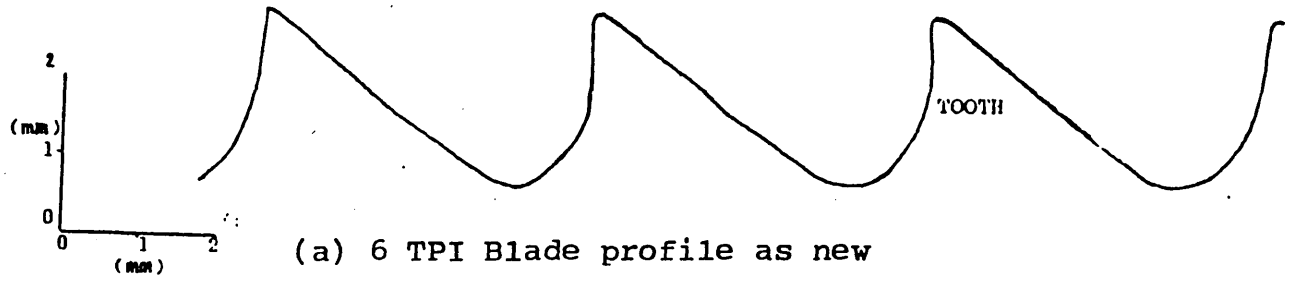

(a) 6 TPI Blade profile as new

(b) 6 TPI Blade profile with every other tooth ground out to root height ie. 3 TPI blade

(c) 6 TPI Blade profile with every other tooth ground out to root height of a 4 TPI blade

Fig. 2.6. Profile of 6 TPI blade as new and modified. Traces were taken on a Shadowgraph.

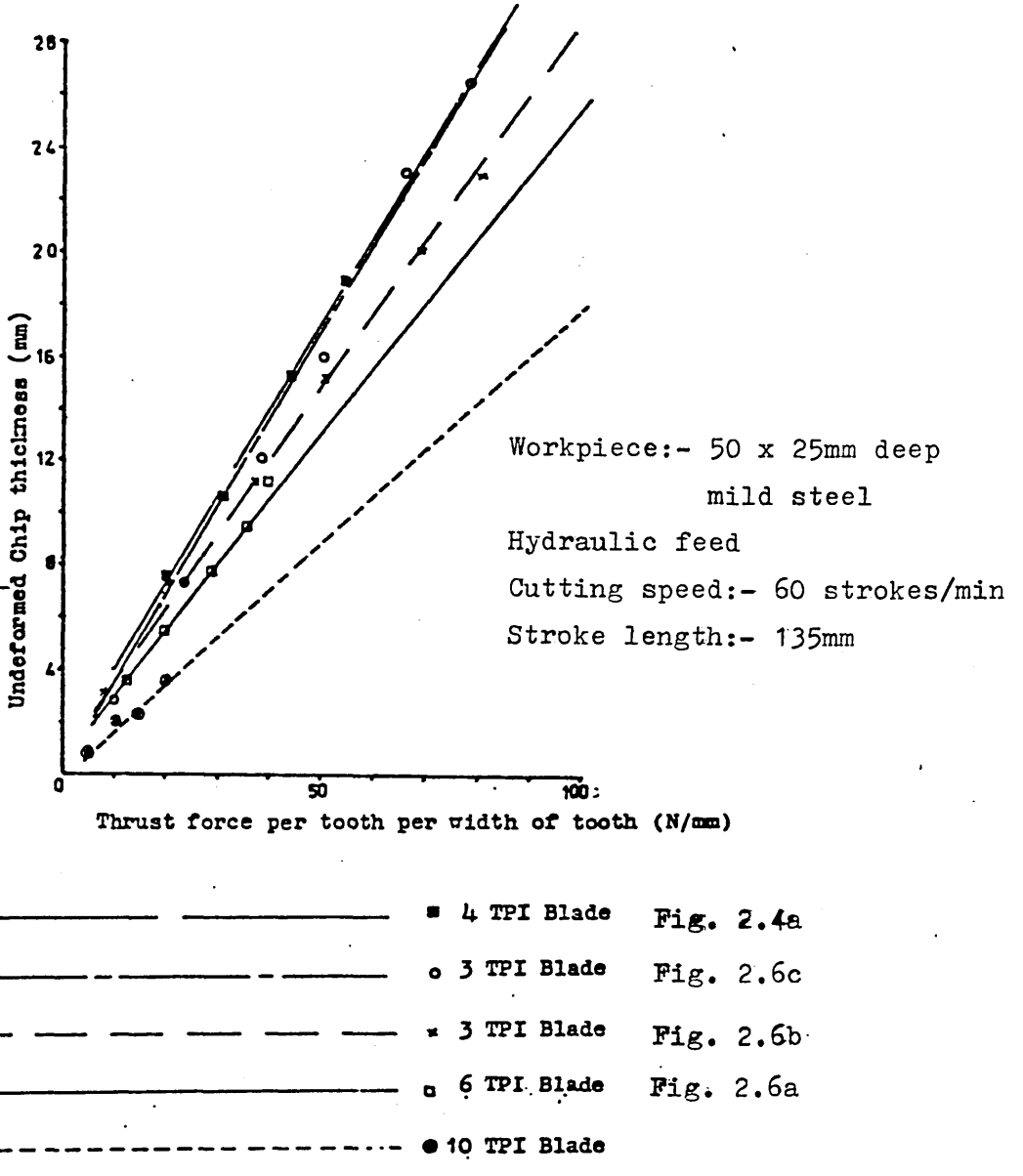

Fig. 2.7. Performance of blades with modified gullets.
50 mm wide x 25 mm deep Mild Steel Workpiece.

Fig. 2.8a.

Small chips and debris cut by a 4 TPI blade. 50 mm wide Mild Steel Workpiece. Magnification x 5

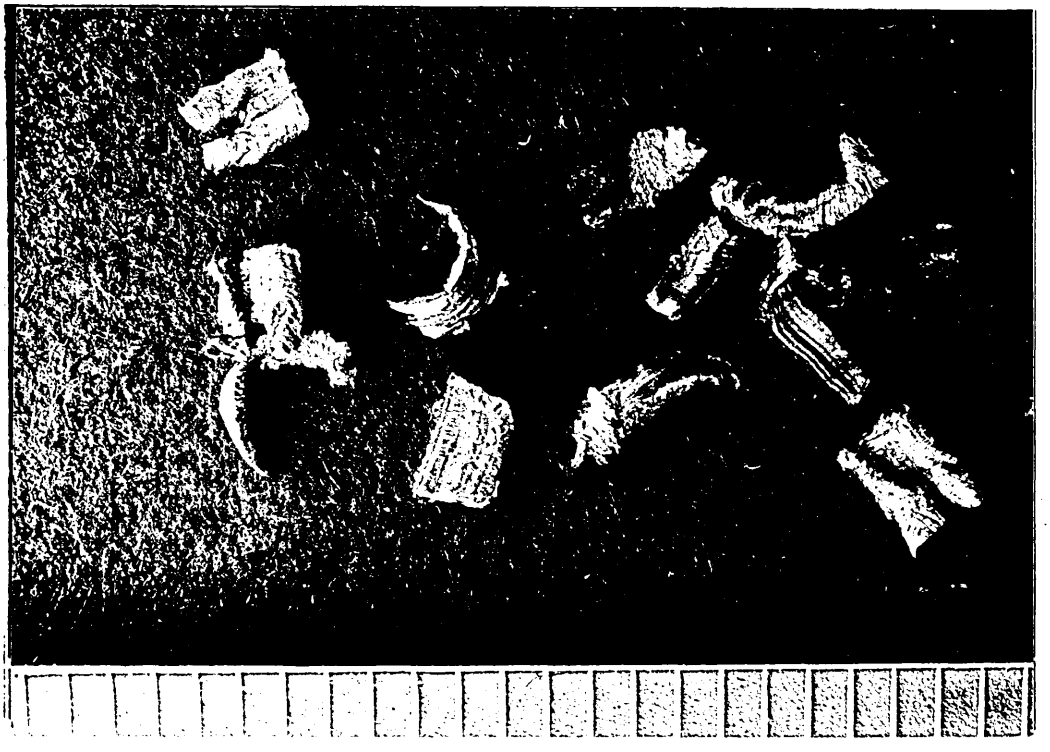

Fig. 2.8b.

Broken chips cut by a 4 TPI blade. 50 mm wide Mild Steel workpiece. Magnification x 5.

Fig. 2.8c. Curly chips cut by a 4 TPI blade.
50 mm wide Mild Steel workpiece.
Magnification x 5.

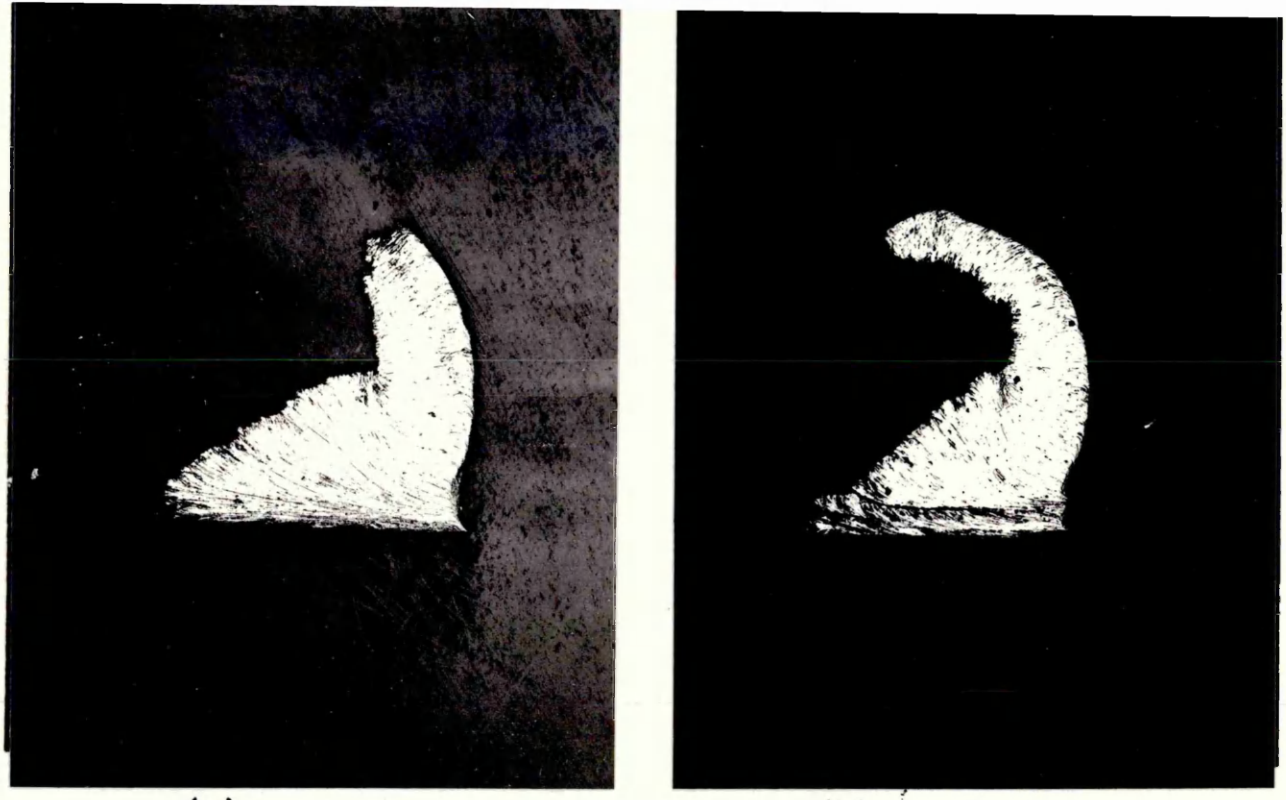

(a) (b)

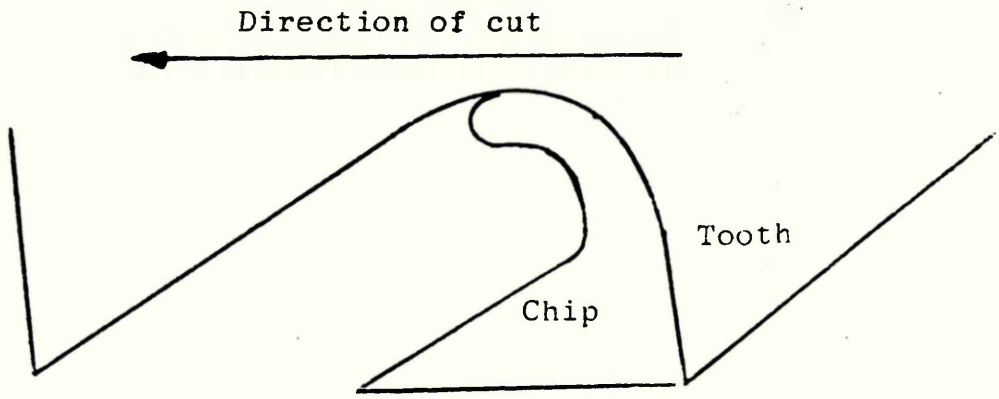

The sketch shows the orientation of the chips in the gullet.

Fig. 2.9 (a-b) Hacksaw chips cut by a 10 TPI blade. 50 mm wide mild steel workpiece. Magnification x 30.

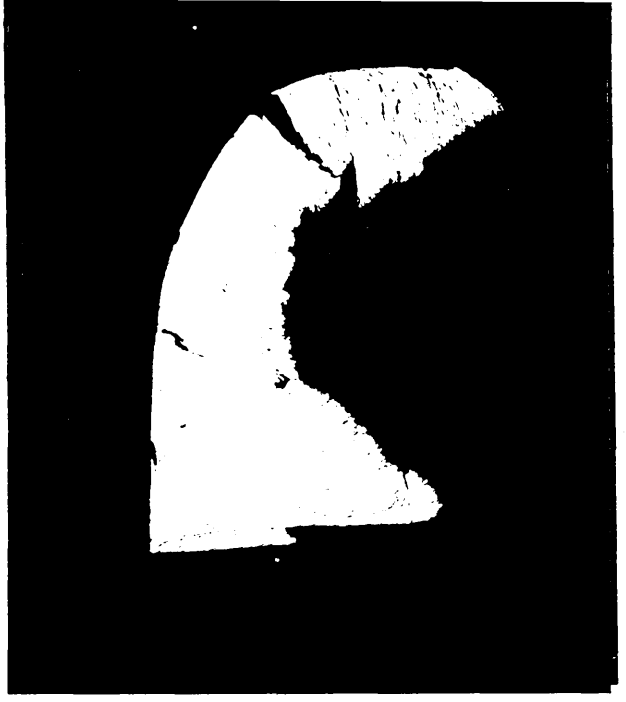

(c)

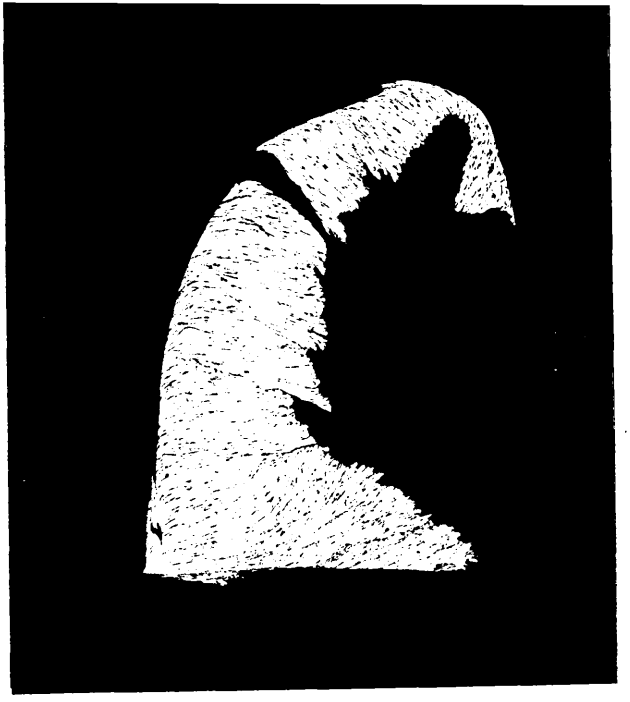

(d)

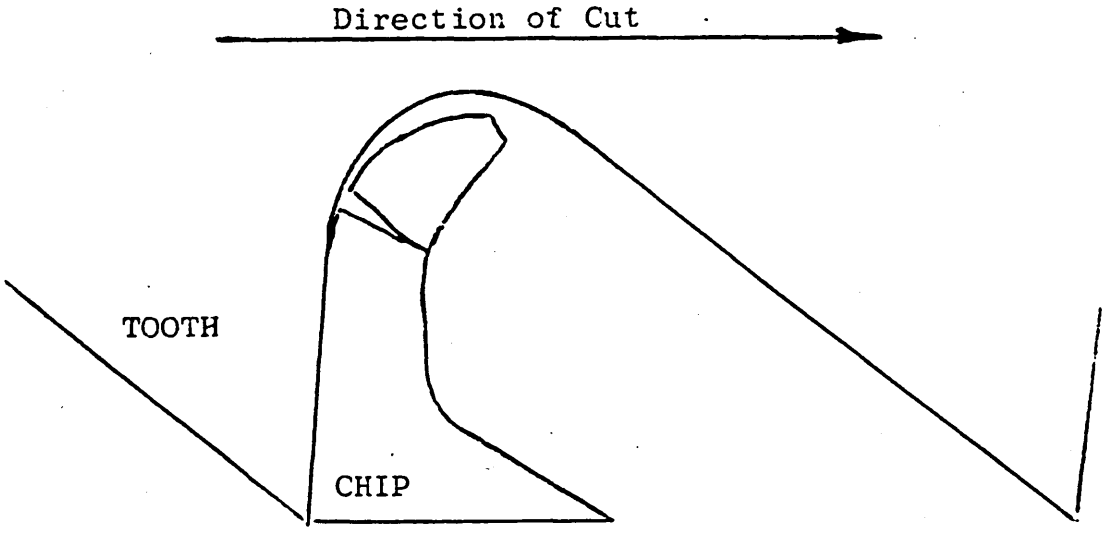

The sketch shows the orientation of the chips in the gullet.

Fig. 2.9 (c-d) Hacksaw chips cut by a 6 TPI blade.
50 mm wide mild steel workpiece
Magnification x 30.

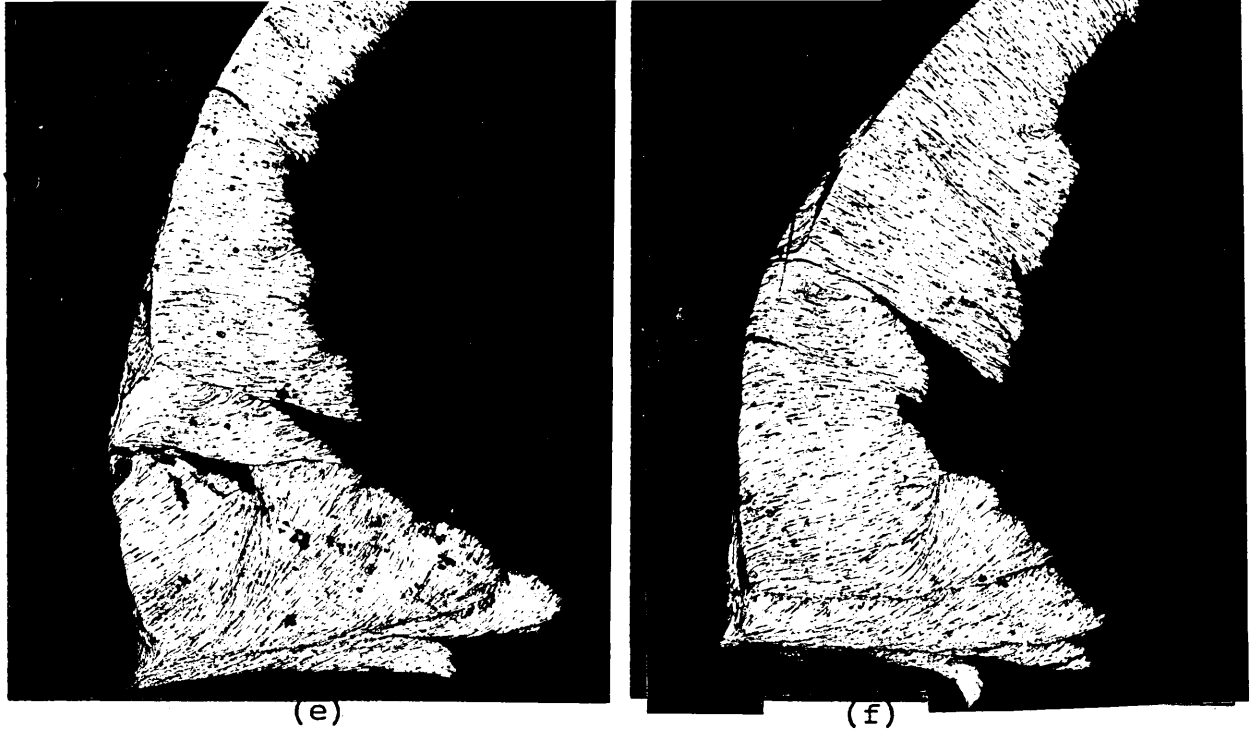

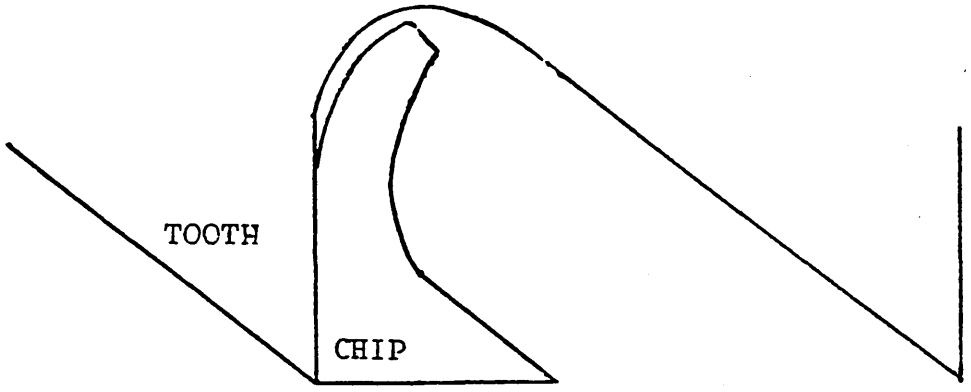

The sketch shows the orientation of the chips in the gullet.

Fig. 2.9. (e-f) Hacksaw chips cut by a 4 TPI blade. 50 mm wide mild steel workpiece. Magnification x 30.

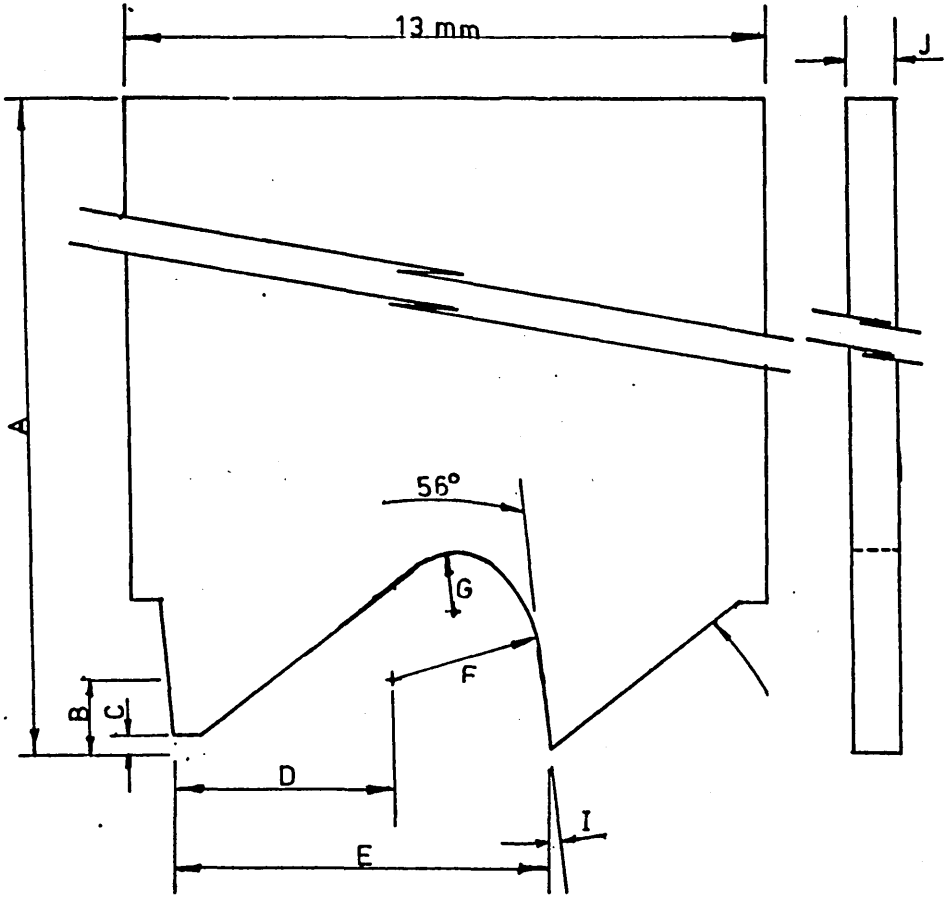

TPI / (mm)	4	6	10
A	40·0	40·0	32·0
B	——	0·85	0·60
C	1·0	1·0	0·5
D	——	2·49	1·49
E	6·35	4·23	2·54
F	——	1·69	1·02
G	1·14	0·69	0·43
I	0°	4°	4°
J	2·0	2·0	1·6

Fig. 3.1. Dimensions of standard single teeth.

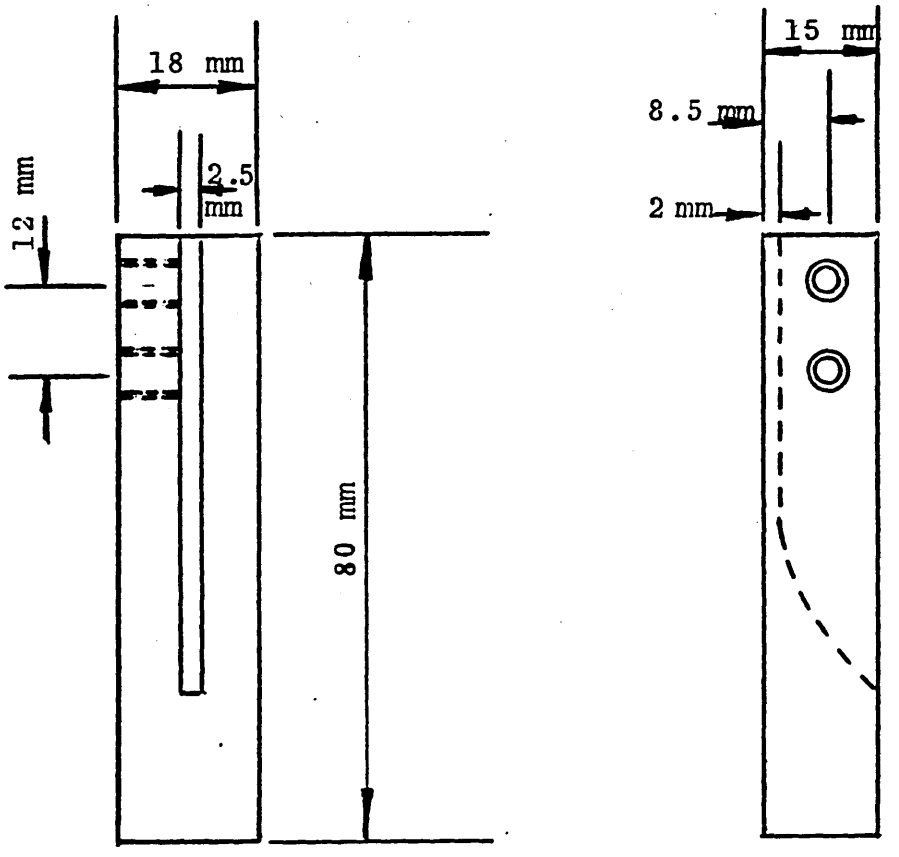

Fig. 3.2. TOOL HOLDER for individual hacksaw teeth
see Fig. 3.1.
The hacksaw tooth is clamped in the 2.5 mm
'slot by two' grub screws.

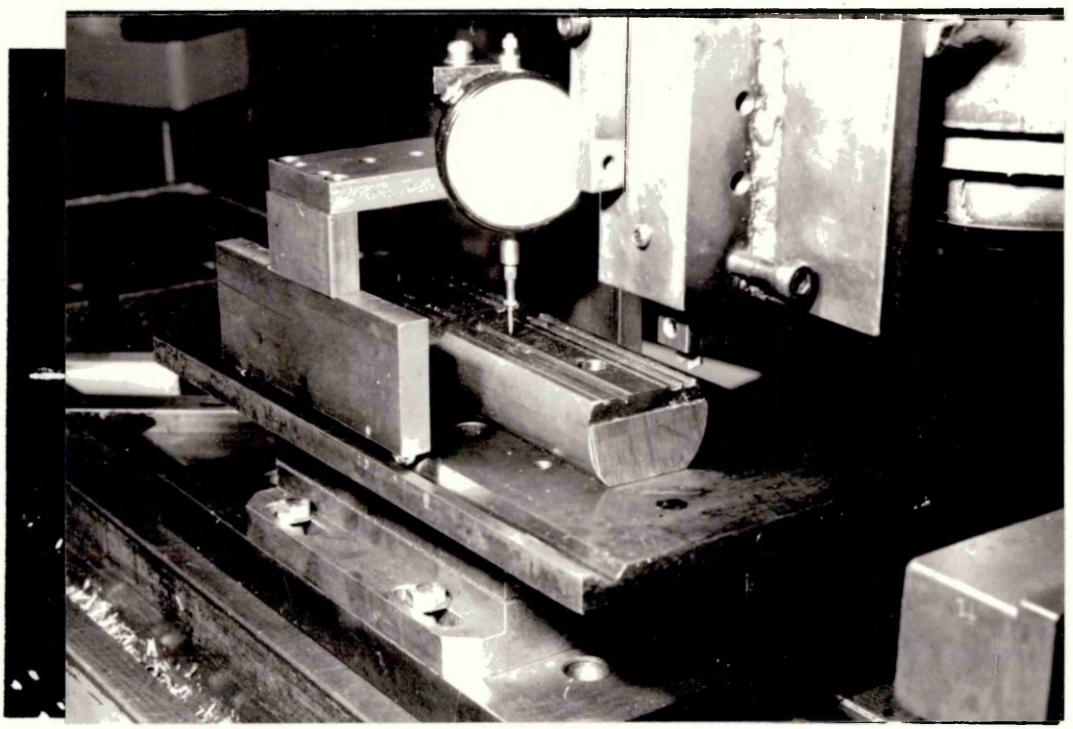

Fig. 3.3. Close up of Bridge and D.T.I. arrangement, for measurement of undeformed chip thickness.

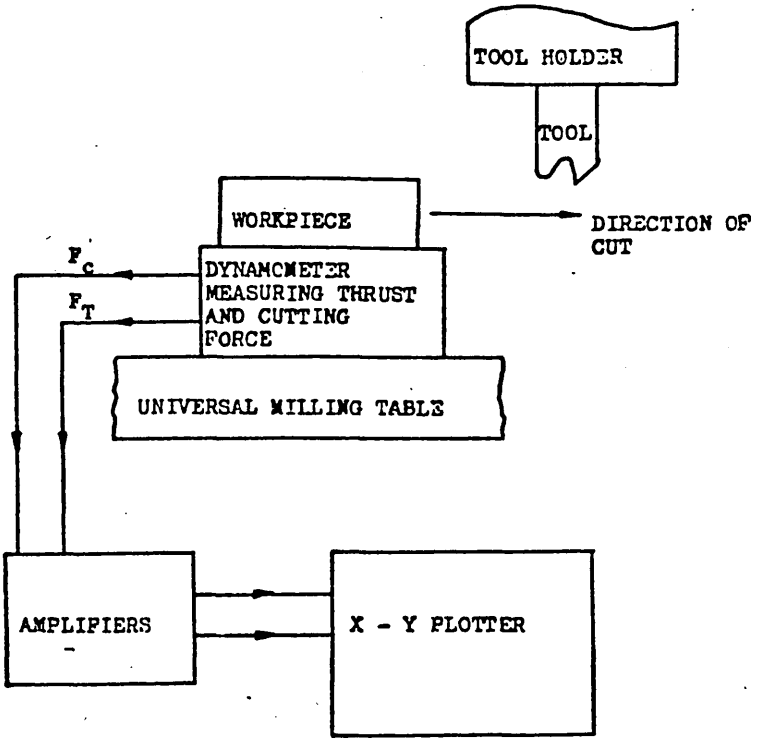

Fig. 3.4. Original design for single tooth and gullet test.

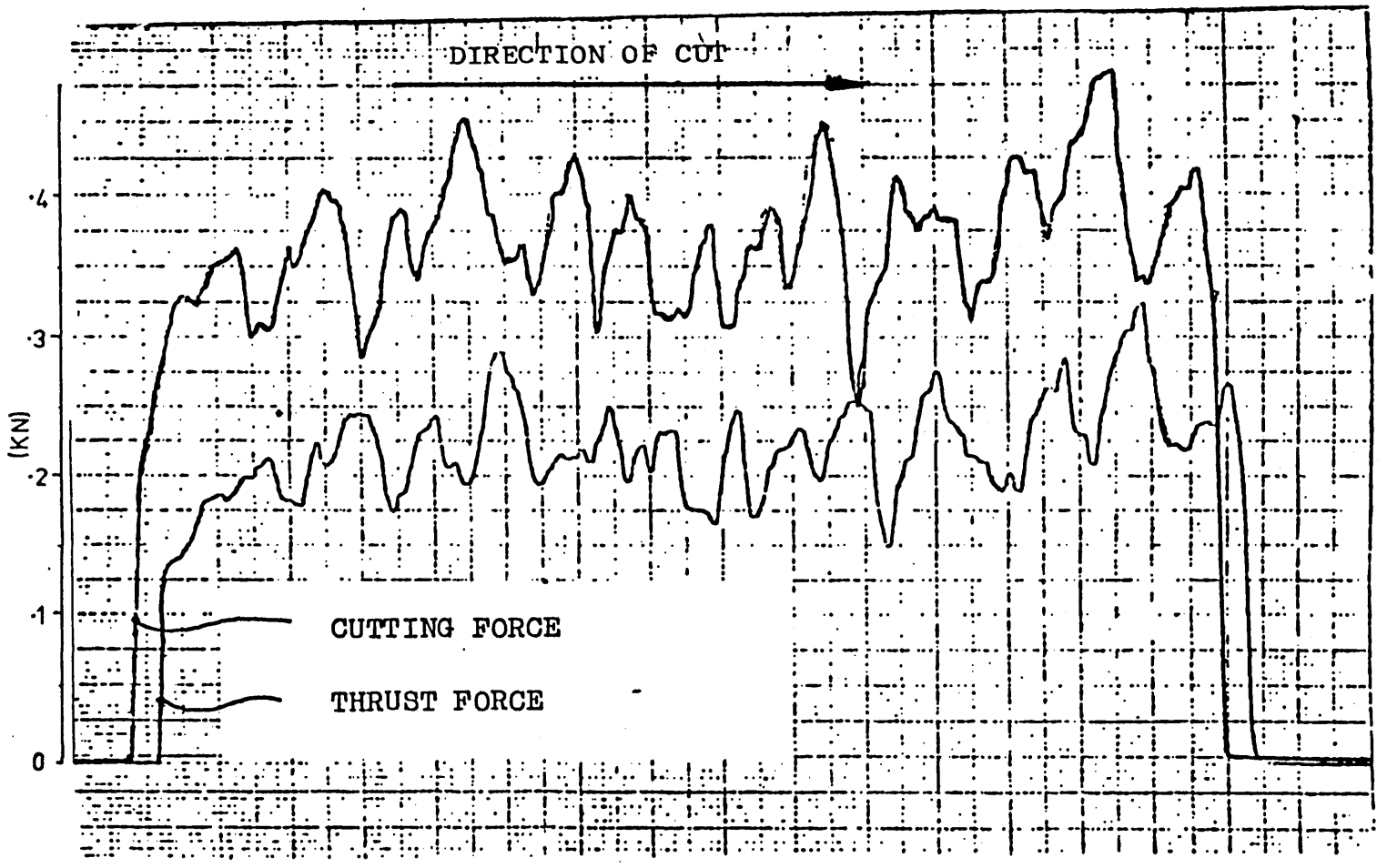

FIG. 3.5. 6 TPI CUTTING AND THRUST FORCE TRACES FOR 0.043mm UNDEFORMED CHIP THICKNESS.

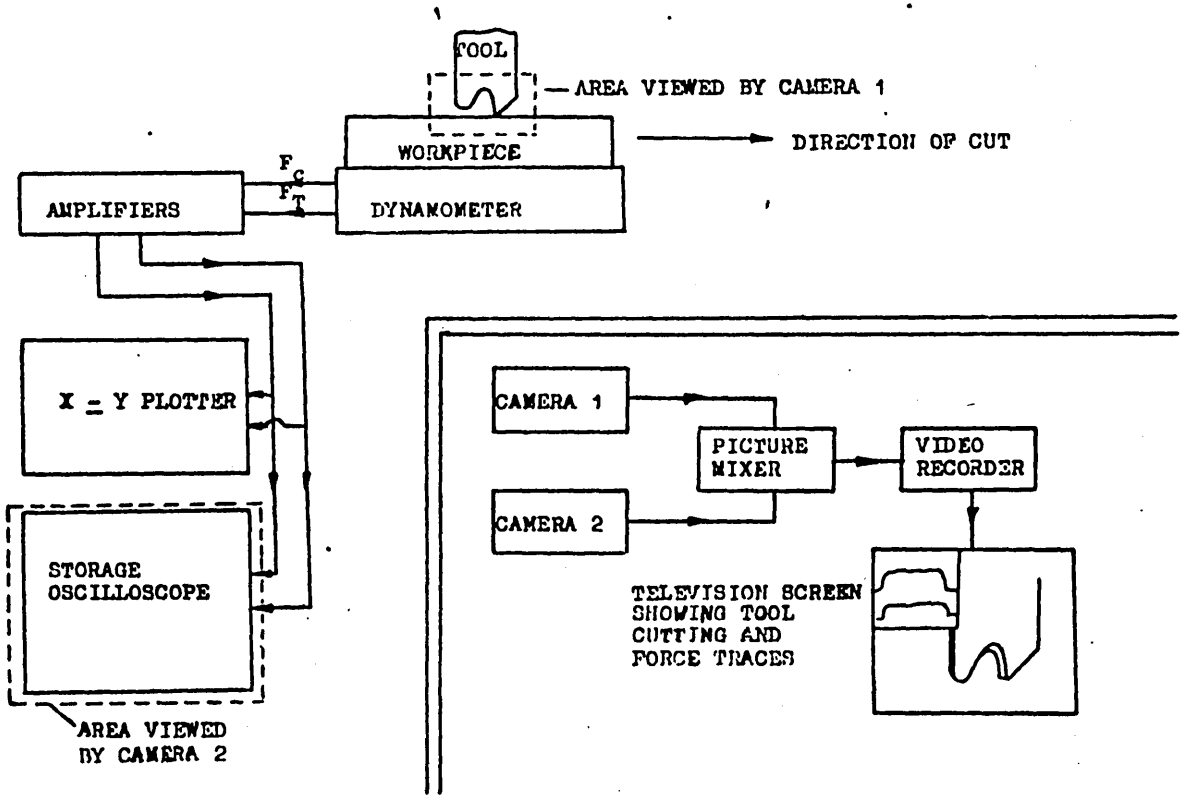

Fig.3.6. Third Design of Single Tooth and Gullet Test

(a)

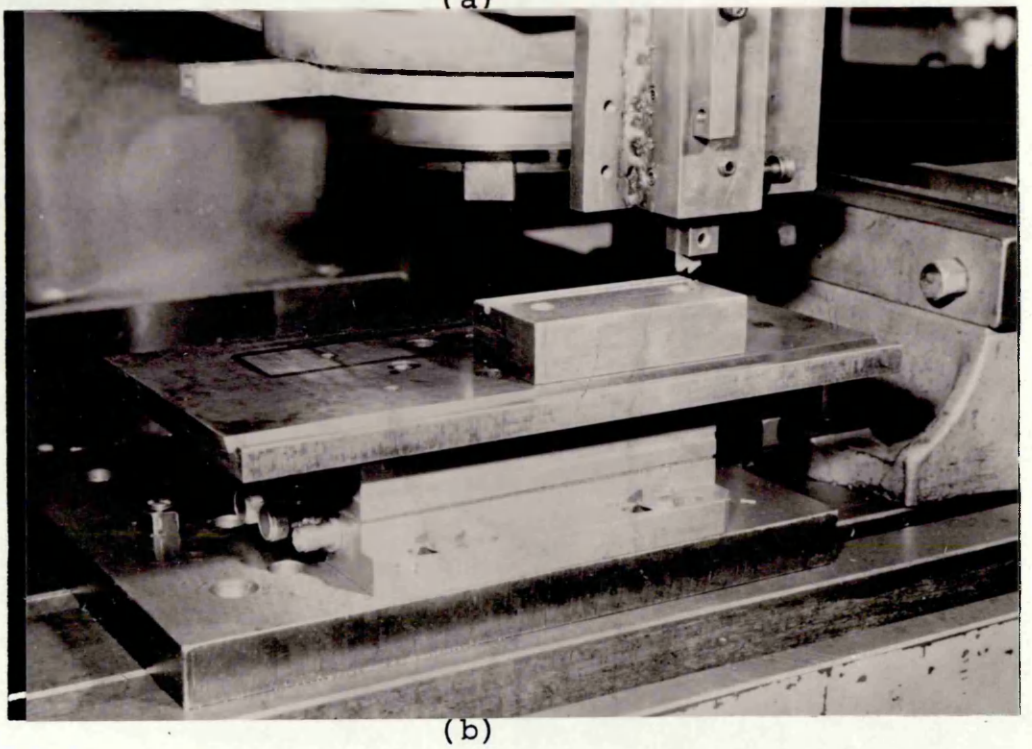

(b)

Fig. 3.7(a). Equipment used for method 3 of the simulation test.

Fig. 3.7(b). Close-up of the workpiece, reference plate, force platform, and flat plate. Also shown a tooth held in the holder and secured to the headstock of the miller.

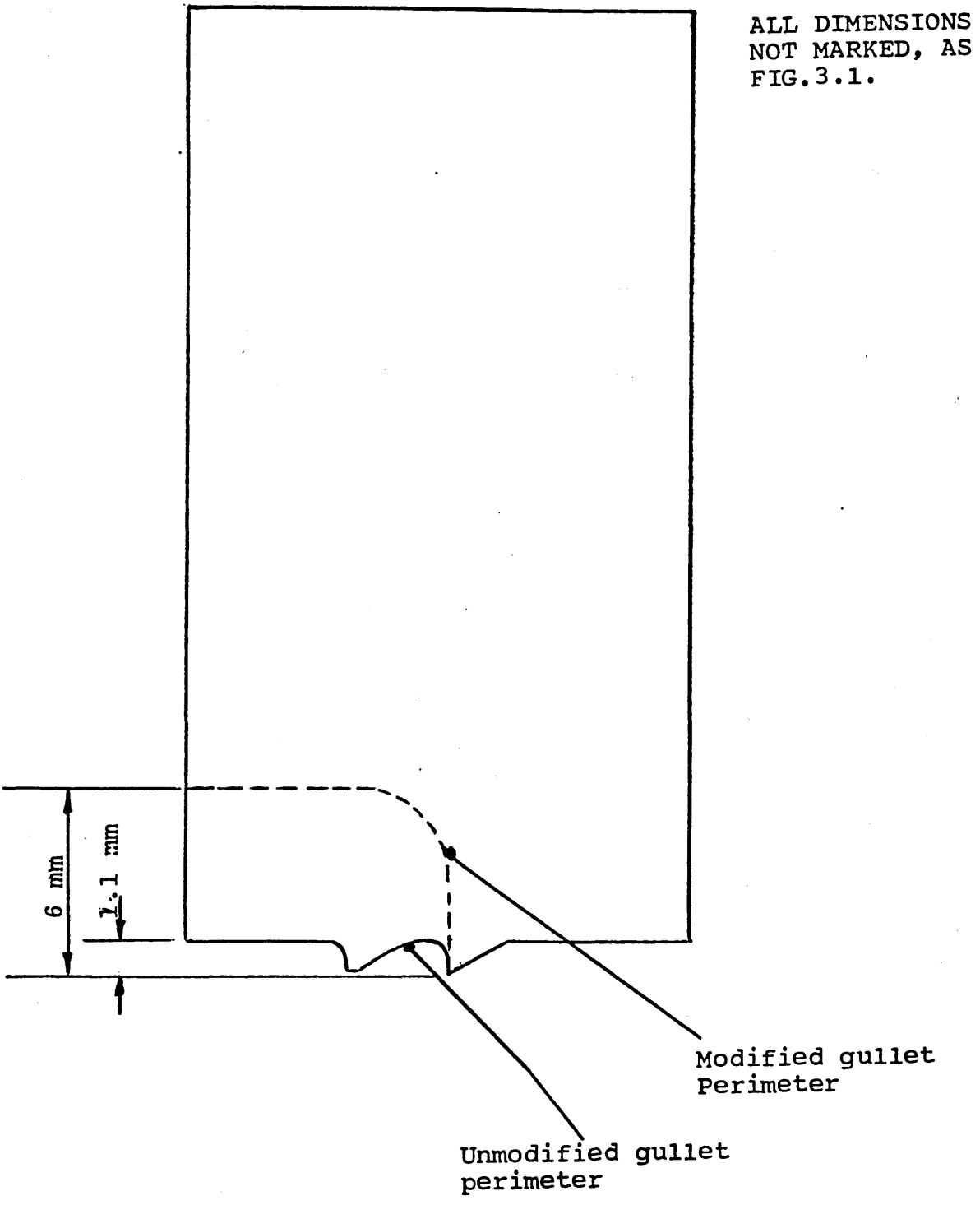

Fig. 3.8. 10 TPI tooth as new and with modified gullet.

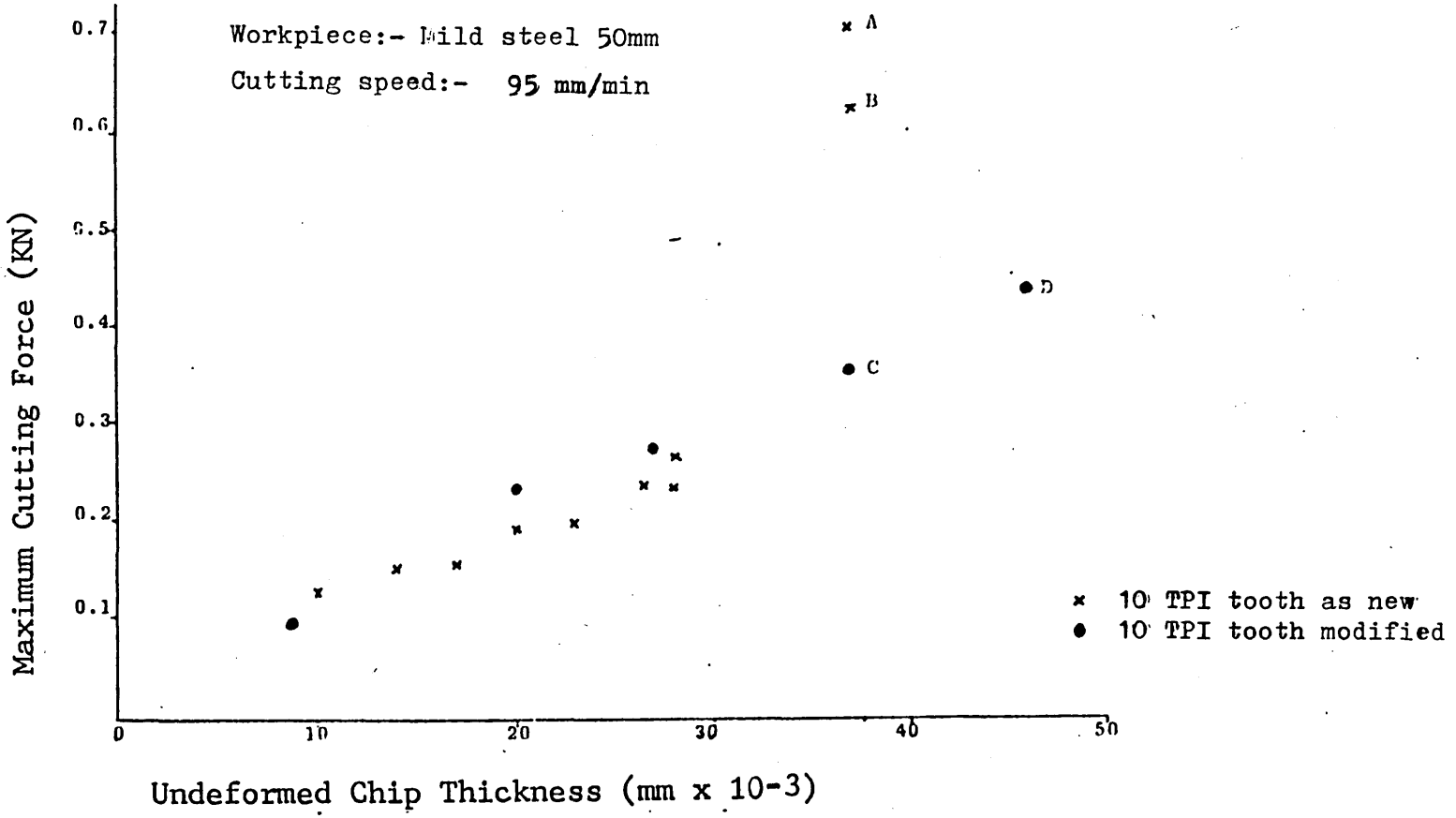

Fig. 3.9. Max. Cutting Force v. Undeformed Chip Thickness.

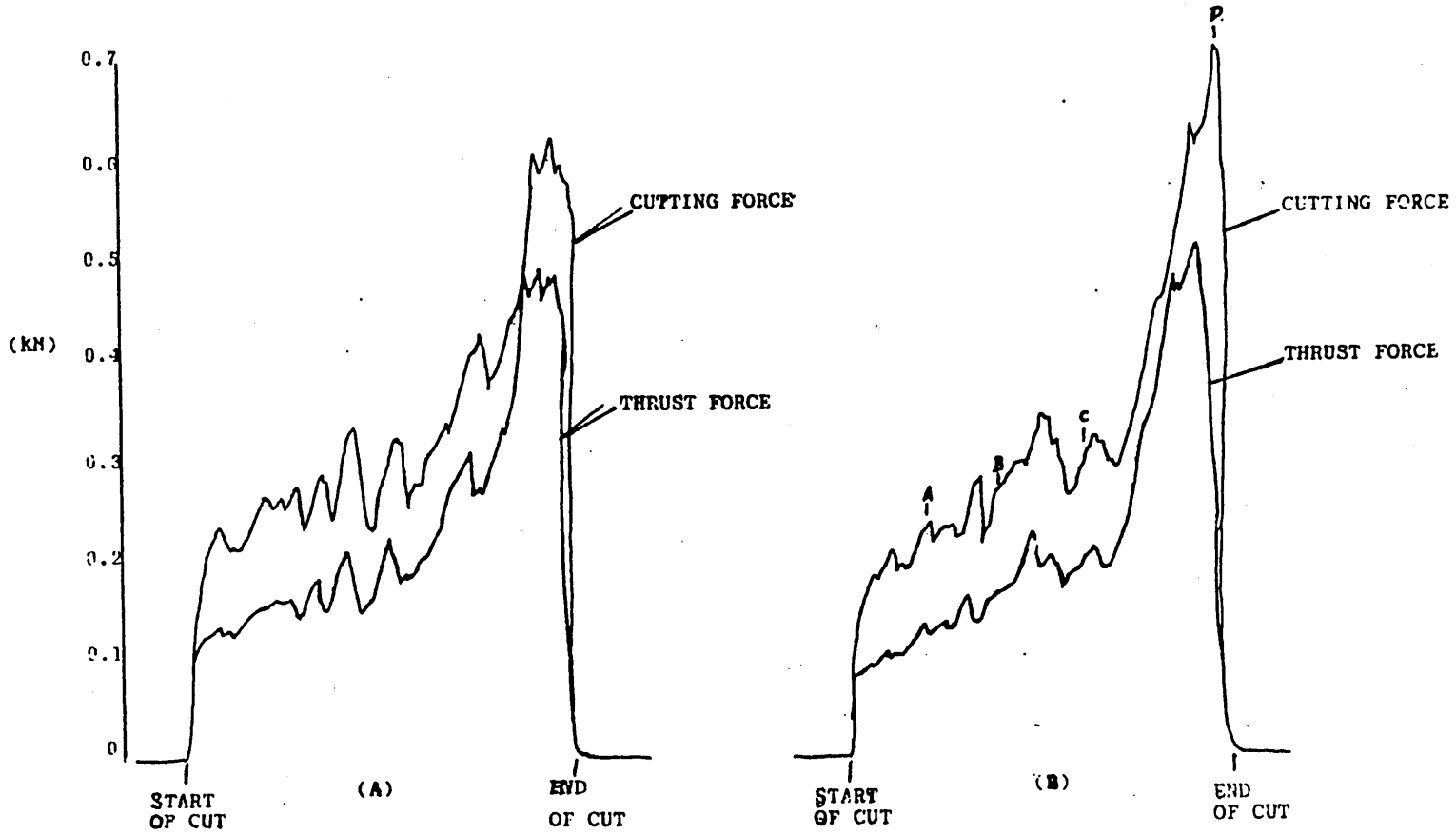

Fig. 3.10. Cutting Force Traces relating to Points A and B on Fig. 3.9.

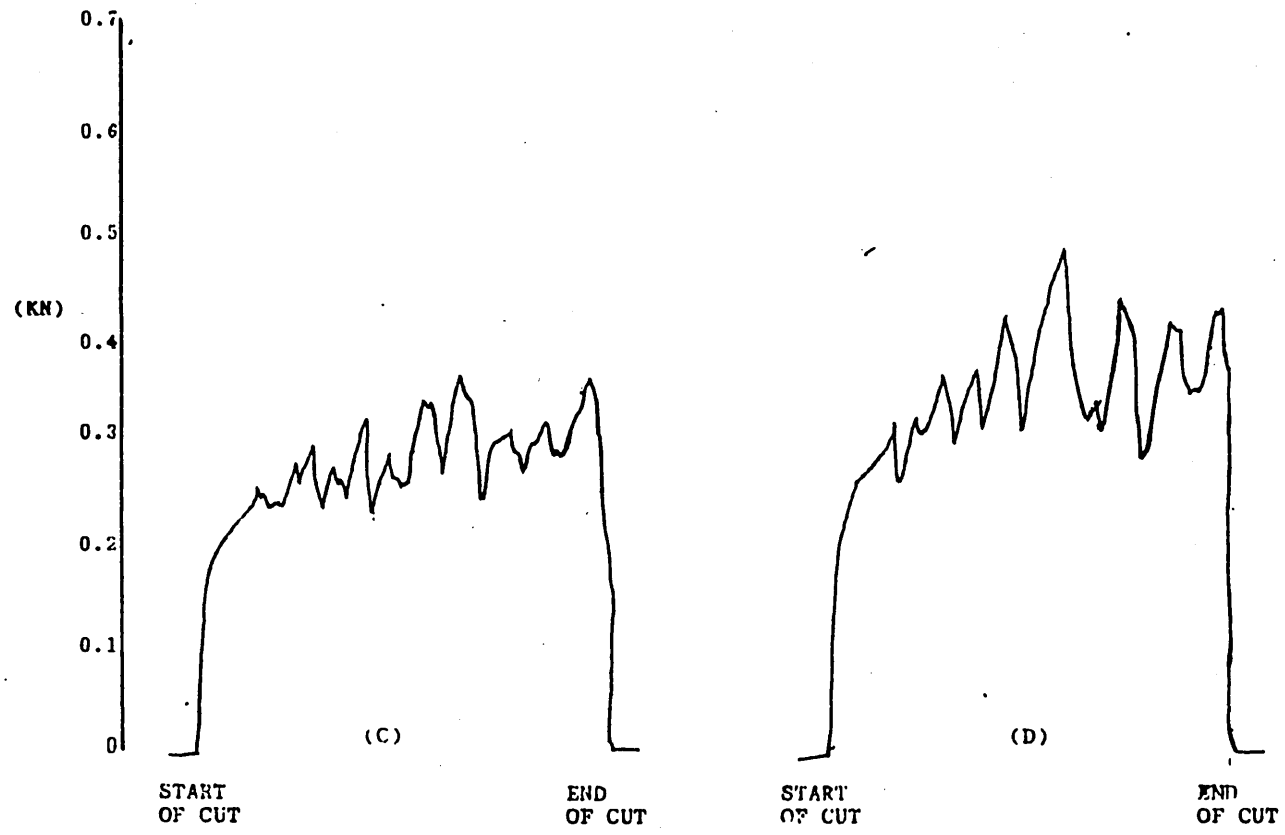

Fig. 3.11. Cutting Force Traces Relating to Points C and D on Fig. 3.9.

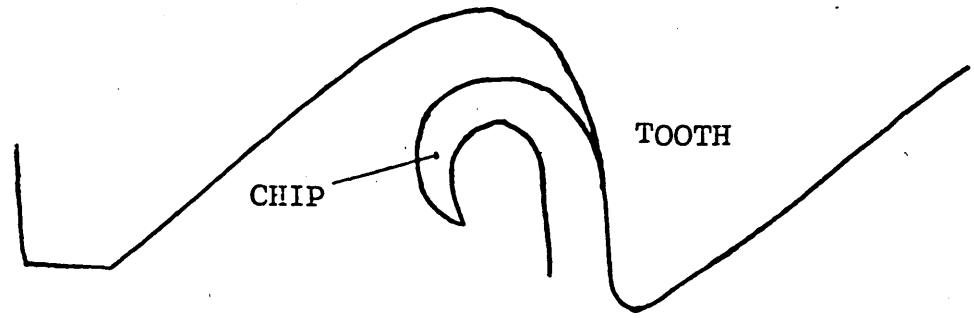

A

The chip curls tightly initially

B

The chip starts to curl again when contact is made with the gullet.

C

The Chip cannot curl further thus its flow up the rake face is restricted.

D

Material builds up in front of the chip, because it cannot flow up the rake face.

Fig. 3.12. Sketches of stages in chip formation in a 10 TPI gullet, cutting mild steel at 95 mm/min. A,B,C and D relate to points on fig. 3.9.

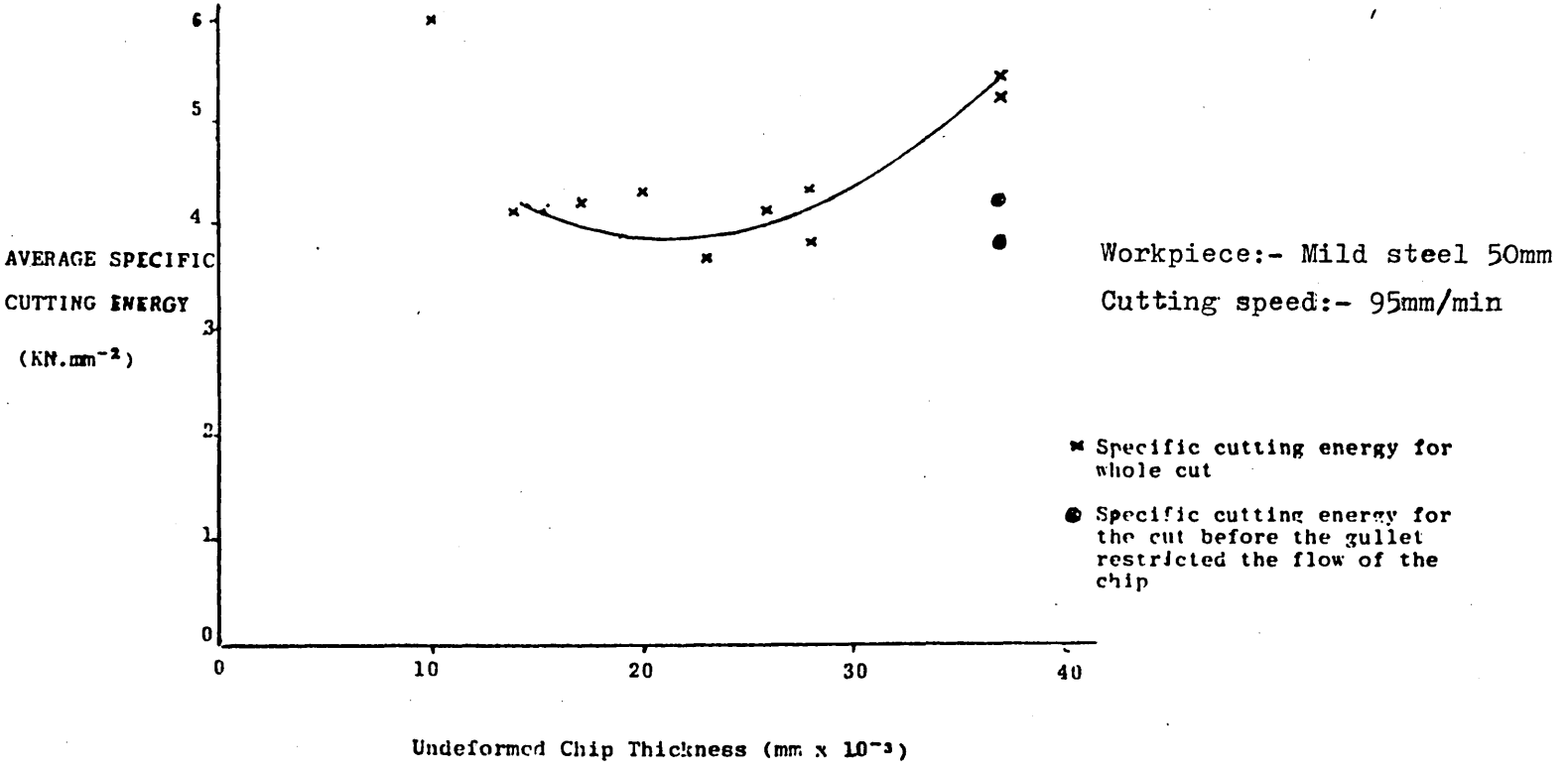

Fig. 3.13. Average Specific Cutting Energy v. Undeformed Chip Thickness for a 10 TPI tooth.

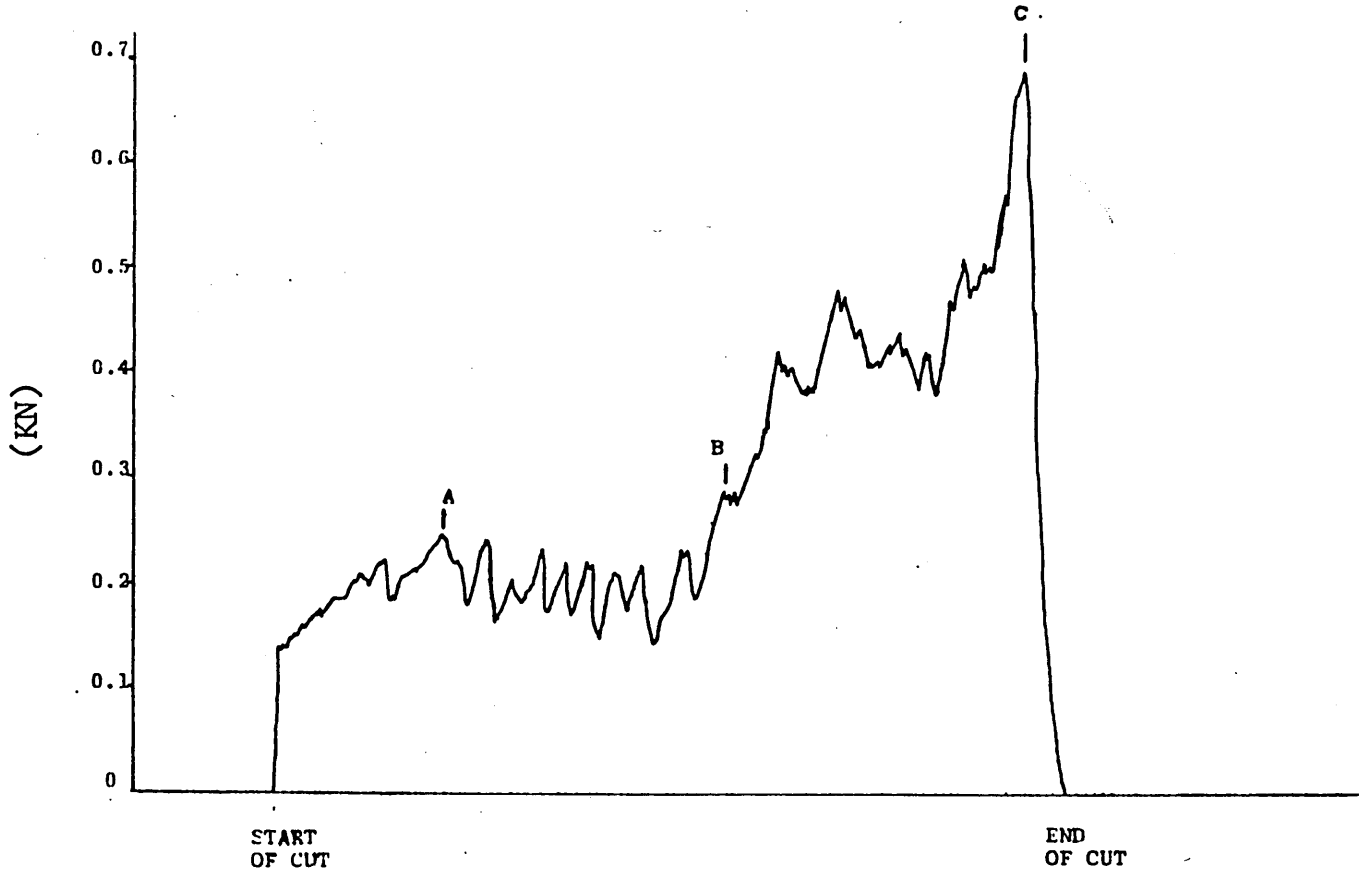

Fig. 3.14. Cutting Force Trace of 10 TPI Tooth Cutting Mild Steel 50 mm Points A, B and C relate to sketches of Chip Formation Fig. 3.14b. Undeformed Chip Thickness 0.029 mm.

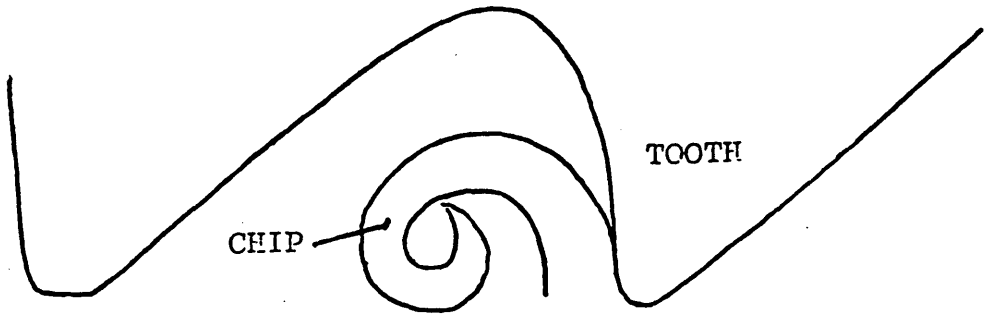

A

Chip curls unrestrained by gullet

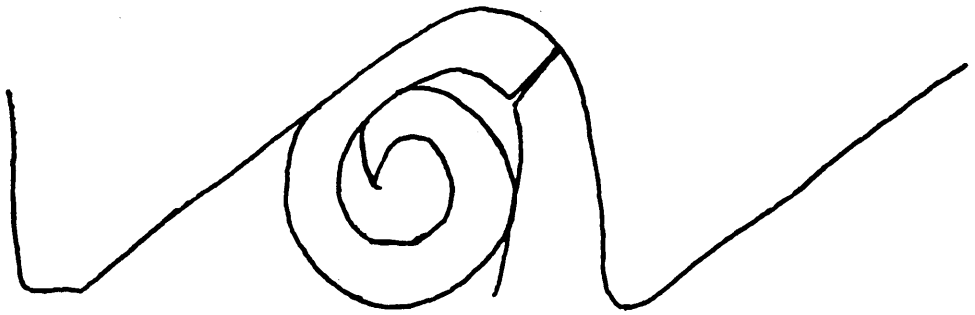

B

Chip stops flowing up the rake face because it can no longer curl

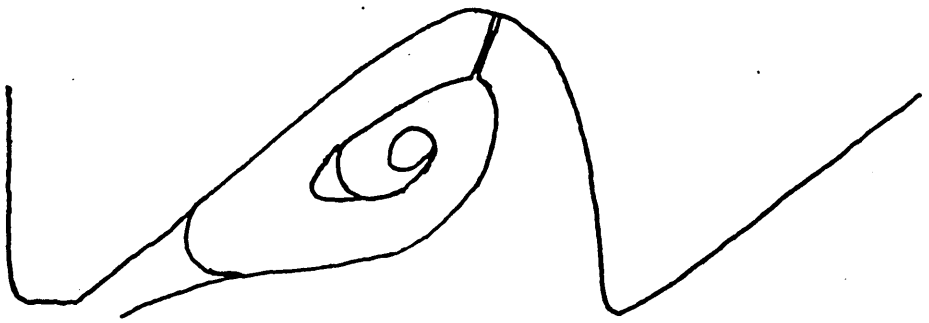

C

Material has piled up in front of the chip because it cannot flow upwards

Fig. 3.14b. Chip Formation in 10 TPI Gullet
A, B and C relate to points on the Force Trace fig. 3.14a.

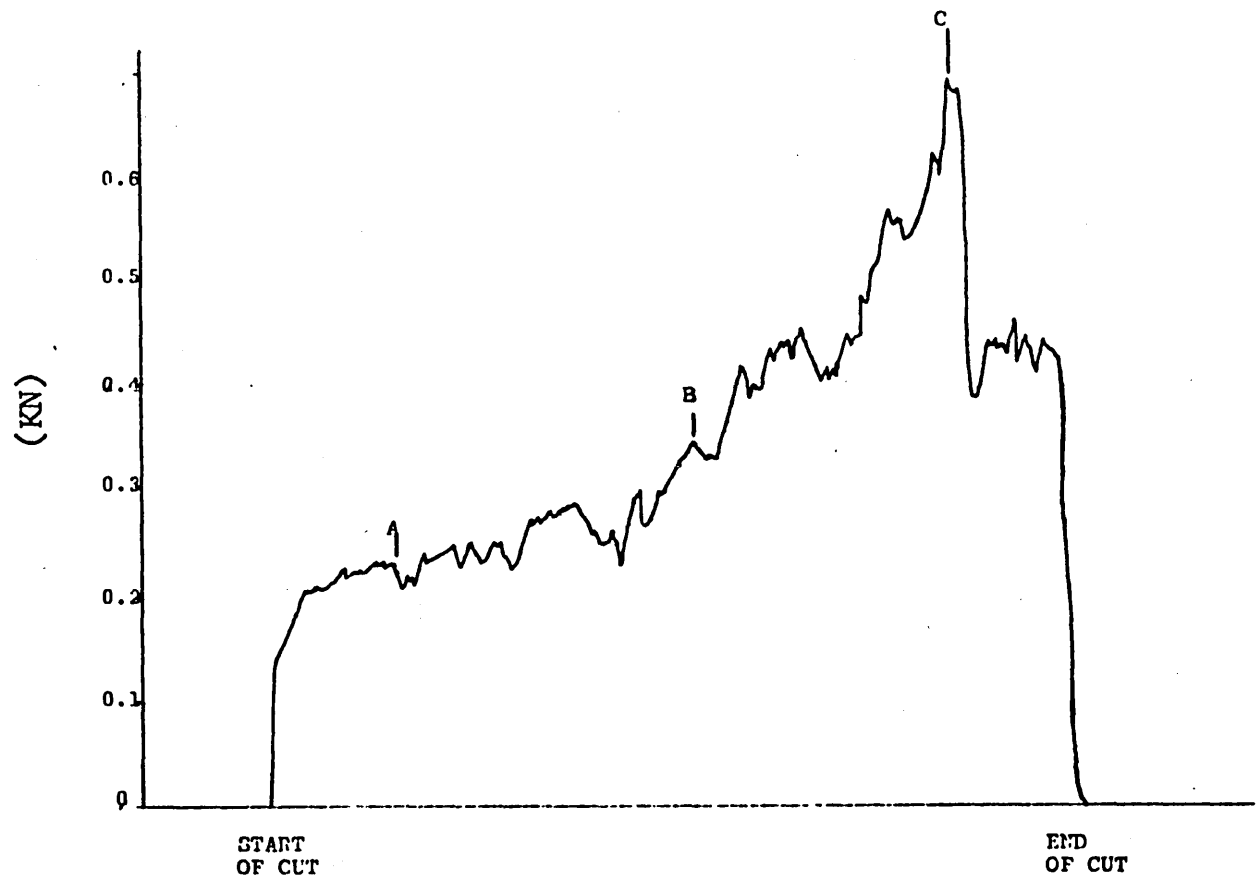

Fig. 3.15.a. Cutting Force Trace of 10 TPI Tooth Cutting Mild Steel 50 mm Points A, B and C relate to sketches of chip formation fig. 3.15.b. Undeformed chip thickness 0.26 mm. The cutting edge broke at point C.

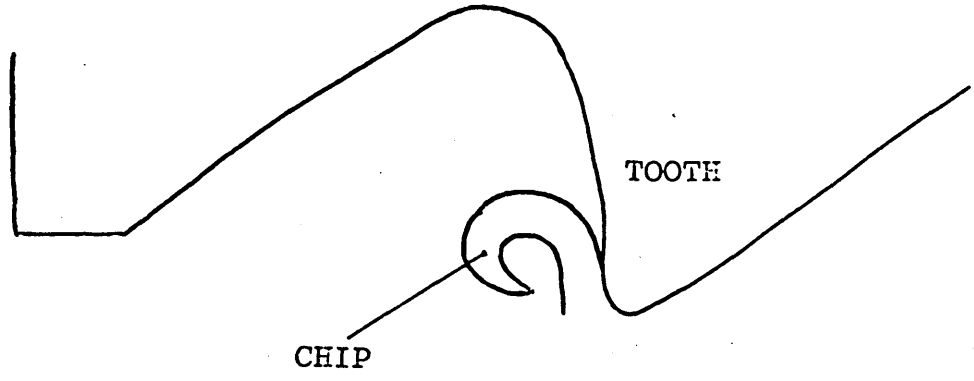

A

Chip curls unrestrained by gullet

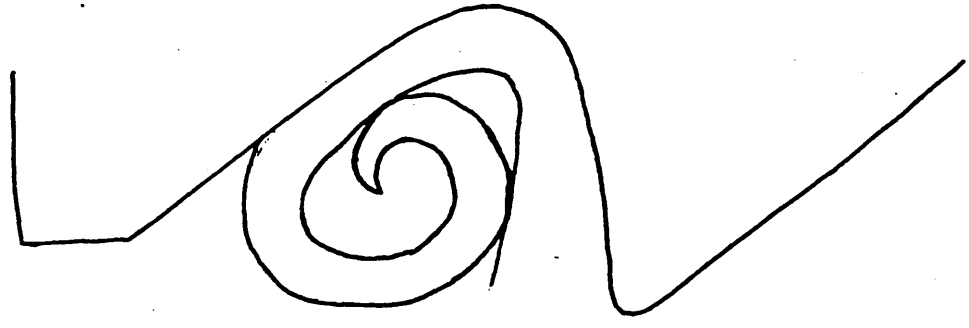

B

Chip has stopped flowing up the rake face, because it can no longer gurl and has started to thicken.

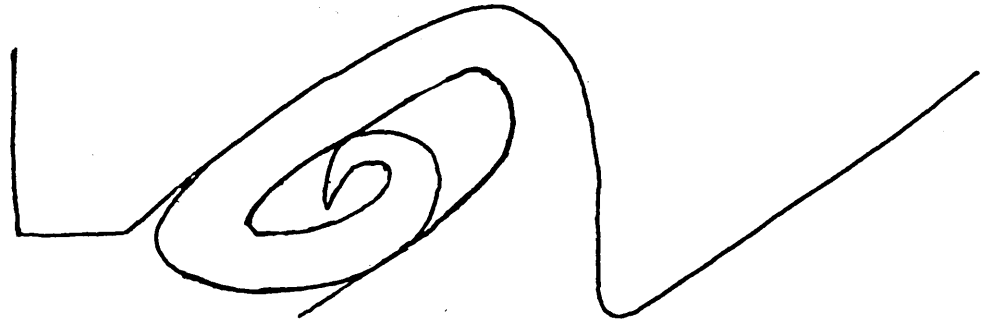

C

Material has piled up in front of the chip because it cannot flow upwards.

Fig. 3.15.b. Chip Formation in a 10 TPI Gullet

A, B and C relate to points on force trace fig. 3.15.a.

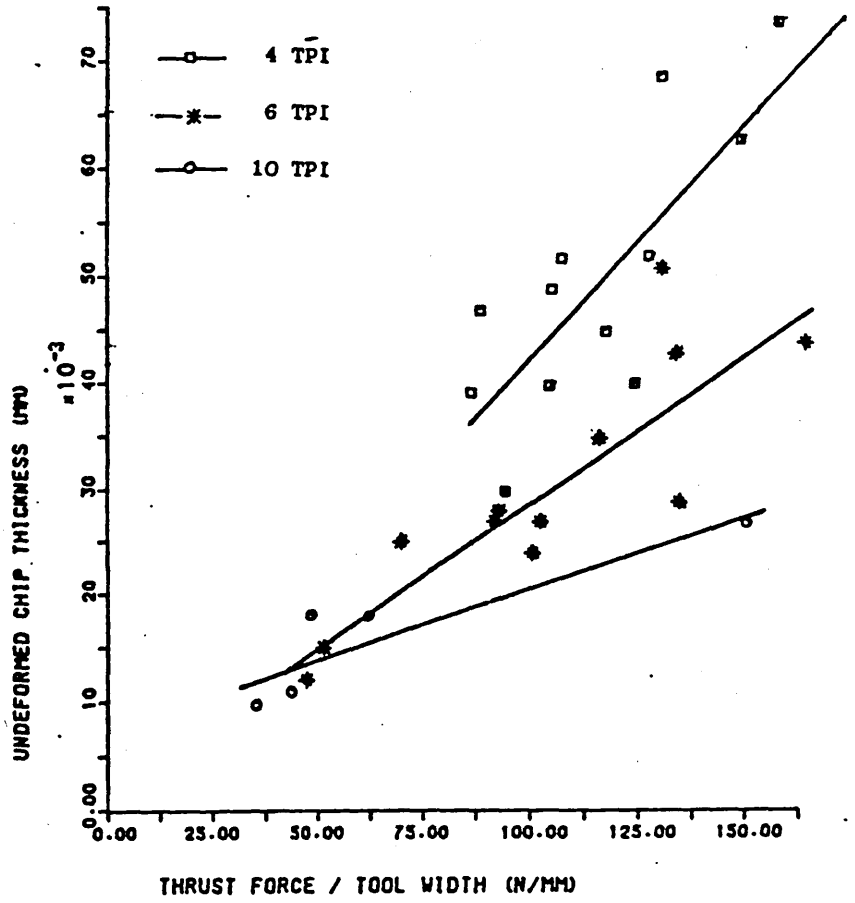

Fig. 3.16. 4, 6 and 10 TPI Tooth and Gullet Cutting 50 mm Mild Steel Workpiece.
Cutting speed 95mm/min

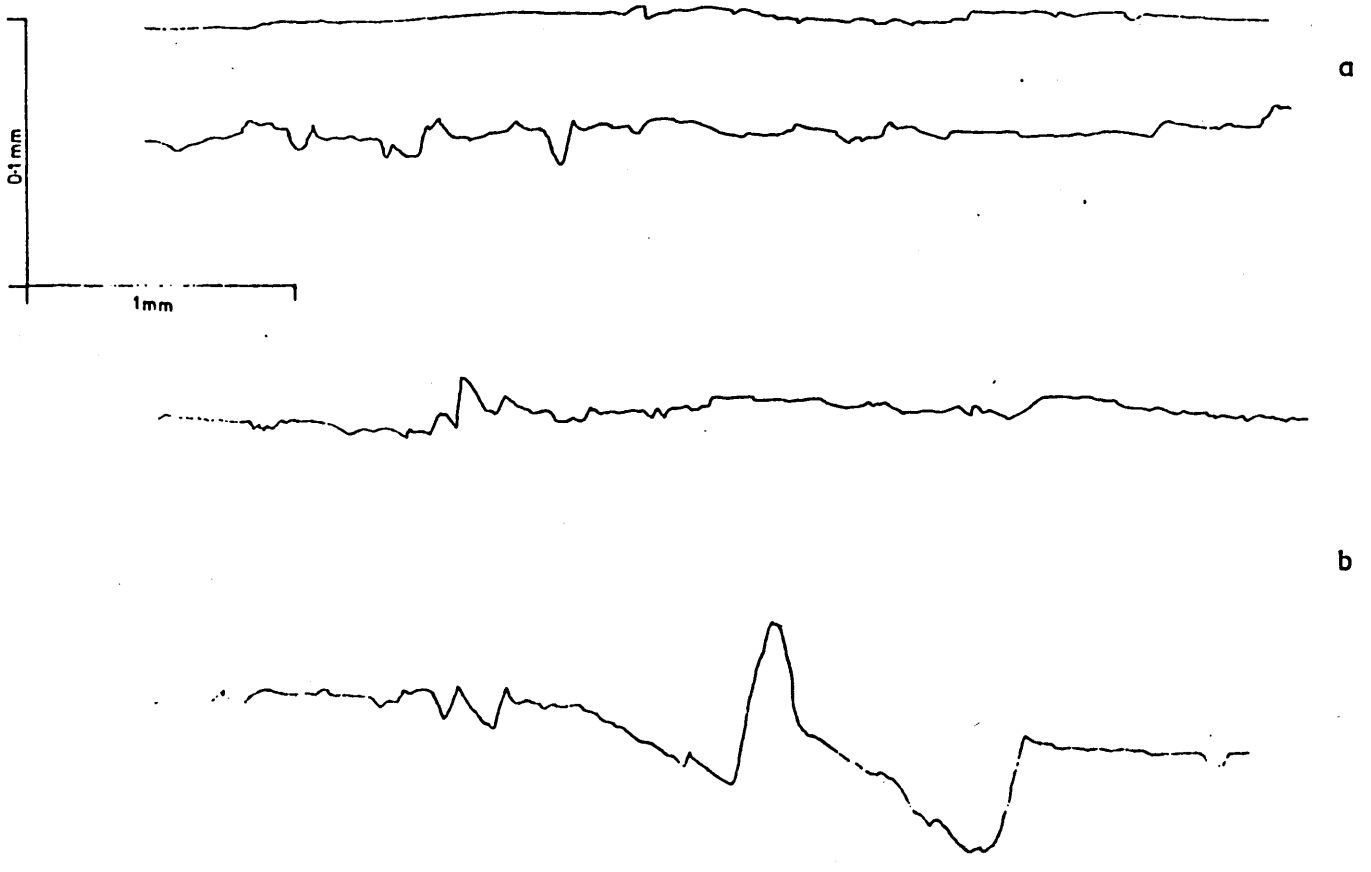

Fig. 3.17. Surface finish traces of:

a) the first and last 5.6 mm of a slot bed produced by sawing
and b) the first and last 5.6 mm of a slot bed produced by a 4 TPI tooth cutting at 95 mm/min.

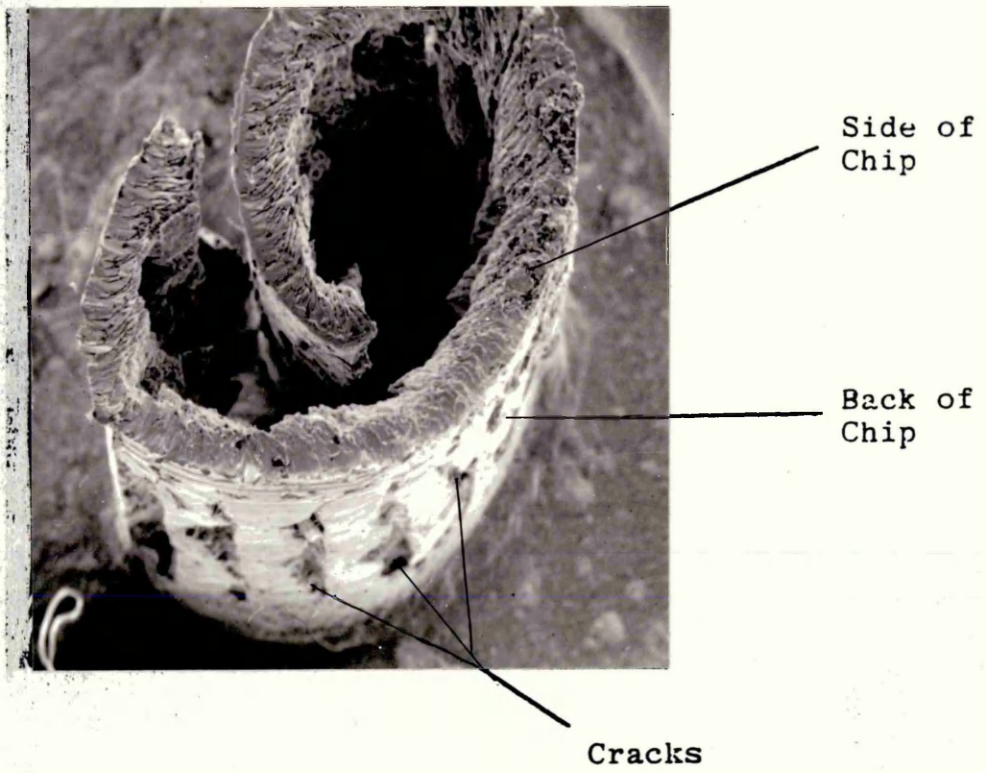

Fig.3.18. SEM photograph of a chip cut by a single 4 TPI hacksaw tooth at 95 mm/min. 50 mm wide mild steel workpiece.

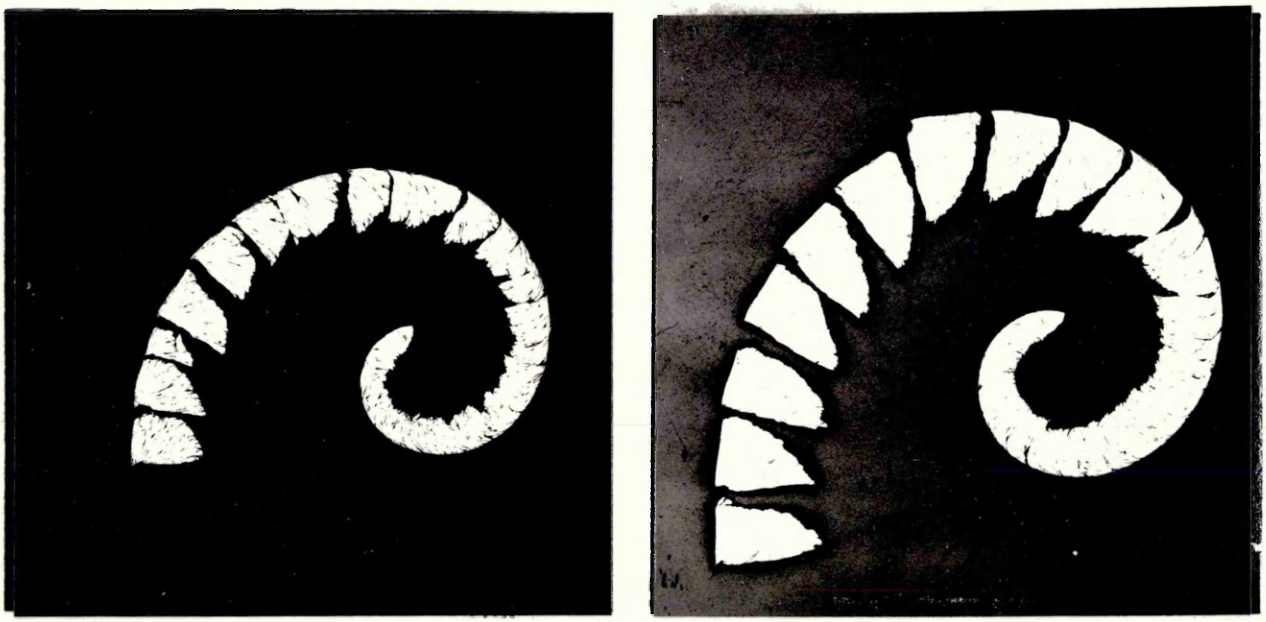

Fig. 3.19.

Chips produced cutting mild steel with single hacksaw teeth at 95 mm/min. 50 mm wide workpiece.

Magnification x 30

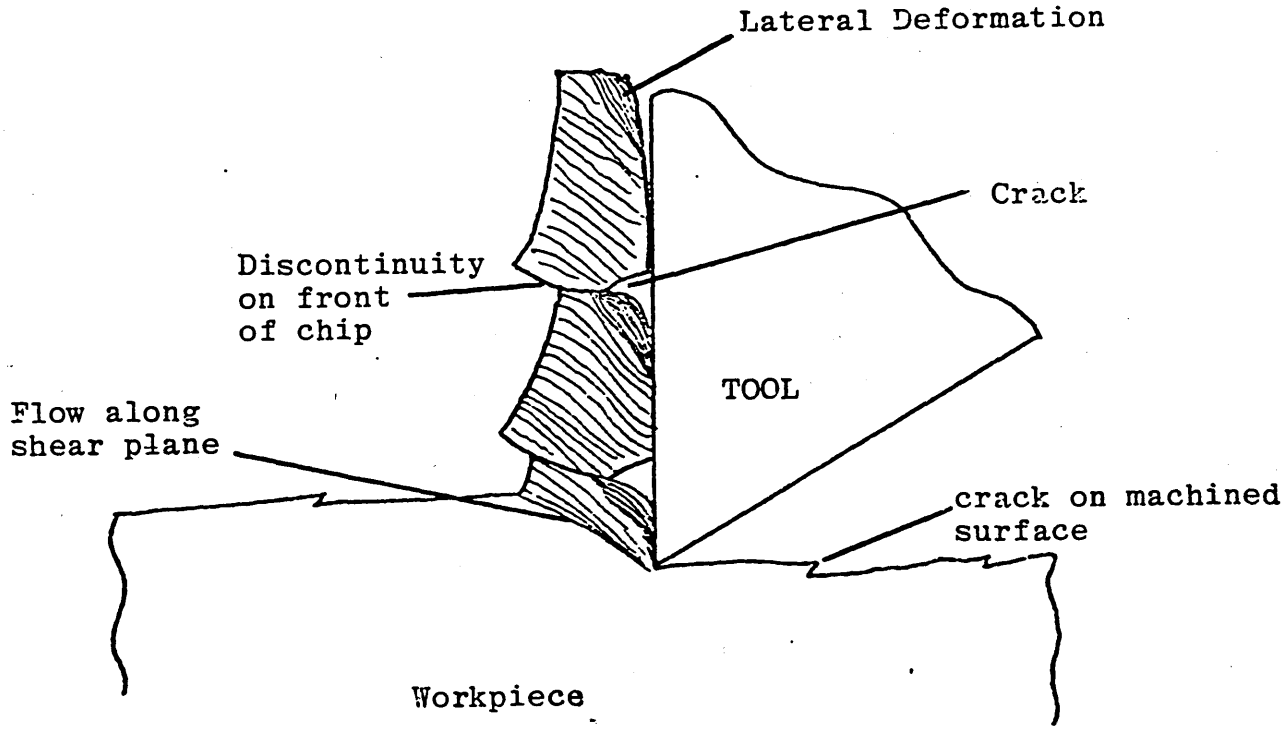

Fig. 3.20. Diagram of 'Non-Built-Up-Edge' chip formation at low speeds, as described by K.L. Chandiramani and N E Cook (ref. 12.)

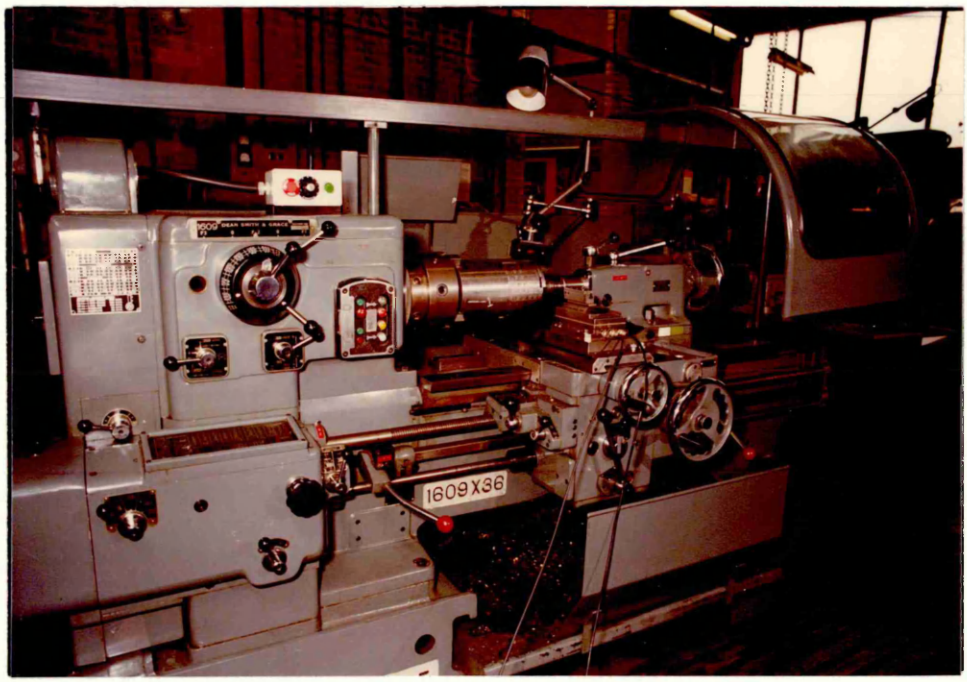

Fig. 4.1. The Screw Cutting Lathe used in the single tooth tests at realistic cutting speeds.

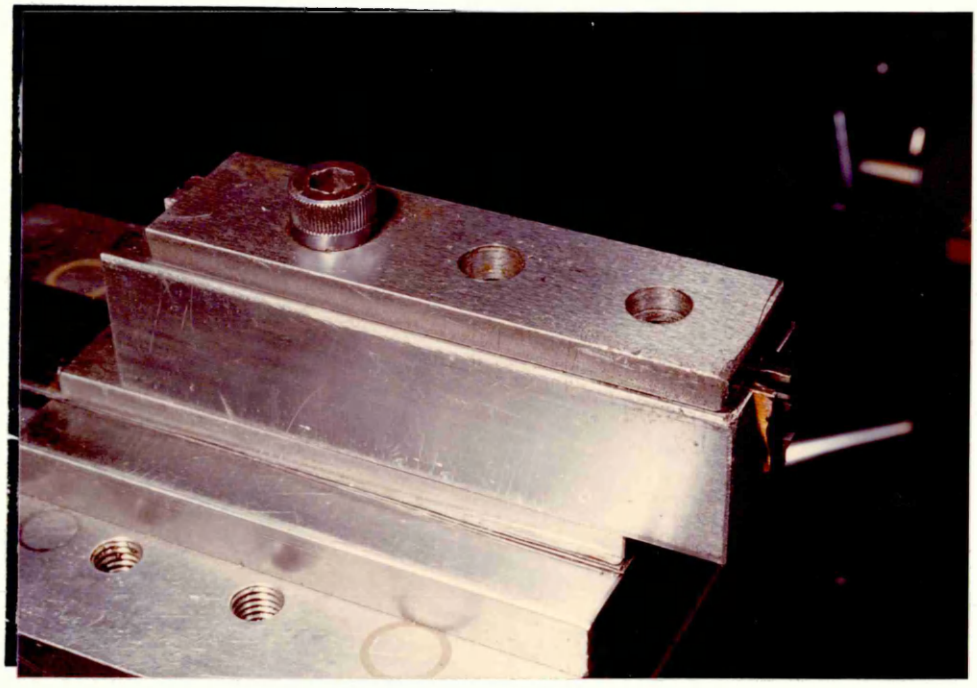

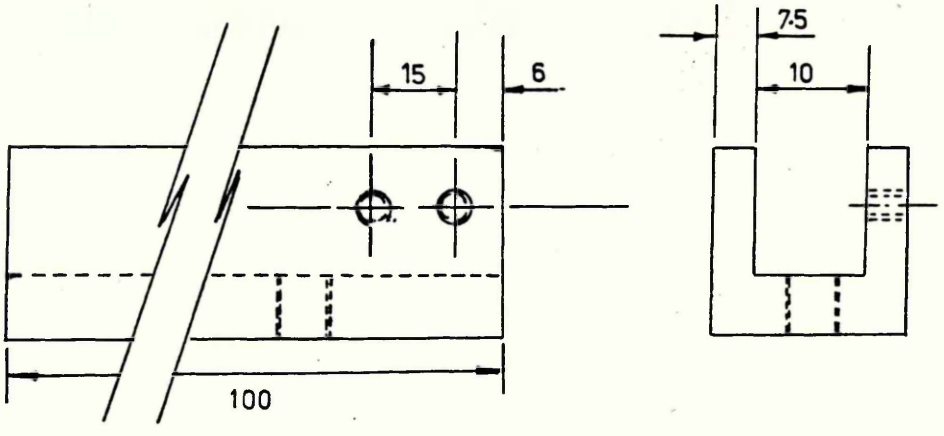

Fig. 4.2. The holder for the single hacksaw teeth in fig. 3.1. Dimensions in millimetres.

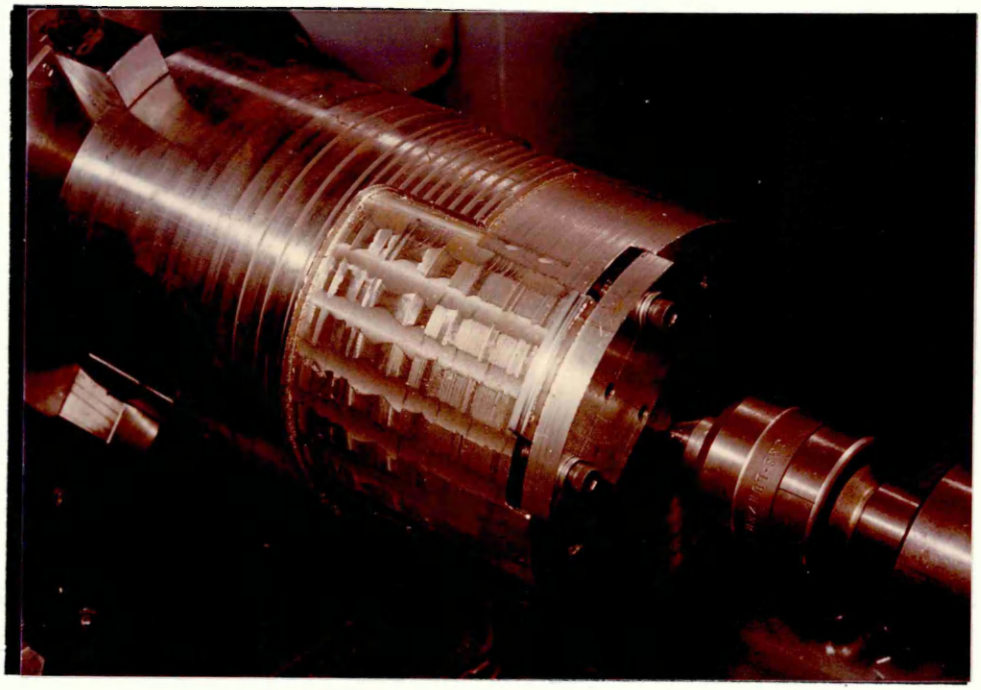

WORKPIECE HOLDER

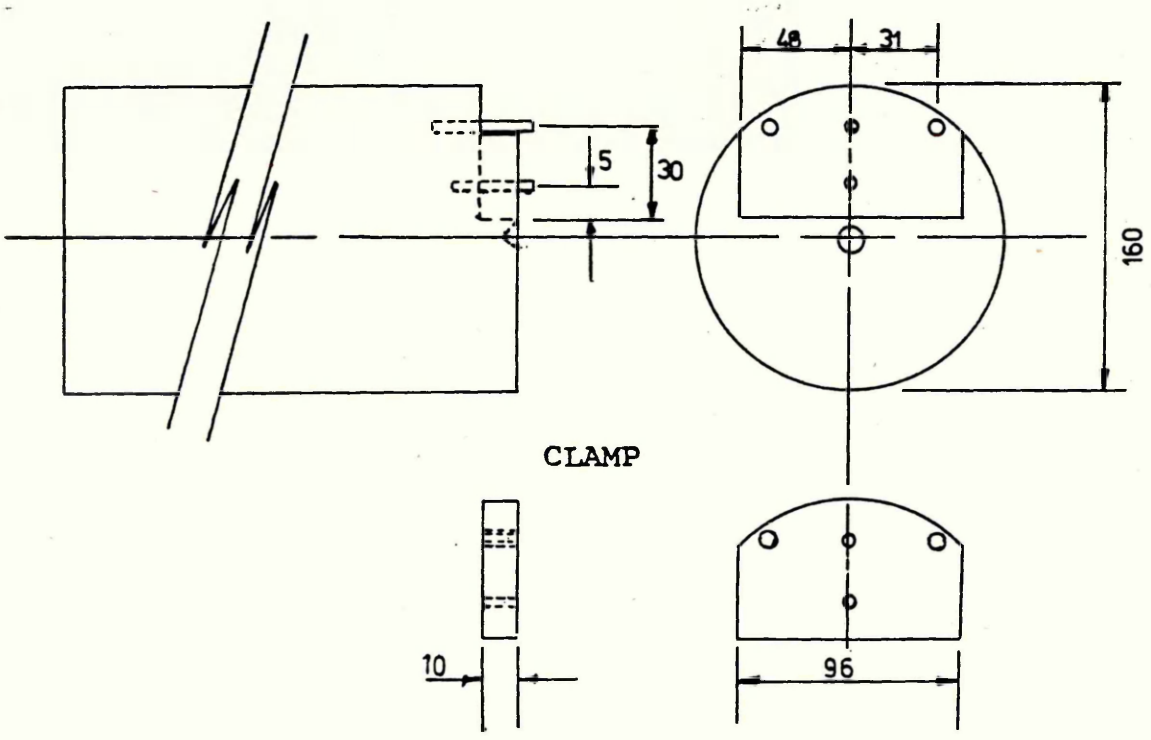

Fig. 4.3. Workpiece holder for Single Tooth Tests at realistic cutting speeds. (Workpieces fig. 4.4.). Dimensions in mm.

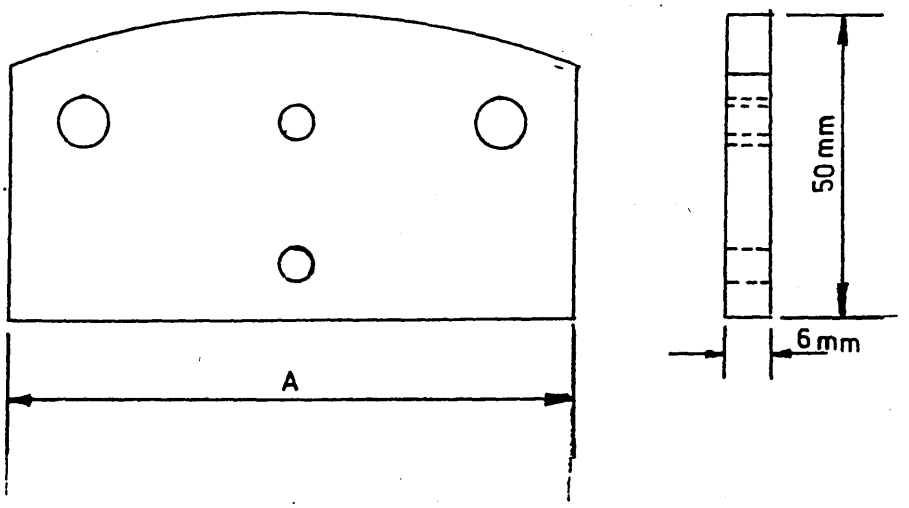

Length of cut (mm)	75	50	25	12
Dimension A(mm)	72	48	24	11.5

Fig. 4.4. Workpiece dimensions for single tooth tests at realistic speeds

Fig. 4.5.a. The Instrumentation used for the Single Tooth Tests at realistic cutting speeds.

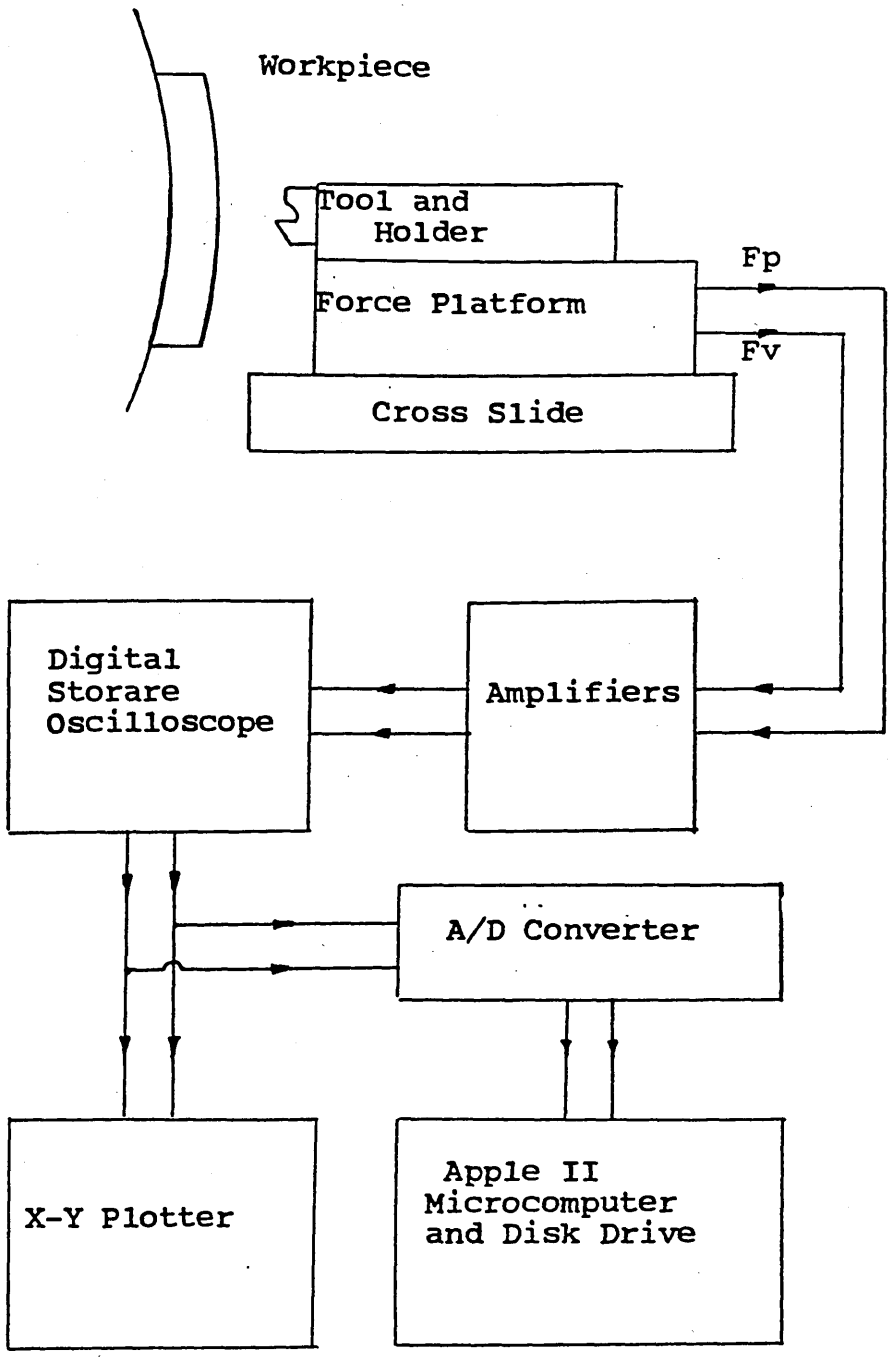

Fig. 4.5.b. Diagrammatic Lay-out of the Instrumentation used for the Single Tooth Tests at realistic cutting speeds.

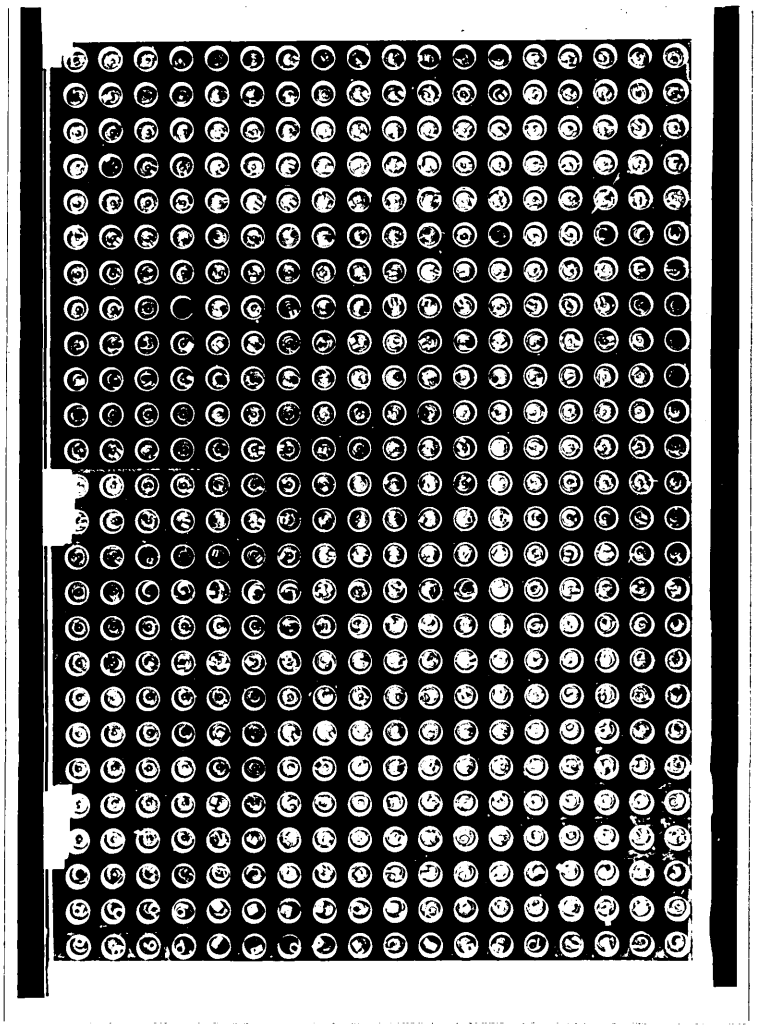

Fig. 4.6. The Perspex Tray used to display the chips produced during the Single Tooth Tests at realistic cutting speeds.

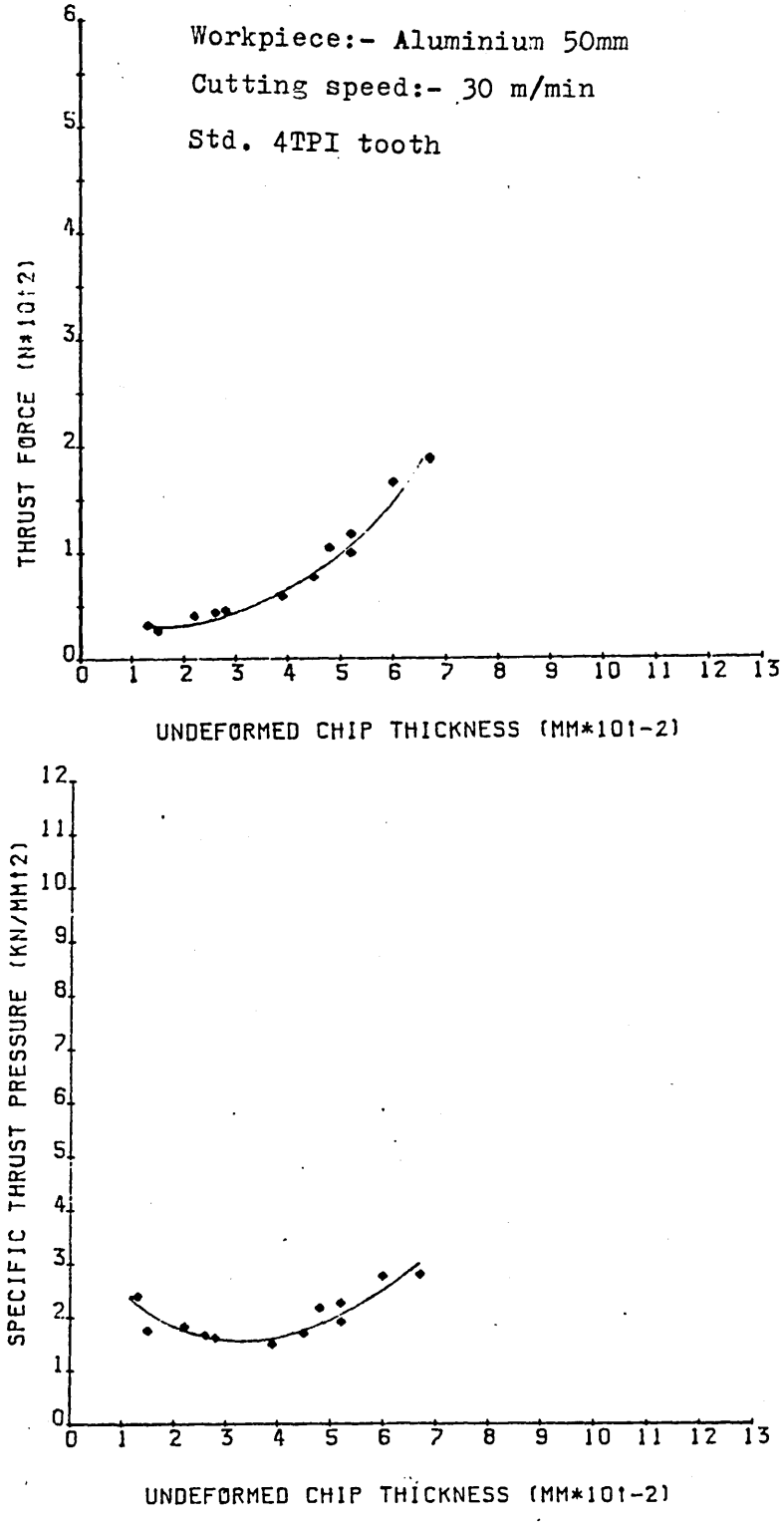

Fig. 4.7. The performance of a 4 TPI tooth cutting aluminium
a) showing thrust force/unit width of tooth v UCT
and b) showing specific thrust pressure v UCT.

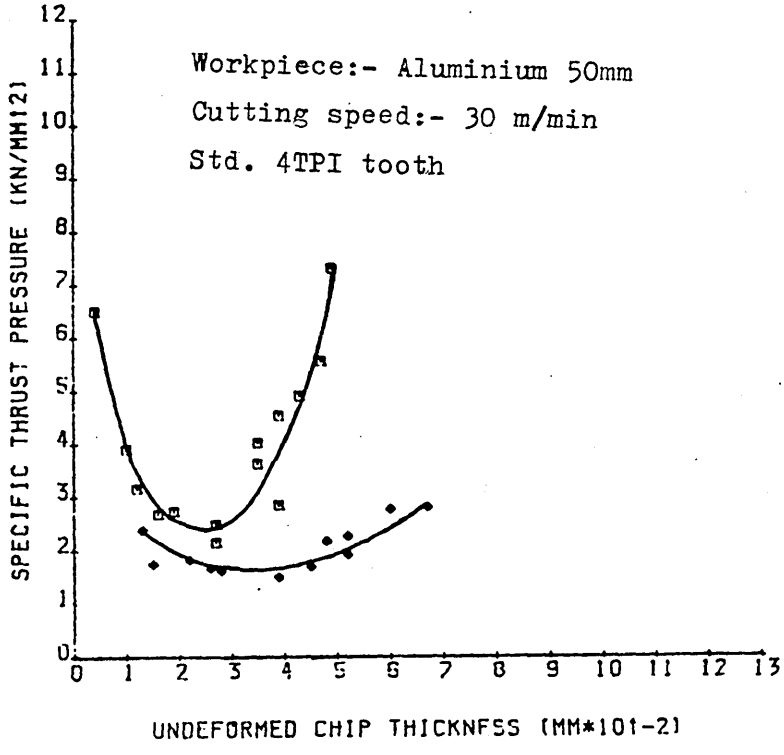

Fig. 4.8. The performance of a 4 TPI tooth cutting aluminium ◇
and the performance of a 6 TPI tooth cutting aluminium ◻

. Length of cut 50 mm

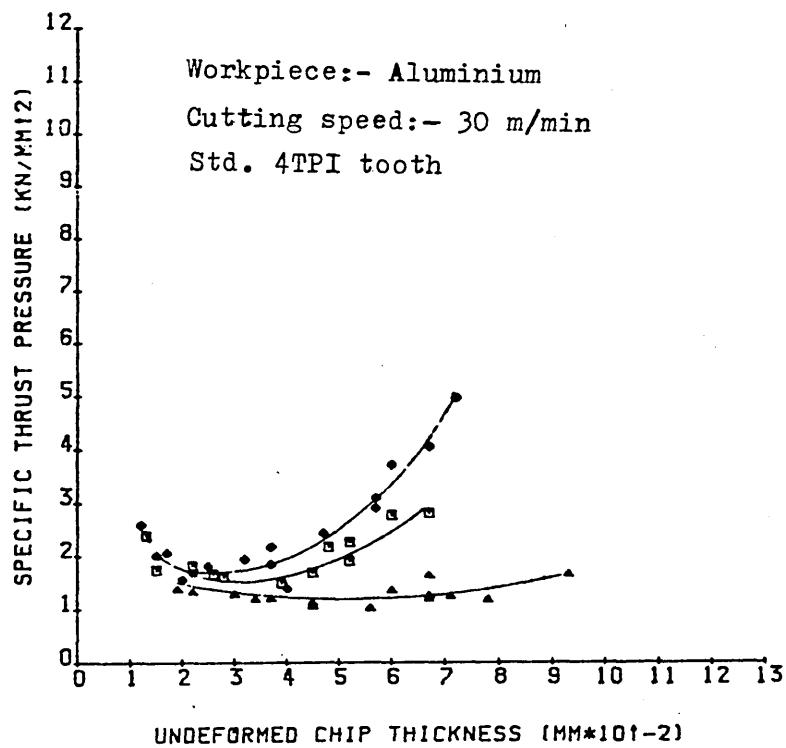

Fig. 4.9. The performance of a 4 TPI tooth cutting aluminium at three different lengths of cut.

◇ 75 mm

⊡ 50 mm

Δ 25 mm

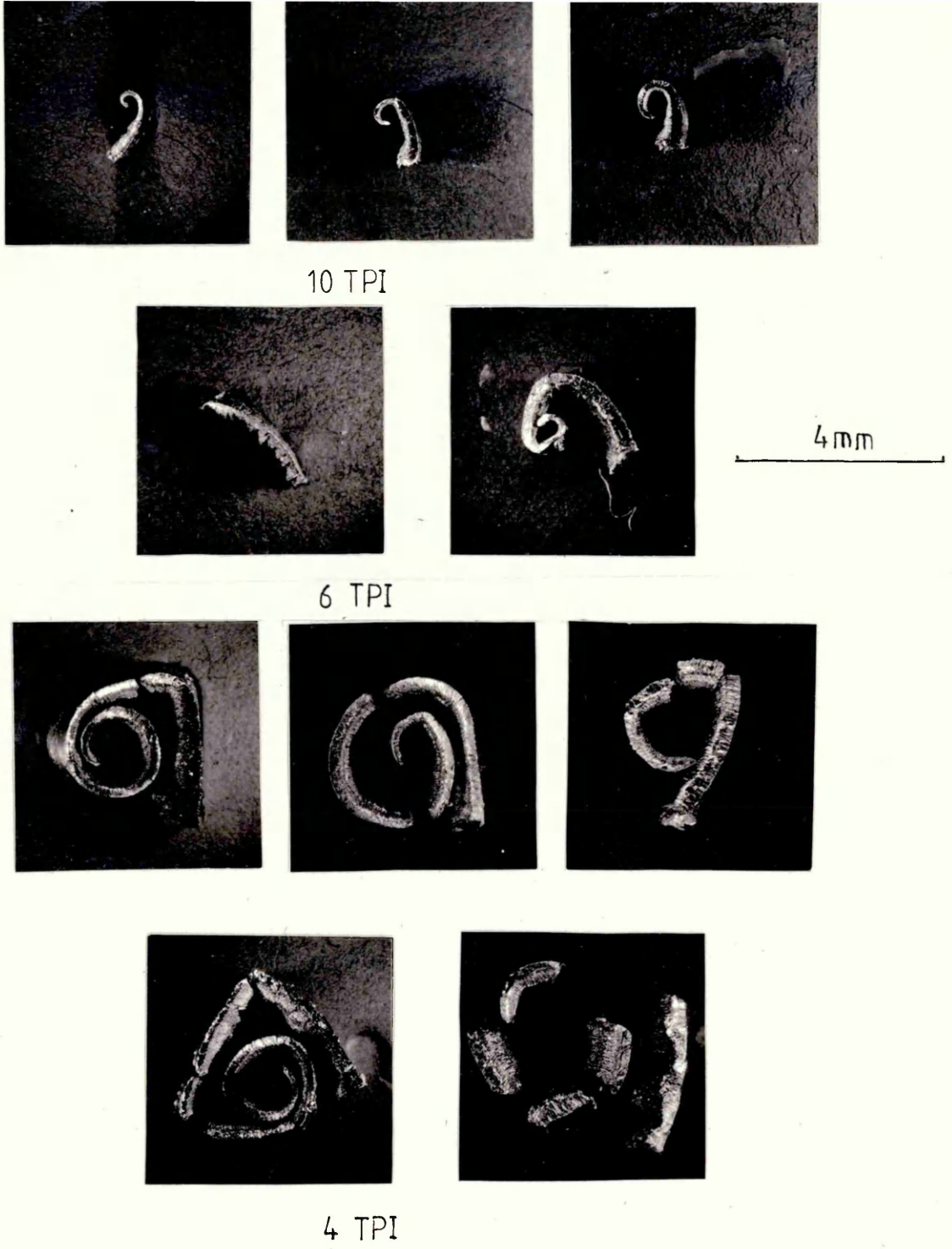

Fig 4.10 Some Mild Steel Chips Produced by Single Hacksaw Teeth Cutting at a Realistic Cutting Speed

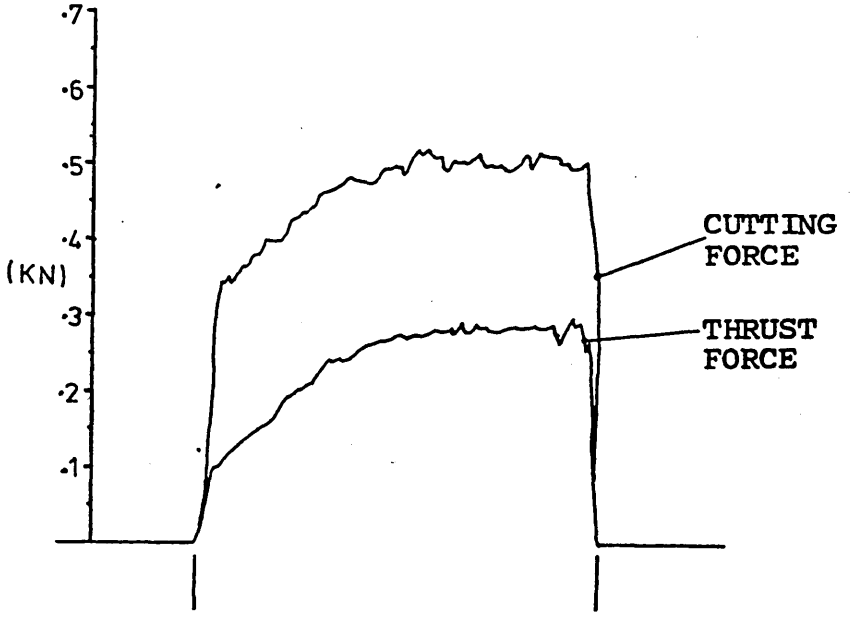

Fig. 4.11. Cutting and thrust force traces for a standard 4 TPI Tooth Cutting 25 mm of Mild Steel. Undeformed Chip thickness 0.071 mm

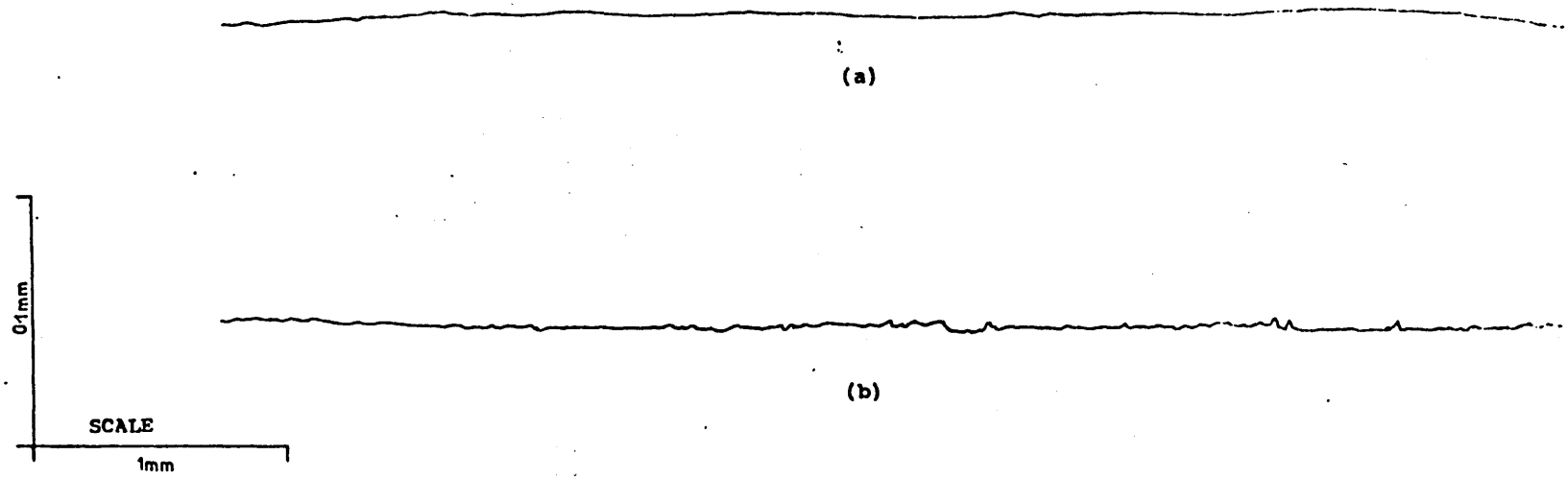

Fig. 4.12. Typical surface finish trace of the slot bed caused by a 4 TPI tooth cutting 50 mm Mild Steel at 30 m/min. Trace (a) is the first 5.6 mm of the slot & trace (b) the last 5.6 mm of the slot.

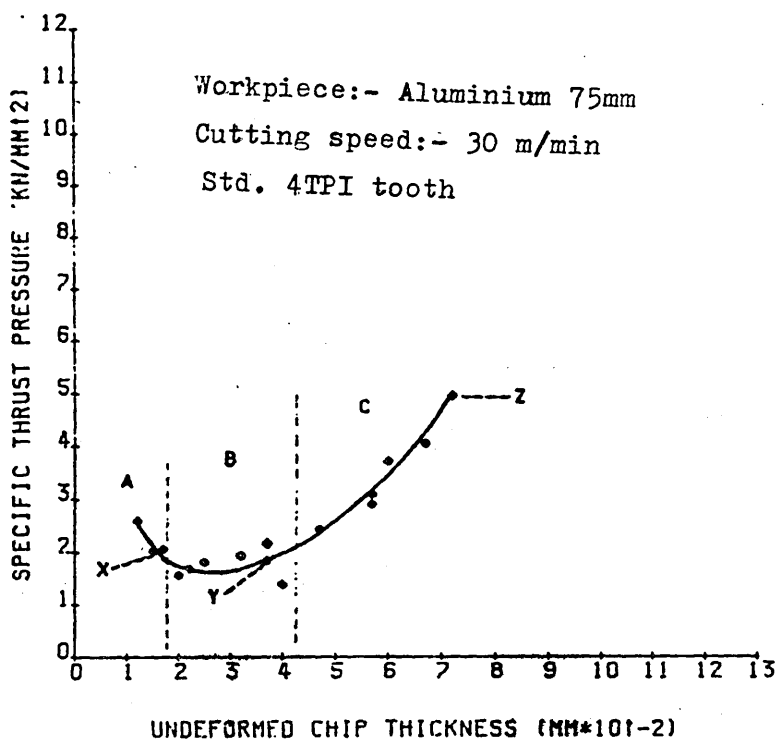

Fig. 4.13. Performance of a standard 4 TPI tooth cutting Aluminium. Length of cut. 75 mm. Cutting speed 30 m/min.

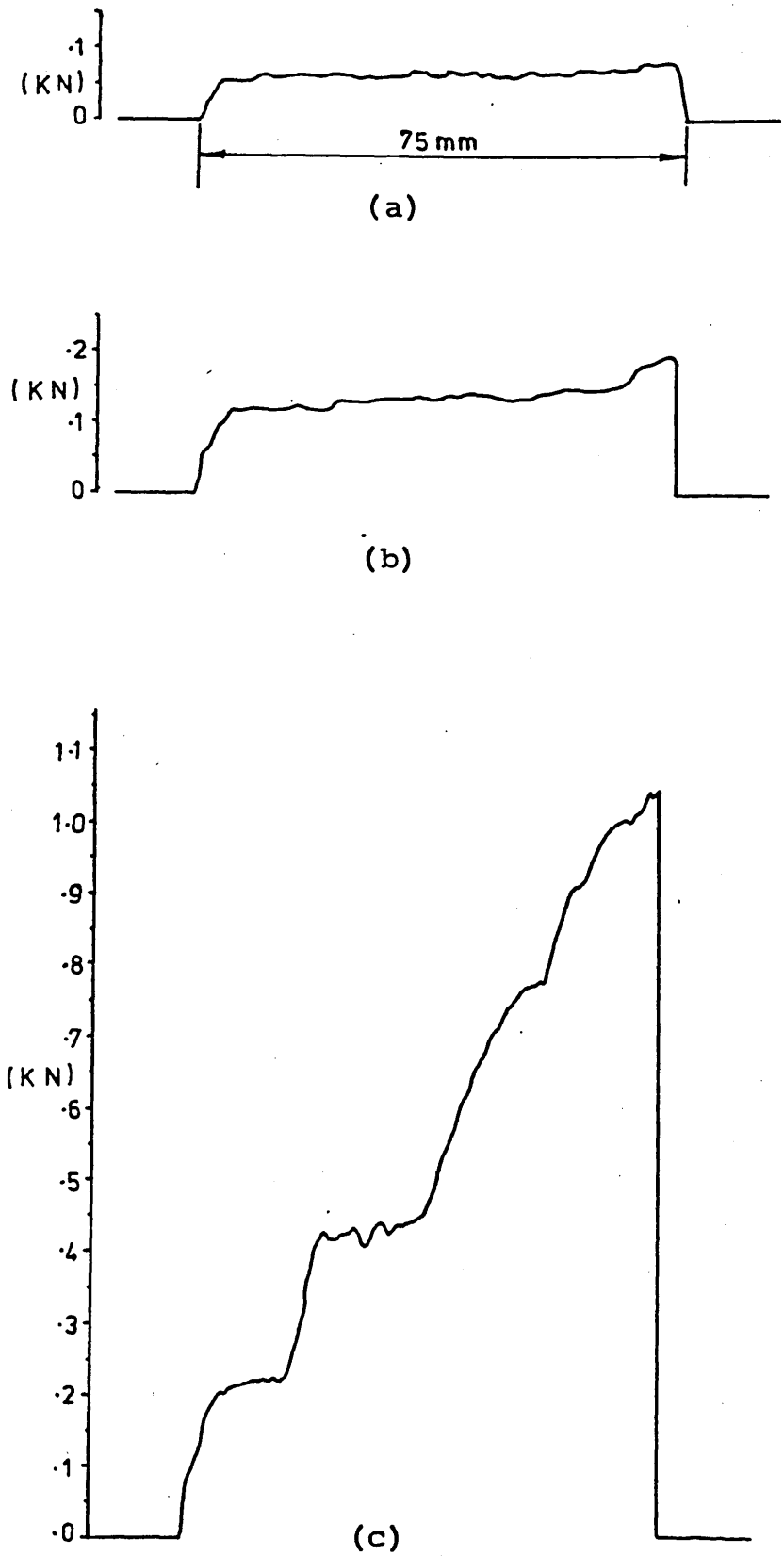

Fig. 4.14. Thrust force traces for points X, Y and Z in fig.4.13. Trace (a) is for point X, (b) is for point Y and (c) is for point Z.

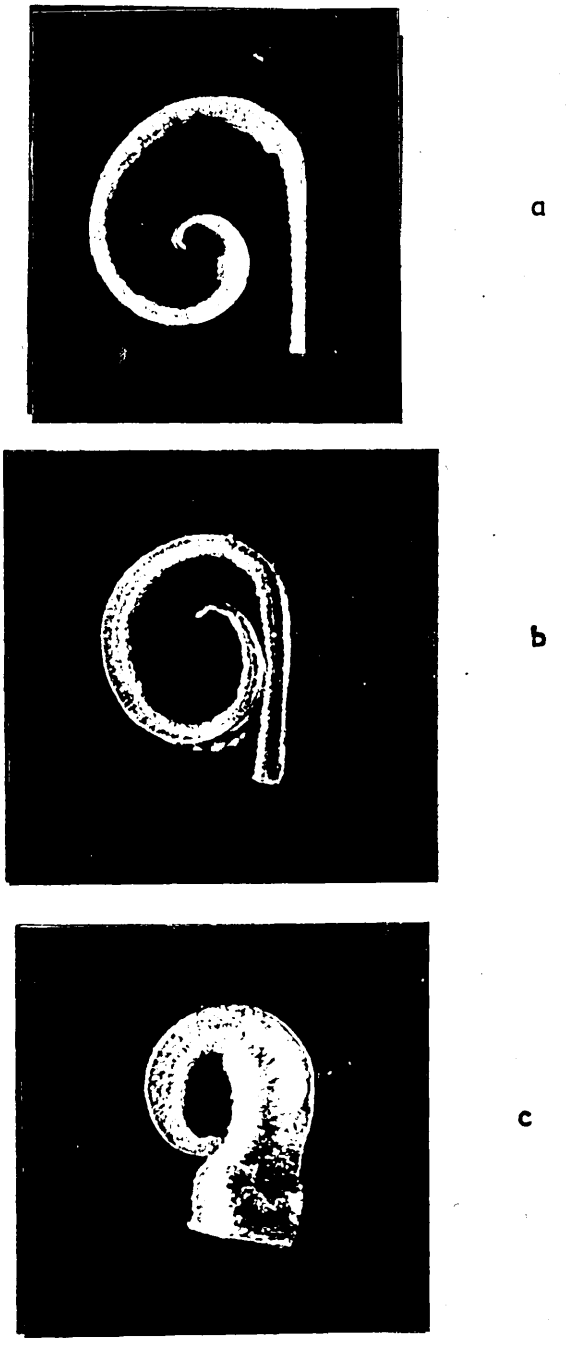

Fig. 4.15. Chips relating to points X, Y and Z in 4.13
Chip (a) relates to point X, (b) to point Y, and (c) to point Z.

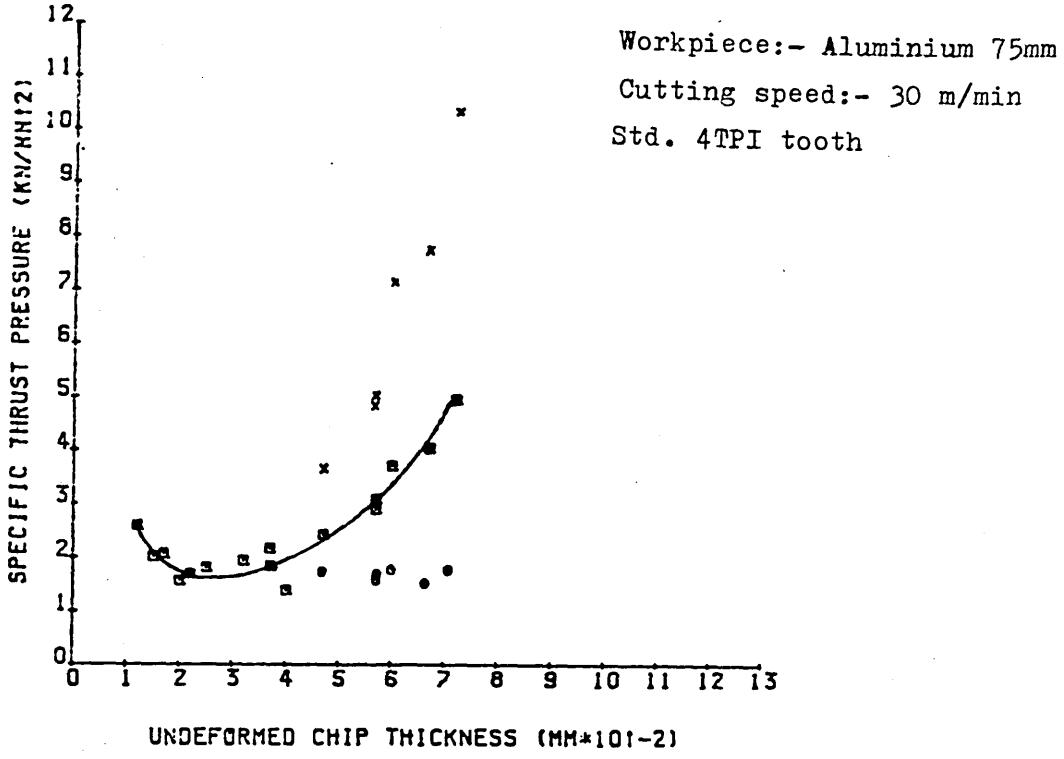

Fig. 4.16. Graph showing, for a standard 4 TPI tooth cutting aluminium
a) the average performance over each cut, ⊡
b) the instantaneous maximum specific thrust pressure, x
and c) the instantaneous specific thrust pressure before restriction of chip flow occurred. ⊙

Length of cut 75 mm. Cutting speed 30 m/min.

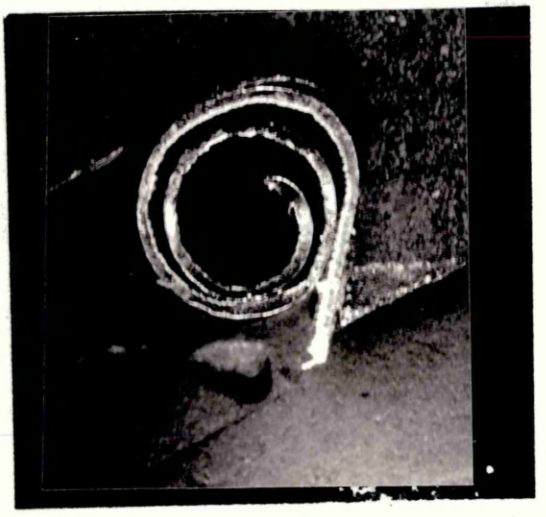

a

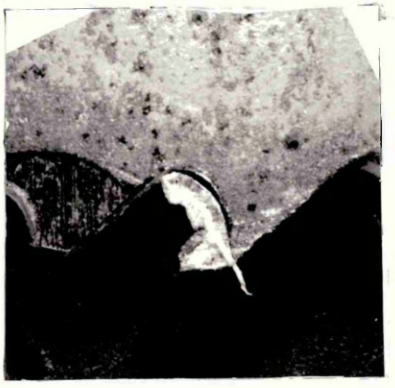

b

Fig. 4.17. Aluminium chips cut by a) a standard 4 TPI tooth
and b) a standard 10 TPI tooth

Undeformed chip thickness for a) was 0.04 mm
and for b) was 0.039 mm

Length of cut for a) was 75 mm
and for b) was 12 mm

Cutting speed 30 m/min.

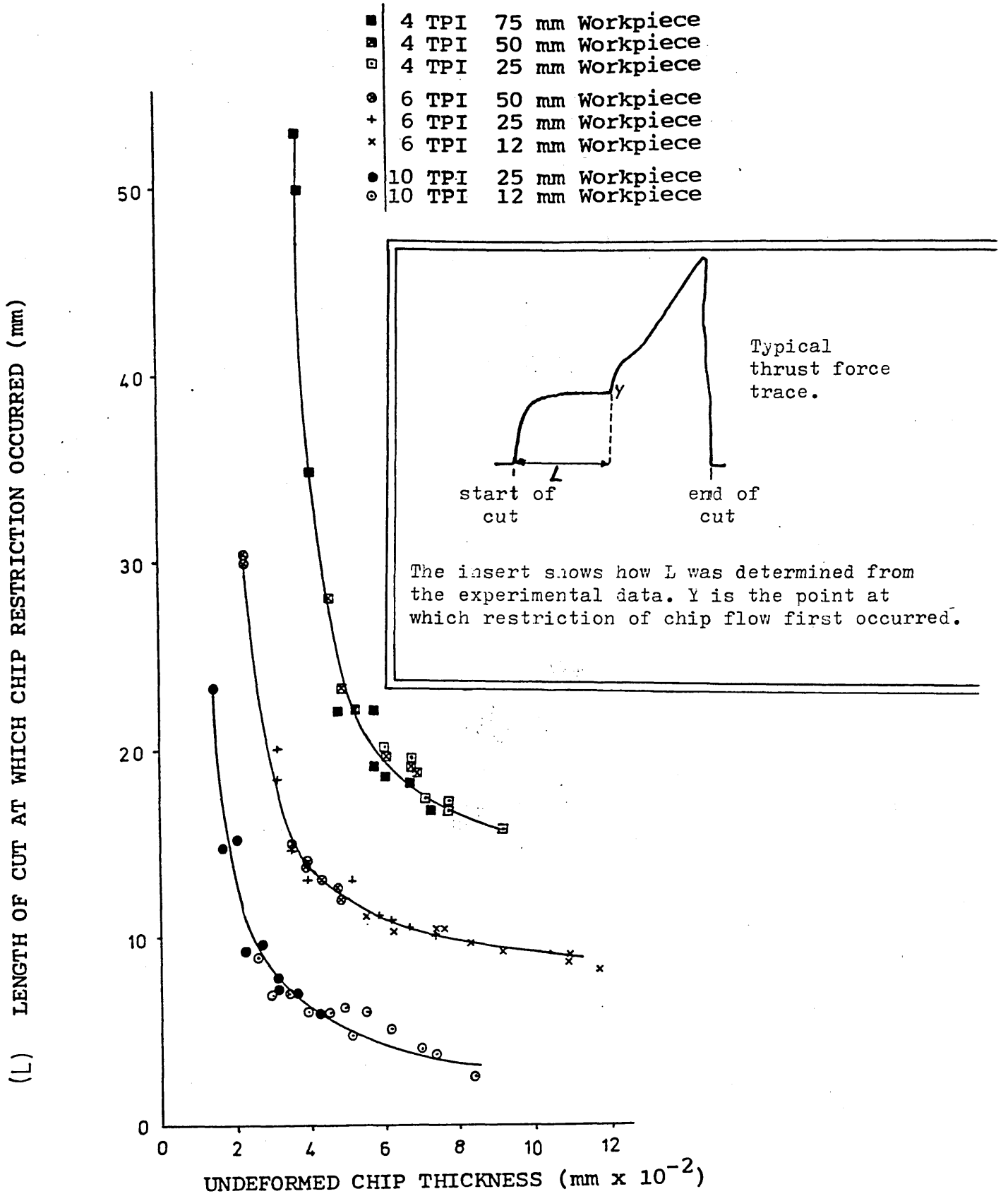

Fig. 4.18. Graph showing the length of cut at which chip flow was first restricted in standard 4, 6 and 10 TPI teeth cutting aluminium at 30 m/min.

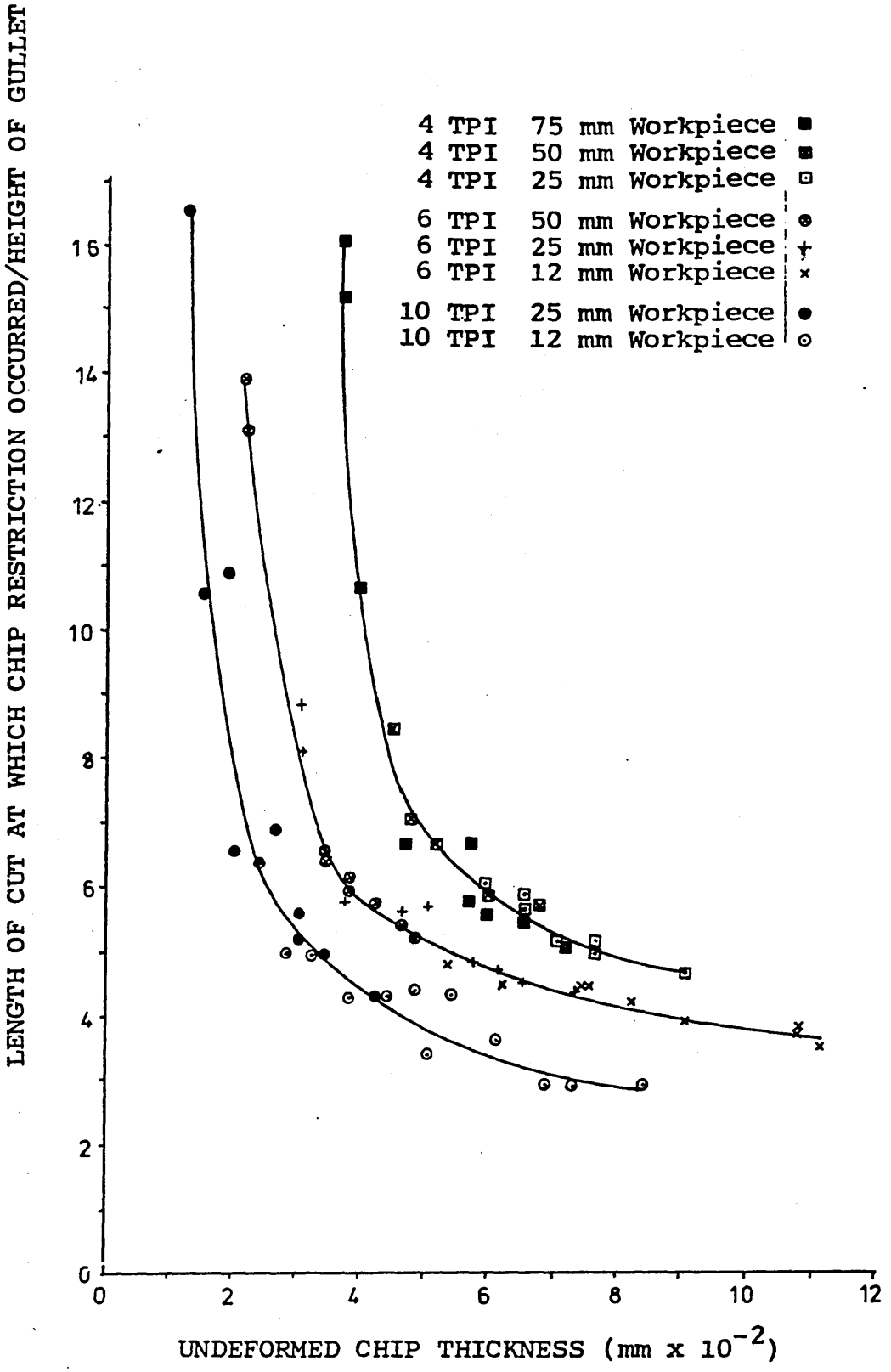

Fig. 4.19. Graph showing the data in fig. 4.18 normalised by the height of the gullet.

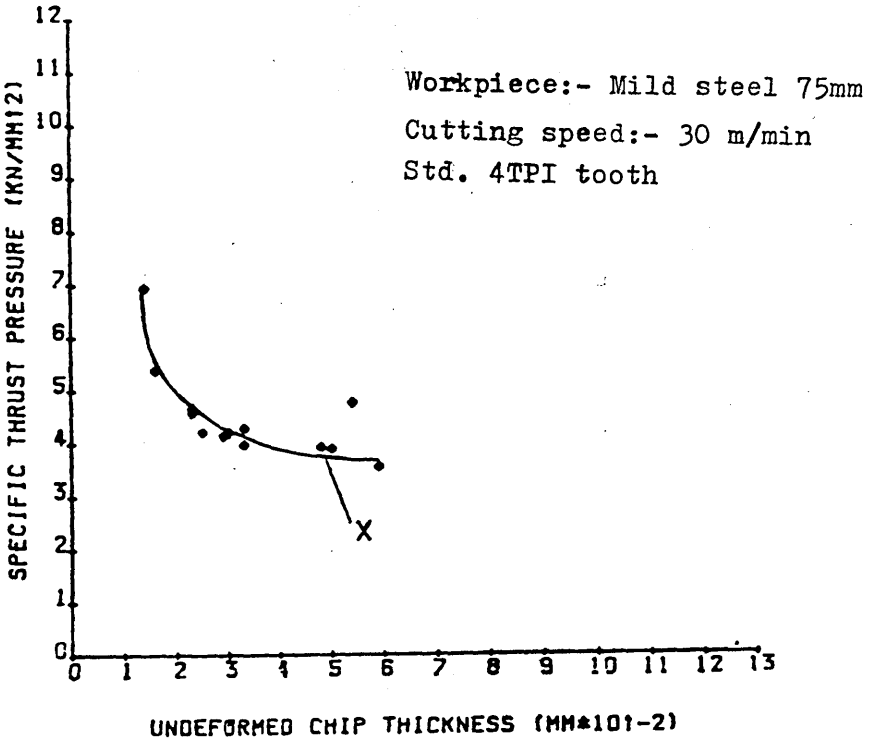

Fig. 4.20. The performance of a standard 4 TPI tooth cutting mild steel. Length of cut 75 mm. Cutting speed, 30m/min.

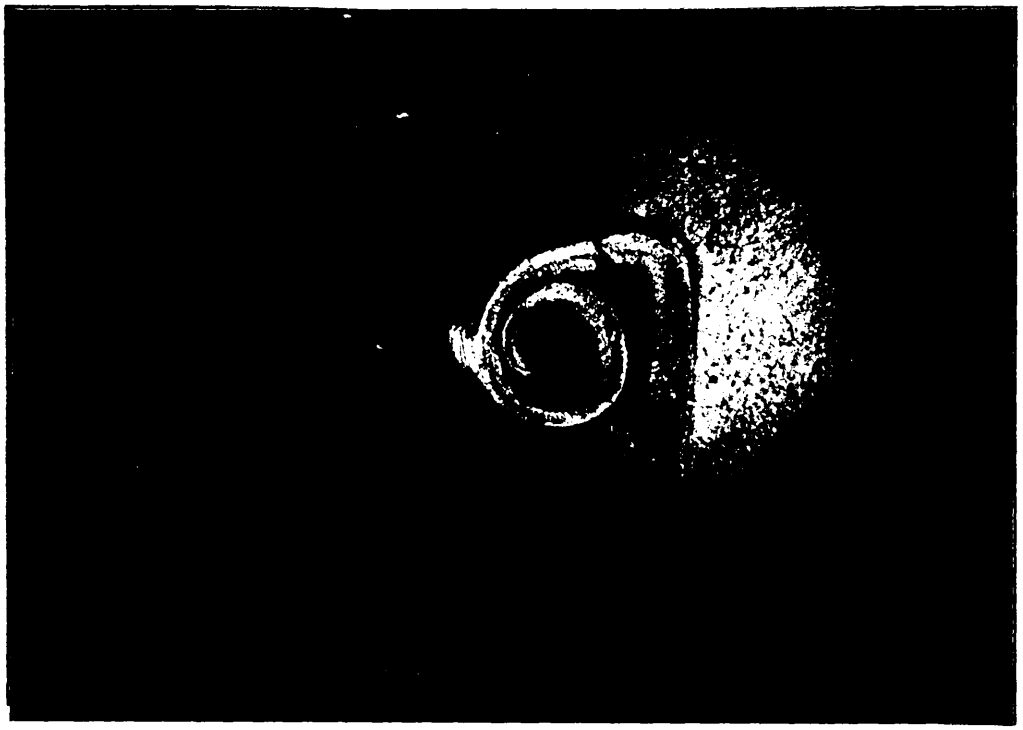

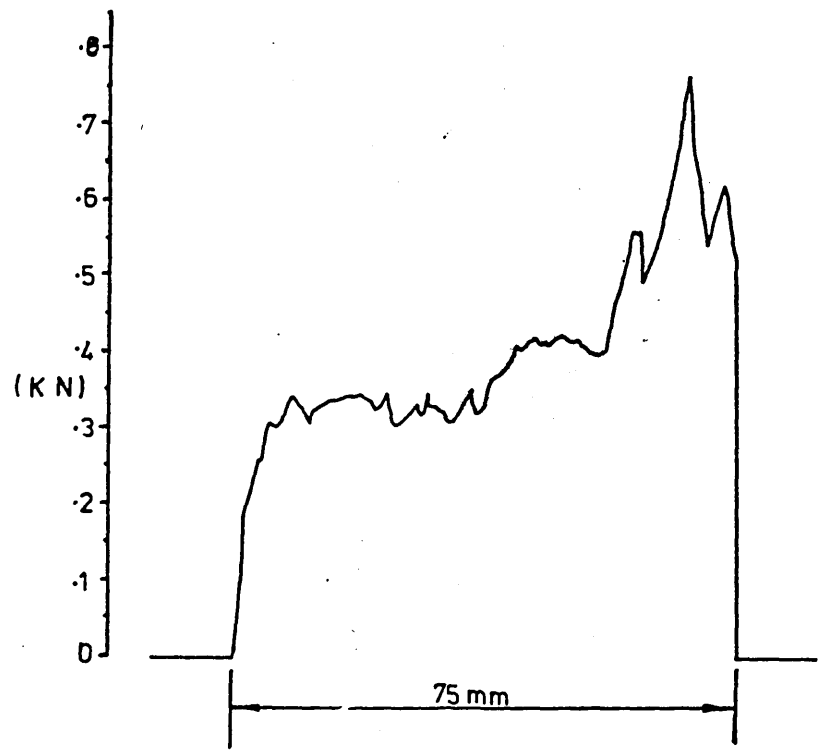

Fig. 4.21. Chip and Associated Thrust Force Trace for a standard 4 TPI tooth cutting a 75 mm Length of Mild Steel.
Both the chip and force trace relate to point X in Fig. 4.20.

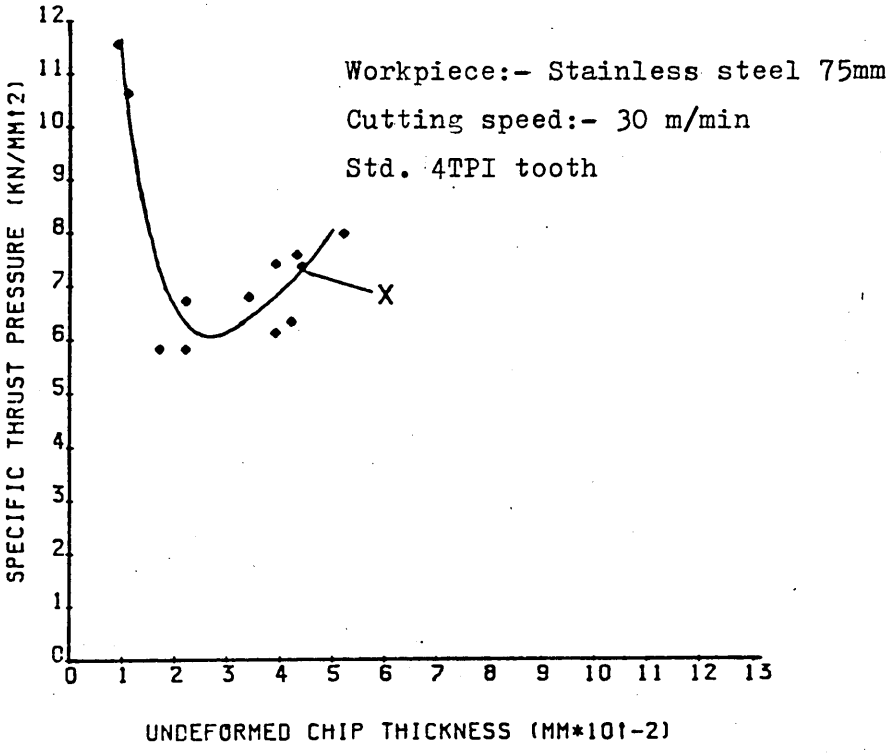

Fig. 4.22. Performance of a standard 4 TPI tooth cutting Stainless Steel. Length of cut 75 mm. Cutting speed 30m/min.

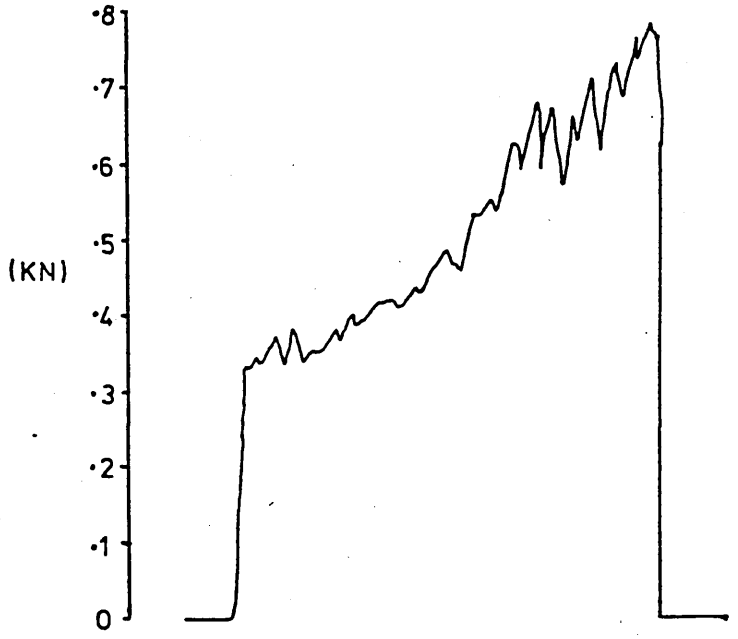

Fig. 4.23. The thrust force trace relating to point X on fig. 4.22.

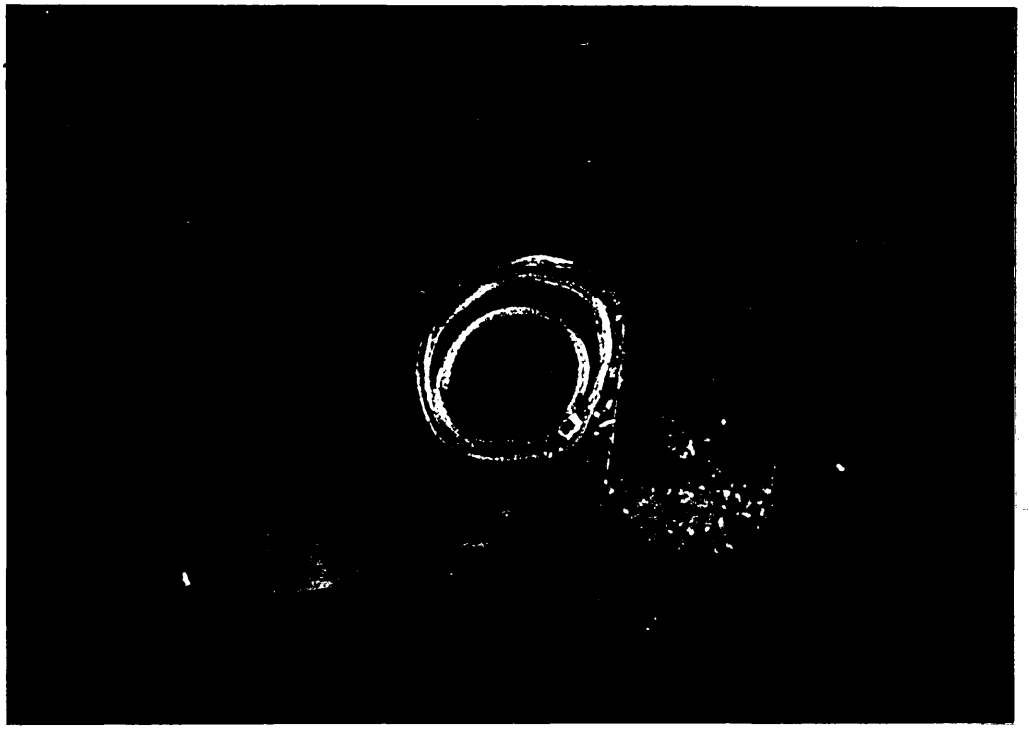

Fig. 4.24. The chip relating to point X on fig. 4.22.

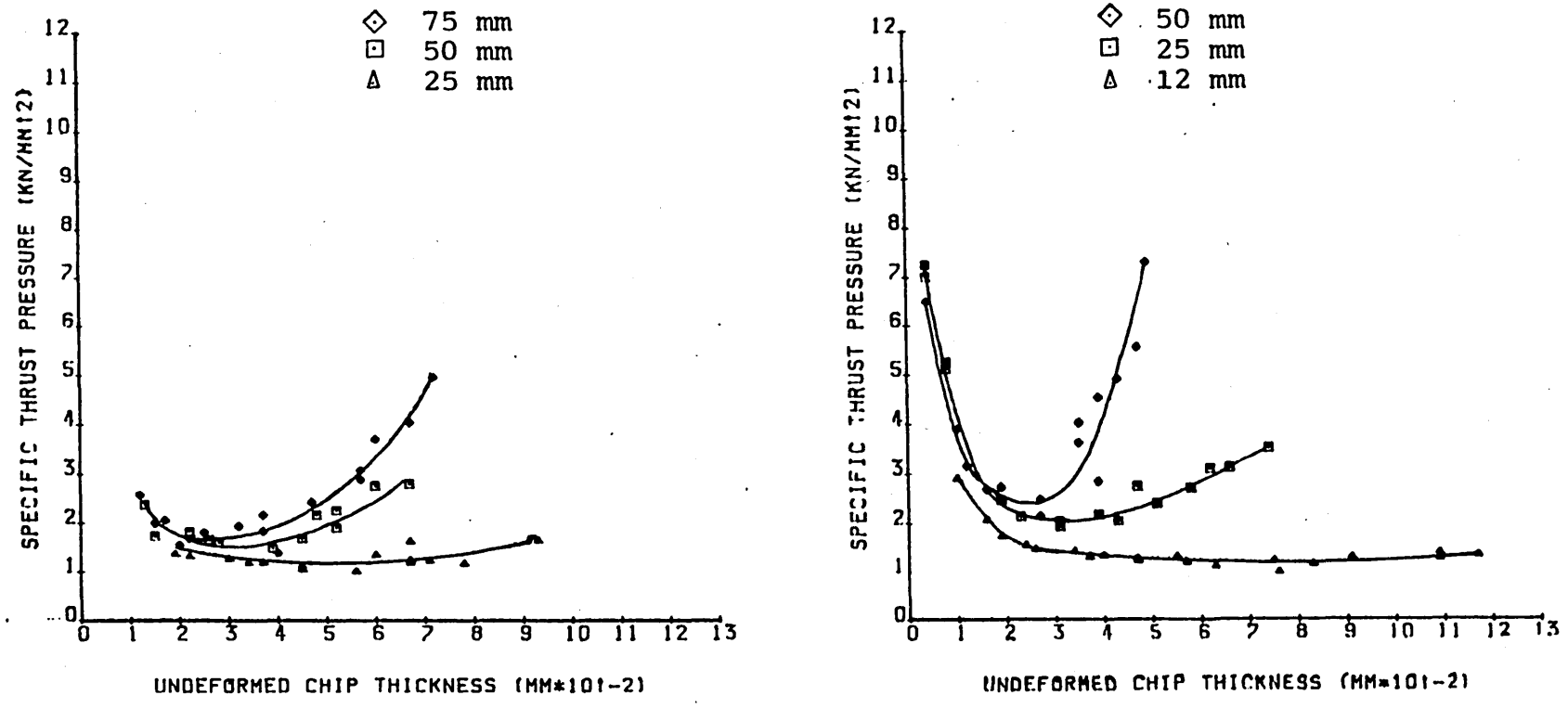

Fig. 4.25.

a) The performance of a 4 TPI tooth cutting various lengths of workpiece

b) The performance of a 6 TPI tooth cutting various lengths of workpiece

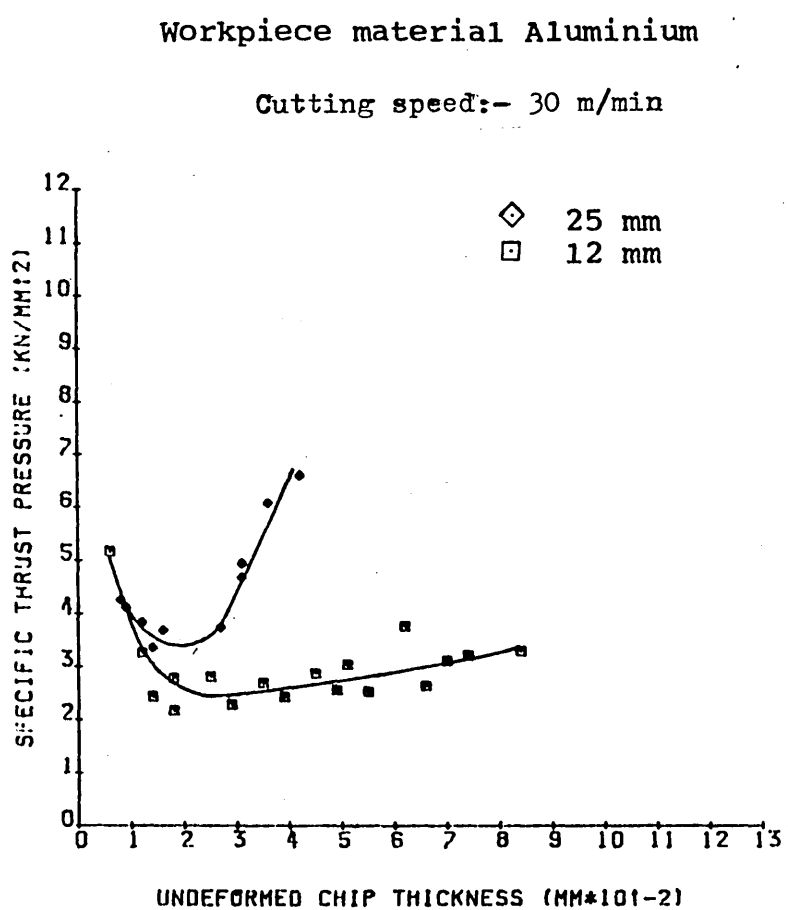

Fig. 4.25.(c) The performance of a 10 TPI tooth cutting two different lengths of workpiece.

Workpiece Mild Steel

Cutting speed:- 30 m/min

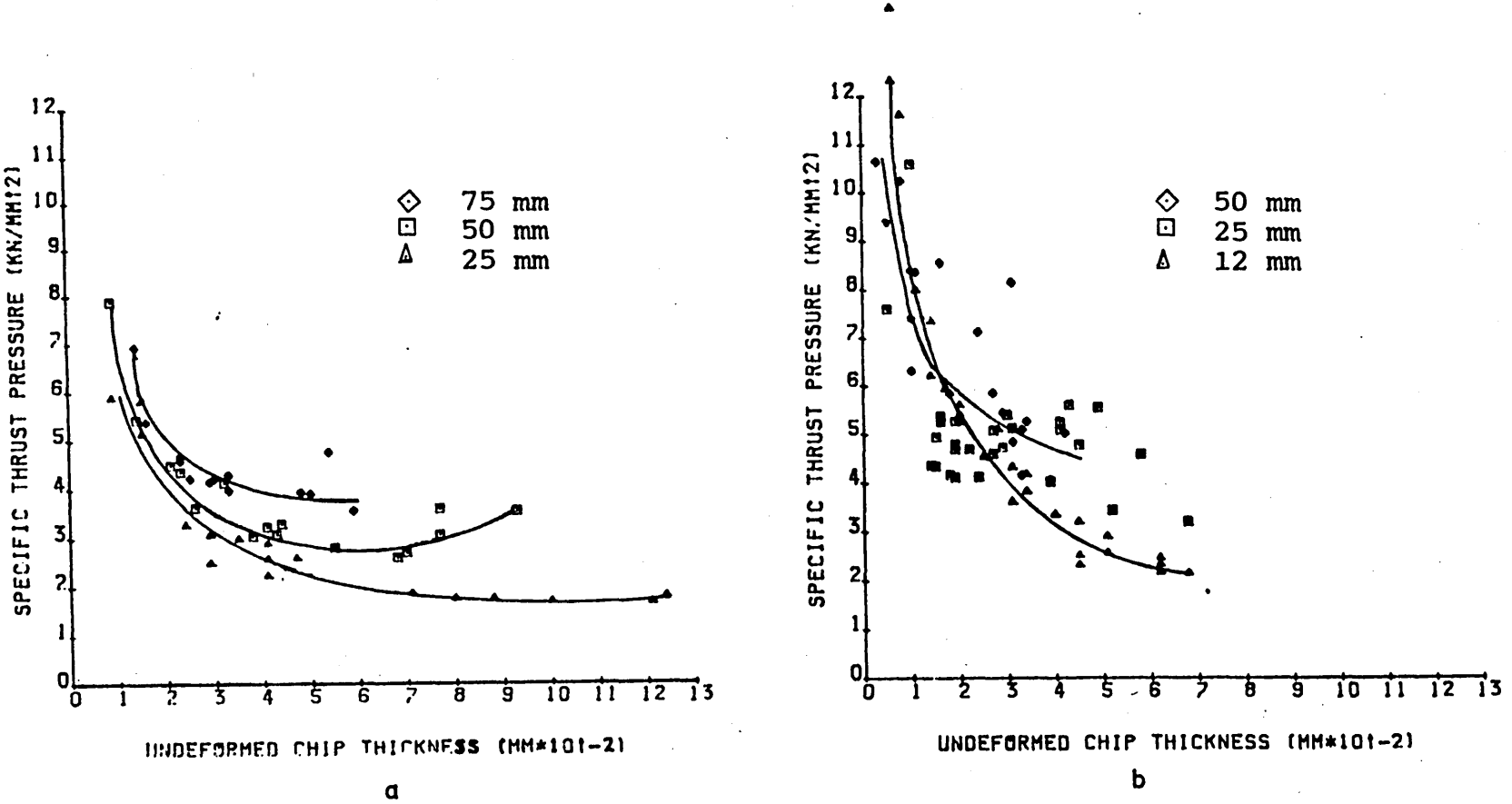

Fig. 4.26. Performance of single hacksaw teeth cutting mild steel as length of cut varies. a) for a 4 TPI tooth
and b) for a 6 TPI tooth

Workpiece Mild Steel

Cutting speed:- 30 m/min

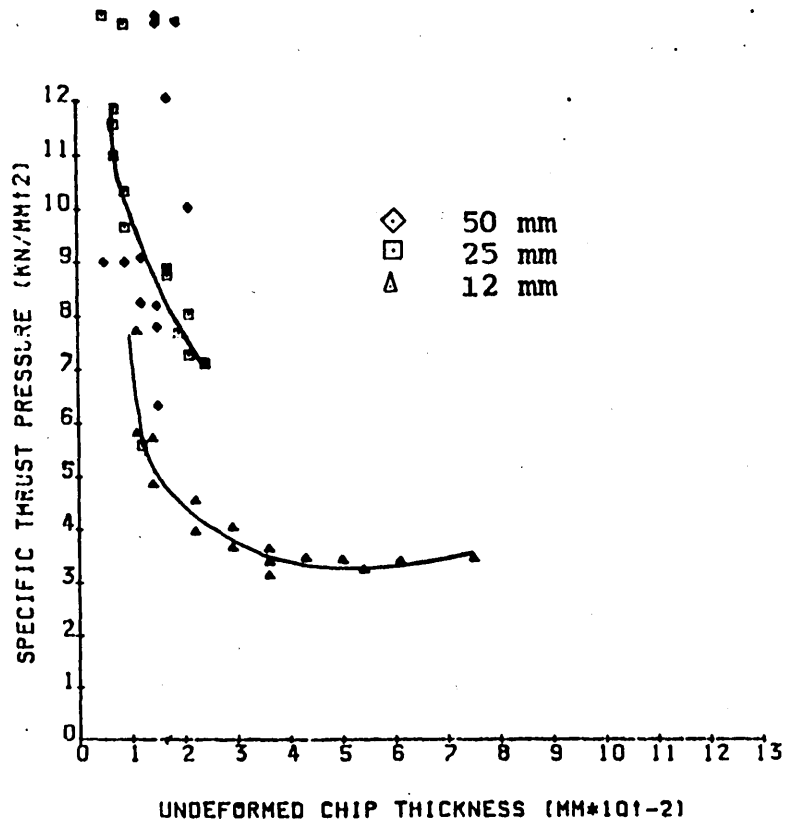

Fig. 4.26(c) Performance of a standard 10 TPI tooth cutting mild steel at various lengths of cut.

Workpiece Stainless Steel

Cutting speed:- 30 m/min

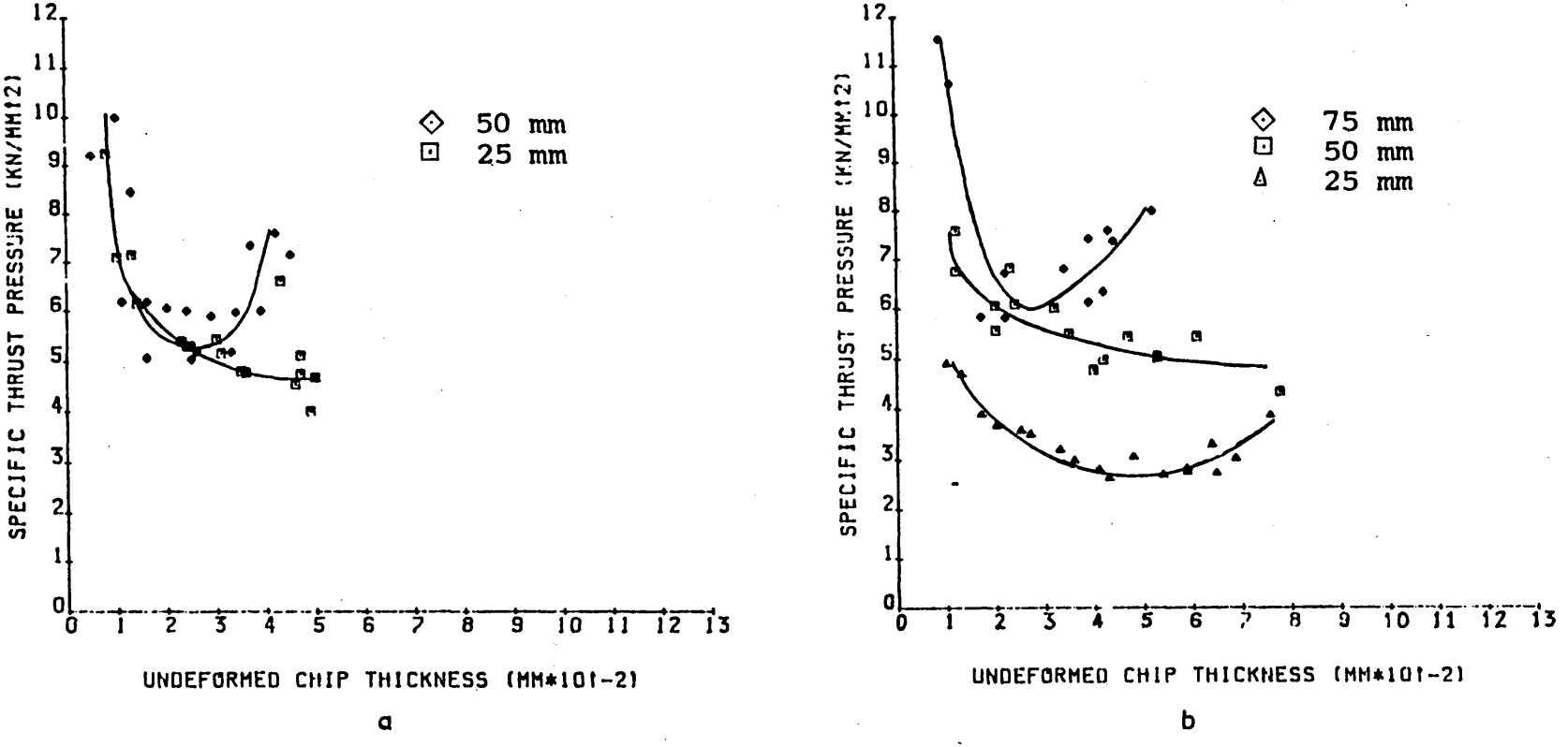

Fig. 4.27. Performance of a single hacksaw tooth cutting stainless steel as length of cut varies (a) for a 6 TPI tooth
(b) for a 4 TPI tooth

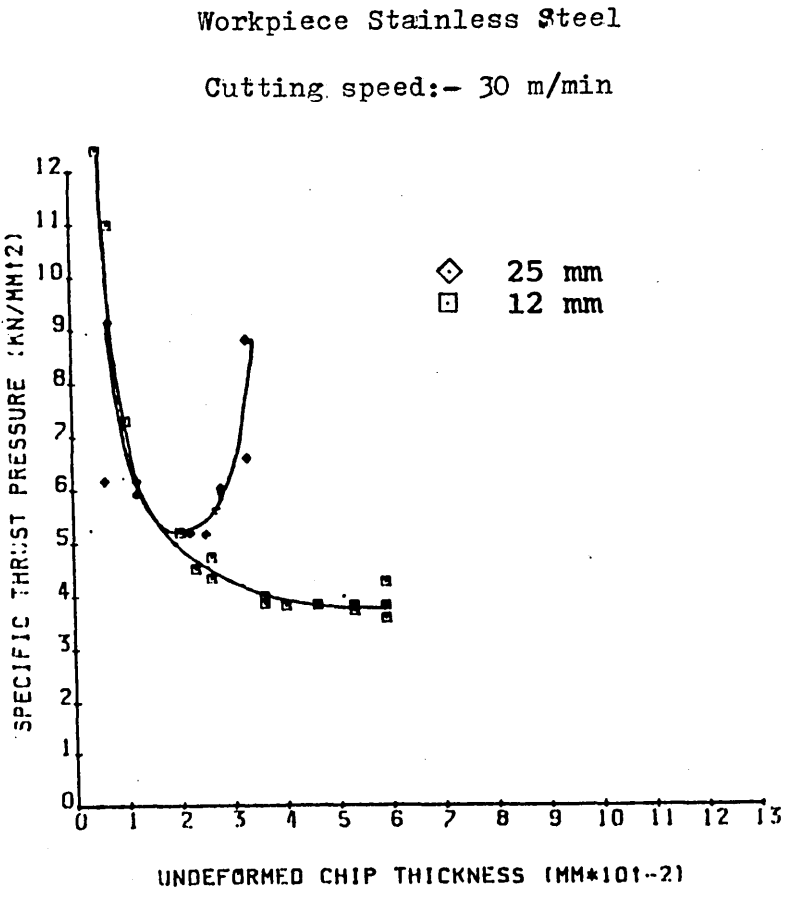

Fig. 4.27(c). Performance of a standard 10 TPI tooth cutting stainless steel at various lengths of cut.

Workpiece Aluminium

Cutting speed:- 30 m/min

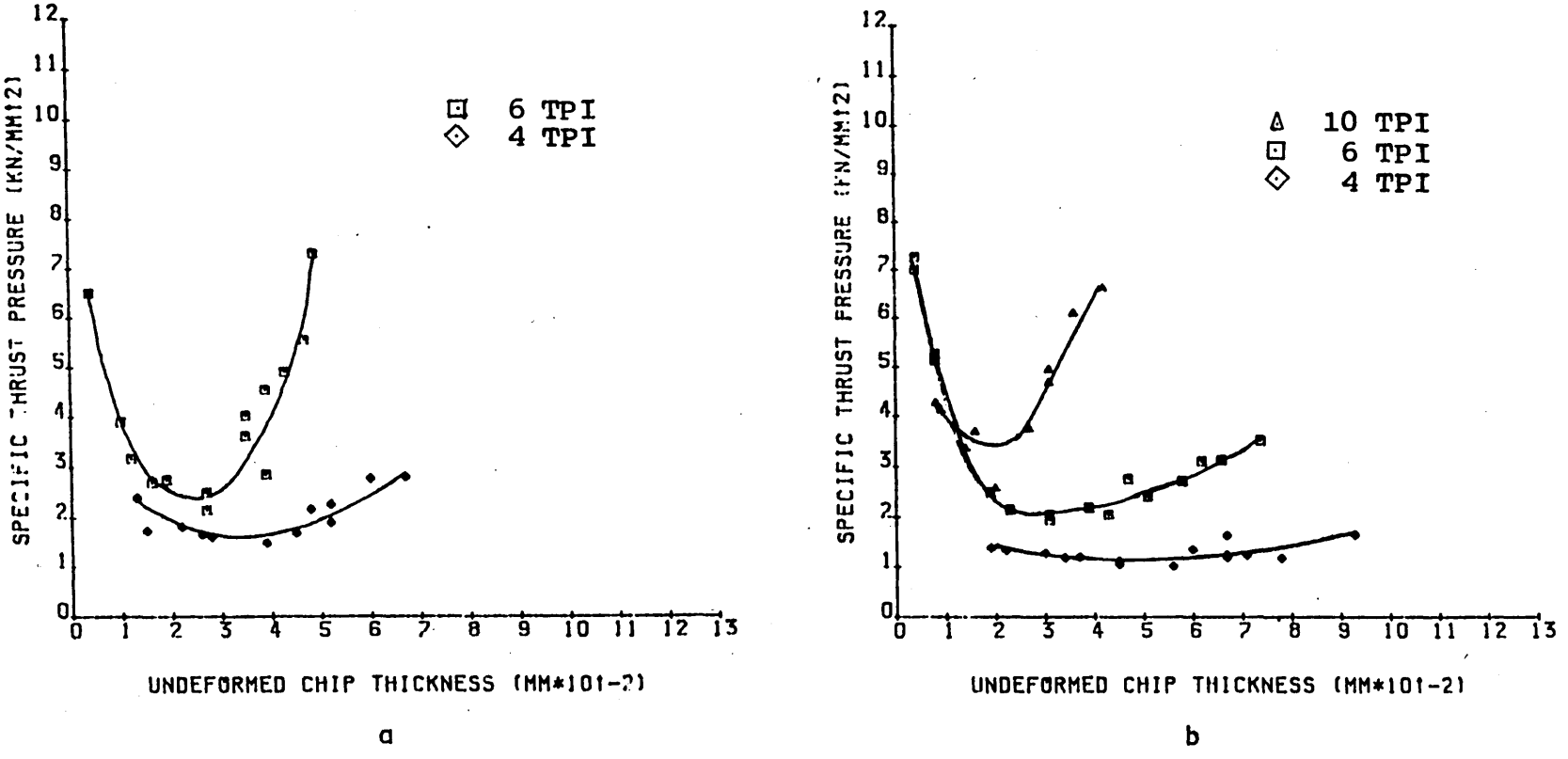

Fig. 4.28. Performance of different pitch standard single teeth cutting aluminium. Length of cut (a) 50 mm
(b) 25 mm

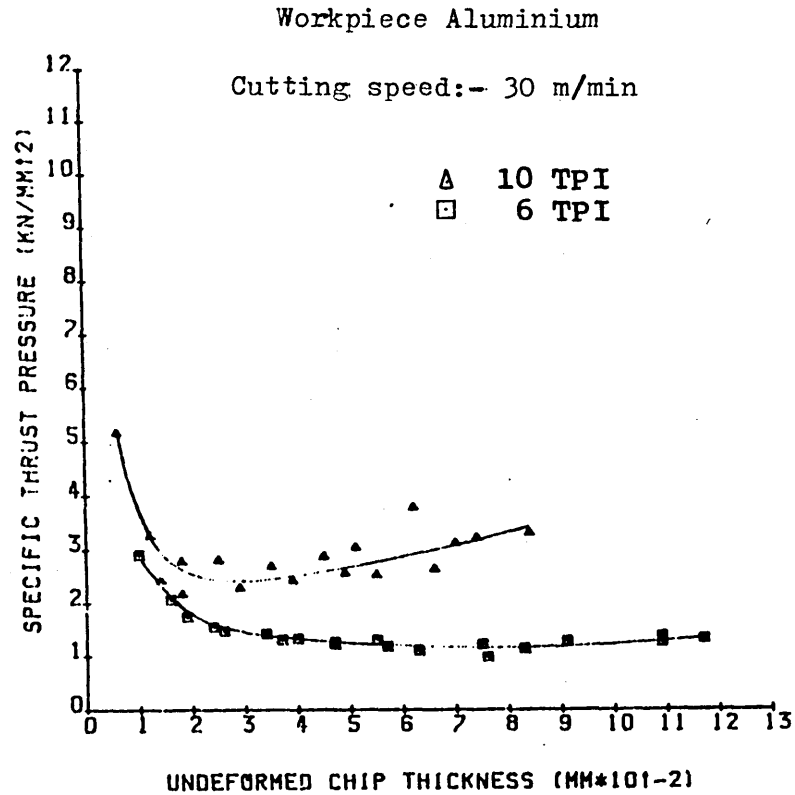

Fig. 4.28(c) Performance of different pitch single teeth cutting aluminium. Length of cut 12 mm

Workpiece Mild Steel

Cutting speed:- 30 m/min

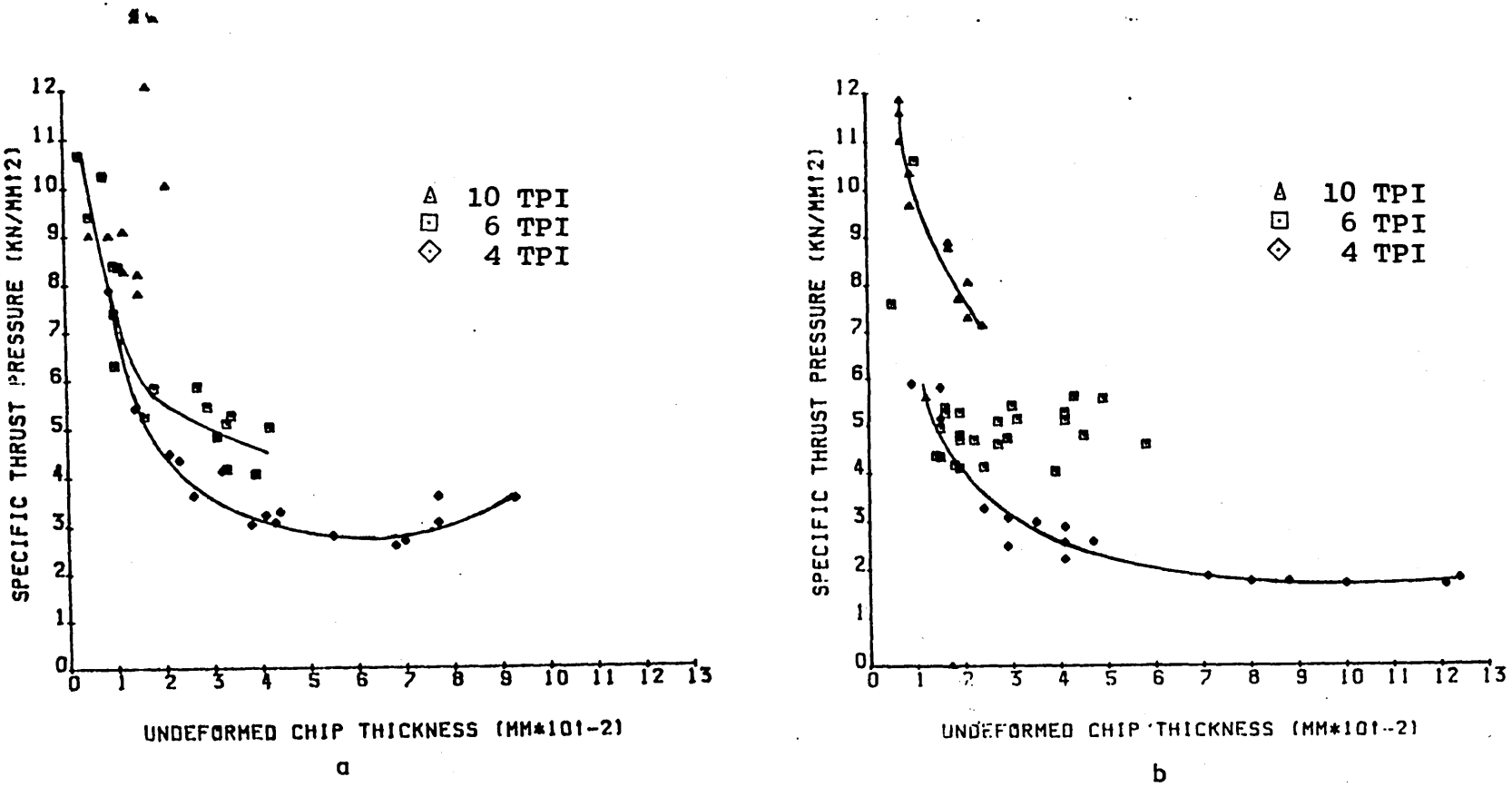

Fig. 4.29. Performance of different pitch standard single teeth cutting mild steel. Length of cut (a) 50 mm
(b) 25 mm

Workpiece Mild Steel

Cutting speed:- 30 m/min

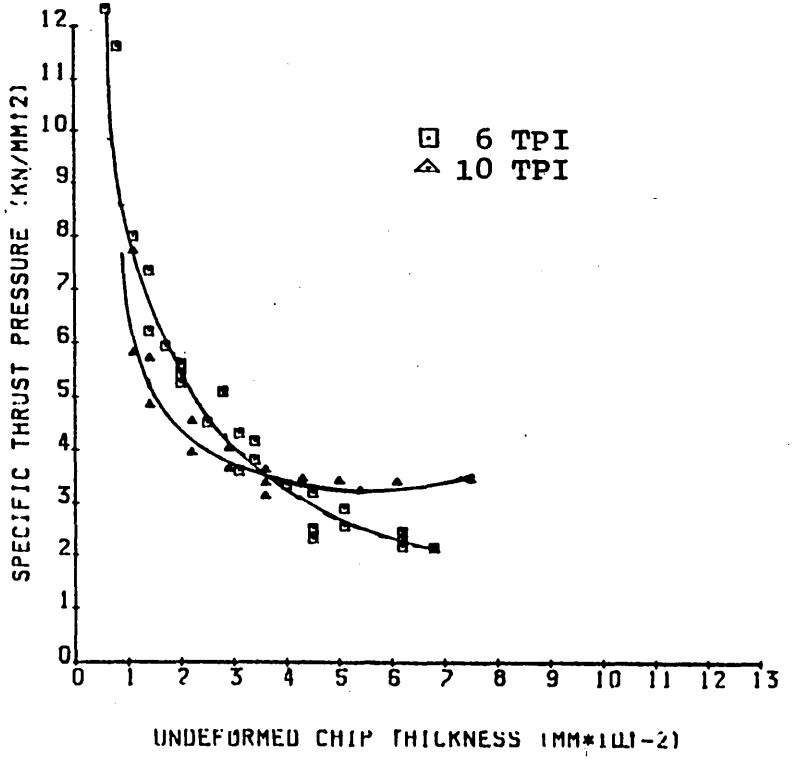

Fig. 4.29(c) Performance of different standard single teeth cutting mild steel. Length of cut 12 mm

Workpiece Stainless Steel

Cutting speed:- 30 m/min

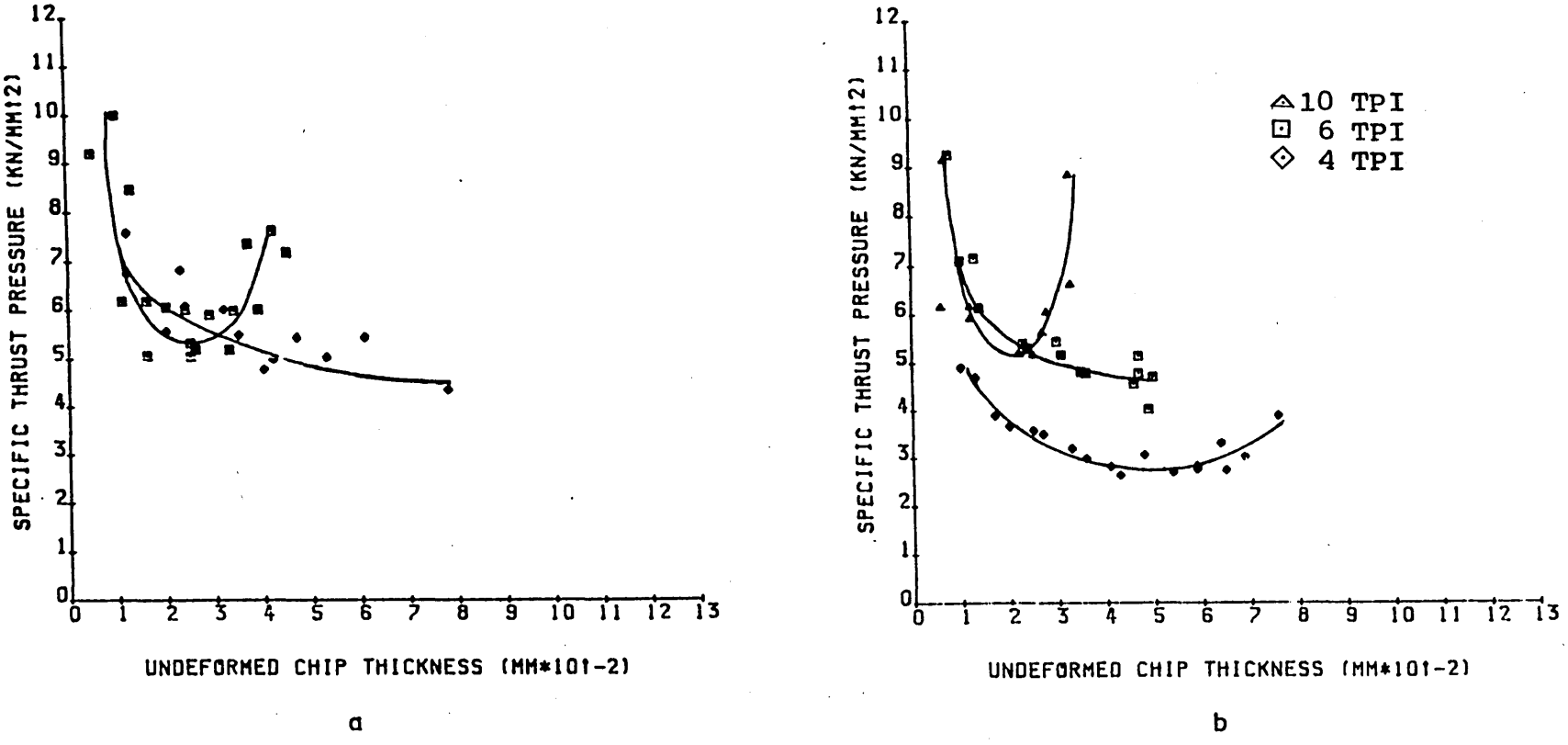

Fig. 4.30. Performance of different pitch standard single teeth cutting stainless steel. Length of cut (a) 50 mm
(b) 25 mm

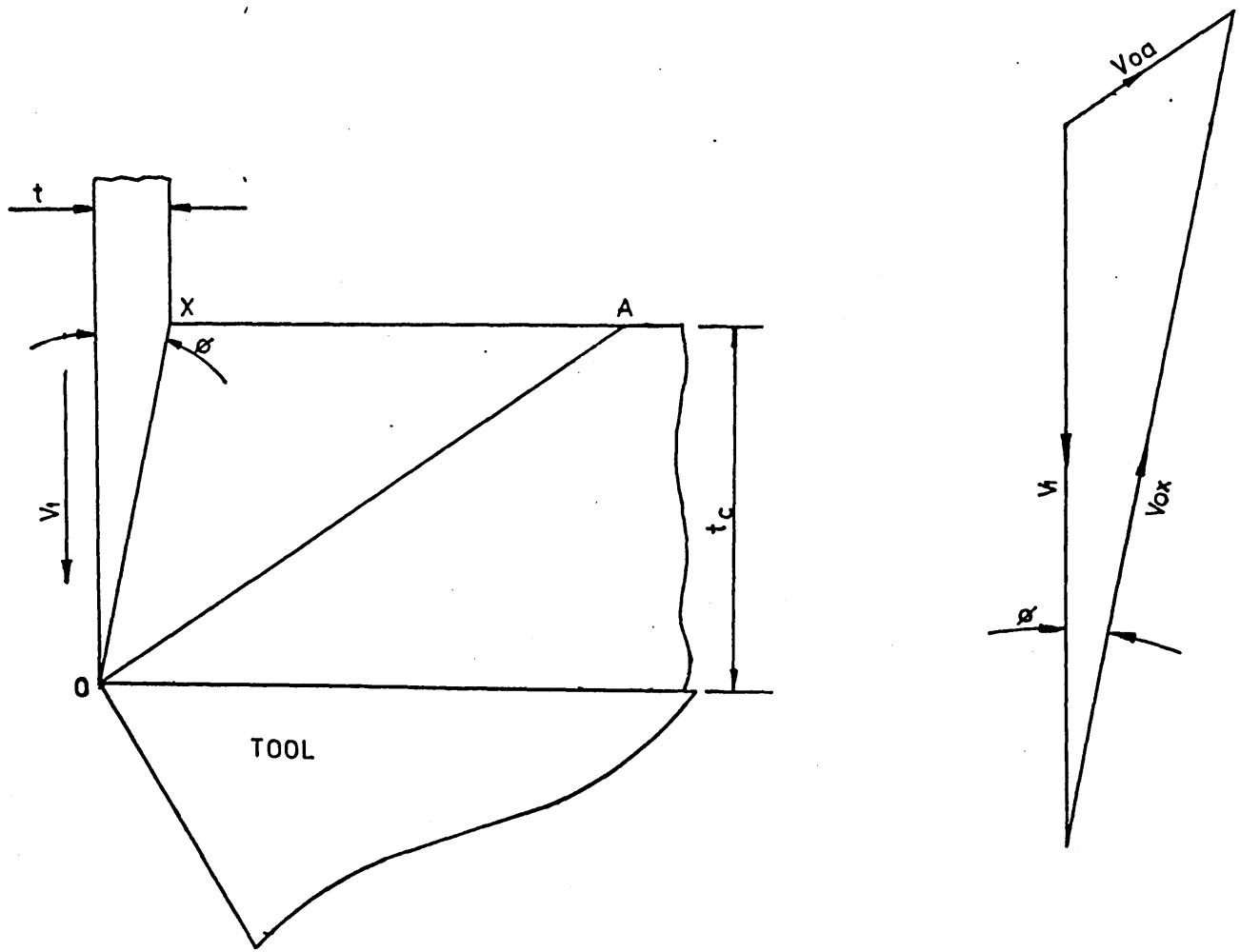

Fig. 5.1. Diagram of the shear planes OX & OA along which the chip material shears when the chip is restricted from flowing along the rake face. The associated hodograph shows the relative velocity of chip material along OX & OA.

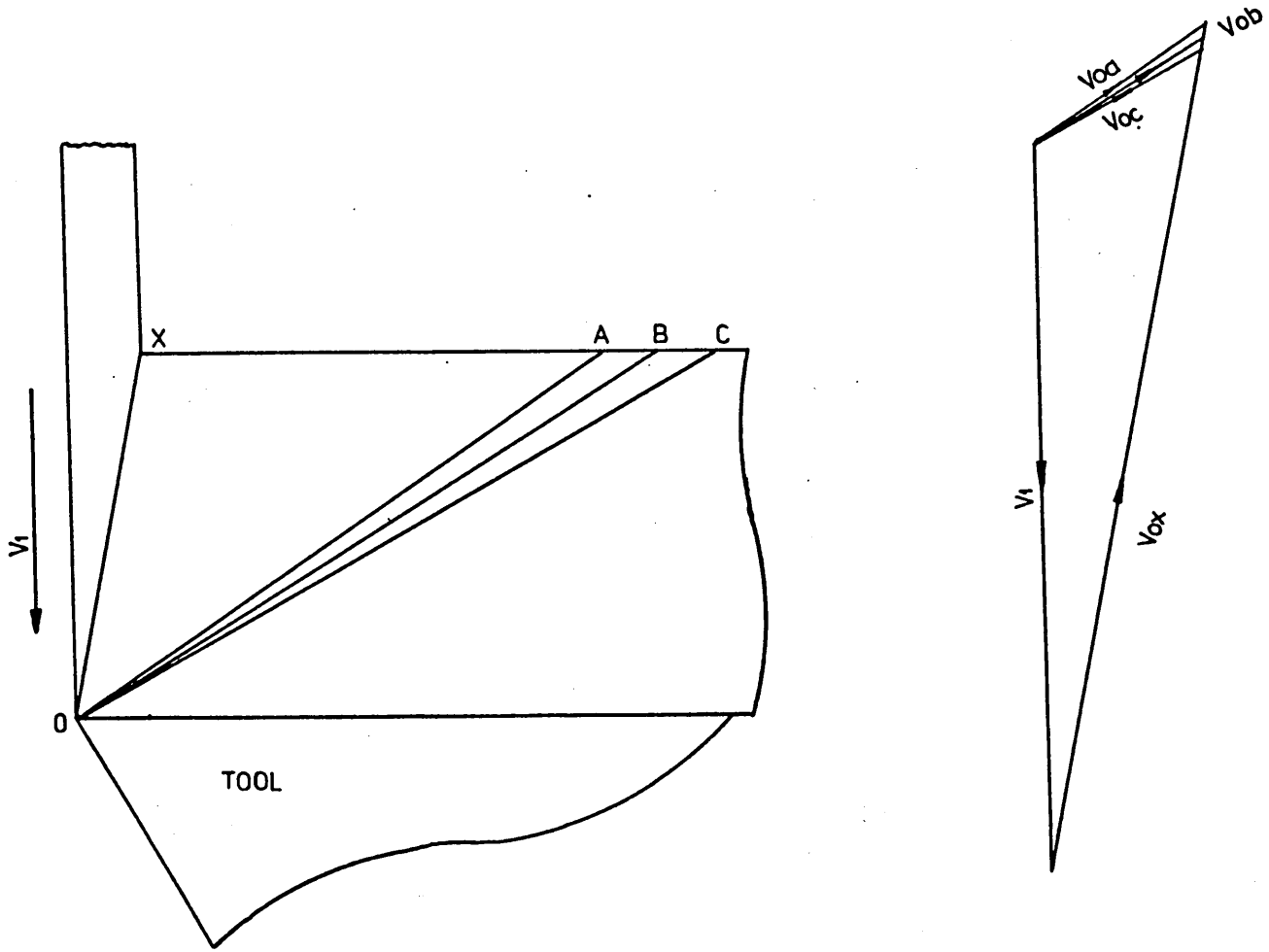

Fig. 5.2. Diagram of alternate secondary shear planes OA, OB & OC and the associated Hodograph

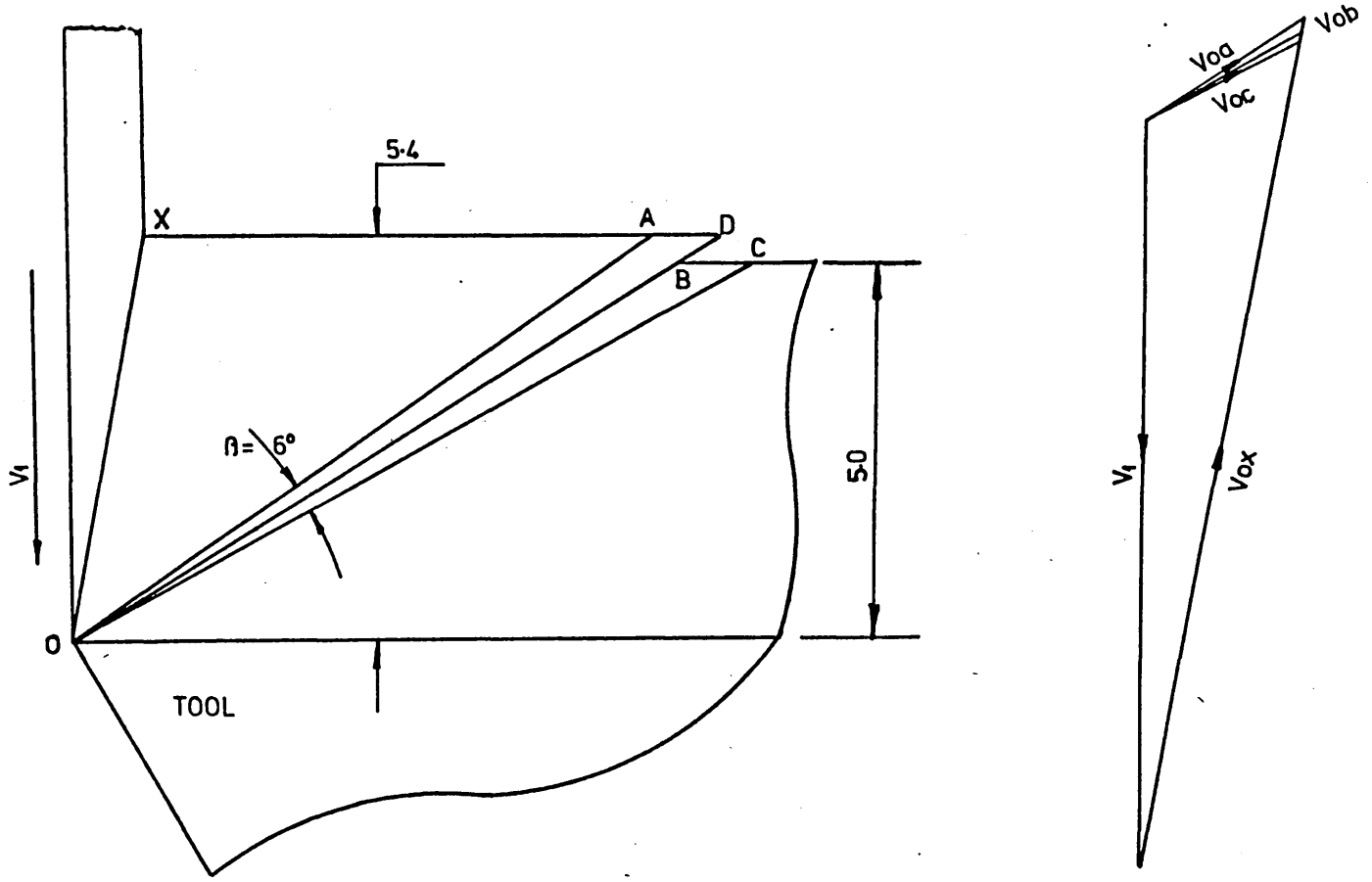

Fig. 5.3. Diagram of chip shape when the tooth has travelled 3t after the chip flow has been restricted.

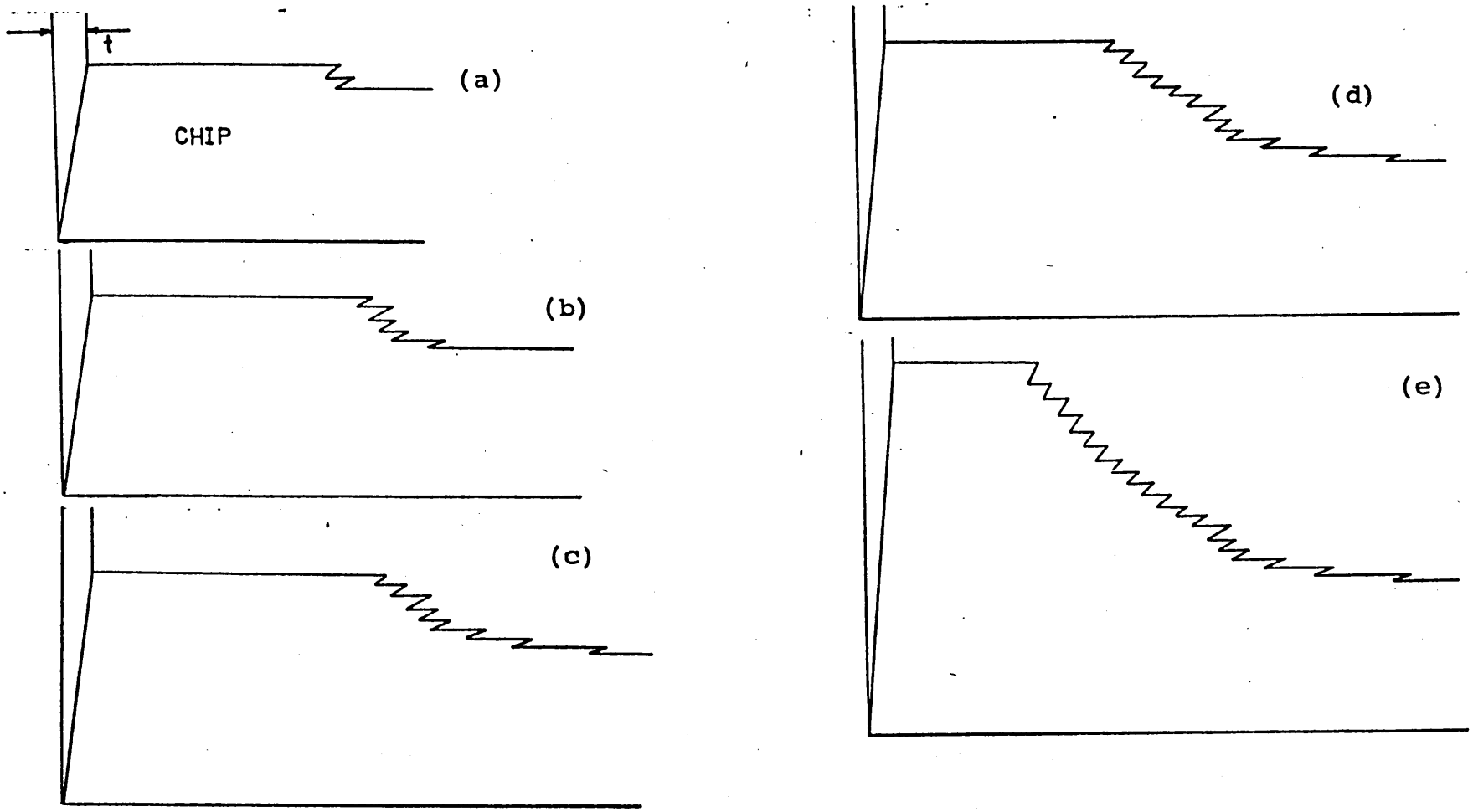

Fig. 5.4. Modelled chip shape at a distance (a) 6t, (b) 15t, (c) 24t, (d) 36t and (e) 54t after chip restriction occurred. Rake angle, 0^{o}.

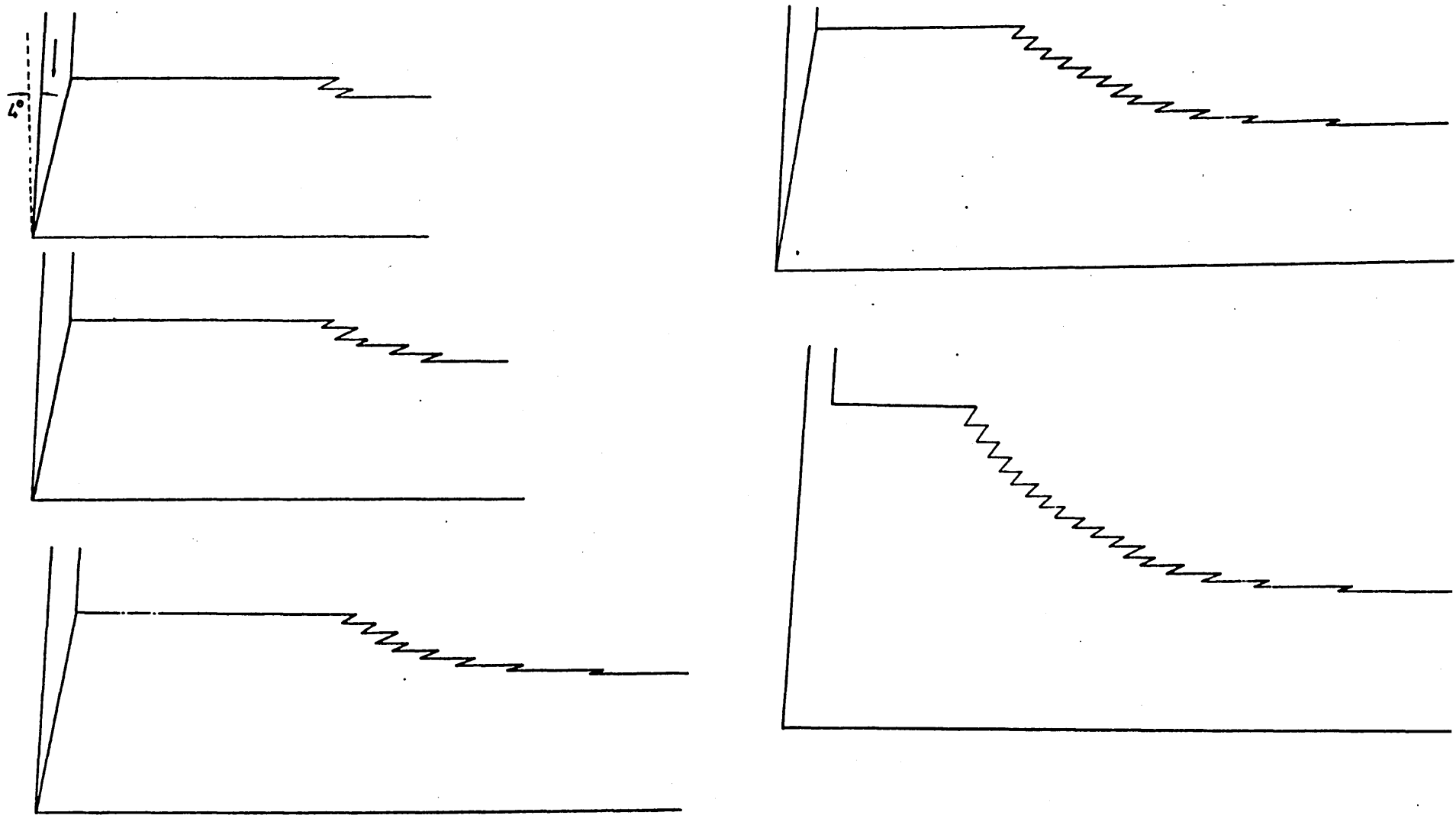

Fig. 5.5. Modelled chip shape at a distance (a) 6t, (b) 15t, (c) 24t, (d) 36t, and (e) 54t after chip restriction occurred. Rake angle, -4^{o}.

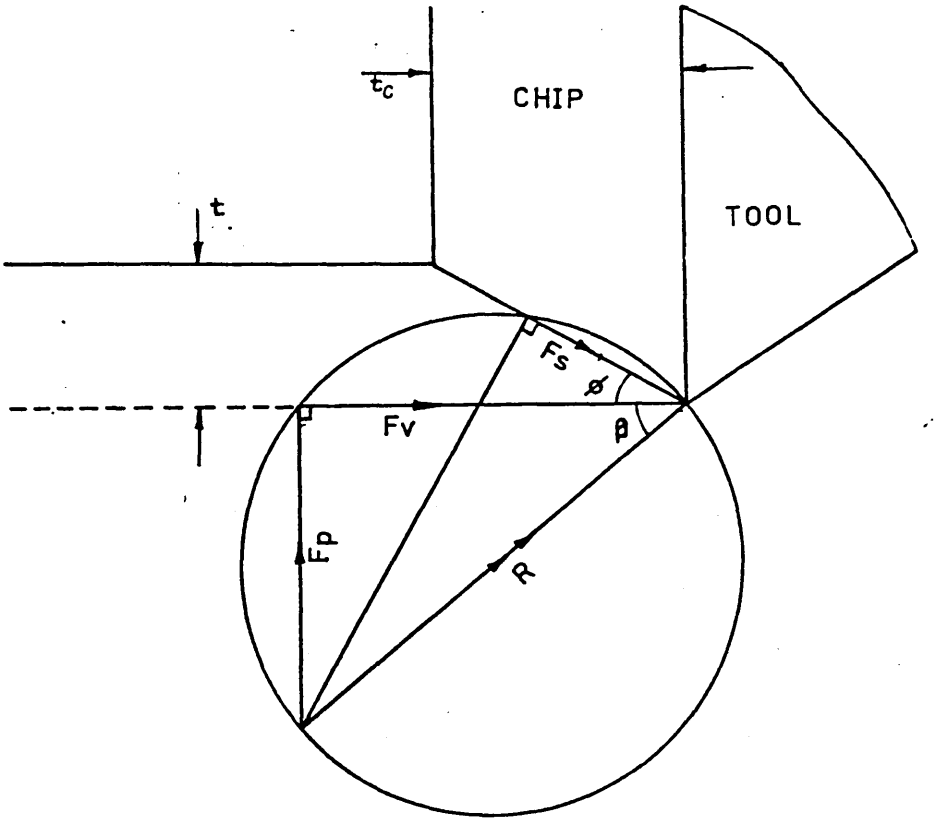

Fig. 5.6. Diagram showing the geometrical relationship between the cutting and thrust forces and the force acting along the shear plane.

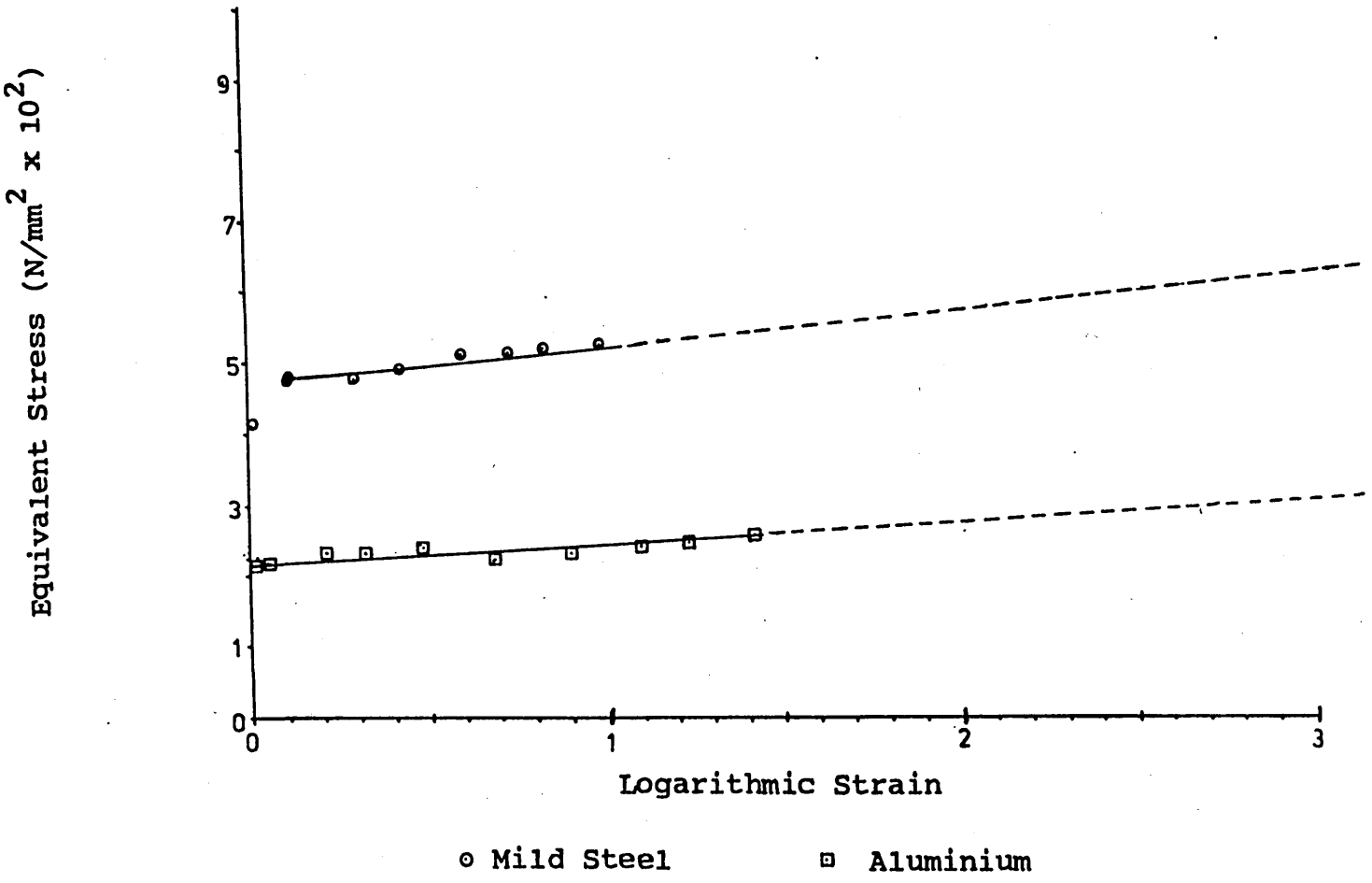

Fig. 5.7. Equivalent Stress v Logarithmic strain for mild steel and aluminium. Data taken from compression tests. Straight line extrapolation has been used.

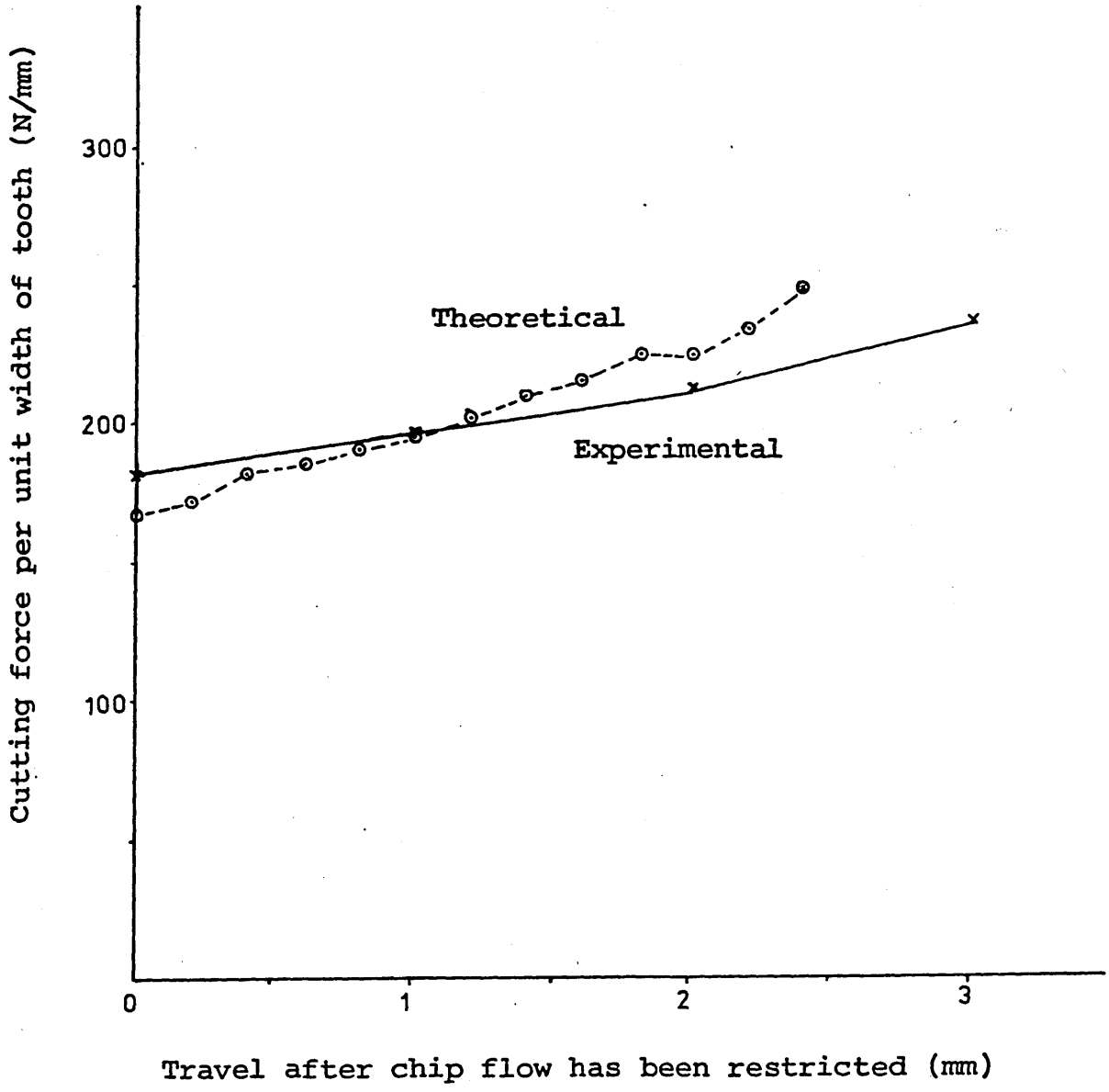

Fig. 5.8a. Theoretical & experimental values of cutting force subsequent to chip flow restriction occurring, for a standard 4TPI tooth cutting aluminium. Undeformed chip thickness is 0.067 mm.

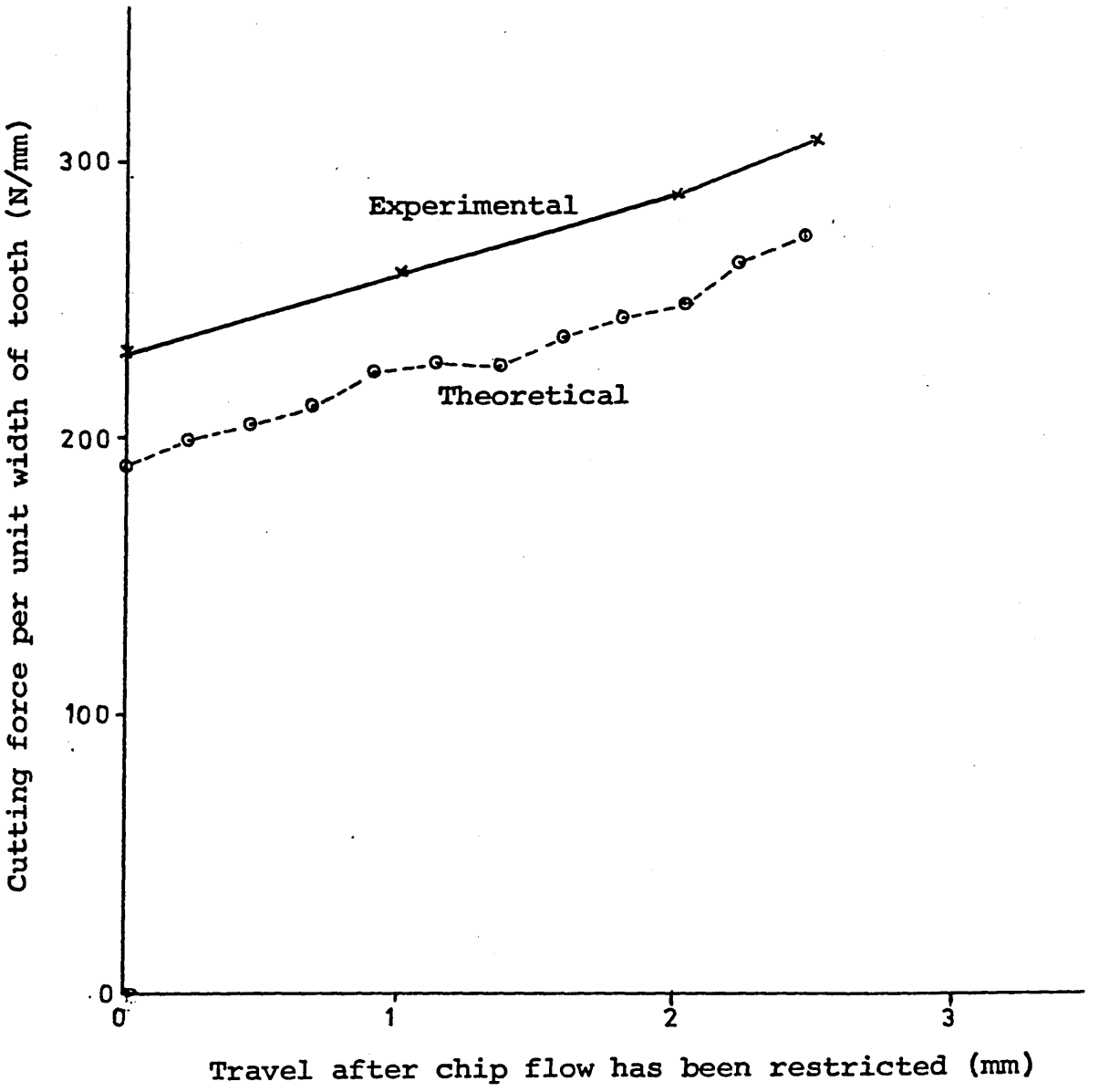

Fig. 5.8.b. Theoretical & experimental values of cutting forces subsequent to chip flow restriction occurring, for a standard 6 TPI tooth cutting aluminium. Undeformed chip thickness is 0.074 mm.

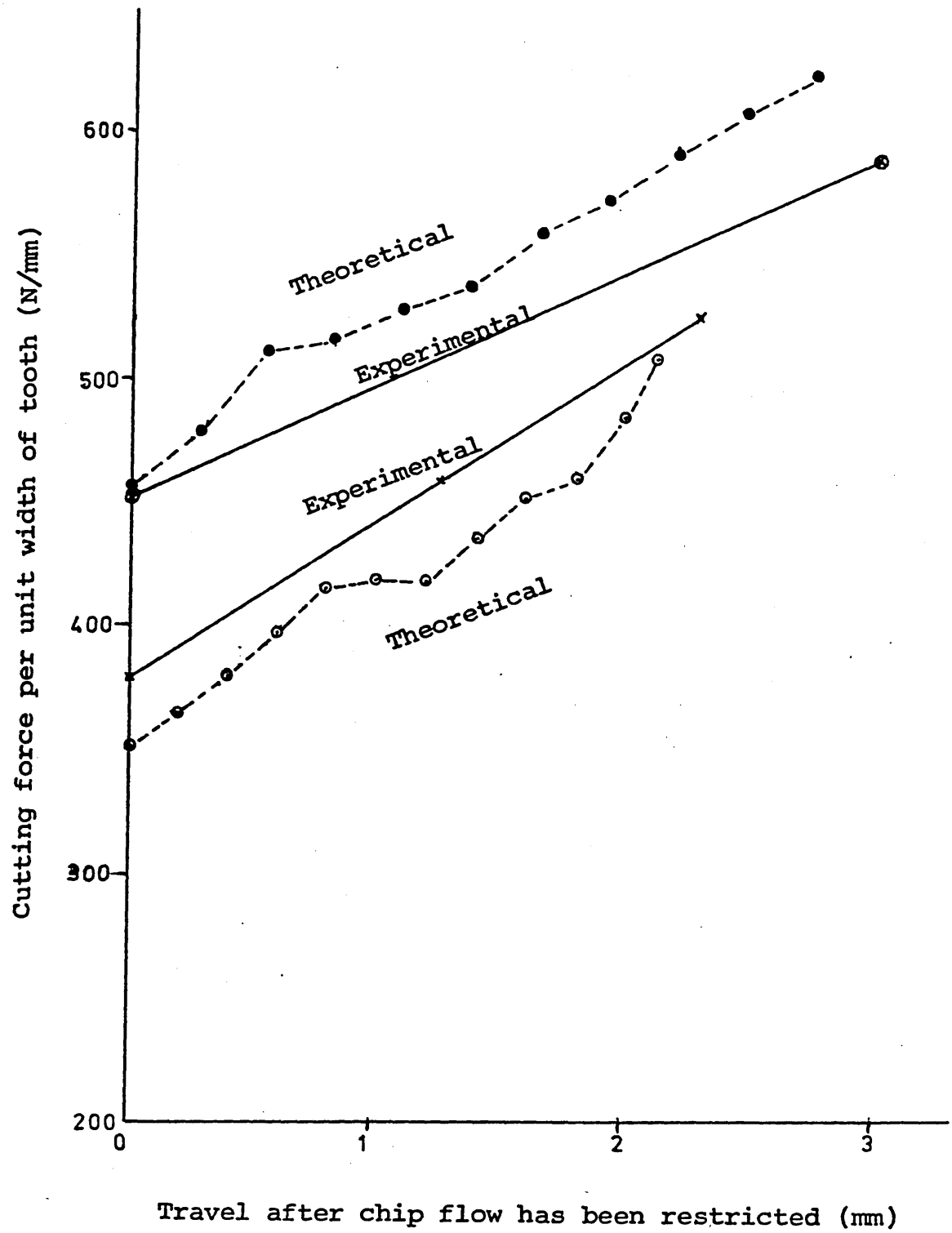

Fig. 5.8c. Theoretical & experimental values of cutting force subsequent to chip flow restriction occurring, for standard 4 TPI and 6 TPI teeth cutting mild steel.

4 TPI 0.093 mm Undeformed chip thickness
6 TPI 0.068 mm Undeformed chip thickness

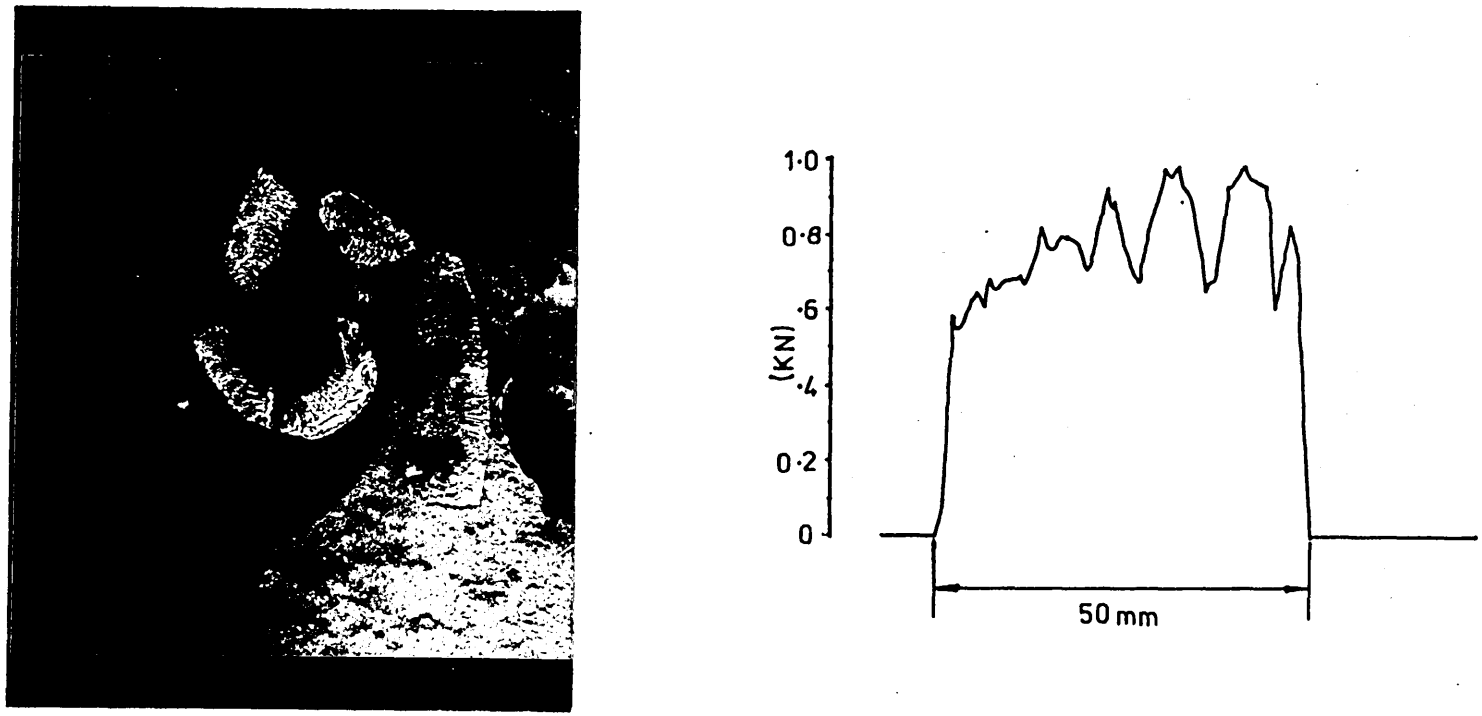

Fig. 5.9. Chip and force trace showing the effect of the chip sticking and then slipping. The peaks are caused by the chip sticking and the subsequent drop in force occurs when the chip slips up the rake face.

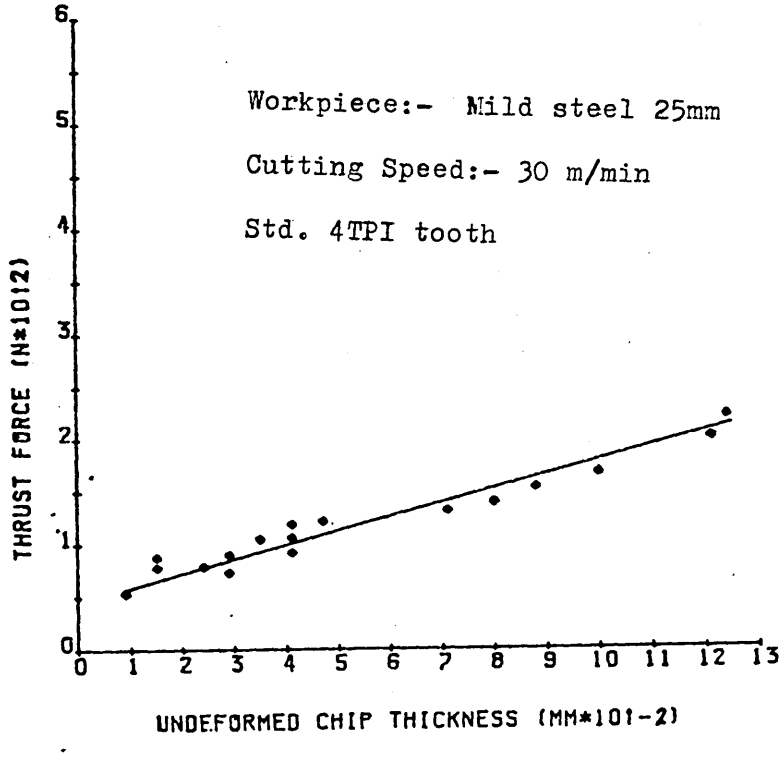

Fig. 6.1. Single tooth data used to predict sawing times, showing thrust force per unit width of tooth v. undeformed chip thickness for standard 4 TPI tooth cutting a 25 mm long mild steel workpiece Cutting speed 30 m/min.

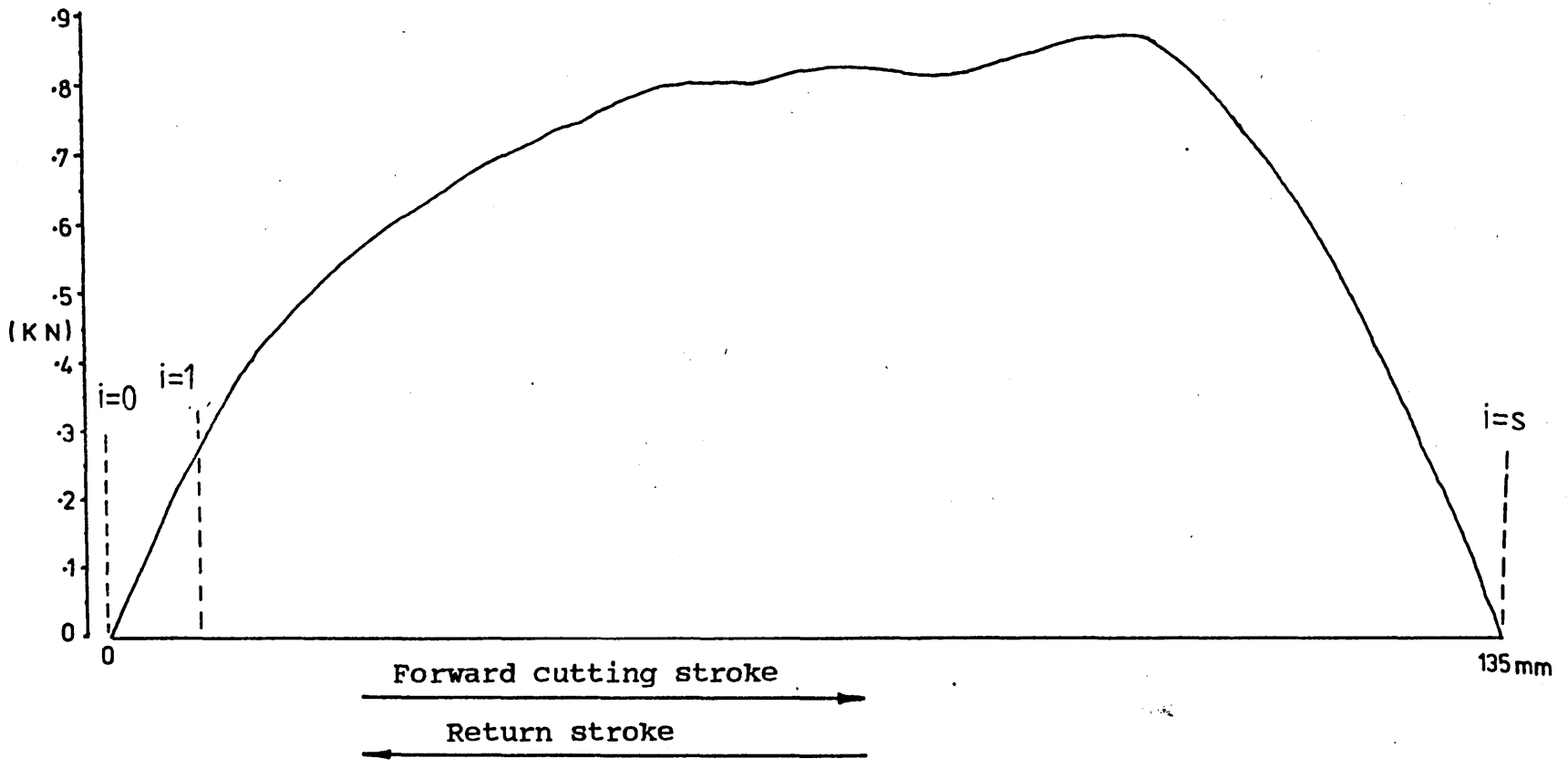

Fig. 6.2. Thrust force trace generated by an hydraulic hacksaw machine.

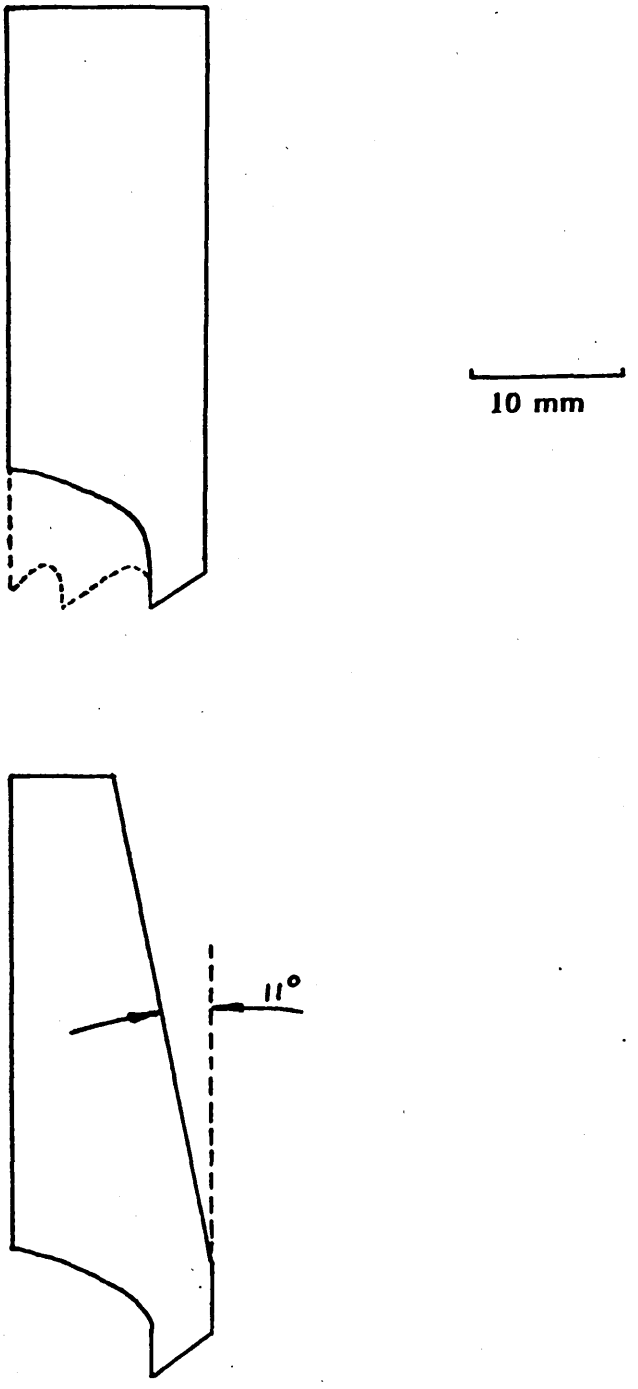

FIG 7.1

4 TPI tooth having no restricting gullet with;-

a) a zero degree rake angle
& b) a 11° rake angle

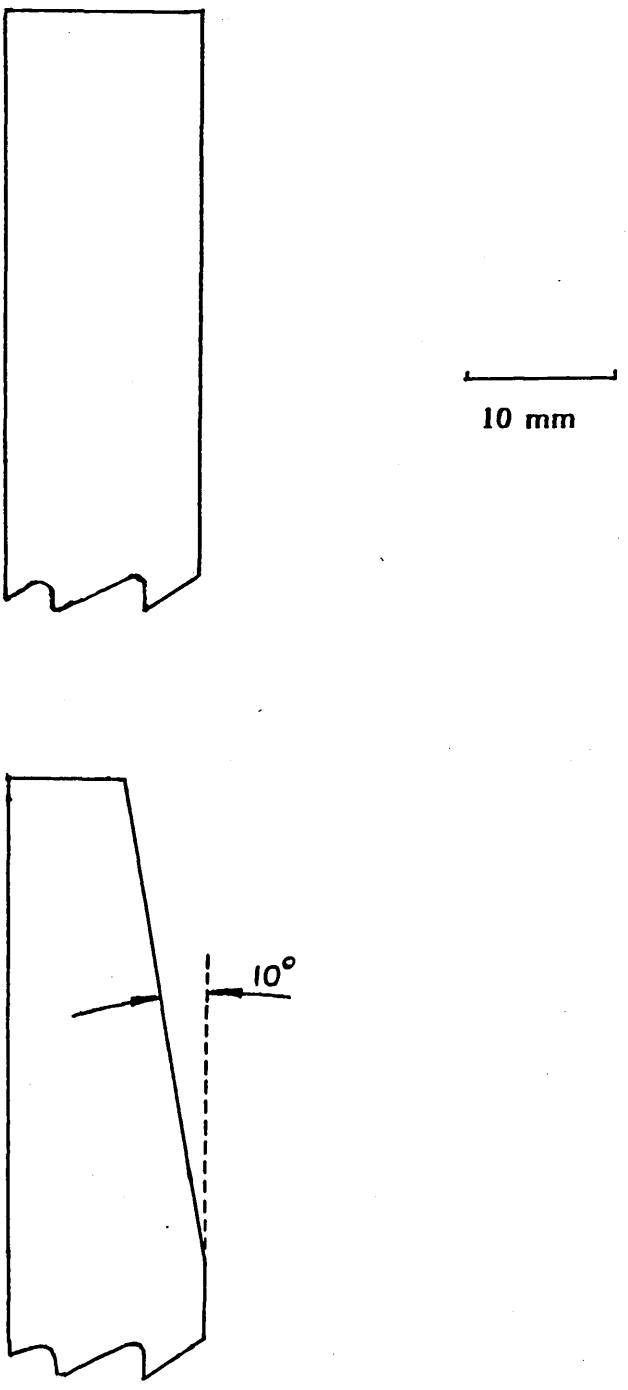

Fig 7.2 Standard 4 TPI Tooth/Gullet Geometry with:

(a) a zero degree rake angle; and
(b) a 10^{o} rake angle

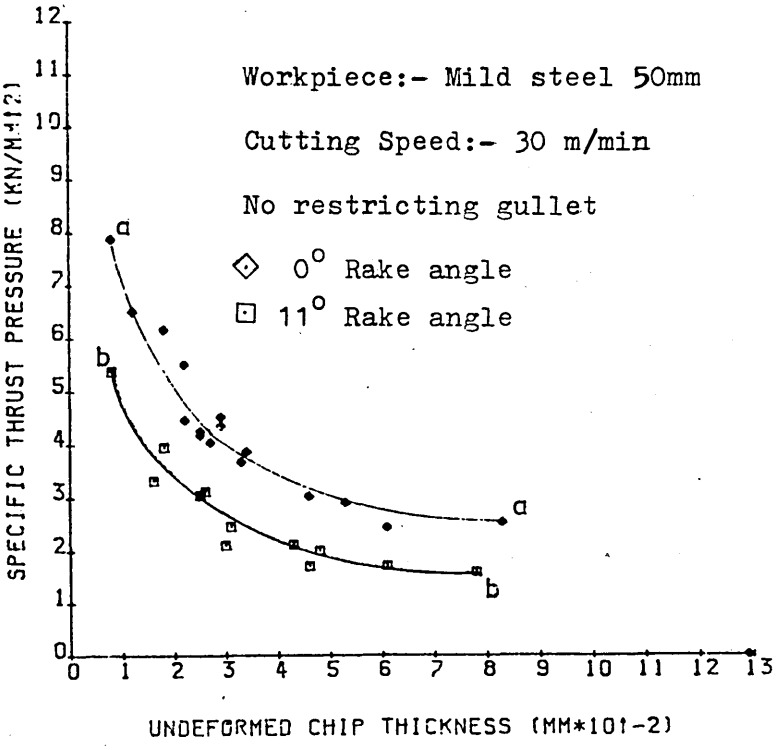

Fig 7.3 Performance of Hacksaw Tooth (4 TPI) with no Restricting Gullet:

(a) with a 0^{o} rake angle; and
(b) with an 11^{o} rake angle

Mild Steel Workpiece, Length of Cut 50 mm
Cutting Speed 30 m/min

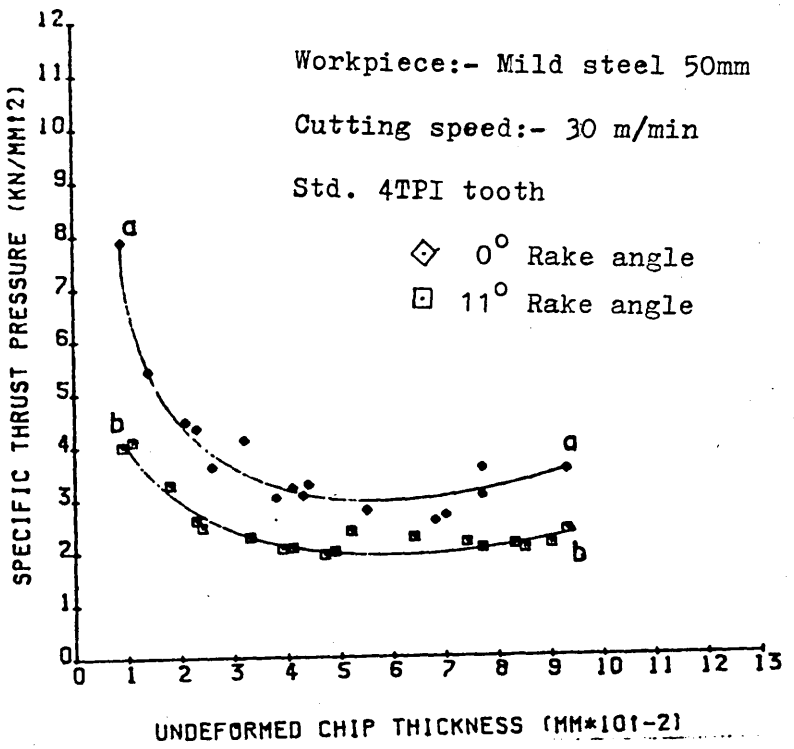

Fig. 7.4 . Performance of a standard 4 TPI tooth
a) with a 0^{o} rake angle.
and b) with a 10^{o} rake angle,
Mild Steel Workpiece, Length of cut 50 mm
Cutting speed 30 m/min.

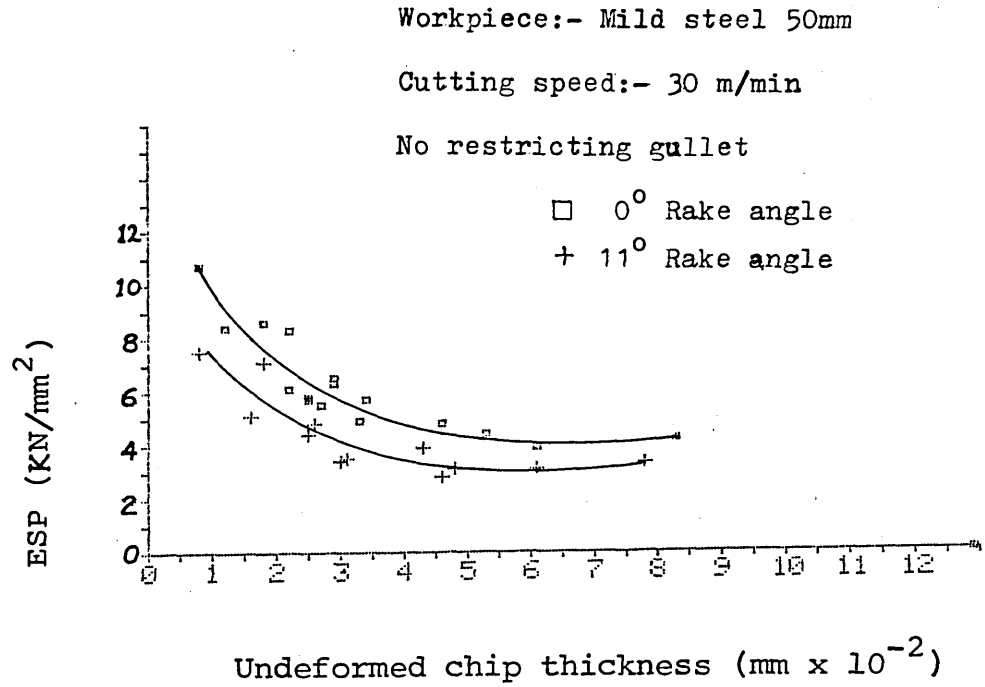

Fig 7.5 Specific Cutting Energy V Undeformed Chip Thickness, for Single Hacksaw Teeth having no Restricting gullet. Workpiece Mild Steel. Length of Cut 50 mm.

a)

x 4 Magn.

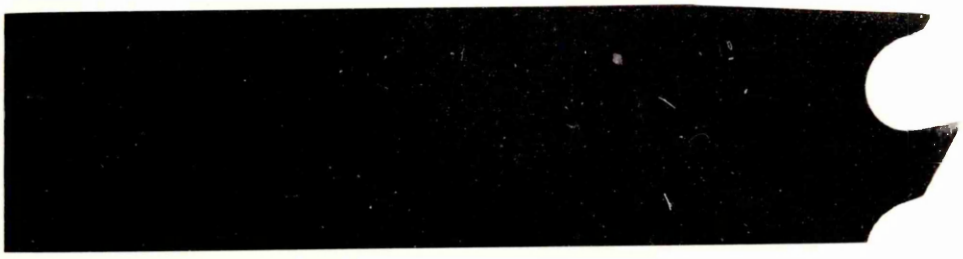

b)

Fig 7.6 Single Hacksaw Teeth Having a Single Radius Root:

(a) 1.25 mm radius
(b) 1.50 mm radius

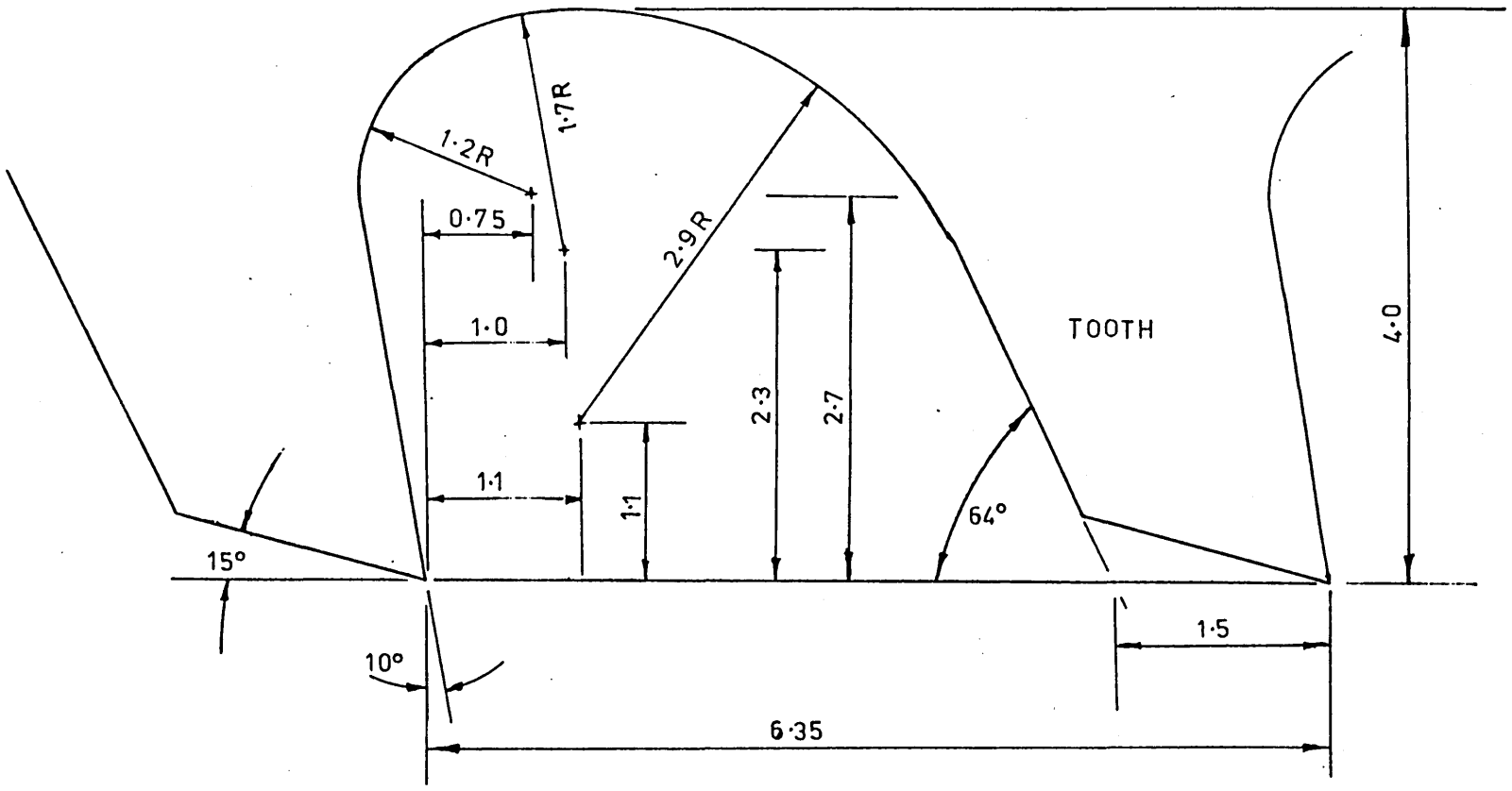

Fig 7.7 New Tooth/Gullet Design for Improved Chip Curl.
All Dimensions in Millimetres.

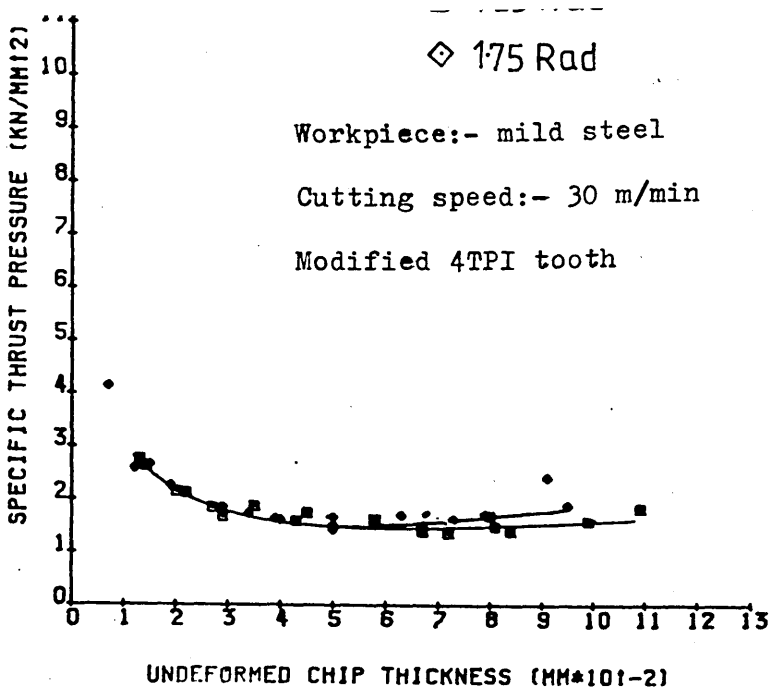

a

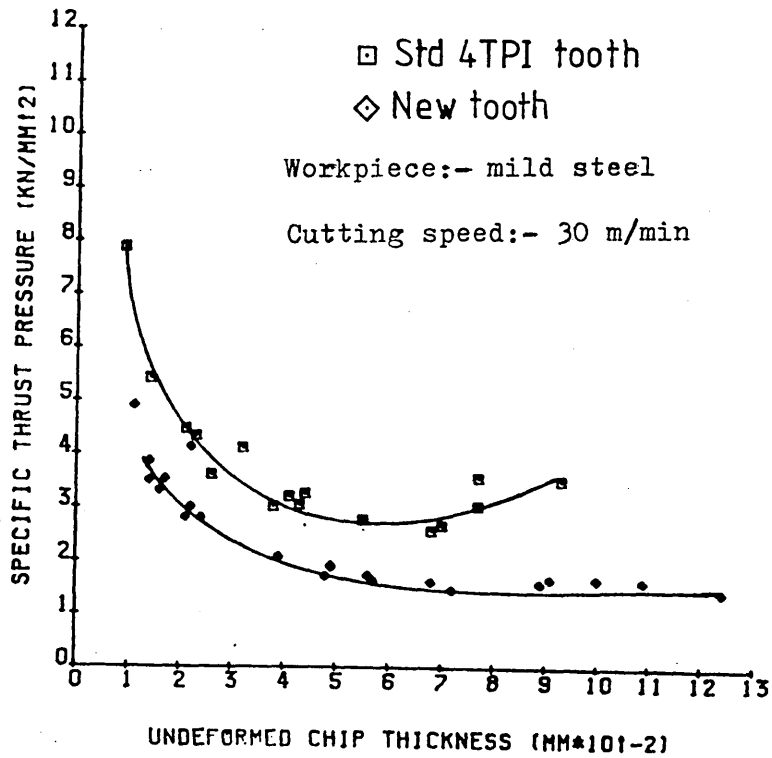

b

Fig 7.8 The Performances of:

(a) the Single Root Radius Teeth, Fig 7.6; and
(b) the New Tooth/Gullet, Fig 7.7

Compared to the Performance of a Standard 4 TPI Tooth Cutting a 50 mm Workpiece.

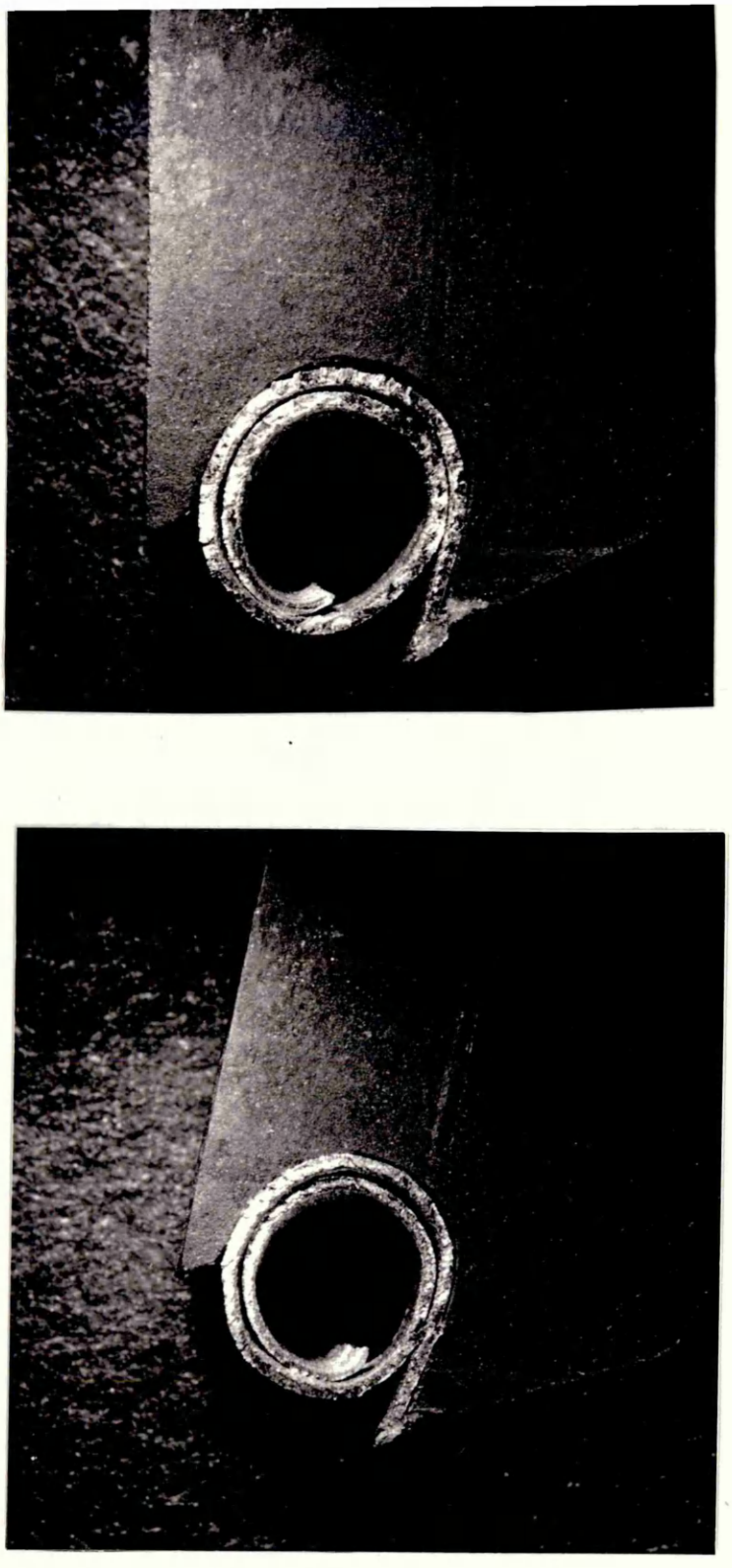

Fig 7.9 The Single Teeth Shown in Fig 7.6 with Chips which have Curled to the Same Radius as the Roots. There is Sufficient Spring in These chips to Prevent Them from Falling Out of the Gullet.

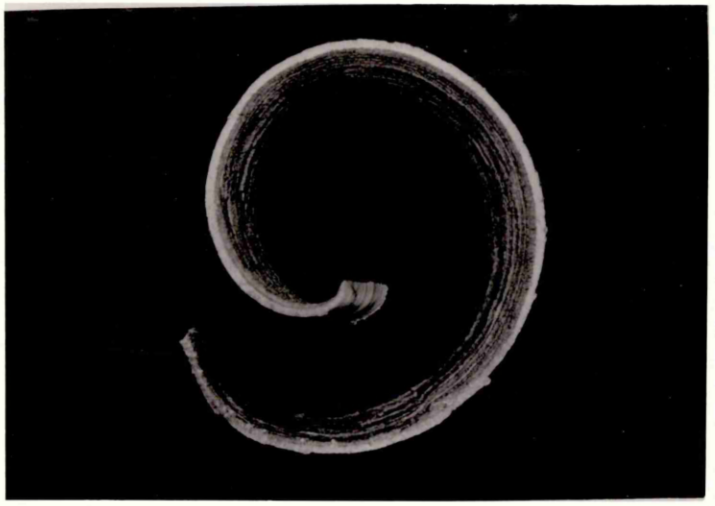

Fig 7.10 Chip Created by a Hacksaw Tooth having no Restricting Gullet.

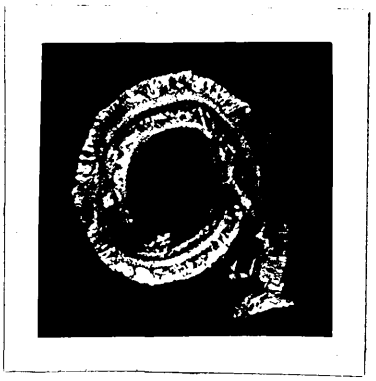

(a) A thin chip which has curled tightly

(b) A thicker chip which could not curl as tightly as (a)

Fig 7.11 Chips Produced by the New Tooth/Gullet, Fig 7.7

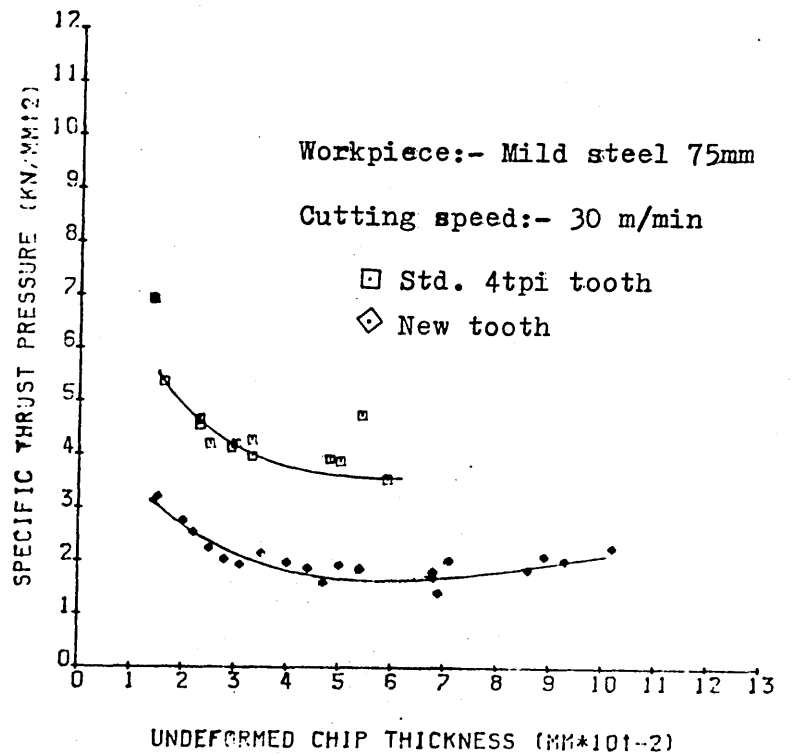

Fig 7.12 The Performances of:

⊡ Standard 4 TPI Tooth/Gullet; and
◇ the New Tooth/Gullet, Fig 7.7

Cutting a 75 mm Mild Steel Workpiece

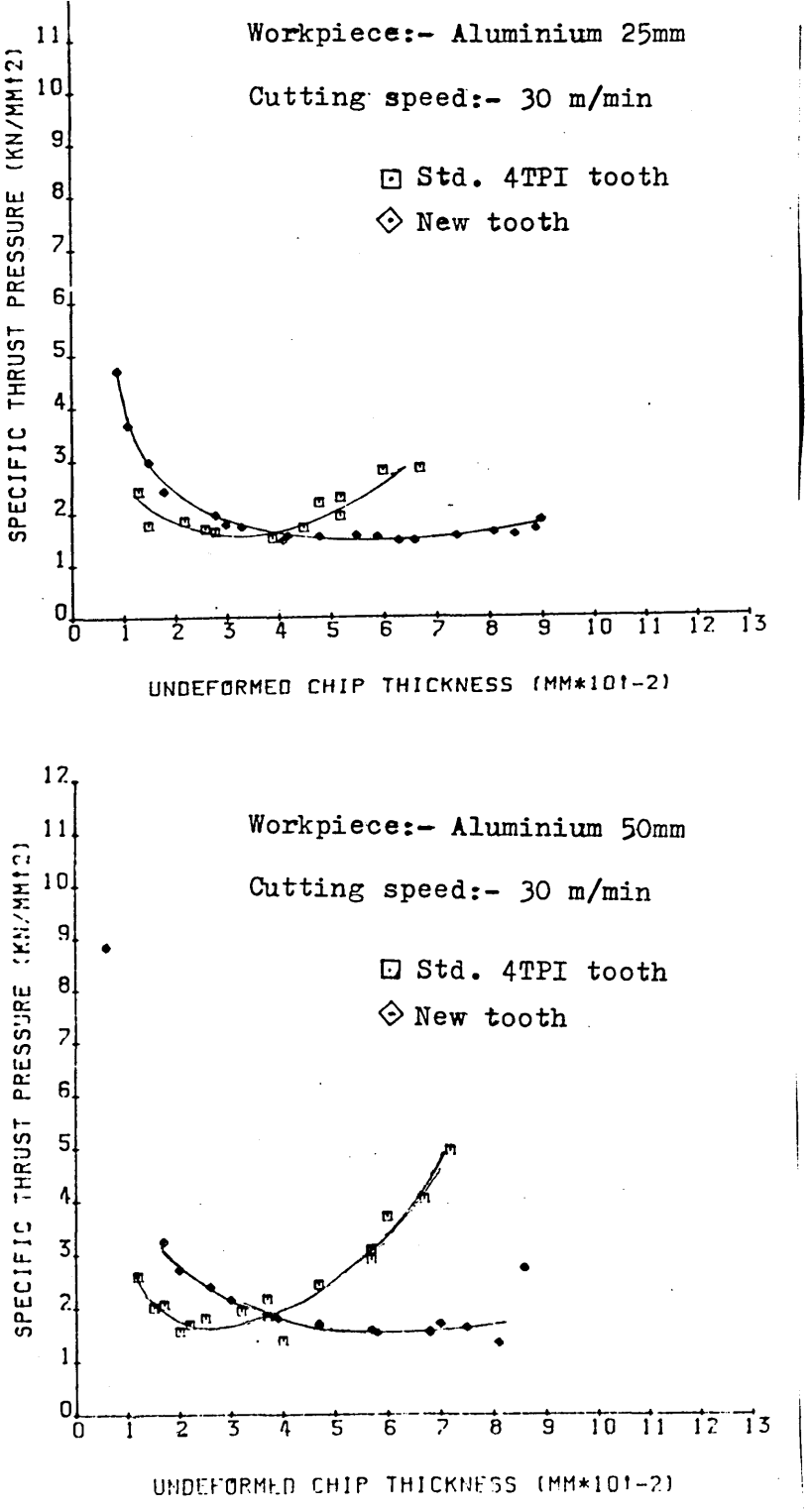

Fig 7.13 The Performances of:

a Standard 4 TPI Tooth/Gullet; and
the New Tooth/Gullet, Fig 7.7

Cutting 25 and 50 mm Aluminium Workpieces

The difference in performance between the std. tooth and the new tooth at low undeformed chip thicknesses is due to a difference in the cutting edge radii of the two teeth

APPENDIX 1

Tooth Size

The author has measured the height of 48 consecutive teeth on a new 350 x 32 x 1.6(6) hacksaw blade. Each tooth height was measured relative to a datum plane using a dial gauge which measured to 0.001 mm. Table A1.1 shows the height of each tooth relative to the tooth preceding it.

The maximum difference in height of the teeth measured was 0.118 mm. This is large compared to the average undeformed chip thickness per tooth (0.002 - 0.03 mm) (1,2).

TABLE A1.1

Blade: 6 TPI

TOOTH NO	SET	HEIGHT DIFFERENCE FROM PREVIOUS TOOTH (mm)
1	Straight	-.051
2	Left	+.042
3	Right	-.014
4	Straight	-.08
5	Left	+.049
6	Right	+.079
7	Straight	-.102
8	Left	+.041
9	Right	+.069
10	Straight	-.134
11	Left	+.023
12	Right	+.035
13	Straight	-.090
14	Left	+.041
15	Right	+.021
16	Straight	-.072
17	Left	+.012
18	Right	+.041
19	Straight	-.090
20	Left	+.031
21	Right	+.009
22	Straight	-.042
23	Left	+.033
24	Right	+.024
25	Straight	-.077
26	Left	+.047
27	Right	+.015
28	Straight	-.077
29	Left	+.054
30	Right	+.042
31	Straight	-.095
32	Left	+.056
33	Right	-.039
34	Straight	-.095
35	Left	+.063
36	Right	+.059
37	Straight	-.109
38	Left	+.015
39	Right	+.104
40	Straight	-.075
41	Left	-.002
42	Right	+.040

TOOTH NO	SET	HEIGHT DIFFERENCE FROM PREVIOUS TOOTH (mm)
43	Straight	-.091
44	Left	+.022
45	Right	+.118
46	Straight	-.088
47	Left	+.066
48	Right	+.008

48 teeth = 8" of blade

APPENDIX 2

High Speed Photography of Hacksawing

A2.1 The Filming Rig

There are two physical problems which have to be overcome in order to film chip formation in hacksawing.

Firstly, the saw cuts in a slot and is therefore hidden from view during cutting. This problem was overcome by cutting on the end of a bar, Figure 2.1. (The guides on either side of the workpiece prevented the blade from running out and the glass prevented the chips from escaping from the gullets during the cut).

The second problem was related to light. Filming at high speeds, in this case 1000 frames/sec, requires a lot of light because the exposure time per frame is very short. The high magnification required also reduced the amount of light available. The close proximity of the lens to the workpiece caused the external light sources to be shone at an oblique angle to the viewing axis which caused shadows to be thrown by the teeth on the gullet area and therefore the chips.

The mirror arrangement, FigureA2.1, was used to shine light parallel to the viewing axis. The centre of the mirror was not silvered so as to allow light reflected from the chips to pass through the mirror to the camera.

A2.2 Discussion of Films

High speed photography is expensive; at 1000 frames/second, a 100 ft film lasts only about 5 seconds. The cost was therefore too high for an extensive study of hacksawing to take place by this method.

However, the films did corroborate the following claims made in the main text of this thesis:

1 Some teeth cut significantly more material than others in the blades new state (Figure A2.2).

2 The saw removes most material at mid stroke when the thrust force is at its highest.

3 Chip flow is restricted by the gullet causing inefficient chip formation (Figure A2.3).

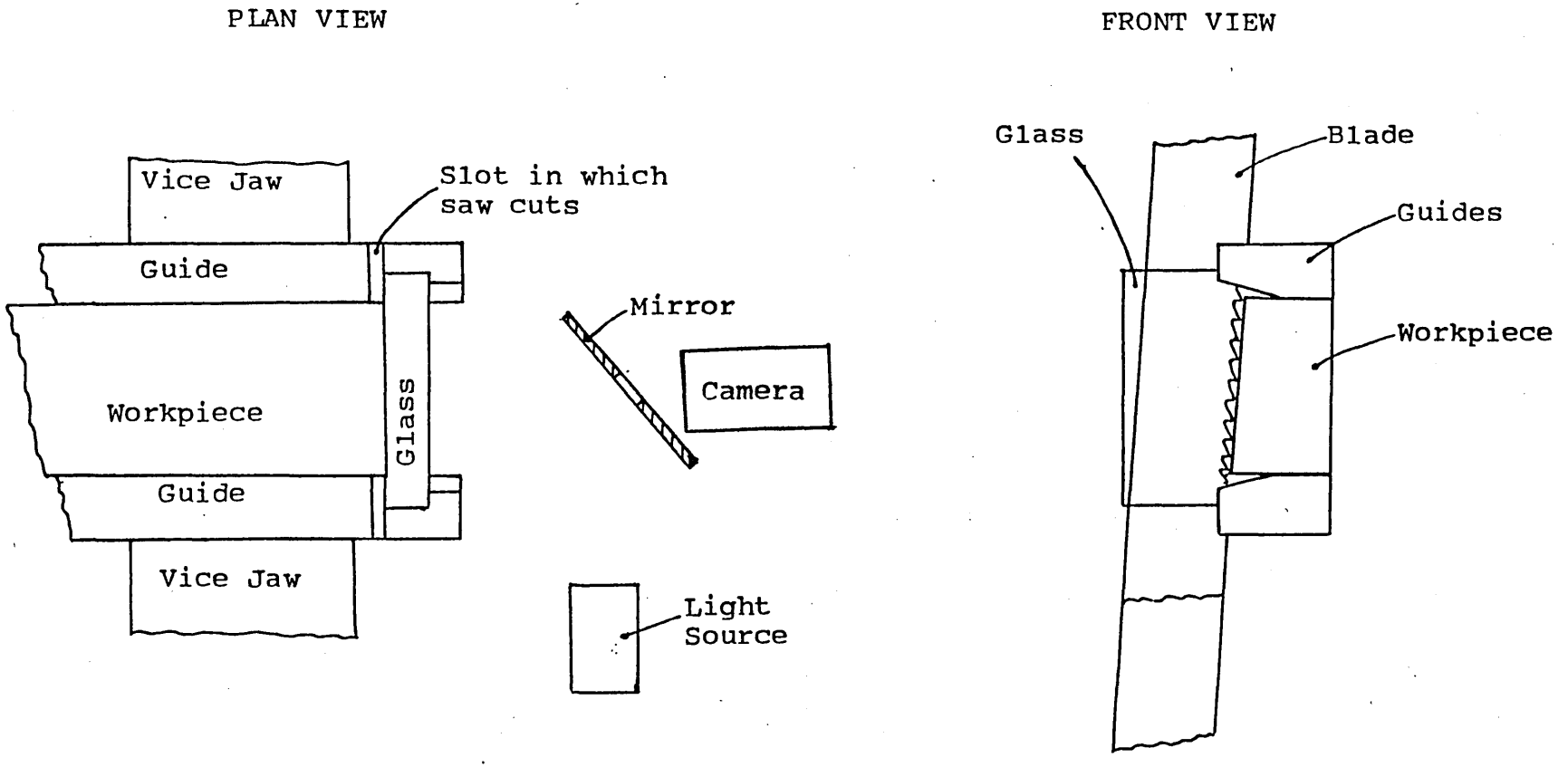

Fig. A2.1. Set up for high speed filming of a hacksaw blade cutting in a power hacksaw machine

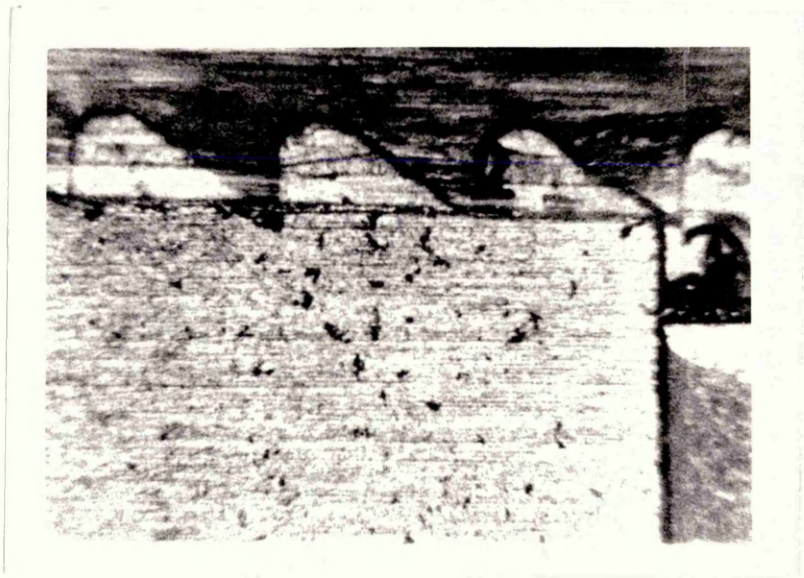

Fig. A2.2. Frame from high-speed film of a 4 TPI hacksaw blade cutting. Only one tooth is cutting.

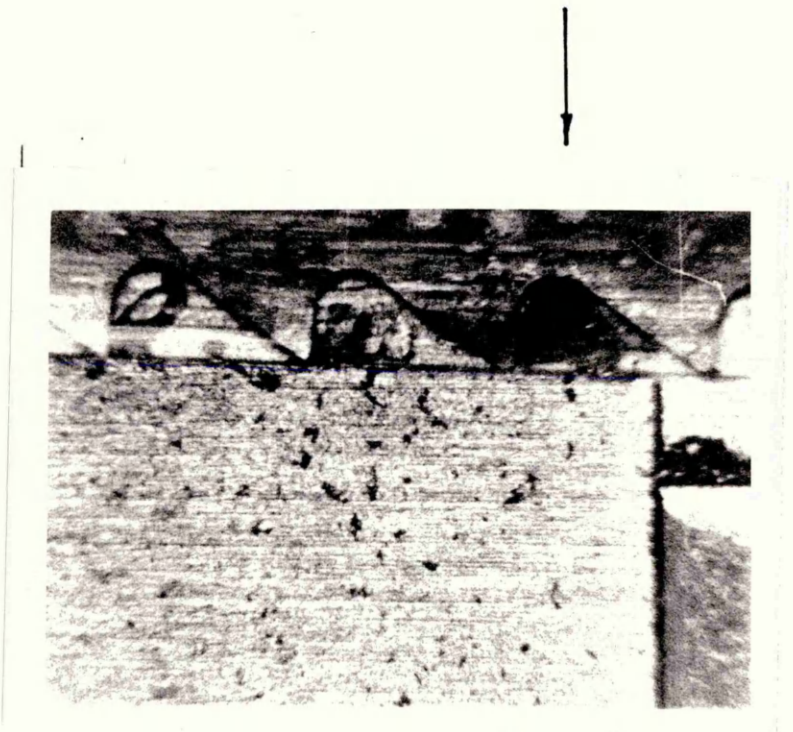

Fig. A2.3. Frame from high-speed film of a 4 TPI hacksaw blade cutting

The indicated chip is forming inefficiently.

APPENDIX 3

Hacksaw Tooth Strength

A3.1 Introduction

Before designing a new tooth and gullet it is necessary to know whether the tooth is strong enough to cut. A theoretical analysis has been made of tooth strength and a short computer program written to show the principal stresses caused by cutting, at various planes in the tooth.

A3.2 Theoretical Analysis

The aim of the analysis is to estimate the maximum principal stress in a hacksaw tooth, given applied cutting and thrust loads, and compare this with the fracture stress of the tooth.

Figure A3.1 shows the cutting and thrust force components, which are assumed to be concentrated at the cutting edge, acting on a standard all-hard hacksaw tooth. It has been assumed in the analysis that the tooth is triangular, ie the rake and clearance faces are straight, which will result in an over-estimation of principal stress.

A3.2.1 The stress caused by the cutting force component:

1 Stress due to shear, σ_{sv}

$$\sigma_{sv} = \frac{Fv}{A} \qquad \text{A3.1}$$

where σ_{sv} is the shear stress at a particular cross section,

F_v is the cutting force component (Figure A3.1);

and A is the cross sectional area at which σ_{sv} occurs.

However,

$$A = t.d \qquad \text{A3.2}$$

where t is the thickness of the tooth and d is the width of the tooth (Figure A3.1).

$$d = L + x.\tan\theta - x.\tan\alpha \qquad \text{A3.3}$$

where L is the width of the tooth at the cutting edge:

x is the height at which σ_{sv} occurs

α is the rake angle

and θ is the wedge angle

Substituting A4.2 and A4.3 in A4.1:

$$\sigma_{sv} = \frac{Fv}{t(L + x(\tan\theta - \tan\alpha)} \qquad \text{A3.4}$$

2 Bending stress (caused by the cutting force component):

$$\sigma_{bv} = \frac{Mv.d/2}{I} \qquad A3.5$$

where σ_{bv} is the bending stress at distance x from the cutting edge. M_v is the bending moment due to F_v and I is the second moment of area of the tooth at distance x from the cutting edge,

therefore:

$$\sigma_{bv} = \frac{Fv.x.d/2}{\frac{t.d^3}{12}}$$

$$= \frac{6.Fv.x}{t.d}$$

$$\sigma_{bv} = \frac{6.Fv.x}{t(L + x(\tan\theta - \tan\alpha)^2} \qquad A3.6$$

A3.2.2 The bending stress due to the thrust force component.

$$\sigma_{bp} = \frac{Fp}{A} + \frac{Mp.d/2}{I}$$

where σ_{bp} is the bending stress due to the thrust force component.

Mp is the bending moment due to the thrust force component = Fp.d/2.

Therefore:

$$\sigma_{bp} = \frac{Fp}{t(L + x(\tan\theta - \tan\alpha)} + \frac{3.Fp}{t.d}$$

$$= \frac{4.Fp}{t(L + x(\tan\theta - \tan\alpha)} \qquad \text{A3.7}$$

A3.2.3 The total stress due to bending:

$$\sigma_b = \sigma_{bv} - \sigma_{bp} \qquad \text{A3.8}$$

where σ_b is the total stress due to bending.

Therefore, substituting A3.6 and A3.7 in A3.8:

$$\sigma_b = \frac{6.Fv.x}{t(L + x(\tan\theta - \tan\alpha)^2} - \frac{4.Fp}{t(L + x(\tan\theta - \tan\alpha)}$$

$$= \frac{6.Fv.x - 4.Fp\ (L - x(\tan\ - \tan\ )}{t(L + x(\tan\theta - \tan\alpha)} \qquad \text{A3.9}$$

A3.2.4 The principal stress at a height x:

$$\sigma_1 = \frac{\sigma b}{2} + \frac{1}{2}\sqrt{\sigma_b{}^2 + 4\sigma_{sv}{}^2} \qquad \text{A3.10}$$

where σ_1 is the principal stress at height x.

Calculating σ_1 for different values of x, O, L, F_v and F_p requires a computer. The program, listed at the end of this appendix, will run on an Apple microcomputer and permits α, θ, L, F_v and F_p to be varied, giving values of σ_{sv}, σ_{bv}, σ_{bp}, σ_b and σ_1 for values of x ranging from 0.5 mm upwards in steps of 0.2 mm.

Table A3.1 shows the principal stresses calculated by the program for a standard all-hard 4 TPI hacksaw tooth. The values of F_v, 1000 N and F_p, 700 N, are taken from the single tooth and gullet cutting data (Chapter Four) for a high undeformed chip thickness cutting a 50 mm mild steel workpiece. The highest value of principal stress is 1102 N/mm^2. This is lower than the blade material's fracture stress of 2 KN/mm^2, which implies that the tooth is strong enough to cut at the specified forces.

A3.3 Deflection of a Standard Set Tooth

The set teeth on a hacksaw blade are subjected during cutting to a net force which deflects the teeth away from the side of the slot on which they are cutting. This reduces the overall set on the blade. A theoretical analysis has been made to estimate the deflection of a hacksaw tooth given a side load W, assumed to be concentrated at the cutting edge.

It is assumed that the tooth is triangular, Figure A3.2, and that it is rigidly supported where it joins the body of the blade.

A3.3.1 The deflection yb due to bending:

$$\frac{d^2yb}{dx^2} = \frac{M}{E.I}$$

where M is the bending moment

E is Young's modulus for the tooth material

x is the distance from the cutting edge

and I is the second moment of area.

Therefore:

$$\frac{d^2yb}{dx^2} = \frac{12.W.x}{bd^3.E} \qquad \text{A3.11}$$

where W is the load

b is the width of the tooth

and d is the thickness of the tooth

However:

$$b = x(\tan\theta - \tan\alpha) \qquad \text{A3.12}$$

where α is the rake angle

and θ is the wedge angle -

Therefore, substituting A4.12 and A4.11:

$$\frac{d^2yb}{dx^2} = \frac{12\ W.x}{(\tan\theta - \tan\alpha).d^3.E} + C \qquad \text{A3.13}$$

where C is a constant.

Applying boundary conditions:

$$\frac{dyb}{dx} = 0 \text{ when } x = h$$

Therefore: $$C = \frac{-12.W.h}{(\tan\theta - \tan\alpha)\, d^3.E} \qquad \text{A3.14}$$

Substituting A3.14 in A3.13:

$$\frac{dyb}{dx} = \frac{12.W.x - 12.W.h}{(\tan\theta - \tan\alpha).d^3.E}$$

Therefore:

$$yb = \frac{6.W.x^2 - 12.W.h}{(\tan\theta - \tan\alpha).d^3.E} + C_1 \qquad \text{A3.15}$$

where C_1 is a constant.

Applying boundary conditions:

$$yb = o \text{ when } x = h$$

Therefore:

$$C_1 = \frac{6.Wh^2}{(\tan\theta - \tan\alpha).d^3.E} \qquad \text{A3.16}$$

Substituting A4.16 in A4.15:

$$yb = \frac{6W}{(\tan\theta - \tan\alpha)d^3.E} (x^2 - 2.h.x - h^2$$

Maximum deflection due to bending occurs at the cutting edge of the tooth, when $x = 0$.

Therefore the maximum deflection due to bending

$$= \frac{6.Wh^2}{(\tan\theta - \tan\alpha)d^3.E} \qquad \text{A3.17}$$

A3.3.2 The deflection due to shear Y_s, of a set tooth at a distance x from the cutting edge.

The average shear stress, $= \frac{W}{d.b}$

$$Y_s = \int_x^h \frac{W}{G.d.b}\, dx \qquad \text{A3.18}$$

where G is the shear modulus.

However:

$$b = x(\tan\theta - \tan\alpha) \qquad \text{A3.19}$$

Substituting A4.19 in A4.18:

$$Y_s = \frac{W}{G.d.(\tan\theta - \tan\alpha)} \quad \frac{1}{x}\, dx$$

Therefore:

$$Y_s = \frac{W.\ln(h) - \ln(x)}{G.d.(\tan\theta - \tan\alpha)} \qquad \text{A3.20}$$

The maximum deflection occurs at the cutting edge when x = o. However, this gives a meaningless value of deflection when used in equation A3.20. Therefore, a value close to the cutting edge must be taken, for example when x = 1 micron.

The maximum deflection of a set tooth, y can be estimated by combining the maximum deflections due to bending and shear (equations A4.17 and A4.20).

$$y = \frac{6.W.h^2}{(\tan\theta - \tan\alpha)d^3.E} - \frac{W.\ln(h)}{G.d.(\tan\theta - \tan\alpha)} \qquad A3.21$$

However, G is very large and therefore the second term in A4.21 can be ignored, giving:

$$y = \frac{6.W.h^2}{(\tan\theta - \tan\alpha)d^3.E} \qquad A3.22$$

A3.4 Deflection of a Non-Standard Hacksaw Tooth Having a Primary and Secondary Clearance Angle

The analysis in Section A3.3.1 has to be extended in order to estimate the deflection of a hacksaw tooth form having both a primary and secondary clearance angle, because the cross-sectional area of the tooth is not directly proportional to its distance from the cutting edge.

It is assumed that the primary clearance angle is 0^o and that the tooth is rigidly supported where it joins the body of the blade. The rake face and secondary clearance face are assumed to be flat. Figure A3.3

A3.4.1 The deflection due to bending, y_b

$$\frac{d^2y_b}{dx^2} = \frac{M}{E.I}$$

where M is the bending moment = $W(x-a)$

E is Young's modulus

I is the second moment of area = $\frac{bd^3}{12}$

x is a distance varying between 'a' and 'h' (Figure A3.3)

a is the distance OB, Figure A3.3

b is the width of the tooth = $x(\tan\theta - \tan\alpha)$

d is the thickness of the tooth

α is the rake angle

and θ is 90^o - the secondary clearance angle

Thus:

$$\frac{d^2yb}{dx^2} = \frac{12\ W.(x-a)}{x(\tan\theta - \tan\alpha)d^3.E}$$

$$= 12\ KW(1 - \frac{a}{x})$$

where $K = \frac{1}{(\tan\theta - \tan\alpha)d^3.E}$

Therefore:

$$\frac{dyb}{dx} = 12\ KWx - 12\ K.W.a\ \ln(x) + C \qquad A3.23$$

where C is a constant.

Applying boundary conditions:

$$\frac{dyb}{dx} = o \text{ when } x = h$$

Therefore $C = 12.K.W.a\ \ln(h) - 12\ K.W.h$ A3.24

Substituting A3.23 in A3.24:

$$\frac{dyb}{dx} = 12.K.Wx - 12\ K.W.a.\ln(x) + 12\ K.W.a.\ln(h) - 12\ K.W.h$$

Therefore:

$$y_b = 6\ KWx^2 - 12\ K.W.a.(x.\ln x - x) + 12\ K.W.a.\ln(h).x - 12\ K.W.hx + C \qquad A3.25$$

Where C is a constant.

Applying boundary conditions:

$y_b = 0$ when $x = h$

Therefore:

$$C = -6\ KWh^2 + 12\ K.W.a.(h.\ln(h) - h) - 12\ K.W.a.h.\ln h + 12\ K.W.h^2 \qquad A3.26$$

Substituting A3.26 in A3.25:

$$y_b = 6\ KW(x^2 - 2a(x.\ln x - x) + 2.a.\ln h.x - 2.h.x. - h^2 + 2a(h.\ln h - h) - 2.a.h.\ln h + 2h^2)$$

Maximum deflection due to bending occurs at the cutting edge when $x = a$.

Therefore, the maximum deflection:

$$= 6\ KW(a^2 + 2a^2 . \ln a + 2a^2 . \ln h - 2.a.h. - h^2 - 2a.h + 2a.h.\ln h - 2ah.\ln h + 2h^2)$$

$$= 6\ KW(3a^2 - 2a^2.\ln a + 2a^2.\ln h - 4ah + h^2) \qquad A3.27$$

A3.4.2 Deflection due to shear, y_s.

Equation A4.20 can be used to find maximum deflection due to shear. For a tooth having both a primary and secondary clearance angle maximum deflection occurs when x = a (Figure A3.3).

Thus:

$$\text{Maximum } y_s = \frac{W.\ln \frac{h}{a}}{G.D.(\tan\theta - \tan\alpha)} \qquad \text{A3.28}$$

A3.3 Total Deflection at the Cutting Edge

Total maximum deflection, y, is calculated by summing the deflection due to bending and shearing (equations A3.27 and A3.28).

Thus:

$$y = 6\ KW(3a^2 - 2a^2.\ln a + 2a^2.\ln h - 4ah + h^2) + \frac{W.\ln \frac{h}{a}}{G.d.(\tan\theta - \tan\alpha)} \qquad \text{A3.29}$$

However G is very large and therefore the second term in equation A3.29 can be ignored.

Thus:

$$y = 6\ KW(3a^2 - 2a^2 \ln a + 2a^2\ .\ \ln h - 4ah + h^2)$$

A3.5 Errors Caused by Assumptions

The assumption that the rake and clearance faces are straight, causes the estimation of tooth width, where the tooth joins the blade, to be under-estimated. Thus, calculated values of principal stresses will be over-estimated, as will values of deflection.

The assumption that the primary clearance angle is zero, section A4.4.1, will cause an under-estimation of tooth deflection, which will be negligible if the primary clearance angle is small, ie less than 25^{o}.

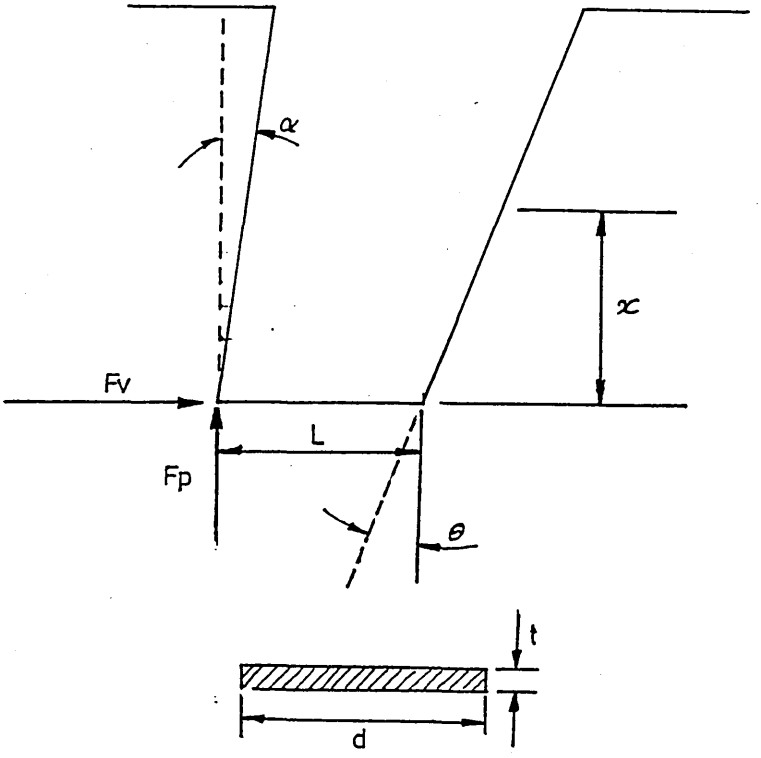

Cross section at height x

Fig. A3.1. Diagram of tooth considered for determination of tooth strength.

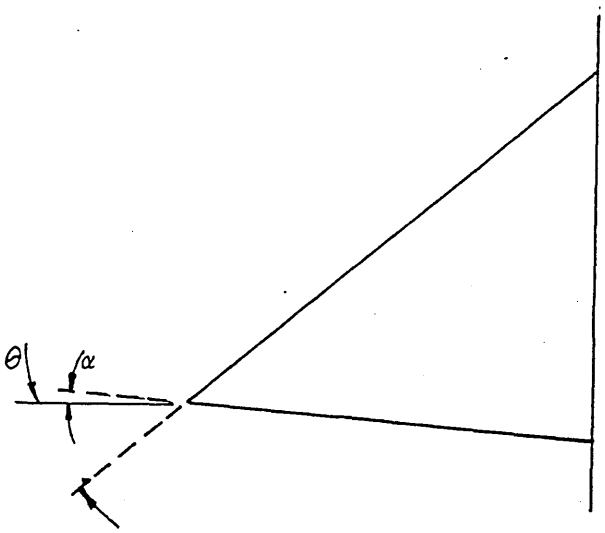

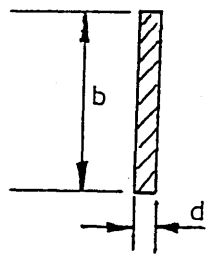

Cross section at distance x from cutting edge

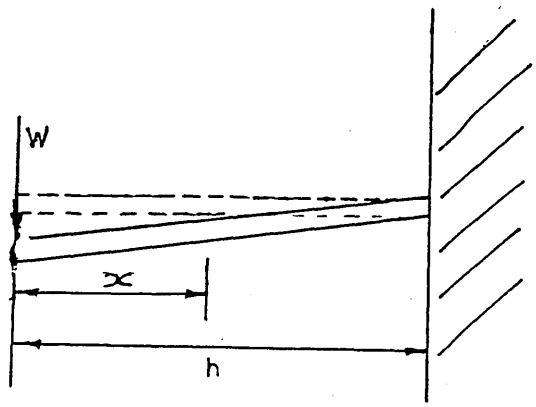

A3.2. Diagram of tooth considered for determination of deflection of a set tooth subjected to a net force W at its cutting edge.

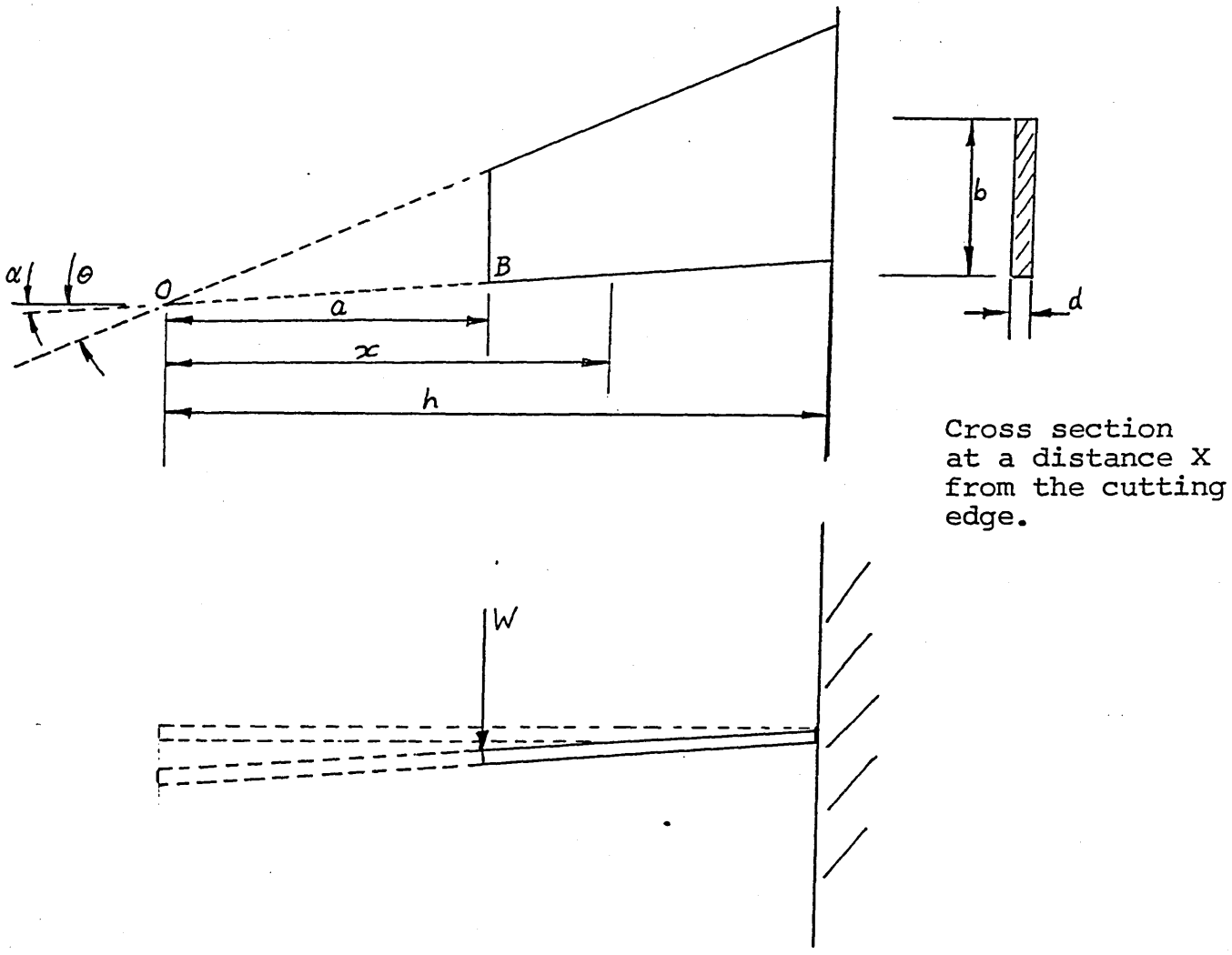

Cross section at a distance X from the cutting edge.

A3.3. Diagram of tooth considered for determination of deflection of a set tooth, having a primary and secondary clearance angle, subjected to a net force W at its cutting edge.

TOOTH WIDTH	2
POINT WIDTH	1.5
RAKE ANGLE	10
BACK ANGLE	26
V FORCE	1000
P FORCE	700

SHEAR STRESS	BENDING STRESS (V)	BENDING STRESS (P)	BENDING STRESS TOTAL	PRINCIPAL STRESS	ANGLE	HEIGHT
301	547	845	-299	187	-27	.5
291	711	814	-104	243	-11	.7
280	851	786	65	315	6	.9
271	971	759	212	397	21	1.1
262	1074	734	339	482	32	1.3
254	1162	711	451	565	41	1.5
246	1238	689	548	642	48	1.7
239	1302	669	633	713	52	1.9
232	1357	649	707	777	56	2.1
225	1404	631	772	834	59	2.3
219	1444	614	830	884	62	2.5
213	1478	598	880	929	64	2.7
208	1506	582	923	968	65	2.9
202	1529	567	962	1003	67	3.1
197	1549	553	995	1033	68	3.3
193	1565	540	1024	1059	69	3.5
188	1577	527	1049	1082	70	3.7
184	1587	515	1071	1102	71	3.9

APPENDIX 4

A4.1 Program Listings

Listings of the tabulating and graphics programs are not given, because the output comamnds are specific to the equipment which the author had available, and will not therefore, be of general interest.

A4.2 Computer Programs used in the Single Hacksaw Tooth Tests at Realistic Cutting Speeds

This appendix contains listings of BASIC programs written by the author for the storage and manipulation of data obtained from the test rig described in Chapter Four.

The function of each program is described below:

1 The "Sample Program" calculates the average and maximum cutting and thrust forces created by each test cut, and stores the data on disk. The data for the calculations is read from a storage oscilloscope via a Mountain Com. Inc. A/D converter.

2 The "Calculations Program" calculates from the weight of each chip and the data created by the Sample Program, and the volume of chip material removed, the undeformed chip thickness, the

specific cutting energy, the average cutting and thrust force per tooth thickness. This data is stored on disk for subsequent analysis.

3 The "Tabulating Program" is used to obtain hard copies of the data stored on disk.

4 The "Graphics Program" is used to compare data from different tests. Graphs can be drawn on a monitor and hard copies can be taken. The data used is that stored on disk by the Calculations Program.

SAMPLING PROGRAM

```
1  REM  ****SAMPLE PROGRAM*****
2  REM   PROG SAMPLES OUTPUT FROM DIGITAL STORAGE OSCILLOSCOPE USING A/D
    CONVERTER.
4  DIM A(300),B(300)
5  DIM VF(30),VN(30),PF(30),PN(30)
6  PRINT : PRINT : PRINT : PRINT "        SAMPLE PROGRAM MENU"
8  PRINT : PRINT : PRINT : PRINT "  SET UP                    TYPE A"
9  PRINT : PRINT : PRINT : PRINT "  SAMPLE 1                  TYPE B": PRINT
    : PRINT : PRINT : PRINT "  SAMPLE 2                  TYPE C"
10  PRINT : PRINT : PRINT : PRINT "  CALCULATIONS             TYPE D": PRINT
    : PRINT : PRINT : PRINT "  CREATE FILE               TYPE E": GET A$: PRINT

11  IF A$ = "A" THEN  GOTO 1000
12  IF A$ = "B" THEN  GOTO 60
13  IF A$ = "C" THEN  GOTO 300
14  IF A$ = "D" THEN  GOTO 490
15  IF A$ = "E" THEN  GOTO 1180
18  REM  **FOR ANALOGUE SAMPLING USING MOUNTAIN COMP. INC. A/D COVERTER**
    *******
60 CHANNEL = 0
70 SLOT = 4
80 AD = 49280 + (SLOT * 16) + CHANNEL
90  REM  **OBTAIN 256 SAMPLES FROM CHANNEL 0*******
100  FOR I = 1 TO 256
110  REM **START CONVERSION********
120 A =  PEEK (AD)
130  REM **READ CONVERTED VALUE*****
140 A(I) =  PEEK (AD)
150  REM **CREATE TIME DELAY*********
160  FOR J = 1 TO 83
165  NEXT J
170  NEXT I
180  GOTO 6
290  REM **OBTAIN 256 SAMPLES FROM CHANNEL 0 FOR SAMPLE 2******
300  FOR I = 1 TO 256
310  REM **START CONVERSION*********
320 A =  PEEK (AD)
330  REM **READ CONVERTED VALUE******
340 B(I) =  PEEK (AD)
350  REM **CREATE TIME DELAY*********
360  FOR J = 1 TO 83
370  NEXT J
380  NEXT I
390  GOTO 6
490  INPUT "CUT NUMBER ?";N
500  REM **CALCULATE AREA UNDER CURVE*****
510 X = 0:Y = 0:Z = A(1)
520  FOR 1 = 1 TO 256
530 X = X + A(I)
540  IF A(I) > A(1) + 5 THEN Y = Y + 1
545  IF A(I) > Z THEN Z = A(I)
550  NEXT I
560 XF = (X - (A\1) * 256)) / Y
570  REM ***CALCULATE AVERAGE CUTTING FORCE******
```

```
580 VF(N) = XP * 10 * CF / 256
590  PRINT "AVERAGE CUTTING FORCE (N)";VF(N)
592  REM **CALCULATE MAX CUTTING FORCE****
610 VM(N) = (Z - A(1)) * 10 * CF / 256
620  PRINT "MAX FV = "VM(N)
700 X = 0:Y = 0:Z = B(1)
710  FOR I = 1 TO 250
720 X = X + B(I)
730  IF B(I) > B(1) + 5 THEN Y = Y + 1
740  IF B(I) > Z THEN Z = B(I)
750  NEXT I
760 XP = (X - (B(1) * 256)) / Y
770  REM ***CALCULATE AVERAGE FORCE 2****
780 PF(N) = XP * 10 * CF / 256
790  PRINT "AVERAGE FORCE (N) = "PF(N)
800 PM(N) = (Z - B(1)) * 10 * CF / 256
805  PRINT "MAX FP = "PM(N)
810  PRINT "TYPE M FOR MENU": GET A$
820  GOTO 6
990  REM  ****SET UP*****
1000  INPUT "NAME OF TOOL    ";B$
1010  INPUT "FORCE CONVERSION FACTOR  ";CF
1020  GOTO 6
1170  REM **FILING FV,FV MAX,FP,FP MAX****
1180  INPUT "NUMBER OF CUTS ?";N1
1190  IF N1 = 0 THEN N1 = N
1200 D$ =  CHR$ (4)
1210  PRINT D$;"OPEN ";B$
1220  PRINT D$;"WRITE ";B$
1230  PRINT N1
1240  FOR I = 1 TO N1
1250  PRINT  INT (VF(I))
1260  PRINT  INT (VM(I))
1270  PRINT  INT (PF(I)): PRINT  INT (PM(I))
1280  NEXT I
1290  PRINT D$;"CLOSE ";B$
1300  END

]
```

```
40  HOME
50  REM **PROG. TO DO CALCULATIONS FOR SINGLE HACKSAW TEETH ON LATHE
60  REM **USES DATA IN FILES CREATED BY SAMPLING PROGRAM******
100  PRINT : PRINT : PRINT : PRINT "                    MENU": PRINT : PRINT
    : PRINT
110  PRINT "  SET UP                          TYPE A": PRINT : PRINT
120  PRINT "  INPUT WEIGHTS                   TYPE B": PRINT : PRINT
130  PRINT "  CORRECTIONS                     TYPE C": PRINT : PRINT
140  PRINT "  CALCULATIONS                    TYPE D": PRINT : PRINT
150  PRINT "  CREATE FILE                     TYPE E": PRINT
160  GET A$: PRINT
170  IF A$ = "A" THEN  GOTO 2000
180  IF A$ = "B" THEN  GOTO 1500
190  IF A$ = "C" THEN  GOTO 1560
200  IF A$ = "D" THEN  GOTO 500
210  IF A$ = "E" THEN  GOTO 890
220  IF A$ <  > "E" THEN  GOTO 40
500  REM  **CALC VOLUMES FROM WEIGHTS MM^3*******
510  DIM VO(NW),UCT(NW)
520  FOR I = 1 TO NW:VO(I) = WT(I) / DN: NEXT I
540  REM **CALC UNDEFORMED CHIP THICKNESS MM*10^-3*******
550  FOR I = 1 TO NW:UCT(I) = VO(I) / WD / LN: NEXT I
570  REM **CALC ESP & ESP(MAX)*******
580  DIM VF(NW),VM(NW),PF(NW),PM(NW)
585  REM **RECALL DATA IN FILE*******
590 D$ =  CHR$ (4)
600  PRINT D$;"OPEN ";B$
610  PRINT D$;"READ ";B$
620  INPUT N
630  FOR I = 1 TO N
632  INPUT VF(I)
633  INPUT VM(I)
634  INPUT PF(I)
635  INPUT PM(I)
637  NEXT I
640  PRINT D$;"CLOSE ";B$
650  DIM VT(N),V(N),PT(N),P(N),ES(N),EM(N)
660  FOR I = 1 TO N:VT(I) = VF(I) / WD
670 V(I) = VM(I) / WD
680 PT(I) = PF(I) / WD
690 P(I) = PM(I) / WD
700 ES(I) = VF(I) / (VO(I) / LN)
710 EM(I) = VM(I) / (VO(I) / LN)
720  NEXT I
730  GOTO 40
880  REM **Z IS THE CUT NO.********
890  DIM Z(N)
900  FOR I = 1 TO N:Z(I) = I: NEXT I
910  REM **CHANGE EVERYTHING INTO3 OR 4 DIGITS**********
920  FOR I = 1 TO N
925 VT(I) =  INT (VT(I) + .5)
926 V(I) =  INT (V(I) + .5)
927 PT(I) =  INT (PT(I) + .5)
928 P(I) =  INT (P(I) + .5)
930 VO(I) =  INT ((VO(I) * 100) + .5) / 100
934 VF(I) =  INT (VF(I) + .5)
```

```
930 PF(I) =  INT ((PF(I) + .5)
940 UCT(I) =  INT ((UCT(I) * 1000) + .5)
950 ES(I) =  INT ((ES(I) / 10) + .5) / 100
960 EM(I) =  INT ((EM(I) / 10) + .5) / 100
965  NEXT I
970  REM **MAKE FILE OF Z,WT,VF,VM,VT,V,PF,PN,PT,P,ES,EM,VO,UCT*****
980  PRINT D$;"OPEN ";B$
990  PRINT D$;"DELETE ";B$
1000  PRINT D$;"OPEN ";B$
1010  PRINT D$;"WRITE ";B$
1011 A = (N * 14) + 7
1020  PRINT A
1022  PRINT B$
1023  PRINT WD
1024  PRINT RT
1025  PRINT M$
1026  PRINT DN
1027  PRINT CS
1028  PRINT LN
1035  FOR I = 1 TO N
1040  PRINT Z(I)
1045  PRINT WT(I)
1050  PRINT VF(I)
1055  PRINT VM(I)
1060  PRINT VT(I)
1065  PRINT V(I)
1070  PRINT PF(I)
1075  PRINT PM(I)
1080  PRINT PT(I)
1085  PRINT P(I)
1090  PRINT ES(I)
1095  PRINT EM(I)
1100  PRINT VO(I)
1150  PRINT UCT(I)
1300  NEXT I
1310  PRINT D$;"CLOSE ";B$
1320  PRINT "FILE CREATED"
1330  END
1500  HOME : PRINT : PRINT
1510  INPUT "HOW MANY WEIGHTS ?   ";NW: PRINT : PRINT
1512  DIM WT(NW)
1515  PRINT "  ENTER DATA    "
1520  FOR I = 1 TO NW
1530  INPUT WT(I)
1540  NEXT I
1550  HOME : PRINT : PRINT
1560  FOR I = 1 TO NW: PRINT "WEIGHT ";I,WT(I)
1570  IF I = 20 OR I = 40 THEN  PRINT " PRESS ANY KEY TO CONTINUE"
1580  IF I = 20 OR I = 40 THEN  GET A$: PRINT
1590  NEXT I
1600  INPUT "  ARE THESE POINTS OK ? Y/N    ";C$
1610  IF C$ = "Y" THEN  GOTO 40
1620  IF C$ <  > "N" THEN  GOTO 1600
1650  REM  CHANGING WEIGHT DATA
1660  PRINT : PRINT : INPUT "  WHICH WEIGHT DO YOU WANT TO CHANGE ? ";I
1670  PRINT : PRINT : PRINT "  REENTER WEIGHT ";I
1680  PRINT : PRINT : INPUT WT(I)
1690  GOTO 1550
2000  HOME : PRINT : PRINT : INPUT "  NAME OF TOOL ?    ";B$
2010  PRINT : PRINT : INPUT "  WIDTH OF TOOL ?    ";WD: PRINT : PRINT
2020  INPUT "  TOOL RADIUS ?    ";RT
2030  PRINT : PRINT : INPUT "  MATERIAL ?    ";M$
2035  PRINT : PRINT : INPUT "  DENSITY OF CHIP ? GM/MM^3    ";DN
2040  PRINT : PRINT : INPUT "  CUTTING SPEED M/MIN ?    ";CS
2045  PRINT : PRINT : INPUT "  LENGTH OF CUT ? MM    ";LN
2050  GOTO 40

]
```